

1990

Development and use of coal washery refuse for strata control in coal mines

John Kwong Hii
University of Wollongong

Recommended Citation

Hii, John Kwong, Development and use of coal washery refuse for strata control in coal mines, Doctor of Philosophy thesis, Department of Civil and Mining Engineering, University of Wollongong, 1990. <http://ro.uow.edu.au/theses/1237>

NOTE

This online version of the thesis may have different page formatting and pagination from the paper copy held in the University of Wollongong Library.

UNIVERSITY OF WOLLONGONG

COPYRIGHT WARNING

You may print or download ONE copy of this document for the purpose of your own research or study. The University does not authorise you to copy, communicate or otherwise make available electronically to any other person any copyright material contained on this site. You are reminded of the following:

Copyright owners are entitled to take legal action against persons who infringe their copyright. A reproduction of material that is protected by copyright may be a copyright infringement. A court may impose penalties and award damages in relation to offences and infringements relating to copyright material. Higher penalties may apply, and higher damages may be awarded, for offences and infringements involving the conversion of material into digital or electronic form.

DEVELOPMENT AND USE OF COAL WASHERY REFUSE FOR STRATA CONTROL IN COAL MINES

A thesis submitted in fulfilment of the requirements
for the award of the degree of

Doctor of Philosophy

from

THE UNIVERSITY OF WOLLONGONG

by



**JOHN KWONG LEE HII, CPEng., B.E.(Hons),
MIEAust., MAusIMM., MAPEA**

**DEPARTMENT OF CIVIL AND
MINING ENGINEERING**

1990

DECLARATION

This is to certify that the work presented in this thesis was carried out by the author in the Department of Civil and Mining Engineering, The University of Wollongong, and has not been submitted to any other university or institute for a Degree.

.....
JOHN KWONG LEE HII

LIST OF PUBLICATIONS

The following publications have appeared as a result of the present study:

- Hii, J.K. and Aziz, N.I., (1989a), Microcomputer Automation of the Strength Testing System for Use in a Rock Mechanics Laboratory, Australasian Instrumentation and Measurement Conference, The Institution of Engineers Australia, Adelaide, South Australia, 14th-16th November, pp. 51-55.
- Hii, J.K. and Aziz, N.I., (1989b), Influence of Water Content on the Mechanical Properties of Cement and Coal Washery Refuse Concrete, First Conference on Concrete and Structures, Malaysia, 3rd and 4th October, 1989, Kuala Lumpur, pp. 47-50.
- Hii, J.K. and Aziz, N.I., (1990), Properties and Behaviour of Cement and Coal Washery Refuse Concrete, Concrete for the Nineties, International Conference on the Use of Fly Ash, Slag, Silica Fume and Other Siliceous Materials in Concrete, Leura (Blue Mountains), New South Wales, Australia, 3rd-5th September, 15 Pages.
- Hii, J.K. and Standish, P., (1989), Data Acquisition Systems for Rock Mechanics Applications, Computer Systems in the Australian Mining Industry, The University of Wollongong, N.S.W., Australia, September, pp. 133-139.
- Hii, J.K., and Wu, Y.H., (1989), Effect of Virgin Stress Fields on the Feasibility of Using Yield Pillar Technique, Computer Systems in the Australian Mining Industry, The University of Wollongong, N.S.W., Australia, September, pp. 107-111.

Hii, J.K. and Yu, A.B., (1989), The Design of CCWR Concrete, First Conference on Concrete and Structures, Malaysia, 3rd and 4th October, Kuala Lumpur, pp. 51-56.

Hii, J.K., Aziz, N.I., Zhang S. and Wu, Y.H., (1990a), Influence of Geometry on Strength and Elasticity of Cement and Coal Washery Refuse Material Models, 3rd International Symposium on the Reclamation, Treatment and Utilization of Coal Mining Wastes, The Kelvin Conference Centre, Wolfson Hall, The University of Glasgow, UK, 3rd-7th September, 7 Pages.

Wu, Y.H., Hii, J.K. and Aziz, N.I., (1989), A New Yield Function for CCWR Concretes, First Conference on Concrete and Structures, Malaysia, 3rd and 4th October, Kuala Lumpur, pp. 173-176.

ACKNOWLEDGEMENTS

The author wishes to thank the many persons who have contributed to the completion of this thesis. Particular appreciation is extended to:

Professor L.C. Schmidt, Head of the Department of Civil and Mining Engineering, The University of Wollongong, for the provision of laboratory facilities and financial support which enabled this work to be carried out.

Dr. N.I. Aziz and Professor R.N. Singh for their suggestions and encouragement during the course of this investigation.

Associate Professor Y.C. Loo, Associate Professor R.W. Upfold, Dr. I. Porter, Dr. V.U. Nguyen and Dr. E.Y. Baafi for their interest in this study and for numerous stimulating discussions.

Staff of the Department of Civil and Mining Engineering, The University of Wollongong and Australian Coal Industry Research Laboratories, Bellambi for their help and advice throughout the course of this thesis.

Dr. R.D. Lama, Manager, Technology and Development, Kembla Coal and Coke Pty. Ltd. for his helpful suggestions in the course of this work.

Mr. Y.H. Wu, Mr. A.B. Yu and Mr. S.A. Lowe for their help and encouragement.

Mr. S. Zhang and Mr. C.C. Choo for their suggestions and encouragement.

All members of the author's family and special acknowledgement is due to his parents for their constant support and encouragement throughout the years.

This research investigation was sponsored in part by Kembla Coal and Coke Pty. Ltd. and in part by grants from The University of Wollongong. The collaboration and financial assistance of Kembla Coal and Coke Pty. Ltd. and The University of Wollongong are sincerely appreciated.

TO DOMINIQUE PAULINE OEI

FOR HER LOVE AND SUPPORT

ABSTRACT

This work involves the development and analysis of a new pump packing material, which utilizes coal washery refuse (CWR) as a raw material, for strata control in underground coal mining operations. A review on the state of the art of pump packing systems is presented, together with an analysis of the cost effectiveness of the new pump packing material as compared to other commercial pump packing materials.

A method is proposed for use in the design of cement and coal washery refuse (CCWR) material mixes to give a required early strength and degree of workability when incorporating CWR. The usefulness of the method is shown by comparison of the results from a large number of tests on CCWR specimens with previously published results. It is shown that the relationship between the strength and curing time of a mix can be accurately described by a simple equation. The effects of the compositions on the strength within the experimental regions are discussed. As expected an increase in the strength of CCWR materials can be obtained either by decreasing the water content or increasing the quantity of OPC used in the mixtures.

This study also investigated the influence of moisture content on the mechanical properties of CCWR material. The unconfined compressive strength, Young's modulus, indirect tensile strength, triaxial strength and drying shrinkage were the primary properties investigated. Results indicate that the moisture content has a significant effect on both the strength and elasticity of CCWR material at all curing times. It is evident from the tests that the drying shrinkage of wet mixes is larger than that of dry mixes. In general, moisture content affects the shrinkage of CCWR material as it reduces the volume of the restraining CWR.

An empirical criterion is proposed for predicting the strength and yield characteristics of CCWR materials. A numerical procedure has been developed to determine the parameters contained in the proposed yield function. It has been demonstrated that the proposed logarithmic yield function can accurately predict the strength and yield characteristics of CCWR materials.

Preliminary tests have also been conducted to determine the influence of moisture content on the flow properties of CWR. The test results indicate that the presence of very fine grains in CWR enhances its flowability remarkably.

Further work investigated the effect of specimen geometry on the strength and elasticity of CCWR material. CCWR models were tested, simulating underground monolithic pack support with different widths in a coal seam of uniform height. The study also investigated the load deformation characteristics of CCWR models under the tests conditions. It is shown that geometry has a significant effect on both the mechanical properties and load deformation characteristics of CCWR models.

A yield pillar technique analysed by the finite element method appears suitable for simulation of excavation of roadways under different virgin stress conditions. Comparison of stability of yield and conventional pillars in several examples substantiates the feasibility of the technique and indicates that yield pillars are practical when the factor k , the ratio of horizontal to vertical stress exceeds 1.6.

TABLE OF CONTENTS

CHAPTER		PAGE
	Title page	(i)
	Declaration	(ii)
	List of Publications.....	(iii)
	Acknowledgements	(v)
	Abstract	(viii)
	Table of Content	(x)
	List of Figures	(xvii)
	List of Tables	(xxvi)
	List of Abbreviations	(xxxii)
	Notation	(xxxii)
1	INTRODUCTION	1-1
2	MONOLITHIC PUMP PACKING SYSTEMS ...	2-1
	2.0 Introduction	2-1
	2.1 Types of Pump Packing System	2-1
	2.2 History of Waste Packing	2-2
	2.3 Application of Monolithic Pump Packing Systems in Australian Underground Coal Mines	 2-7
	2.4 Properties of Pump Packing Materials	2-20
	2.4.1 Thyssen	2-22
	2.4.2 Warbret	2-23
	2.4.3 Anhydrite	2-24
	2.4.4 Aquapak	2-25
	2.4.5 Tekpak	2-26
	2.4.6 Flashpak	2-27
	2.4.7 Tailings pak	2-28
	2.4.8 Monier 'Big Bag'	2-29
	2.5 Survey of the Types of Packing Materials Used in the Southern Coalfields	 2-30
	2.6 Summary	2-33

CHAPTER		PAGE
3	THEORETICAL CONSIDERATIONS.....	3-1
3.0	Introduction	3-1
3.1	Principles of Pump Packing	3-1
3.1.1	Purpose of pump packing.....	3-1
3.1.2	Detached block theory	3-2
3.1.3	Roof beam tilt theory	3-4
3.1.4	Practical requirements for the use of pump packing	3-5
3.1.5	Longwall strata behaviour and the generation of pack load	3-5
3.1.6	Basic requirements	3-7
3.1.6.1	Short term support requirements	3-7
3.1.6.2	Long term support requirements	3-8
3.2	Suitability of Pump Packing under Australian Conditions with Special Reference to the Bulli Seam	3-10
3.3	Development of CCWR Material for Strata Control	3-12
3.3.1	Design of CCWR material	3-12
3.3.2	Correlation of the strength and the curing time	3-12
3.3.3	Optimum design of CCWR material	3-18
3.4	Application of the Experimental Design with Mixtures	3-23
3.5	Development of a New Yield Function for CCWR Material	3-27
3.5.1	General form of the yield function	3-27
3.5.2	Determination of parameters in the yield function	3-28

CHAPTER		PAGE
	3.5.3 The procedure for the computation of parameters A, B and C	3-30
4	EXPERIMENTAL INVESTIGATIONS	4-1
	4.0 Introduction	4-1
	4.1 Material Used in the Experiments	4-2
	4.1.1 Sampling and collection of CWR	4-2
	4.1.2 Processing of CWR.....	4-4
	4.1.3 Grain size analysis of CWR using mechanical method.....	4-5
	4.1.4 X-ray diffraction analysis	4-6
	4.1.5 Ordinary Portland cement	4-7
	4.1.6 Calcium chloride	4-9
	4.2 Outline of the Experimental Programme	4-10
	4.3 Experimental Equipment	4-14
	4.3.1 Strength testing system	4-14
	4.3.2 Instron 8033 testing machine	4-15
	4.3.3 Data acquisition system components	4-17
	4.3.4 Device dependence of strain measurements of CCWR material specimens	4-21
	4.3.5 Experimental apparatus for flow tests of CWR	4-22
	4.4 Experimental Procedures	4-23
	4.4.1 Test specimens identification coding	4-23
	4.4.2 Design and construction of sample moulds	4-24
	4.4.3 Sample preparation	4-24
	4.4.4 Mixing of concrete	4-25

	PAGE
4.4.4.1 Batch size	4-25
4.4.4.2 Mixer	4-25
4.4.4.3 Charging sequence	4-25
4.4.5 Pouring of CCWR material specimens..	4-26
4.4.6 Curing of CCWR material specimens ...	4-28
4.4.7 Observations of the physical appearance of various CCWR material mixes	4-29
4.4.8 CCWR test specimen bulk density determination	4-29
4.4.9 Determination of the grain mass M_s of CCWR specimens	4-30
4.4.10 Method for measuring the physical properties of CCWR specimens	4-31
4.4.11 Method for determining the sound (sonic) velocity of CCWR specimens	4-31
4.4.12 Strength test procedures	4-33
4.4.12.1 Unconfined compressive strength tests	4-33
4.4.12.2 Indirect tensile strength tests	4-36
4.4.12.3 Triaxial strength tests	4-37
4.4.13 Experimental technique for flow tests of CWR	4-38
4.4.14 Testing procedures for flow tests of CWR	4-39
4.5 Mechanical Properties Evaluation of CCWR Material	4-41
4.6 Effect of Water Content on the Mechanical Properties of CCWR Material	4-41
4.7 A New Yield Function for CCWR Material	4-43

CHAPTER	PAGE
4.8	Effect of Water Content on the Flow Properties of CWR 4-43
4.9	Effect of Geometry on the Properties and Behaviour of CCWR Material Models 4-44
5	EXPERIMENTAL RESULTS AND DISCUSSION 5-1
5.0	Introduction 5-1
5.1	Effect of Crushing on the Grain Size Distribution of Minus 10mm CWR 5-1
5.1.1	Discussion and conclusions drawn from sieve analyses 5-2
5.2	Results from X-ray Diffraction Analyses and Discussion 5-5
5.3	Mechanical Properties Evaluation of CCWR Material 5-9
5.3.1	Unconfined compressive strength test results 5-10
5.3.2	Triaxial strength test results 5-15
5.3.3	Brazilian test results 5-37
5.3.4	Sonic velocity values measured during curing 5-37
5.3.5	Moist weight values measured during curing 5-42
5.3.6	Observations and analyses of CCWR specimen behaviour 5-42
5.3.6.1	Physical properties of CCWR specimens 5-42
5.3.6.2	Specimen failure modes ... 5-44
5.3.7	Discussion of results 5-44

CHAPTER		PAGE
	5.3.7.1 Mechanical properties of CCWR specimens	5-46
	5.3.7.2 CCWR pack characteristics in relation to strata behaviour	5-48
5.4	Effect of Water Content on the Mechanical Properties of CCWR Material	5-49
	5.4.1 Effect of water content on the drying shrinkage of CCWR material	5-54
5.5	A New Yield Function for CCWR Material	5-59
5.6	Effect of Water Content on the Flow Properties of CWR	5-63
	5.6.1 Slump test results	5-63
	5.6.2 Flow test results	5-66
	5.6.3 Discussion of flow test results.....	5-66
5.7	Effect of Geometry on the Properties and Behaviour of CCWR Material Models	5-69
	5.7.1 Effect of geometry on the strength of CCWR material models	5-75
	5.7.2 Effect of geometry on the axial modulus of CCWR material models	5-76
	5.7.3 Effect of geometry on the Poisson's ratio of CCWR material models	5-77
	5.7.4 Effect of geometry on the stiffness of CCWR material models	5-77
	5.7.5 Discussion of test results	5-78
6	ALTERNATIVE METHOD OF IMPROVING GATEROAD STABILITY USING YIELD PILLAR TECHNIQUE	6-1
	6.0 Introduction	6-1

CHAPTER	PAGE
6.1 Review of Past Work	6-2
6.1.1 Stress control methods	6-4
6.2 Theoretical Considerations of Stress Control Design	6-5
6.3 Effect of Virgin Stress Fields on the Feasibility Study of Yield Pillar Technique	6-8
6.3.1 Method of analysis	6-9
6.3.2 Computation of stresses in pillars	6-9
6.3.3 Determination of factor of safety	6-16
6.3.4 Scheme of analysis	6-16
6.4 Results and Discussion	6-18
6.5 Conclusions	6-22
7 CONCLUSIONS	7-1
BIBLIOGRAPHY	R-1
APPENDIX I PROGRAM PRINTOUT	AI-1
APPENDIX II EXPERIMENTAL DATA	AII-1
1. Sieve Analysis Results	AII-1
2. Sonic Velocity Data	AII2-1
3. Specimens Moist Weight Data	AII3-1
4. Calculated Compressive Strength Test Results and Specimen Experimental Data	AII4-1
5. Post-Failure Modulus and Residual Strength Results	AII5-1
6. Plots of Sonic Velocity and Strength Relationships of CCWR specimens	AII6-1
7. Flow Test Results	AII7-1

LIST OF FIGURES

LIST OF FIGURES

FIGURE	TITLE	PAGE
2.1	Use of Monier "Big Bag" chocks as Longwall gateroad support at Appin Colliery	2-8
2.2	Wooden crib roadway support at South Bulli Colliery	2-10
2.3	Proposed pump pack support system	2-11
2.4	Typical single pass wide heading layout	2-12
2.5	Typical double pass wide heading layout	2-13
2.6	Centre roadway packwall	2-14
2.7	Monier 'Big Bag' supports	2-15
2.8	Side roadway packwall	2-15
2.9	Maingate packwall	2-16
2.10(a)	Concept of single entry dividing wall - driveage layout	2-16
2.10(b)	Concept of single entry dividing wall - partial extraction by Longwall with single entry	2-17
2.11	Advancing Longwall Panel	2-17
2.12	Shortwall entry driveage system with pump packing	2-18
2.13	Shortwall extraction system with pump packing, no development is required	2-19

LIST OF FIGURES

FIGURE	TITLE	PAGE
2.14	Kemcol Beaver with pump packing	2-19
2.15	Uniaxial compressive strength of cement based materials and industry by products	2-22
2.16	Layout of wooden chock installations per 60m of Longwall 6 gateroads at Tahmoor Colliery	2-32
3.1	"Big Bag" chocks at West Cliff Colliery	3-3
3.2	Detached block theory	3-3
3.3	Generalised view of roof tilt	3-4
3.4	Floor heave problem	3-9
3.5	Support failure leads to excessive roof to floor closures	3-10
3.6	Plots of the measured strength against curing time for each mix	3-14
3.7	Comparison between calculated and measured strength	3-16
3.8	Plots of $\ln S$ against $1/\sqrt{t}$ for mixes 2 through 5	3-16
3.9	Plots of $\ln S$ against $1/\sqrt{t}$ for mixes 1, 7, 8, 11, 12 and 13	3-17
3.10	Plots of $\ln S$ against $1/\sqrt{t}$ for mixes 6, 9 and 10	3-17
3.11	Plots of $\ln S$ against $1/\sqrt{t}$ for mixes 14 through 17	3-18

LIST OF FIGURES

FIGURE	TITLE	PAGE
3.12	Comparison between the measured strength and the calculated (by eqns 13 and 14) strength	3-21
3.13	Final strength contour plots	3-22
3.14	Contour plots for 28 day strength	3-22
3.15	The dependence of the strength on R1 for different R2 (28 day strength)	3-24
3.16	The dependence of the strength on R1 for different R2 (Final strength)	3-24
3.17	The dependence of the strength on R2 for different R1 (28 day strength)	3-25
3.18	The dependence of the strength on R2 for different R1 (Final strength)	3-25
3.19	Flow chart for logarithmic yield function program	3-31
4.1	Model of West Cliff Coal Washery	4-3
4.2	Collection of CWR sample	4-3
4.3	Typical grain shapes of West Cliff CWR	4-5
4.4	Grain shapes of West Cliff CWR	4-6
4.5	Grain size distribution curves of the processed CWR	4-7

LIST OF FIGURES

FIGURE	TITLE	PAGE
4.6	The servo controlled stiff testing machine	4-15
4.7	A closed loop servo block diagram	4-16
4.8	The interface of LVDT and HP data acquisition and control system	4-17
4.9	Flow chart for the LVDT program	4-19b
4.10	The interface of strain gauges and HP data acquisition and control system	4-21
4.11	Schematic of the flow-tube experimental apparatus	4-23
4.12	CCWR material specimen moulds	4-24
4.13	'Bennett' Mixer	4-25
4.14	Slump test	4-27
4.15	'ICAL Syntron Packer, Model VP65B'	4-28
4.16	Simplified 'Pundit' system diagram	4-32
4.17	'Pundit' sonic velocity apparatus	4-33
4.18	CCWR material specimen mounted in the LVDT strain measurement rig during the unconfined compressive strength test	4-35
4.19	LVDT strain measurement rig	4-35

LIST OF FIGURES

FIGURE	TITLE	PAGE
4-20	Indirect tensile strength (Brazilian) test rig	4-37
4-21	Triaxial cell applied to the LVDT strain rig	4-38
5.1	The grain size distribution curve of CWR before processing ...	5-4
5.2	The grain size distribution curve of CWR after processing	5-5
5.3	Plots of the measured strength against curing time for mixes 1 to 5	5-13
5.4	Stress-curing time curves of various mixes of CCWR specimens for up to 5 hours curing time	5-13
5.5	Stress-curing time curves of mixes 2 to 5 CCWR specimens for up to 24 hours curing time	5-14
5.6	Triaxial strength test results for CCWR specimens at different confining pressure (15.6% cement, mix 1)	5-22
5.7	Triaxial strength test results for CCWR specimens at different confining pressure (12.5% cement, mix 2)	5-22
5.8	Triaxial strength test results for CCWR specimens at different confining pressure (10.0% cement, mix 3)	5-23
5.9	Triaxial strength test results for CCWR specimens at different confining pressure (7.5% cement, mix 4)	5-23
5.10	Triaxial strength test results for CCWR specimens at different confining pressure (5.0% cement, mix 5)	5-24

LIST OF FIGURES

FIGURE	TITLE	PAGE
5.11	Peak strength Mohr's envelopes for 15.0%C-21.0%W mix....	5-25
5.12	Peak strength Mohr's envelopes for 15.0%C-14.7%W mix....	5-26
5.13	Peak strength Mohr's envelopes for 12.5%C-19.1%W mix....	5-27
5.14	Peak strength Mohr's envelopes for 12.5%C-16.5%W mix....	5-28
5.15	Peak strength Mohr's envelopes for 12.5%C-13.0%W mix....	5-29
5.16	Peak strength Mohr's envelopes for 10.0%C-19.1%W mix....	5-30
5.17	Peak strength Mohr's envelopes for 10.0%C-16.5%W mix....	5-31
5.18	Peak strength Mohr's envelopes for 7.5%C-19.1%W mix.....	5-32
5.19	Peak strength Mohr's envelopes for 7.5%C-16.5%W mix....	5-33
5.20	Peak strength Mohr's envelopes for 7.5%C-12.6%W mix....	5-34
5.21	Peak strength Mohr's envelopes for 5.0%C-13.0%W mix....	5-35
5.22	Peak strength envelope of CCWR specimens for mixes 1 to 5	5-36
5.23	Peak strength envelope of CCWR specimens for mixes 7, 8, 10, 11, 12 and 13	5-36
5.24	Small axial cracks appeared just before the maximum compressive strength was reached - indicating tensile cleavage failure	5-45

LIST OF FIGURES

FIGURE	TITLE	PAGE
5.25	A typical hour glass failure shape	5-45
5.26	Shear cone with splitting above	5-46
5.27	Effect of nominal water content on the strength of CCWR specimens at different curing time (15% OPC)	5-52
5.28	Effect of nominal water content on the strength of CCWR specimens at different curing time (12.5% OPC)	5-52
5.29	Effect of nominal water content on the strength of CCWR specimens at different curing time (10% OPC)	5-53
5.30	Effect of nominal water content on the strength of CCWR specimens at different curing time (7.5% OPC)	5-53
5.31	The effect of water content on the drying shrinkage of CCWR specimens	5-59
5.32	Measured and predicted triaxial strengths of CCWR mix 1	5-62
5.33	Measured and predicted triaxial strengths of CCWR mix 2	5-62
5.34	Measured and predicted triaxial strengths of CCWR mix 4	5-63
5.35	Effect of water content on the slump values of CWR	5-65
5.36	A comparison of the flowability of CWR for all mixes at different slopes	5-68
5.37	Effect of water content on the flowability of CWR	5-69

LIST OF FIGURES

FIGURE	TITLE	PAGE
5.38	Effect of geometry on the unconfined compressive strength of CCWR material models	5-75
5.39	Effect of geometry on the axial modulus of CCWR material models	5-76
5.40	Effect of geometry on the Poisson's ratio of CCWR material models	5-77
5.41	Effect of geometry on the stiffness of CCWR material models	5-78
5.42	CCWR models with distinct shear plane at complete failures (diameter=55.5mm).....	5-80
5.43	CCWR models at complete failures (diameter=75.5mm).....	5-81
5.44	CCWR models at complete failures (diameter=102.8mm).....	5-81
5.45	CCWR models at complete failures (diameter=149.5mm).....	5-82
5.46	CCWR models at complete failures (diameter=206mm).....	5-82

LIST OF FIGURES

FIGURE	TITLE	PAGE
5.47	CCWR models at complete failures (diameter=242mm).....	5-83
5.48	CCWR models at complete failures (diameter=314.5mm).....	5-83
5.49	Various CCWR models at complete failures (Elevation A).....	5-84
5.50	Various CCWR models at complete failures (End elevation B)..	5-84
5.51	Various CCWR models at complete failures (End elevation C)..	5-85
6.1	Principle of stress control method	6-6
6.2	Formation of Pillar A	6-10
6.3	Flow chart of the iterative scheme	6-15
6.4	Finite element mesh for yield pillar scheme	6-17
6.5	Principal stress field in the yield pillar scheme	6-19
6.6	Principal stress field in the conventional pillar scheme	6-19
6.7	Distribution of stress along a cross-section of pillar	6-20
6.8	Safety factor versus k (σ_{oh}/σ_{ov})	6-21

LIST OF TABLES

LIST OF TABLES

TABLE	TITLE	PAGE
2.1	Survey of the distribution of monolithic pump packing systems in the United Kingdom	2-3
2.2	Cost and pipeline pumping life of tailings pak 2 (UK)	2-20
2.3	Cost and pipeline pumping life of packing materials for various pump pack systems	2-21
2.4	Thyssen material properties	2-23
2.5	Warbret material properties	2-24
2.6	Anhydrite material properties	2-24
2.7	Aquapak material properties	2-25
2.8	Tekpak material properties	2-26
2.9	Flashpak material properties	2-27
2.10	Tailings pak material properties	2-28
2.11	CCWR material properties	2-29
2.12	Australian Monier "Big Bag" material properties	2-30
2.13	Types of packing materials used in the Southern Coalfields ...	2-31
3.1(a)	Measured unconfined compressive strength of CCWR materials at different curing times	3-13a

LIST OF TABLES

TABLE	TITLE	PAGE
3.1(b)	Measured unconfined compressive strength of CCWR materials at different curing times	3-13b
4.1	Physical properties of oil samples	4-4
4.2	Chemical and mineralogical compositions of Type A Portland cement	4-8
4.3	Summary of tests	4-12
4.4(a)	Batching and pouring details of various mixes of CCWR materials	4-13a
4.4(b)	Batching and pouring details of various mixes of CCWR materials	4-13b
4.5	Descriptions of the physical appearance of various CCWR material mixes	4-30
5.1	The grain size distribution of CWR before processing	5-3
5.2	The grain size distribution of the processed CWR	5-3
5.3	Chemical compositions of West Cliff CWR	5-7
5.4	Average major geomechanical compounds in fine discards (UK)	5-8
5.5	Chemical composition of coal preparation wastes for four main coalfields of the Soviet Union	5-9

LIST OF TABLES

TABLE	TITLE	PAGE
5.6(a)	Summary of results of compressive strength tests	5-11
5.6(b)	Summary of results of compressive strength tests	5-12
5.7	Results of triaxial tests for CCWR material specimens (mixes 1 through 3)	5-16
5.8	Results of triaxial tests for CCWR material specimens (mixes 4 and 5)	5-17
5.9	Results of triaxial tests for CCWR material specimens (mixes 7 through 8)	5-18
5.10	Results of triaxial tests for CCWR material specimens (mixes 10 and 11)	5-19
5.11	Results of triaxial tests for CCWR material specimens (mixes 12 and 13)	5-20
5.12	Summary of triaxial test results for CCWR specimens	5-21
5.13	Results of Brazilian tests for CCWR material specimens (mixes 3 through 5)	5-38
5.14	Results of Brazilian tests for CCWR material specimens (mixes 7 through 8)	5-39
5.15	Results of Brazilian tests for CCWR material specimens (mixes 10 through 11)	5-40
5.16	Results of Brazilian tests for CCWR material specimens (mixes 12 through 13)	5-41

LIST OF TABLES

TABLE	TITLE	PAGE
5.17	Physical properties of CCWR specimens for different mixes ...	5-43
5.18	Effect of water content on the unconfined compressive strength of CCWR materials at different curing times	5-50
5.19	Effect of water content on the unconfined compressive strength of CCWR materials at different curing times	5-51
5.20	Drying shrinkage values for 15.0%C-12.0%W specimens	5-55
5.21	Drying shrinkage values for 15.0%C-21.0%W specimens	5-55
5.22	Drying shrinkage values for 12.5%C-16.5%W specimens	5-56
5.23	Drying shrinkage values for 12.5%C-19.1%W specimens	5-56
5.24	Drying shrinkage values for 10.0%C-12.0%W specimens	5-57
5.25	Drying shrinkage values for 10.0%C-19.1%W specimens	5-57
5.26	Drying shrinkage values for 7.5%C-16.5%W specimens	5-58
5.27	Drying shrinkage values for 7.5%C-19.0%W specimens	5-58
5.28	Comparisons of predicted and measured values for various CCWR materials	5-60
5.29	Slump test results of CWR	5-64

LIST OF TABLES

TABLE	TITLE	PAGE
5.30	Results of compressive strength testing for series VI experiments (Effect of geometry on the strength and elasticity properties of CCWR material models with diameters of 55.5mm and 75.5mm)	5-70
5.31	Results of compressive strength testing for series VI experiments (Effect of geometry on the strength and elasticity properties of CCWR material models with diameters of 102.8mm and 149.5mm)	5-71
5.32	Results of compressive strength testing for series VI experiments (Effect of geometry on the strength and elasticity properties of CCWR material models with diameters of 206mm and 242mm)	5-72
5.33	Results of compressive strength testing for series VI experiments (Effect of geometry on the strength and elasticity properties of CCWR material model with a diameter of 314.5mm)	5-73
5.34	Summary of results of compressive strength testing for series VI experiments (Effect of geometry on the strength and elasticity properties of CCWR material models)	5-74
6.1	Virgin stress fields	6-17
6.2	Properties of rocks	6-18

LIST OF ABBREVIATIONS

ACIRL	Australian Coal Industrial Research Laboratories Ltd.
CCWR	Cement and Coal Washery Refuse
CWR	Coal Washery Refuse
KCC	Kembla Coal and Coke Pty. Ltd.
MG	Main Gate
MPPS	Monolithic Pump Packing System
MRDE	Mining Research and Development Establishment
NCB	National Coal Board
NERDDC	National Energy Research, Development and Demonstration Council
NSW	New South Wales
OPC	Ordinary Portland Cement
PFA	Pulverised Fly Ash
ROM	Run of Mine
TEA	Triethanolamine
TG	Tail Gate
UK	The United Kingdom
USA	The United States of America

NOTATION

A and B	unknown positive parameters (for Section 3.3);
A, B, C	parameters to be considered by experiments (for Section 3.5);
$[B]$	the derivative matrix of $[N]$;
β	the slope of stress - diametric strain curve of CCWR model;
C	cohesive strength;
$[D], [D_{ep}]$	the elasticity matrix and elastic-plastic matrix respectively;
$\delta u, \delta \epsilon$	the virtual displacements and the corresponding strain in domain Ω respectively;
$\{\Delta a\}$	the vector of nodal displacement increments;
$\{\Delta \sigma_o\}$	the initial stress increment;
Δb_v	the increment of body force;
$[\Delta F_o]$	the iterative term of the nodal force;
$[\Delta F_v]$	the nodal force due to the increment of the body force;
$[\Delta F_\tau]$	the boundary traction;
Δp	the increment of boundary traction;
$\Delta \sigma_A$	the increment of stress in the pillar due to the excavation of Roadways 1 and 2;
E_{ps}	denotes the allowable tolerance;
$f(t)$	a monotone increasing function of t ;
ϕ	angle of internal friction;
Γ	boundary of the domain Ω ;
Γ_e	boundary element;
$[K]$	the stiffness matrix;
k	ratio of σ_{oh}/σ_{ov}

k, m, n	unknown parameters;
n	a constant for any mix formulation;
N	number of triaxial tests;
$[N]$	the matrix of specified shape functions;
Ω	domain;
Ω_e	elements connected at the nodes;
Q	the error of prediction;
R_1	the ratio of $X_1/(X_3 + X_4)$;
R_2	the ratio of X_3/X_4 ;
S	unconfined compressive strength of CCWR specimens;
SF	the safety factor;
S_{28}	unconfined compressive strength of CCWR specimens at 28 day curing time;
S_{final}	final unconfined compressive strength of CCWR specimens;
σ_A	the redistributed stress in the pillar;
σ_{A0}	the virgin stress determined by in-situ stress measurement;
σ_{oh}	horizontal virgin stress;
σ_{ov}	vertical virgin stress;
σ_c	unconfined compressive strength;
σ_1	major principal stress;
σ_3	minor principal stress;
$\sigma_{1i} (\sigma_{3i})$	predicted major principal stress under minor principal stress σ_{3i} condition;

$\sigma_{1i}^* (\sigma_{3i})$	experimental major principal stress under minor principal stress σ_{3i} condition;
σ_{3i}	minor principal stress;
$\sigma_s (\sigma_3)$	the strength of the rock, which is the function of σ_3 ;
t	curing time of CCWR specimens;
X_1	mass percentage of water;
X_2	mass percentage of calcium chloride accelerator;
X_3	mass percentage of ordinary Portland cement;
X_4	mass percentage of coal washery refuse;
X_i	the proportion of the i'th component in the mixture.

CHAPTER ONE

INTRODUCTION

CHAPTER 1

INTRODUCTION

The main theme of this thesis is the development of a pump packing material, which utilizes coal washery refuse (CWR), for strata control in Australian underground coal mining operations. The thesis is also intended to provide an introduction to the current state of the art design principles, applications and some on-going research activities of pump packing for both mine operators and researchers interested in pump packing technology, as well as providing to others a general understanding of how cement and coal washery refuse (CCWR) material can be used for strata control in coal mines.

An attempt is made to critically assess the present state of knowledge in the development and utilization of CWR as a pump packing material in Australian underground coal mines, and understand the importance of the research in relation to future field application. It is anticipated that the contribution made with regard to the treatment and utilization of wastes from the coal washery will play a major role in future mine planning as a result of the increasing importance of environmental issues; such as the disposal of CWR and surface subsidence.

In New South Wales, Australia, the raw coal production in the year 1987-1988 alone was 76.3 million tonnes of which 12.3 million tonnes was extraneous dirt. According to NSW Government (1983), it is estimated that by the year 2000, the existing and planned coal mining activities could generate some 104 million tonnes of CWR in the Southern Coalfields alone, while the existing and planned surface emplacements have a capacity for only 30 million tonnes of CWR. There is

a need for a full study of the problems associated with the generation, utilization and disposal of CWR in this state. The disposal of CWR in particular was considered to be a significant economic and environmental issue which needed to be resolved as a matter of urgency in the Illawarra region. It is anticipated that similar problems may be faced in other coalfields (NSW Government, 1983).

At present, there is a growing interest in the utilization of wastes from the coal washery, both as cementing medium and aggregate, for the construction of monolithic pump pack (McCarthy and Robinson, 1981, Richmond et al, 1985, Thomas, 1986, Atkins et al, 1984, 1986, 1987, Hii and Aziz, 1986a, 1986b, 1987a, 1987b, 1987c, 1987d, 1989, Zadeh et al, 1987, Hii and Yu, 1989). In recent years the potential use of CWR has also been investigated.

Apart from the expensive commercial materials for pump packing, the utilization of CWR would have a two-fold advantage in costs reduction. There would be a reduction in both the dirt disposal costs and commercial materials costs. Much work however needs to be done in this field since many problems are being experienced in obtaining a consistent mix owing to the variation in products from the coal washery.

In order to substitute the expensive commercial materials for pump packing, it is necessary to improve its geotechnical characteristics. A comprehensive laboratory testing programme was therefore devised to investigate the geotechnical properties of CWR as a function of various cement mixes over a 365 day period. The research programme aims at producing the most cost effective and economical monolithic pump packing system for strata control and increased recovery of coal.

The investigation also aims: to optimize particular mechanical properties of CCWR materials, to develop a cheaper binding material, to increase the initial

strength of the mixture, and to develop a material which is pumpable but can still give sufficient strength for use as a pack material in Australian underground coal mining operations. The study also investigates the effect of water content on the mechanical properties and behaviour of CCWR material containing calcium chloride admixture.

The effect of water content on the flow properties of CWR is also examined. The objective of this study was to determine the optimum water content for flowability of CWR. The test results from consistency measurements and flow tests are used to characterize the flow properties of minus 10mm CWR with different nominal water contents.

Cost-effective analysis of CCWR pump packing material as compared to other commercial pump packing materials has been carried out.

A method is proposed for use in the design of CCWR material mixes. It has been demonstrated that the relationship between the strength and curing time of a mix can be accurately described by a simple equation. Based on the results of laboratory strength tests, empirical equations were formulated to correlate the strength of a mix to the composition of the mix through regression analysis. The procedure for determining the parameters contained in the proposed empirical equations is presented in Chapter 3 (Section 3.3). It is substantiated that an increase in the strength of CCWR materials may be acquired either by decreasing the water content or increasing the quantity of OPC utilized in the mixtures.

An empirical criterion is also proposed for predicting the strength and yield characteristics of CCWR material. The parameters contained in the yield function have been determined from routine material strength test results. A procedure for the determination of the parameters is presented in Sections 3.5.1 and 3.5.2 (Chapter

3). The logarithmic yield function program, written in FORTRAN, has been developed to facilitate data processing of test results and a listing of the fundamental FORTRAN code is given. The study has indicated that the proposed logarithmic yield function can predict the strength and yield characteristics of CCWR material in a satisfactory manner.

Research is required to understand the tectonic forces which prevail in Australian mining conditions. The research work in turn could help in selecting the most effective pump packing systems. The following basic works on strata movement that have been conducted are:

- (i) the understanding of the nature of load/deformation characteristics (ground reaction curves) of the areas where pump packing system is intended for support;
- (ii) the evaluation of the strength and deformation characteristics of various pump packing materials;
- (iii) the selection of a suitable pump packing material based on the strength and cost; and
- (iv) an examination of the pump packing material characteristics in relation to strata behaviour.

Further work investigated the influence of specimen geometry and end constraint on the strength and elasticity of CCWR material. The feasibility of the yield pillar technique under different virgin stress field conditions in underground mining operations is also investigated.

CHAPTER TWO

MONOLITHIC PUMP PACKING SYSTEM

CHAPTER 2

MONOLITHIC PUMP PACKING SYSTEMS

2.0 INTRODUCTION

This Chapter presents a literature review of monolithic pump packing systems with particular reference to their applications in the United Kingdom, Germany and Australia. A review of the current state of the art design principles and some on-going research activities of monolithic pump packing systems is also included. Monolithic pump packing technologies which include the development of pack materials, pack design principles, manpower and cost for pack installations, pack material handlings and pack constructions have been reported previously (McCarthy, 1974, Farmer and Robertson, 1975, Hodgkinson, 1977, Whittaker and Woodrow, 1977, Lewis and Stace, 1981, Richmond, 1981, Smart et al, 1982, Freeman, 1982, Buddery, 1984, Clark and Newson, 1985, Batten, 1985, Richmond et al, 1985, Hii and Aziz, 1986). Attention is focused on the history and technology of waste packing and the properties of pump packing materials.

2.1 TYPES OF PUMP PACKING SYSTEM

Common types of pump packing systems which have been used in coal mines include the following:

- (i) Anhydrite system (first used in 1964);
- (ii) Thyssen system (first used in 1973);
- (iii) Warbret system (first used in 1976);

(iv) Monolithic pump packing systems using:

- (a) Aquapak;
- (b) Tekpak;
- (c) Flashpak; and
- (d) Mine tailings.

Clark and Newson (1985) presented a statistics on the current distribution of monolithic pump packing systems in Britain (Table 2.1). It is noted that the number of Tekpak installations was significant. This gave a good indication of the popularity and the unique properties of Tekpak installations.

2.2 HISTORY OF WASTE PACKING

Support of mine working in the form of waste packing underground has been practised as long as some form of pillar extraction has been adopted, more specifically in Longwall mining methods. Waste packing was initially confined to hand packing in the form of building walls constructed from roof stone and stone bands in the waste area. Hand packing was normally confined to strip packing, because of the lack of material for solid stowing.

Total stowing in the form of hydraulic placing of stowage material in the waste in mines was first reported about 1880. Although of unknown origin, the system was practised in both U.S.A. and Silesia in the year mentioned above. It was some 20 years later that hydraulic stowing was first used in coal mines in the UK (Harlech, 1925).

Table 2.1 Survey of the distribution of monolithic pump packing systems
in the United Kingdom
(after Clark and Newson, 1985)

Area	Installations	Aquapak		Tekpak		Thyssen		Others*
		M/G	T/G	M/G	T/G	M/G	T/G	
Scottish	11		3			7	4	
North East	Nil							
North York	Nil							
Doncaster	2	1	1					1
Barnsley	Nil							
South Yorks	3	1		1	1			
North Notts	Nil							
South Notts	9		2	5	2			
North Derby	1							3
South Mids	6	4	2			2	2	
Western	22	4	4	11	10	2	2	3
South Wales	7		1			4	3	
Total	60	23		30		26		7
				(Face Ends)				

*Other installations are:

Doncaster Area	-Synthetic Anhydrite	- 1 Face End
North Derby Area	-Warbret	- 3 Face Ends
Western Area	-Flash pack	- 1 Face End
Western Area	-GP7	- 2 Face Ends

(Pack Reinforcement)

The early fifties saw the emergence of mechanized dry pack "stowing" for roadside packing, with the main objective being strata control in roadways for advancing Longwall faces. This was soon followed by a new concept of roadway packing using monolithic packs constructed using some form of hydraulically

placed material. Anhydrite packing was the first type of monolithic packing system to emerge as a new method of waste-side packing. The first trial of the Anhydrite packing system was carried out at Holland Colliery, West Germany in 1964 (Heinrich, 1971, Recklinghausen et al, 1972). Following an initial success, the Anhydrite packing system gained wide acceptance in the Saar and Ruhr Coalfields. The advantages claimed were (Buddery et al, 1982):

- (i) improved gate road stability;
- (ii) improved face end ventilation, by preventing short circuiting of the airflow across the goaf;
- (iii) reducing the risk of spontaneous combustion in the goaf area.

Interest in the UK began in 1973, when a pump packing system was installed in Brynliw Colliery, South Wales. A detailed description of Thyssen system has been published previously (Hodgkinson, 1977). This system was developed by Thyssen (UK), and utilized up to 50%, -19mm run of mine (ROM) fines, the rest was made of a bentonite component (flowmat), and a cementing agent. However, it was soon realised that the system did not live up to expectations when applied to seams with high clay impurities. The swelling factor of clay present in the ROM material reduced the "pumpability" of the coal slurry to such a degree that the system required to be discontinued on some occasions. Furthermore, since coal constituted nearly half of the pack material, the system suffered in some cases from the effects of spontaneous combustion which could not be eliminated.

In 1976, the modified Warbret system was developed. According to Buddery and Ashika (1982), the likelihood of pipe blockages due to bleeding and segregation is diminished by pre-mixing the bentonite suspension so that gelling is complete before it is added to the aggregate, whereas, in the Thyssen system gelling

of the suspension takes place in the pipeline and hence is inhibited by the aggregate causing blockages.

The deficiencies in the Thyssen and Warbret systems prompted British Coal - formerly the National Coal Board (NCB) - to experiment with new products. This resulted in the development and introduction of the Aquapak system in 1979 (Nixon et al, 1982). The system, which contained a very high proportion of water was first tried at Hem Heath Colliery. The objective being to alleviate the disadvantages encountered by the coal slurry systems. The large quantity of water in the Aquapak material required the use of cement with a high affinity for water. Therefore, Monopak, which is basically a blend of three cementitious materials, was subsequently developed to suit the requirement. This was further helped by the incorporation of a thixotropic medium such as bentonite clay which kept the Monopak in suspension until it had set.

In Great Britain, by 1980, packing by mechanized methods was employed at some 20% of advancing face ends (Stokes and Kitching, 1980). About 55% of the systems used dirt collected insitu, 21% used ROM material only and 24% used ROM material with a cement additive.

In 1981, Australian Coal Industry Research Laboratories (ACIRL) investigated the use of monolithic pump packing as a means of underground roof support (Richmond, 1981). Also in 1981, Monier Resources Australia established their mining services section. They now have a market for "Big Bag" chocks which, when filled with their "Minegrout H" mix, provide load bearing capacities of up to 500 tonnes.

In 1983, there were 85 monolithic pump packed face end systems used in Britain, with monolithic pump packing system (MPPS) still providing the largest

single group and constituted some 10% of all advancing Longwall face end system (Clark and Newson, 1985). The material cost in 1983 was approximately \$85 per cubic meter. The total annual expenditure including the capital cost and material transportation cost was over \$15.4 million for 67,800 tonnes of material.

Continued research into the development of pump packing material led to the development of Tekpak. As with Aquapak, two materials are separately pumped in solution and then mixed in the packing bag to form a quick setting monolithic pack. The materials are Tekcem, which is based on high alumina cement and Tekbent which is a mixture of Bentonite and accelerators. The advantages claimed include: less use of solid materials in the pack construction in comparison to Aquapak (nearly 73% by weight of Aquapak); longer pumping life of the cement; hence less risk of pipe blockages; less risk of cement burns as Tekcem is less aggressive than Aquacem; and a lower cost of cement materials used.

Further studies by the Mining Research and Development Establishment (MRDE) of the British Coal, resulted in the development of a low cost product called Flashpak which could be used to form a satisfactory monolithic pack. The principle of the system consisted of pumping two grouts which when mixed in the packhole, formed a monolithic pack. The attractive property of Flashpak material is that when the two grouts are completely mixed together they form a gel, and hence Flashpak does not require a waterproof containing bag.

Finally, development work has already started on a new phase, that of using mine tailings and fly ash both of which are waste products. As well as improving gate road strata control, this type of packing has the added advantage of disposing of undesirable materials in a cost-effective manner (Atkins et al, 1984, Atkins et al, 1986).

National Energy Research, Development and Demonstration Council (NERDDC) has major on-going research and field investigation into the evaluation of cementitious support for increased recovery from coal mines (Richmond et al, 1985). NERDDC, in association with ACIRL, Monier Resources Ltd., The University of Wollongong and Kembla Coal and Coke (KCC) Pty. Ltd. initiated a research programme aimed at producing the most effective and economical method of monolithic pump packing system for strata control and increased recovery of coal.

2.3 APPLICATION OF MONOLITHIC PUMP PACKING SYSTEMS IN AUSTRALIAN UNDERGROUND COAL MINES

The Australian pump packing experience has been reported previously (Richmond, 1981, Todd, 1983, Schaller and Savidis, 1983, Richmond et al, 1985, Batten, 1985, Thomas, 1985, Hii and Aziz, 1986). It is evident that to date no Australian underground coal mine has used a bulk monolithic pump packing system for roadway support. The fact that all Australian underground Longwalls are retreating and not advancing (advancing Longwalls are used in UK) means that bulk monolithic pump packing has not been needed to support roadways behind the face on the goaf edge.

However, monolithic pump packing systems in the form of Monier "Big Bag" chocks have been used in an attempt to keep a goaf side return airway partially open back to the last cut through (Todd, 1983). Monier "Big Bag" chocks (1m diameter) were set at 4m centres in the roadway following the passage of the face as illustrated in Figure 2.1. The trial was a failure because before the next open cut through was reached the chocks had crushed out and subsequently the airway was lost to the goaf. The internal partitioning of the bag was recognised as an inherent

weakness, especially when controlling vertical as well as horizontal forces at the goaf edge. It was found that eight sections had induced cleavage planes into the bags and this was rectified in future Monier "Big Bag" chocks. It was realised that the failure of the grout to reach sufficient strength in the short time allowed and the wide spacings of single bags along the goaf edge indicated that too much had been expected of the system.

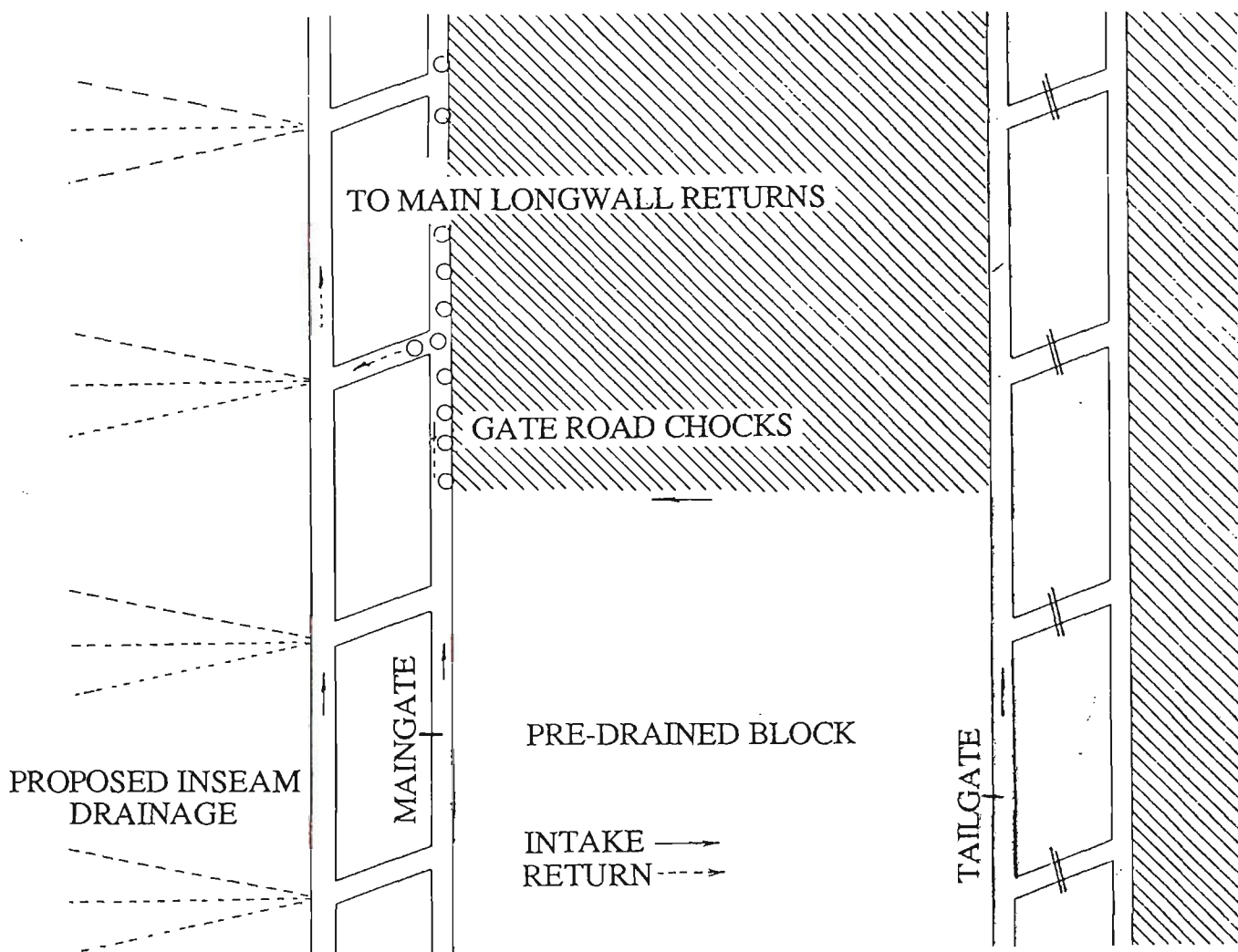


Figure 2.1 Use of Monier "Big Bag" chocks as Longwall gateroad support at Appin Colliery.

(after Todd, 1983)

The use of Monier "Big Bag" chocks has introduced several Australian underground coal mines such as South Bulli, West Cliff, Darke Forest and others to the material and technology used in monolithic pump packing systems. The properties of Monier "Big Bag" material will be reported in Section 2.4.8. A general review on the properties, the load/deformation behaviour, the availability and the cost of different Monier Minegrouts has been published previously (Batten, 1985).

In Australia, interest is now being shown in monolithic pump packing system utilizing wastes from power plants (flyash) and coal washeries (CWR). A pneumatic bulk handling system has been installed at West Cliff Colliery with the aim of constructing continuous lengths of monolithic pump pack support (using flyash and cement mixture) in Longwall gateroads. However, this has not been successful in terms of cost-effectiveness. The author and other researchers have been committed to the evaluation of CWR for disposal and strata control in underground coal mines. Results obtained thus far have been very encouraging.

Due to the need to continually maximize productivity levels in the Australian underground coal mining industry, several alternative Longwall panel layouts utilizing pump packing technology have been proposed by various researchers (Richmond, 1981, Hebblewhite, 1983, Richmond et al, 1985, Marshall and Lama, 1986, Lama, 1988). Some have the potential for increased development rate and/or improved recovery.

Richmond (1981) conducted a laboratory simulation of the insitu load-deformation characteristics of a wooden crib (chock) and compared the support capabilities of the wooden crib support system and the pump pack support system. Figure 2.2 illustrates the layout of the wooden crib support system for the tailgate of Longwall N at South Bulli Colliery. Figure 2.3 schematically shows the proposed pump pack support system. It was estimated that a 2m (weak) pump pack system

would offer approximately 20 times the maximum support load density provided by the wooden crib system. Richmond (1981) reported that in addition to the significantly higher support capacity of the pump pack system it would also offer a stiffer support.

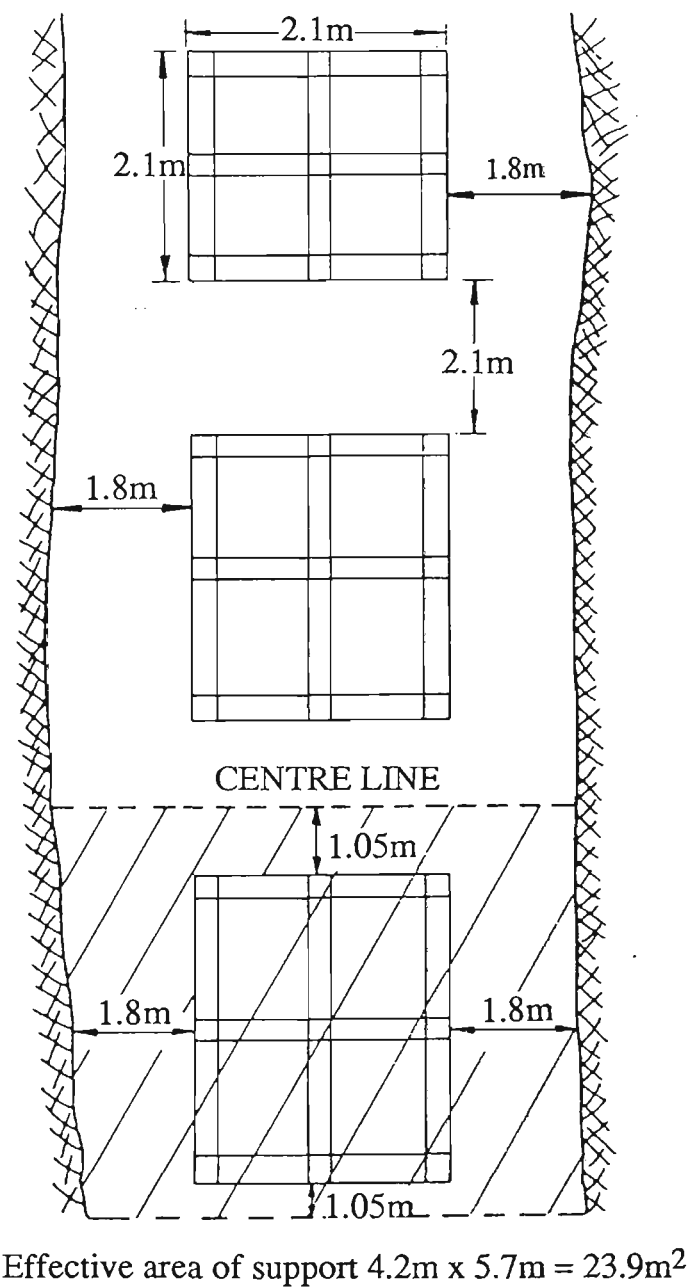


Figure 2.2 Wooden crib roadway support at South Bulli Colliery.
(Richmond, 1981)

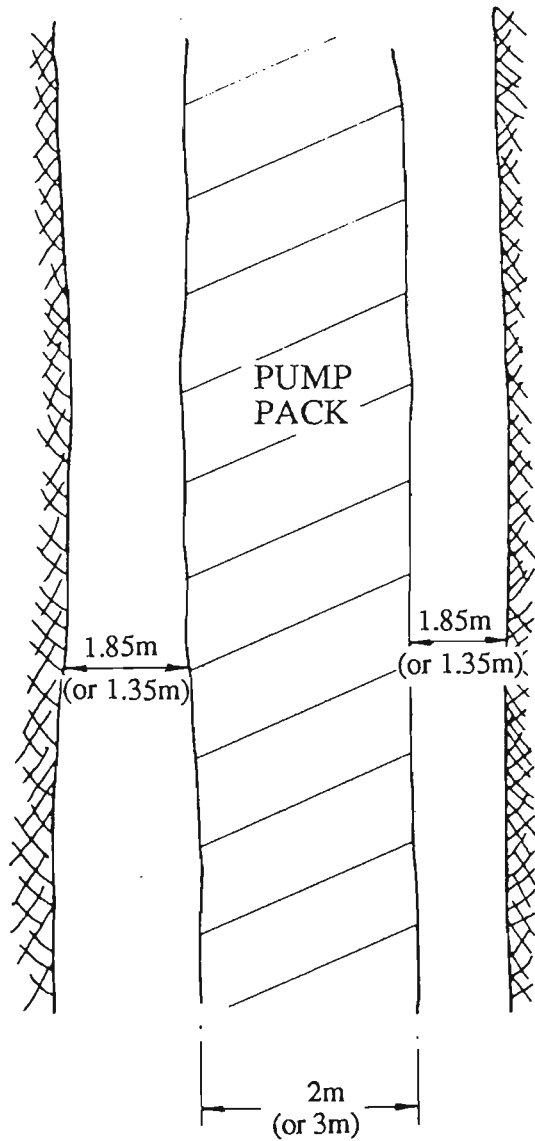


Figure 2.3 Proposed pump pack support system.

(after Richmond, 1981)

Hebblewhite (1983) proposed an advancing 12m wide single entry system with a 3m central monolithic pack as shown in Figure 2.4.

Advantages claimed of the proposed system over a narrow single entry are:

- (i) the two separate headings can act as an intake and return airway; and
- (ii) the pack can be broken at regular intervals for emergency access.

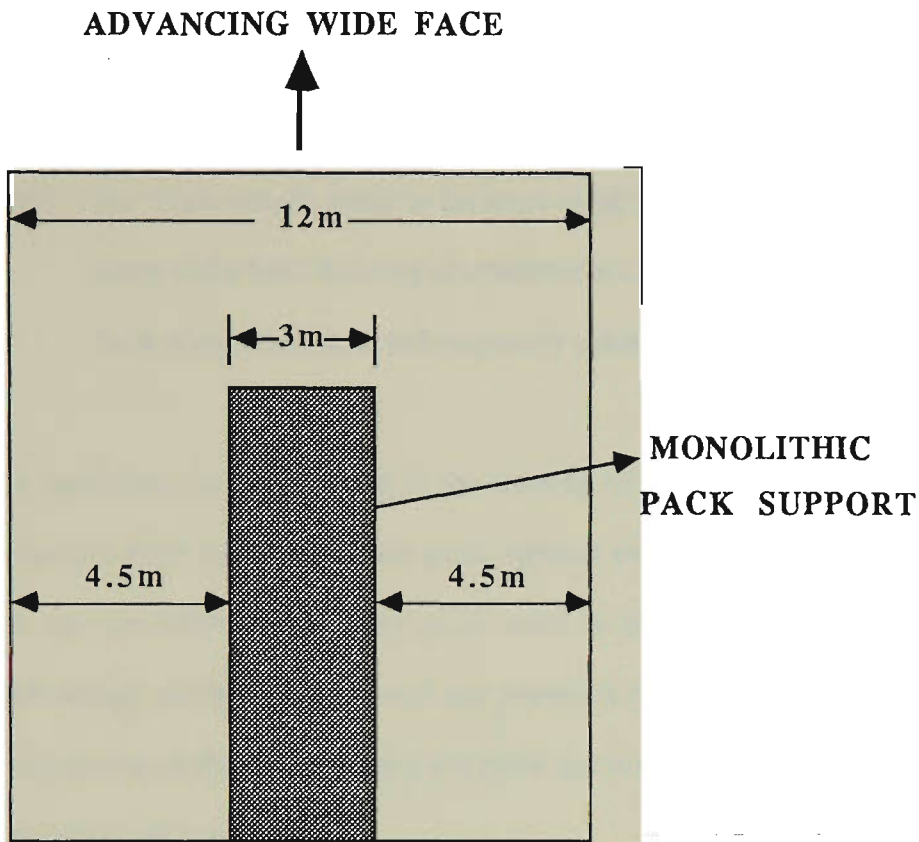


Figure 2.4 Typical single pass wide heading layout.

(after Hebblewhite, 1983)

Limitations of the proposed system are:

- (i) economic considerations, the costs of installing pump pack supports have to be compared with savings generated by the system;
- (ii) the NSW Coal Mines Regulations Act stipulates the maximum width of a heading as 5.5m therefore exemption would be needed;
- (iii) technological problems in obtaining the most appropriate mining equipment;
- (iv) inability of the support system to provide initial control of the roof strata in bad conditions;

- (v) deterioration in roadways after the first Longwall face passes due to high pack loadings on the goaf edge; and
- (vi) the pack would need to be kept quite close to the face and have early load bearing characteristics, and this could cause face congestion and subsequently a loss in production.

A variation on this system is the mining of two roadways, firstly a 7.5m wide roadway which has a 3m wide pack against one rib and secondly a 'second pass' face on the other side of the pack wall as illustrated in Figure 2.5. The obvious advantage of this method over the previous one is that it would not require as much shuttering or the need to keep the pack as close behind the face for effective initial support of the roof.

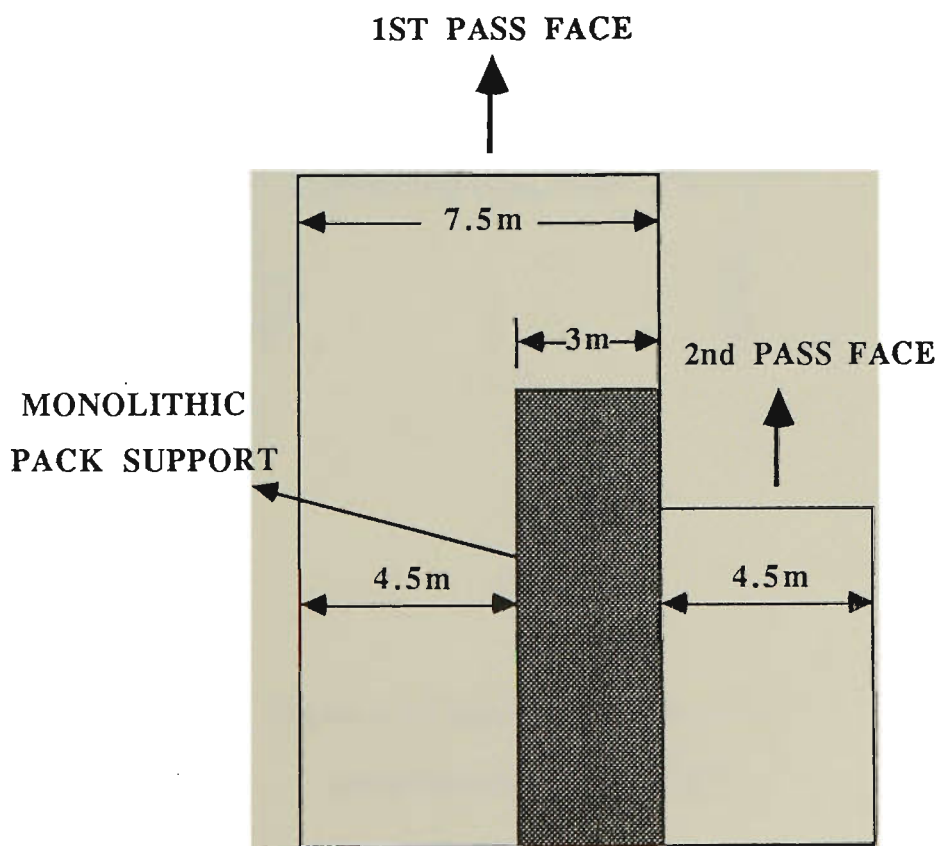


Figure 2.5 Typical double pass wide heading layout.

(after Hebblewhite, 1983)

Richmond et al. (1985) have proposed several alternative Longwall panel layouts utilizing pump packing technology as shown below:

- (i) retreating Longwall gateroad support both as piers or continuous wall structure (see Figures 2.6 through 2.9);
- (ii) dividing walls in single entry headings (see Figure 2.10); and
- (iii) advancing Longwall monolithic emplacement (see Figure 2.11).

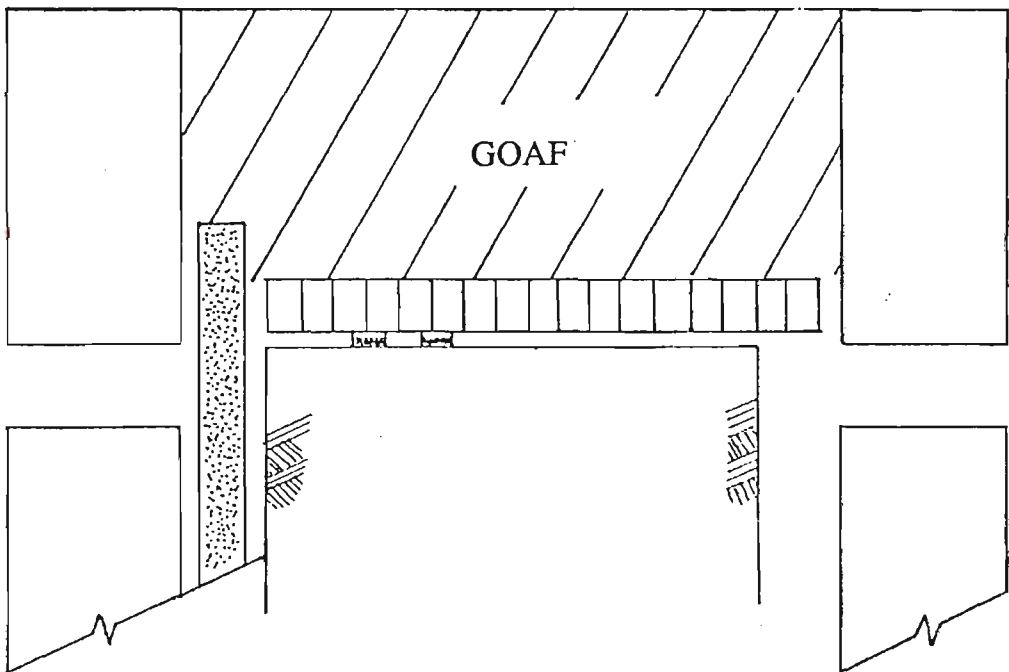


Figure 2.6 Centre roadway packwall.

(after Richmond et al, 1985)

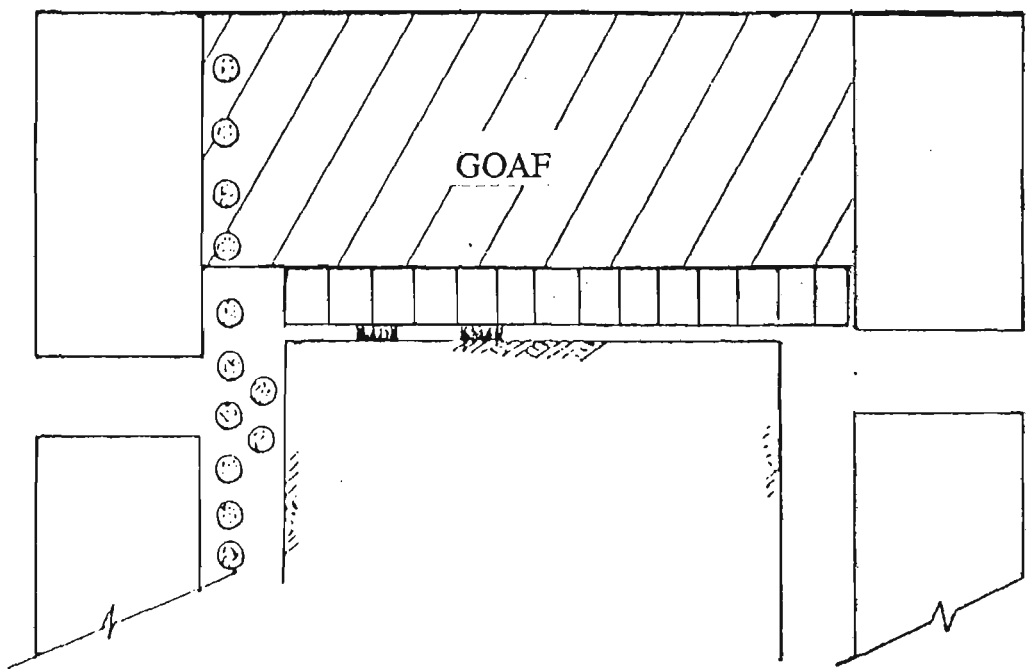


Figure 2.7 Monier 'Big Bag' supports.
(after Richmond et al, 1985)

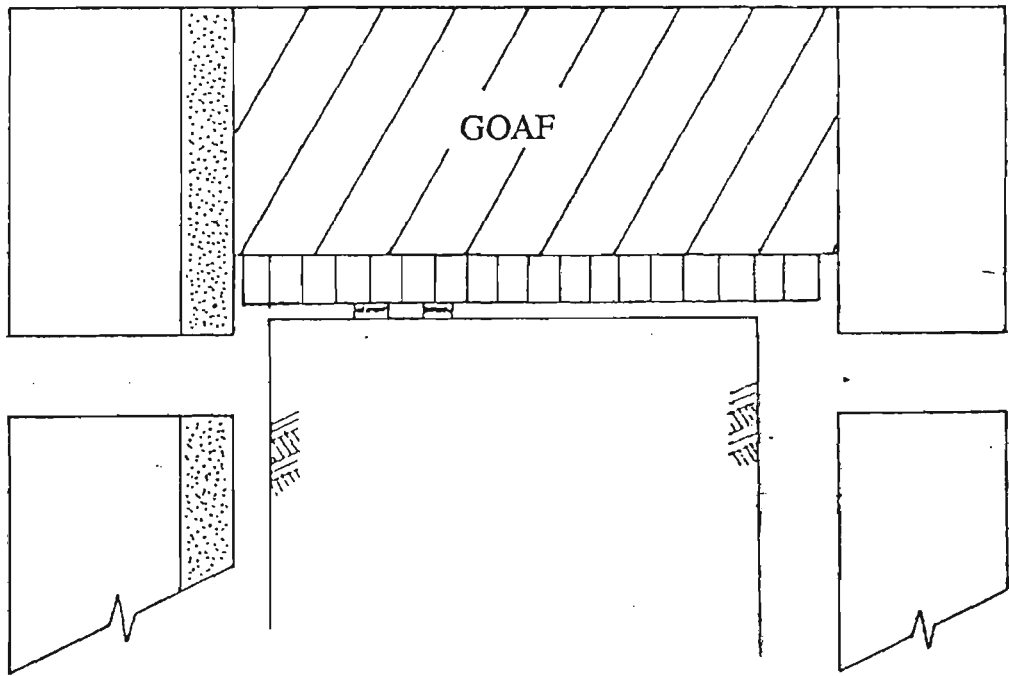


Figure 2.8 Side roadway packwall.
(after Richmond et al, 1985)

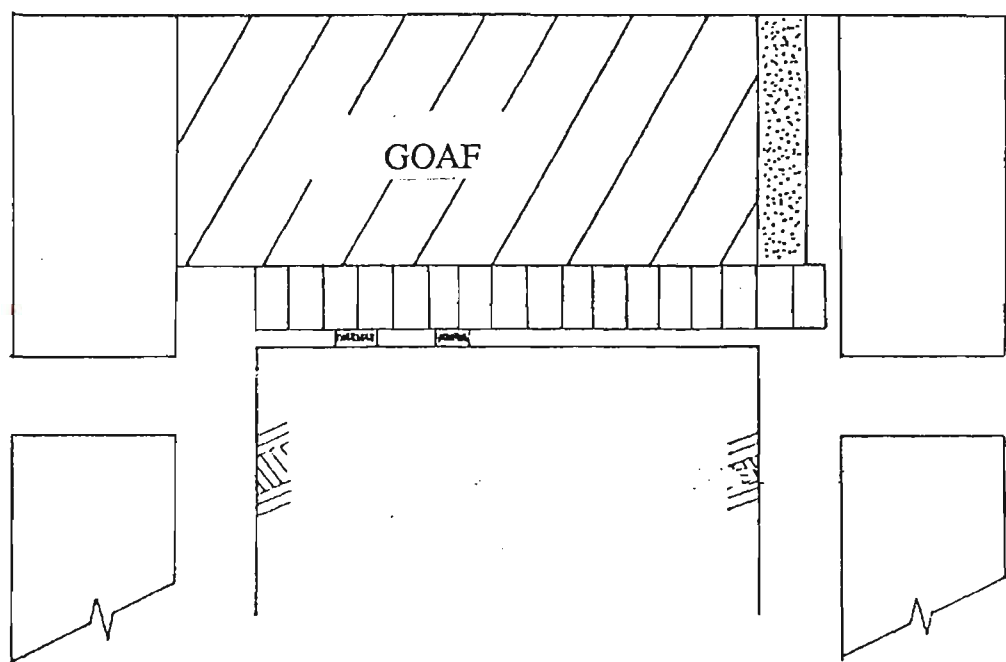


Figure 2.9 Maingate packwall.
(after Richmond et al, 1985)

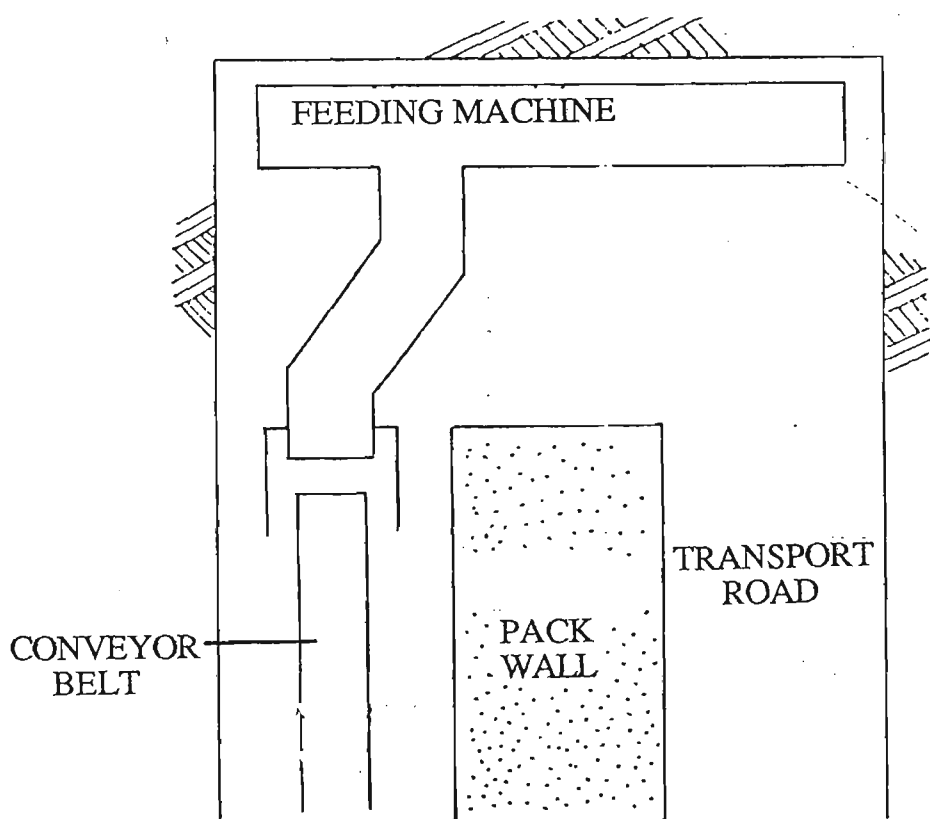


Figure 2.10(a) Concept of single entry dividing wall - driveage layout.
(after Richmond et al, 1985)

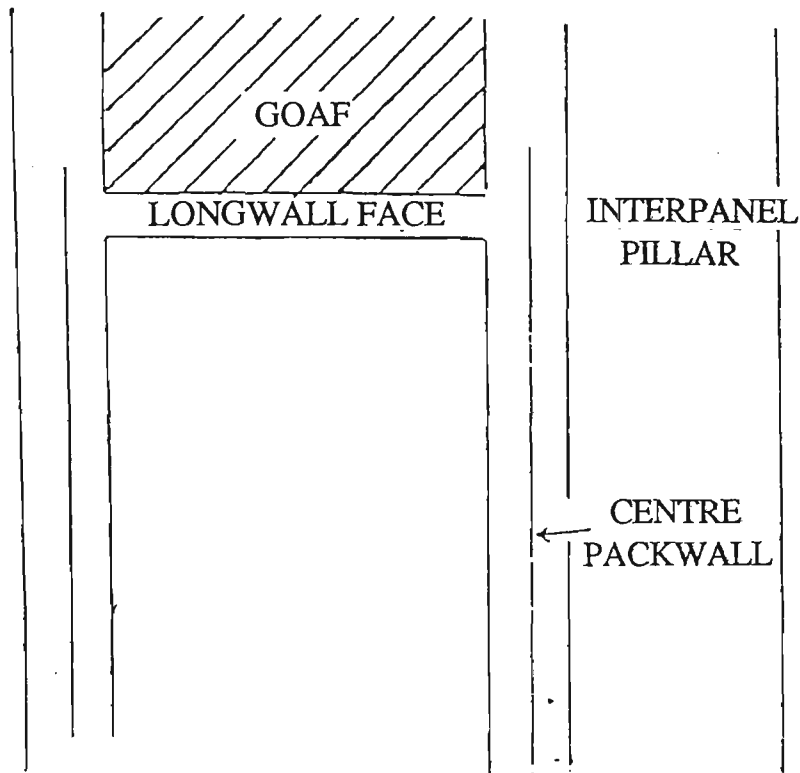


Figure 2.10(b) Concept of single entry dividing wall - partial extraction by Longwall with single entry.
(after Richmond et al, 1985)

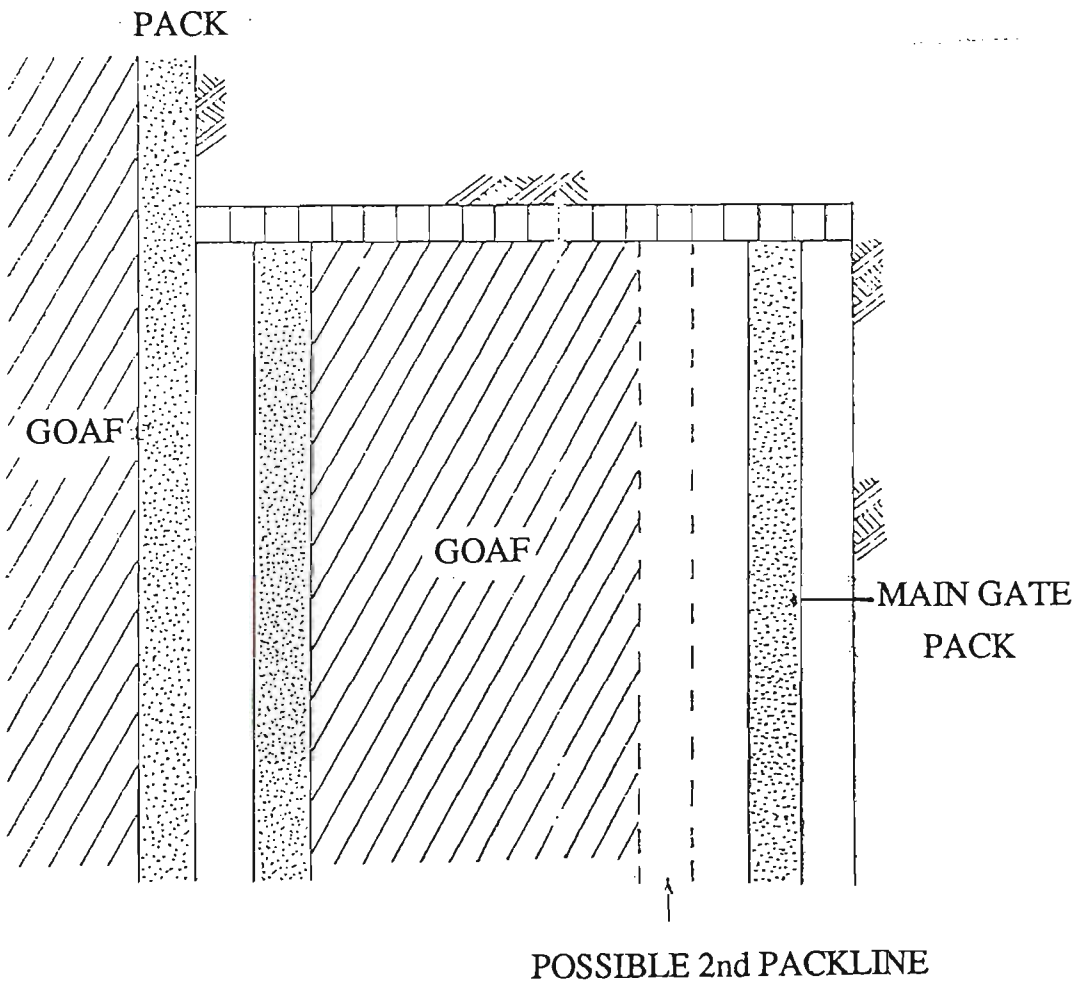


Figure 2.11 Advancing Longwall Panel.
(after Richmond et al, 1985)

According to Lama (1988), besides the development of new machines, further improvement in development rates is also possible by adopting the following approaches:

- (i) develop systems so that more than one roadway may be driven simultaneously, for example, use Shortwall with pump packing to divide the roadway into two or more headings (see Figure 2.12);
- (ii) develop systems so that roadways are driven simultaneously with Longwall extraction, hybrid advance retreat system (See Figure 2.13); and
- (iii) use of multiple machines to develop parallel single entries for future mines (Marshall and Lama, 1986) (see Figure 2.14).

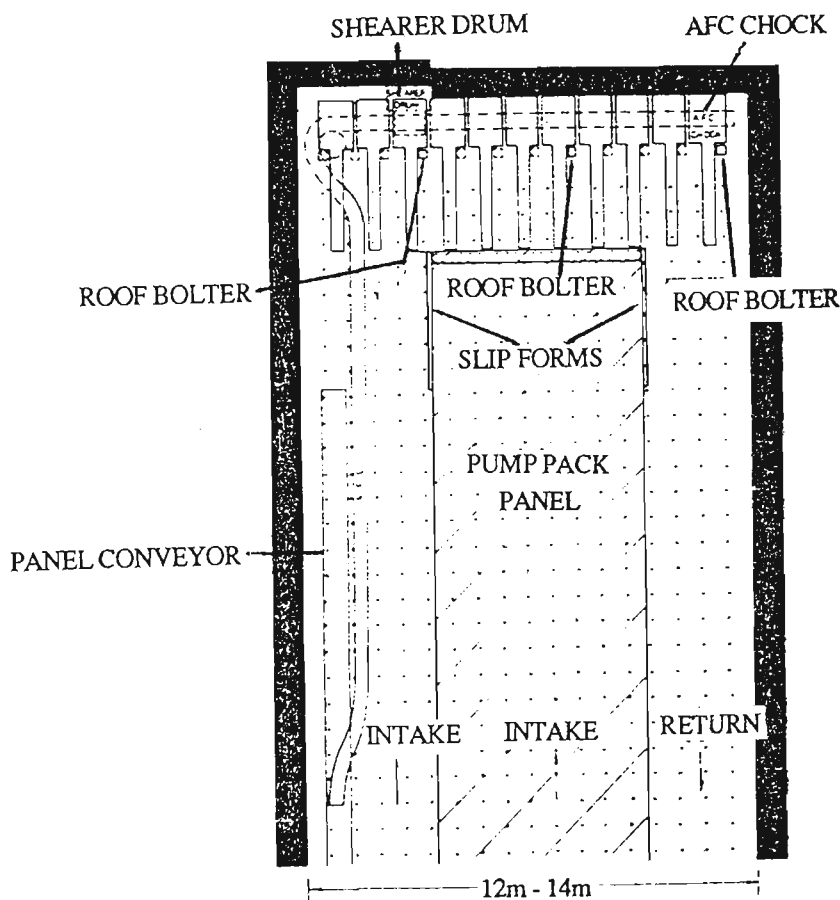


Figure 2.12 Shortwall entry drivage system with pump packing.

(after Lama, 1988)

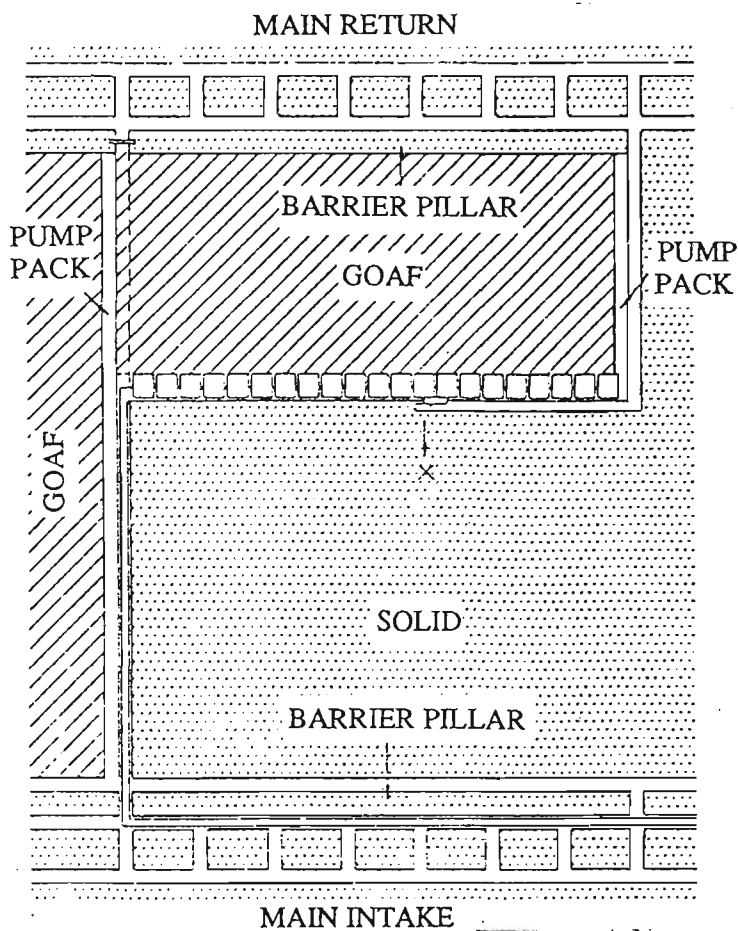


Figure 2.13 Shortwall extraction system with pump packing,
no development is required.

(after Lama, 1988)

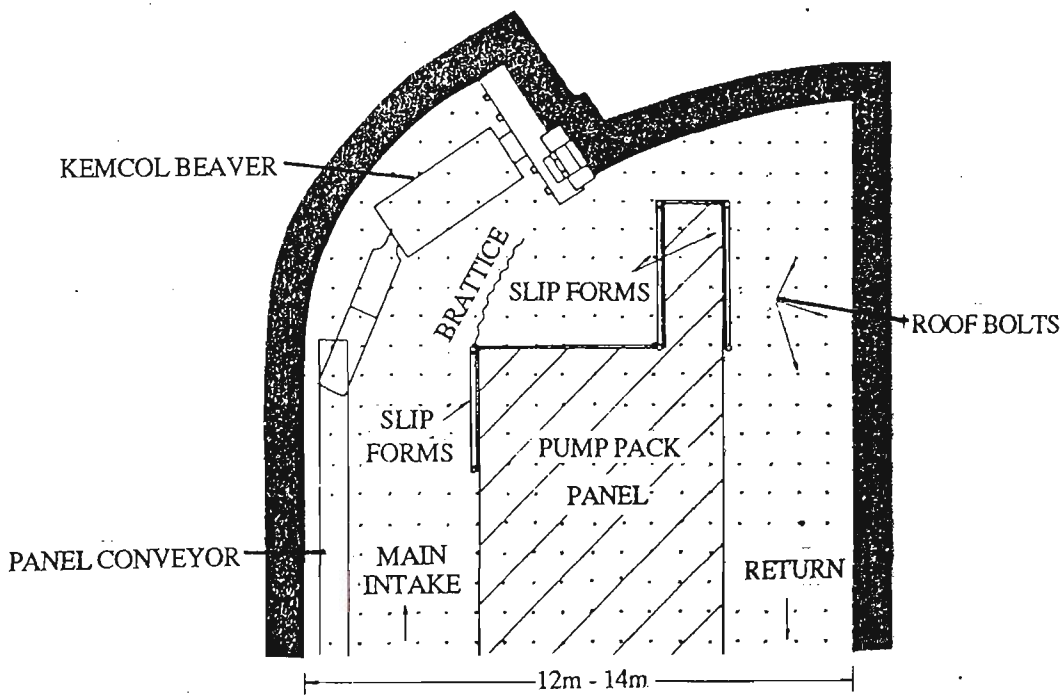


Figure 2.14 Kemcol Beaver with pump packing.

(after Marshall and Lama, 1986)

2.4 PROPERTIES OF PUMP PACKING MATERIALS

The cost and pipeline pumping life of various pump packing materials currently available in the market are given in Tables 2.2 and 2.3. The prices quoted, with the exception of Monier "Big Bag", are based on the UK market, and converted to Australian dollars by a factor of \$2=£1 sterling (exchange rate, 1986). The strength properties of various pump packing materials are presented in Sections 2.4.1 through 2.4.8. The use of pack materials for the control of roof in roadways has been very successful in Germany. Materials used for early bearing strength include alpha-hemihydrate and for late bearing strength comprise mixtures of alpha-hemihydrate, flyash and sand (Ruston et al, 1988). Figure 2.15 graphically illustrates the properties of the materials most suited for various purposes. More than 20 different types of pack materials have been developed in Germany. They have been used in a number of underground mining operations to counteract abnormal strata conditions.

Table 2.2 Cost and pipeline pumping life of tailings pak 2 (UK)
(after Atkins et al, 1986)

Tailings pak 2 (UK)				
Products	OPC	Additives	PFA	Tailings
Pipeline pumping life (mins)	120	IND	IND	IND
kg/m ³ of placed material pack	280	21	214	857
Imported material cost/m ³ of pack			\$57	

Note: IND means indefinite.

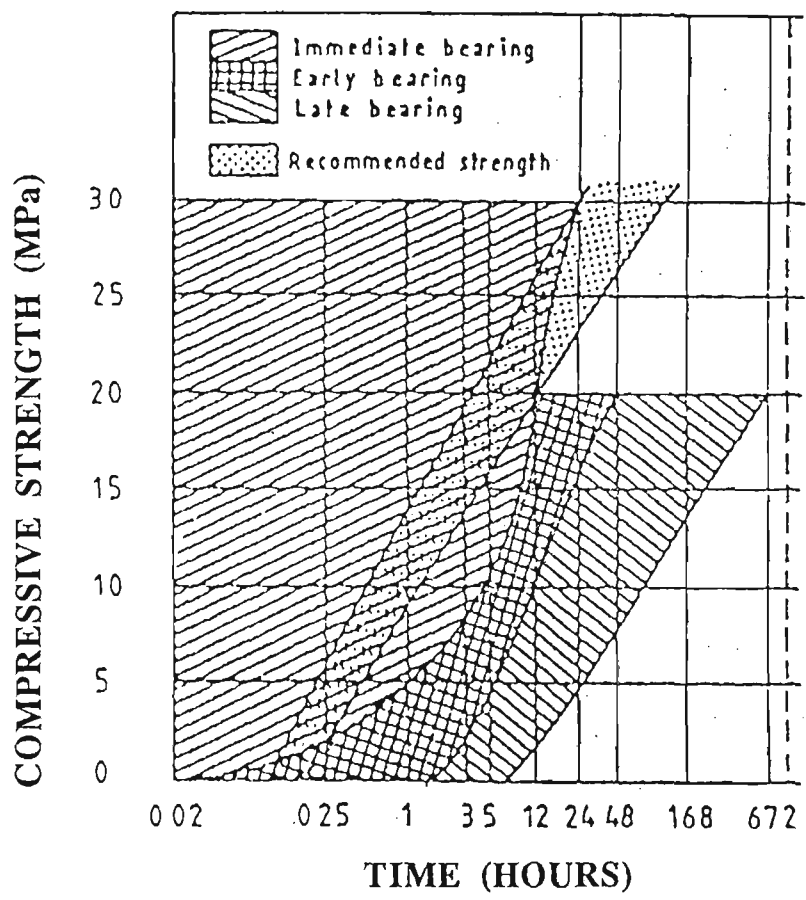


Figure 2.15 Uniaxial compressive strength of cement based materials and industry by products.
(after Ruston et al, 1988)

2.4.1 Thyssen

Table 2.4 presents the composition and strength properties of material for the Thyssen pump packing system. The packbind grout is capable of setting in 30 minutes, however, the additional quantities of water within the mix can increase the overall setting time of the finished pack to 60 minutes.

Table 2.4 Thyssen material properties
(after Hodgkinson, 1977)

Product	Materials Formulation	Setting Time	Strength Properties
Thyssen	10.4% Packbind (cement)	60 mins	0.4 MPa after 2 hours
	1.4% Flowmat (Bentonite)		0.5 MPa after 1 day
	51.5% Coal (-19mm)		1.0 MPa after 7 days
	36.7% Water		5.0 MPa after 28 days (maximum strength)

During the setting period the pack has no measurable strength, and during the strength development stages the pack will yield slightly under pressure. This demonstrates a hydraulic characteristics so desired in any packing system.

2.4.2 Warbret

This is a modification of the material used in the Thyssen system in which the following changes were made:

- (i) mixing of bentonite;
- (ii) using of OPC; and
- (iii) using of cement accelerator triethanolamine (TEA) 51.

As can be seen from Table 2.5, the final strength of the Warbret material is greater than Thyssen material by as much as 5 MPa.

Table 2.5 Warbret material properties
(after Woodley et al, 1980)

Product	Materials Formulation	Setting Time	Strength Properties
Warbret	48.0% Coal	60 mins	0.1 MPa after 1 hour
	29.0% Water		1.2 MPa after 1 day
	1.2% Bentonite		7-10 MPa
	19.2% Accelerator (TEA 51)		(final strength)

2.4.3 Anhydrite

The strength characteristics of material for Anhydrite pump packing system is shown in Table 2.6. The material has slow setting characteristics in the natural state, and the addition of an accelerator in the ratio of 1:100 by weight is thus desirable.

Table 2.6 Anhydrite material properties
(after Batten, 1985)

Product	Materials Formulation	Setting Time	Strength Properties
Anhydrite	89.9% Crushed Anhydrite	4 hours	0.1 MPa after 2 hours
	0.9% Accelerator		6.0 MPa after 1 day
	9.3% Water		8.9 MPa after 7 days

2.4.4 Aquapak

Table 2.7 shows the setting time and strength properties of Aquapak material. Aquapak is quite a remarkable development in that the pack comprises 85% water, 14% Aquacem and 1% Aquabent by volume. Aquabent contains bentonite to prevent water/cement separation and sodium carbonate accelerator. Even though it is considered a weak cement from a civil engineering view point, its properties have been proven ideal in meeting the requirement for pack applications.

Table 2.7 Aquapak material properties
(after Highton et al, 1984, Clark et al, 1985)

Product	Materials Formulation	Setting Time	Strength Properties
	33.3% <u>Aquacem</u>		0.35 MPa in 1 hour
	High alumina cement		0.6 MPa in 2 hours
	Portland cement		1.2 MPa in 24 hours
	Anhydrite calcium sulphate		5.0 MPa after 28 days
Aquapak	3.7% <u>Aquabent</u>	20 mins	
	Accelerator		
	Sodium Carbonate		
	(Soda ash)		
	Bentonite		
	63.2% <u>Water</u>		

The popularity of Aquapak system in the UK mines was attributed to the smaller delivery pipe size (25mm), and the reduced size and lower cost of the power packs, pumps and mixing tanks. Later experiences showed that the material could

be pumped from the outbye end of the district, which saved the transport of materials to a station close to the coalface as was necessary with Packbind.

2.4.5 Tekpak

Table 2.8 shows the details of the strength properties of Tekpak material. The unconfined compressive strength of Tekpak material has been shown to approximate that of Aquapak material. Water makes up to 91% of the pack by volume. However, the material quantities used were only about 73% of that used in the Aquapak pump packing system.

Table 2.8 Tekpak material properties
(after Highton et al, 1984, Clark et al, 1985)

Product	Materials Formulation	Setting Time	Strength Properties
Tekpak	14.2% Tekcem	30 mins	0.7 MPa in 2 hours
	14.2% Tekbent		2.5 MPa in 24 hours
	71.6% Water		5.0 MPa after 7 days

Foseco Technik has now designed a new product called Tekpak XX which gives a minimum 24 hours pumping life. When Tekcem XX is mixed with Tekbent XX in the packbag, the hardening action is said to be at least as swift as with the standard Tekpak.

More recently, Masol, a cementitious binder for pump packing with coal slurries, has been introduced into the "Tekpak technology". Masol is described as a

blend of non-aggressive high alumina cement and it is a modified form of Tekbent. However, the performance of this new product in the field is yet to be assessed.

2.4.6 Flashpak

Table 2.9 shows the strength properties of Flashpak material. The Flashpak material can set almost immediately after mixing. This reaction therefore requires no particular packhole preparation or containing bag. Hence, simple steel sheets suspended from the packhole supports are all that is required.

Table 2.9 Flashpak material properties
(after Highton et al, 1984, Clark et al, 1985)

Product	Materials Formulation	Setting Time	Strength Properties
Flashpak	66% <u>Fly ash mix slurry</u>		0.5 MPa after 2 hours
	Fly ash (64.5%)		1.6 MPa after 1 day
	Aluminium sulphate (0.03%)		4.4 MPa after 7 days
	Water (35.47%)	Flash set	
	34% <u>Cement mix slurry</u>		
	OPC (62.5%)		
	Water (37.5%)		

The pack is virtually built up layer upon layer until the pack is completed. Additionally, according to Clark and Newson (1985), the excellent adherence of the material to the roof, sides and pack wall itself helps to reduce air leakage.

2.4.7 Tailings pak

Table 2.10 shows the strength characteristics of the material used in the tailings/PFA system. At this stage, tailings pak material is still under experimental stage. However, the laboratory test results have been very encouraging, and the results strongly show that tailings pak would have wide application in the foreseeable future.

Table 2.10 Tailings pak material properties
(after Atkins et al, 1985)

Product	Materials Formulation	Setting Time	Strength Properties
Tailings Pak	10% Tekcem	30 mins	0.3 MPa after 2 hours
	10% Tekbent		0.8 MPa after 1 day
	16% PFA		1.44 MPa after 2 days
	64% Tailings		1.85 MPa after 7 days

Studies on the use of CWR were carried out by Thomas (1985). CWR crushed down to -10mm size was used for the sample preparation. The details of the test results are shown in Table 2.11.

It can be seen from the test results that the strength of CCWR material is considerably greater than that of tailings pak material. This increase in strength is considered to be attributed to the presence of 12.3% of Portland cement.

Table 2.11 CCWR material properties
(after Thomas, 1986)

Product	Materials Formulation	Setting Time	Strength Properties
CCWR	12.3% Portland cement	N/A	0.2 MPa after 1 hour
	0.37% Calcium chloride		0.35 MPa after 2 hours
	69.7% -10mm coal		5.17 MPa after 7 days
	washery refuse		6.53 MPa after 14 days
	17.6% Water		6.78 MPa after 28 days

2.4.8 Monier "Big Bag"

Table 2.12 shows the strength characteristics of Monier "Big Bag" material. The Monier "Big Bag" chocks, which are said to be a fire resistant roof support system are constructed from specially formulated materials including Portland cement. The system offers high initial resistance to roof movement and it also provides load bearing capacities of up to approximately 500 tonnes.

In Australia, Monier "Big Bag" chocks have been used as an additional roof support system at "sensitive" roadways intersections. Studies carried out by Batten (1985) and field observations have shown that the Monier "Big Bag" chock/material tends to suffer from a lack of cohesion when loaded, which is not a desirable feature as a pump packing material.

Table 2.12 Australian Monier "Big Bag" material properties
(after Batten, 1986)

Product	Materials Formulation	Setting Time	Strength Properties
Monier "Big Bag"	OPC	10-16 hours	1.5 MPa after 1 day
	PFA		2.7 MPa after 3 days
	Expansion Agents		3.7 MPa after 7 days
	Plasticiser for better		6.3 MPa after 28 days
	flow		10.46 MPa in 42 days 18.7 MPa in 90 days

2.5 SURVEY OF THE TYPES OF PACKING MATERIALS USED
IN THE SOUTHERN COALFIELDS

The Author conducted a survey of the types of packing materials used in the Southern Coalfields, Australia as shown in Table 2.13. The survey indicates that wooden chocks and Monier "Big Bag" chocks (a type of monolithic pump packing system) are the two most popular types of packing materials. It is noted that the number of wooden chocks used is significant. This gives a good indication of the popularity and the relative ease of wooden chock installations. Monier "Big Bag" chocks have been installed in several collieries since its introduction in 1981. At present, most collieries have stopped using Monier "Big Bag" chocks because they are not cost-effective for use as roof supports. The undesirable insitu load/deformation characteristics of Monier "Big Bag" chocks have been discussed in Section 2.4.8.

Table 2.13 Types of packing materials used in the Southern Coalfields.

TYPES OF PACKING MATERIALS USED			
Colliery	Wooden chock	Steel chock	"Big Bag" chock
Appin	Yes	--	Yes
Bulli	Yes	--	Yes
Coal Cliff	Yes	--	Yes
Cordeaux	Yes	--	Yes
Corrimal	Yes	--	Yes
Darke Forest	Yes	--	Yes
Huntley	Nil	--	Nil
Kemira	Yes	Yes	Yes
Metropolitan	Yes	--	Yes
North Cliff	Yes	--	Nil
Nebo	Yes	--	Yes
South Bulli	Yes	--	Yes
Tahmoor	Yes	--	Nil
Tower	Yes	--	Yes
West Cliff	Yes	--	Yes
Wongawilli	Yes	--	Yes

In the Southern Coalfields, Australia, wooden chocks are generally used as extra supports when roof conditions deteriorate in gateroads and main development headings and/or as preventive measures where overlying pillars are left in the Bulli Seam and cause major stresses in the roof. It is evident that wooden chocks are erected in the maingate and tailgate cut throughs prior to the extraction of the

Longwall pillar. In Kemira Colliery, typically some 40 wooden chocks are used as secondary roof supports in each Longwall, 20 chocks for the maingate and 20 chocks for the tailgate.

In Tahmoor Colliery, BP Coal Australia which is now a subsidiary of Kembla Coal and Coke Pty. Limited, extensive wooden chocks have been used to secure the roof of Longwall gateroads because of difficult roof conditions. Some 300 mini chocks and 70 big chocks have been used for each Longwall. Some 130 mini chocks and 6 big chocks have also been used for Longwall recovery. Typically, for every 60m of Longwall gateroads, 4 mini chocks and 1 big chock are used for the maingate, and 7 mini chocks are used for the tailgate. Figure 2.16 diagrammatically shows the layout of wooden chock installations per 60m of Longwall gateroads at Tahmoor Colliery.

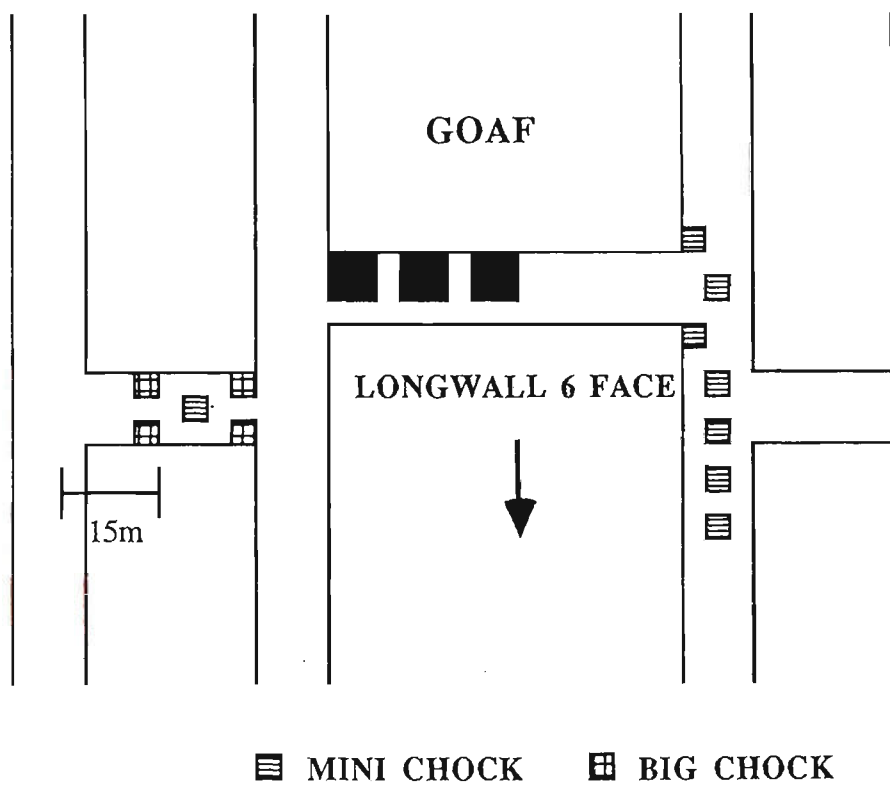


Figure 2.16 Layout of wooden chock installations per 60m of Longwall 6 gateroads at Tahmoor Colliery.

2.6 SUMMARY

It can be inferred from the literature survey that the selection of any type of packing material for use in the Australian coal mines would obviously be influenced by the availability of the product at a competitive price and its function as a support material. Given the existing environmental constraints imposed on the coal mine operators, the utilization of CWR as a packing material is an attractive proposition.

In the likely event of high tonnage demand for packing material, the crushed CWR can be piped down from the surface to the packing site, where it will be readily mixed with other ingredients and pumped into the pack form or bag.

Other desirable features of a packing system should include:

- (i) good packing characteristics (the behaviour and suitability of the pump packing material with reference to strata control requirement);
- (ii) contain a minimum of imported material;
- (iii) flexibility and ease of material handling, bulk pneumatic and hydraulic pipeline conveying;
- (iv) longer pipeline pumping life; and
- (v) most importantly the cost-effectiveness of the system.

In general, pump packs are designed to yield and thus control convergence, and are often built to an optimum size to save manpower and material costs. In addition, as German experience has shown, pump packs greater than a critical width lead to floor heave as the packs do not yield under load (Lewis and Stace, 1981).

Extensive studies over the years have established the following criteria for pack strengths: the strength of 0.1 MPa for deshuttering purposes, and initial strengths of 0.4-0.5 MPa in 4 hours, and 1.0-1.4 MPa in 24 hours are desirable. A more important criterion is that the pack should be able to develop strength as quickly as possible, and the final strength should be in the order of 6-10 MPa (Whittaker et al, 1977, Issac et al, 1982, Smart et al, 1982a, 1982b, Buddery, 1984, Clark and Newson, 1985, Smart, 1986, Isaac and Payne, 1986).

It is important to note that the above criteria for pack strength apply especially for the United Kingdom conditions. Therefore, it is in the opinion of the author that the pack strength for Australian conditions should be higher in order to accommodate the excessive load of the massive sandstone roof (Hii and Aziz, 1986a). The strength of the pump packing material can only be determined from field trials and monitoring programmes.

The state-of-the-art review of pump packing system has led to the following conclusions and recommendations.

The planning of an efficient pump packing system requires a high level of prediction, both of geological conditions and those likely to be caused by mining. It is noted that the continued effective control of the roof strata in the vicinity of a roadway is only achieved when the pack supports are capable of sustaining the variations which arise from the changing mine layout, the ground stress conditions and the variations in the geological conditions.

Judging from experiences gained in the United Kingdom and Germany, the elimination of chain pillars leading to the pillarless Longwall mining can be an attractive proposition. The re-use of roadways to serve adjacent Longwall faces should be approached with caution. Excessive floor heave at the face ends is just

one example of the many problems encountered at Betws Colliery, South Wales, where pillarless mining was successfully attempted (Issac et al, 1982).

An attempt has been made to emphasize the importance of understanding the tectonic forces which prevail in mining. Consequently, an improvement in this understanding can help to effectively control these forces by the selective use of pump packing systems.

It has been proposed that considerations of the reaction of the pump pack within its structural environment suggests that in heavy strata loading conditions, increased pack strengths would be beneficial to strata control, ensuring maximum control over convergence (Smart et al, 1982a, Hii and Aziz, 1986a).

Research has indicated that the material properties of tailings pak products are ones of the most cost-effective pump packing materials, and are therefore recommended for field trials in the Bulli seam.

The integrated methods of colliery waste disposal for ground control as proposed by Atkins et al. (1986) are of particular interest to the coal mining industry. The tailings pak pump packing system undoubtedly will have a large contribution to make to the mining industry in the foreseeable future.

CHAPTER THREE

THEORETICAL CONSIDERATIONS

CHAPTER 3

THEORETICAL CONSIDERATIONS

3.0 INTRODUCTION

This Chapter focuses on the principles of pump packing and the suitability of pump packing under Australian conditions with particular reference to the Bulli Seam. The Chapter is also concerned with the development of CCWR material for strata control, the application of the experimental design with mixtures and the development of a new yield function for CCWR material.

3.1 PRINCIPLES OF PUMP PACKING

3.1.1 Purpose of pump packing

In general, the purposes of pump packing can be outlined as follows:

- (i) to provide support for the roadway behind an advancing longwall face and the packs provide support to the immediate beds of strata as the face advanced;
- (ii) to effect a breaking off line at the waste edge to maintain the competence of the immediate roof measures;
- (iii) to facilitate the disposal of the controversial liquid tailings from coal washery plant and pulverised fly ash from power stations, this factor being pertinent to the use of tailings/fly ash packing system; and

- (iv) to prevent or minimize air leakage across the waste area.

It is envisaged that the first two points are strata control aspects and the last two are environmental ones. It can be recalled that elimination of chain pillars by the re-use of roadways has been successfully practised in Britain (Smart et al, 1982a). In most cases, this has been achieved by employing pump packing techniques.

The two main reasons for the elimination of substantial chain pillars between adjacent retreating longwall coal faces are: to improve recovery of reserves (by preventing sterilisation of reserves); and to reduce the amount of development required for retreating longwall faces through reuse of roadways.

In Australia, "Big Bag" packs have been used at some roadway intersections as a secondary means of support. Figure 3.1 illustrates "Big Bag" chocks which are used for roof support at West Cliff Colliery, N.S.W., Australia. However, research has indicated that pump packing can also be used as an initial means of strata control.

3.1.2 Detached block theory

The detached block theory has been successfully implemented to explain the deformation mechanisms around both face lines and roadways in underground coal mines (see Figure 3.2). The fundamental of detached block theory has been reported in Wilson (1975) and Whittaker and Woodrow (1977). The actual caving height and the geometry of the detached block are the major parameters in the theory, and it is assumed that the caving characteristics of the waste govern the caving height. It can be used to predict the load generated from the detached block in the strata and the actual strength required for a pack.



Figure 3.1 "Big Bag" chocks at West Cliff Colliery.

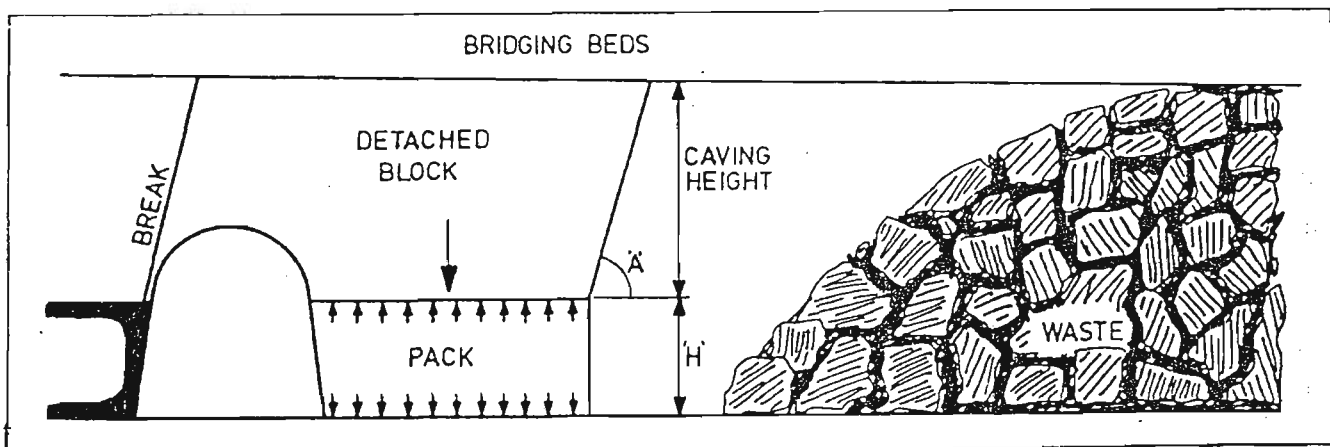


Figure 3.2 Detached block theory.

(after Clark and Newson, 1985).

In the United Kingdom, the detached block theory together with appropriate safety factors have been widely used for roof support design on face lines. It is cautioned that consideration should be taken of the imposed loading generated by the bridging beds assuming the subsidence profile. This is because the measured pack load has indicated that the pack at some distance behind the face line is not solely supporting the dead weight of a detached block (Clark and Newson, 1985).

3.1.3 Roof beam tilt theory

The roof beam tilt theory has been reported in details elsewhere (Smart et al, 1982, Smart, 1986). The roof beam tilt approach recognises the imposed loading generated by the downward movement of the bridging beds around the roadway. Figure 3.3 schematically shows the support mechanisms of roof beam tilt theory.

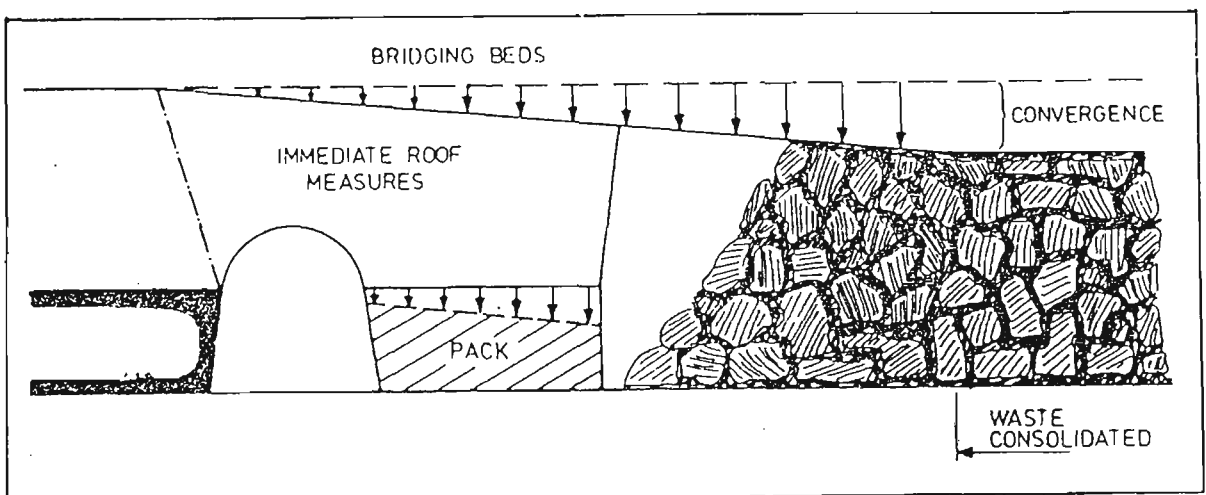


Figure 3.3 Generalised view of roof tilt.

(after Clark and Newson, 1985)

The theory suggests that the immediate roof tilt towards the waste about a pivot point in the ridside. Although the amount of downwards movement of the roof can be controlled by the pack, it is unavoidable. In fact this phenomenon may be modelled as a simple lever problem.

3.1.4 Practical requirements for the use of pump packing

In the light of several changes in the form and type of construction of gateside packs that have been introduced in recent years with respect to longwall mining, the basic requirements regarding the provision of roof support have remained unchanged. The recent changes have been directed towards mechanizing pump packing operations and achieving earlier and higher supporting resistance. Progressive developments towards improving the optimum pack support resistance is conditional upon full knowledge of the pack design requirements (Smart, Isaac and Roberts, 1982, Smart, 1986).

In order to understand the implications of materials properties of pump packing systems in an underground environment, it is necessary to appreciate and briefly discuss the nature of strata behaviour above a longwall panel. Of particular interest is the role of the pack in relation to the strata behaviour and support load requirements about longwall faces.

3.1.5 Longwall strata behaviour and the generation of pack load

There is a general agreement that the longwall face disturbs the equilibrium stress field of the strata. The immediate roof begins to sag away from the overlying strata and subsequently becomes destressed as the face moves away from the standing position. Eventually after a critical length of advancement the immediate roof begins to cave.

As the face continues to advance the vertical and horizontal forces gradually rearrange to their former condition after a prolonged period. In the working area, it is envisaged that the pack should be able to accept the movement associated with the redistribution of stresses without compromising its ability to accept later loading. One of the important requirements of a pack as reported by Buddery, Hassani and Singh (1984) is to prevent bed separation above the roadway which would promote strata failure in the roof.

In Australia, the caving material sometimes does not expand sufficiently to completely fill the void, because the geology of roof often consists of massive sandstones interrupted by shale and mudstone layers. However, under these conditions, the bridging beds remain relatively stable but fracturing may occur.

Previous work by Smart et al. (1982b) suggested that under ideal caving conditions, overburden pressure is believed to be taken by the solid coal in front of the face and over the waste through the bridging beds. The purpose of pump packing therefore is to control the immediate roof (the cantilever beam) by restricting convergence of the roof, and consequently to prevent the beam from breaking along the coal face. The amount of convergence to be allowed is very much dependent upon the geology of the immediate roof.

Over the past years, various researchers have carried out extensive study into pump packing technology needs (Hodgkinson, 1977, Whittaker et al, 1977, Richmond, 1981, Smart et al, 1982a, 1982b, Buddery and Ashika, 1982, Issac et al, 1982, Buddery, 1984, Lerche and Renetzeder, 1984, Clark and Newson, 1985, Richmond et al, 1985, Singh et al, 1985, Thomas, 1986, James, 1986, Smart, 1986, Issac and Payne, 1986, Hii and Aziz, 1986a, 1986b, 1987a, 1987b, 1989, Atkins et al, 1984, 1986, 1987, Zadeh et al, 1987, Hii and Yu, 1989).

3.1.6 Basic requirements

It has always been recognised that, ideally, a packing medium must be able to fulfil both the short term and long term support requirements. There is a general agreement that early effective support is necessary to achieve good strata control. Therefore, the early load-bearing capacity of a pack system is absolutely essential. It is indicative that the pack must always be built in contact with the roof, and preferably as near as possible to the coal face. It is also required that the pack be built of a suitable material, and in such a way that the best use is made of the available material.

3.1.6.1 Short term support requirements

The examination of the resistance of the existing packs indicates that reliance is placed on the resistance of the "pack wall" in the early life of the packs. It is of paramount importance that the packs be able to absorb the vertical closure without bulging and weakening the wall.

Therefore, the pack should be able to accommodate 5-10% strain (in most geological conditions) without undergoing failure. Unfortunately, not every condition allows the building of suitable packs and resort is made to other measures such as timber or other imported materials. However, roadways conditions often hinder the transport of material in bulk.

The pump packing system has the distinct advantages of relatively short setting time in relation to face operations and also early load-bearing characteristics. However, sometimes the early support property of the system can be neglected due to poor workmanship. This can result in inadequate roof contact or the existence of unfilled cavities and broken roof which may render packing less effective.

In normal face strata control, the break-off line which usually occurs at the rear of powered supports can be diverted away from the face-end area by the provision of the pump packing support which can also be a suitable packhole support. In ground prefractured by interaction, it has been proven to be especially advantageous to use pump packing for additional support.

It is envisaged that a large amount of initial movement is necessary for the stability of the strata and the pack should be able to accept this movement without compromising its later strength. One of the important requirements of a pack is to prevent bed separation which would promote strata failure in the roof.

3.1.6.2 Long term support requirements

It is often recognised that no matter how important the pack might be in offering early resistance, it is equally important that the pack gives long-term yield support at the side of the roadway.

The phenomenal lowering of the upper beds behind a longwall face is governed by the condition existing in the waste area. It is anticipated that the pack must offer sufficient resistance to maintain the immediate roof in contact with the upper beds and allow all the strata to lower at the same rate, otherwise adverse conditions in the associated roadway will occur.

However, too great a resistance could lead to the floor bearing capacity being exceeded and consequently floor lift would occur (see Figure 3.4). The pack long term support requirement is to be able to support the height of strata "caving height" that is free to move under its own weight.

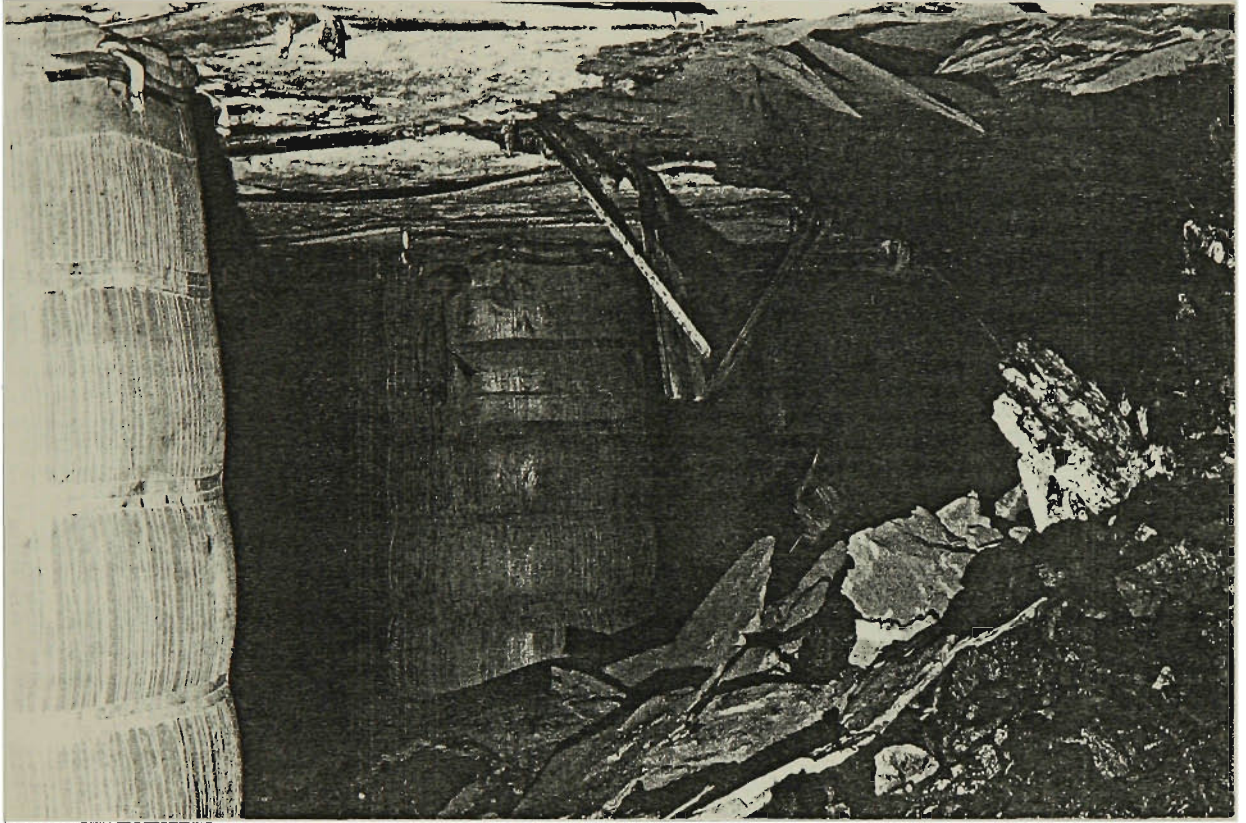


Figure 3.4 Floor heave problem.

(Source: Monier Resources, Australia)

The success of pump packing suggests that its properties are close to those required. Although the ultimate strength can be attained by many pump packing systems, many packs (mechanically and poorly built hand packs) offer negligible resistance initially, and consequently they cannot control the movement of the immediate roof, other packs which are either made of wood or concrete offer too high an early resistance damaging the structural integrity of the surrounding rock mass and resulting in excessive roof to floor closures (see Figure 3.5).



Figure 3.5 Support failure leads to excessive roof to floor closures
(West Cliff Colliery).

3.2 SUITABILITY OF PUMP PACKING UNDER AUSTRALIAN CONDITIONS WITH SPECIAL REFERENCE TO THE BULLI SEAM

The coal mines in Australia, especially those in the Southern Coalfields, have been using pump packing in the form of "Big Bag" chocks since 1981. However, to date bulk monolithic pump packing system for roadway support has not found a general application in Australian collieries. The excellent geological condition of Australian mines, with high production capacity, has placed little importance in the past on the maximization of percentage extraction of the workable reserves.

In addition to its present form as "Big Bag", in providing stability to roadways and intersections, the pump packing technique has a significant role in contributing towards the success of the pillarless longwall mining method as suggested by Marshal and Lama (1986). Such a system should be attempted in Bulli Seam, in view of the less complicated geological conditions of the Southern Coalfields of NSW. However, in the experimental stage, care must be taken to provide means of minimising the possible effects of floor heave at the gate ends.

A careful study of the geological conditions of the mines in both Australia and the United Kingdom has indicated a marked difference in the mining conditions between the two countries (Smart and Aziz, 1986, Porter and Aziz, 1988). Therefore, it is most important to be able to distinguish the difference in the geological conditions, and thus modify the pump packing system before any transfer of pump packing technology from Europe to Australian coal mines can be successful.

In Australia, the average powered support setting load density is 0.625 MPa, and this is about 2.3 times higher than that used in the United Kingdom (Porter and Aziz, 1985). This level of support density indicates that for successful application of pump packing systems in Australian conditions a higher pack strength is required.

Therefore, more laboratory testing of the properties of tailings pack material which is the "key" pump packing material used in this particular research is highly desirable. This research is necessary to develop cheaper alternatives and to match the strength of the pack to the surrounding strata in Australia.

The characteristics of pump packing which would be suitable to act as a means of underground roof support in Australian conditions include rapid initial

setting and steady increase in strength from 1.0 MPa in one day to 5.0 MPa or more in 28 days.

3.3 DEVELOPMENT OF CCWR MATERIAL FOR STRATA CONTROL

3.3.1 Design of CCWR material

Although numerous methods of concrete mix design have been developed, each method is applicable only under conditions similar to those for which it is developed. All methods of mix design are deduced from empirical information and follow substantially the same procedure. Loo and Ahmad (1982) have conducted a comparative study of four popular concrete mix design methods. To substitute the expensive commercial materials for pump packing, a method for use in the design of CCWR material mixes is proposed.

This research program aims at producing the most cost effective and economical CCWR material for strata control and increased recovery of coal. The investigation also aims: to optimise particular mechanical properties of CCWR material, to develop a cheaper binding material, to increase the initial strength of the mixture, and to develop a material which is pumpable but can also give sufficient strength for use as a pack material in Australian underground coal mining operations.

3.3.2 Correlation of the strength and the curing time

Figure 3.6 shows the plot of the measured strength against curing time for each mix (see Table 3.1). It is obvious from Figure 3.6 that the strength of a mix increases with an increase in the curing time, which has also been reported (Knissel

Table 3.1(a) Measured unconfined compressive strength of CCWR materials at different curing times.

Mix	X1 (Water) %	X2 (CaCl2) %	X3 (OPC) %	X4 (CWR) %	Unconfined Compressive Strength, MPa											
					1 Hr.	1.5 Hr.	2 Hrs.	4 Hrs.	1 Day	7 Days	14 days	28 days	60 days	90 days	A	B
1	12.660	0.124	4.154	83.062	--	--	--	1.208	1.208	1.876	2.041	2.432	2.493	3.388	3.399	1.379
2	19.000	0.182	6.061	74.757	--	--	--	--	0.321	0.823	0.924	1.111	1.616	1.617	2.064	2.560
3	16.500	0.187	6.249	77.064	--	--	--	--	0.594	1.289	1.213	1.680	1.864	2.097	2.306	1.456
4	13.040	0.195	6.508	80.257	--	0.038	0.042	0.166	1.629	2.664	3.152	3.379	4.105	4.625	6.088	2.250
5	19.120	0.242	8.064	72.574				0.659	1.703	2.011	2.183	2.724	2.886		3.342	1.794
6*	16.200	0.250	8.356	75.194	0.032		0.048		2.650	3.070	3.410				4.378	1.327
7	13.790	0.234	7.816	78.160		0.039	0.042	1.799	3.449	3.882	4.344	4.699	5.631		8.516	2.903
8	12.000	0.263	8.774	78.963	0.036	0.047	0.078	0.271	3.495	6.305	6.232	7.474	7.433	7.795	8.959	1.011

* (after Thomas, 1986).

% denotes percentage by weight.

Table 3.1(b) Measured unconfined compressive strength of CCWR materials at different curing times.

Mix	X 1	X 2	X 3	X 4	Unconfined Compressive Strength, MPa											
	(Water)	(CaCl2)	(OPC)	(CWR)	1 Hr.	1.5 Hr.	2 Hrs.	4 Hrs.	1 Day	7 Days	14 days	28 days	60 days	90 days	A	B
	%	%	%	%												
9	19.120	0.302	10.072	70.506					1.152	2.800	3.117	3.394	4.803	4.900	5.729	1.960
10	16.500	0.312	10.397	72.791	0.009			0.013	1.365	3.895	4.670	5.134	7.029	7.100	8.724	2.180
11	13.040	0.325	10.829	75.806		0.082	0.151	1.021	5.138	8.859	10.612	10.838	15.073	16.599	18.308	1.610
12	19.730	0.360	11.986	67.924					1.289	2.870	3.111	4.248	4.623	5.443	6.171	1.994
13*	17.620	0.369	12.302	69.709	0.025		0.046			5.170	6.530	6.780			9.076	1.415
14	14.720	0.338	13.252	71.690					2.589	5.774	6.620	7.539	9.325	10.282	13.927	2.580
15	11.760	0.386	14.849	73.005	0.068	0.111	0.231	0.892	6.714	8.552	8.682	8.126	9.493	12.773	12.005	0.822
16*	15.960	0.501	16.707	66.832	0.051		0.229			11.700	14.100	15.190			19.843	1.361
17*	16.300	0.623	20.770	62.307	0.104		0.551			14.690	18.500	21.800			32.285	2.082

* (after Thomas, 1986).
% denotes percentage by weight.

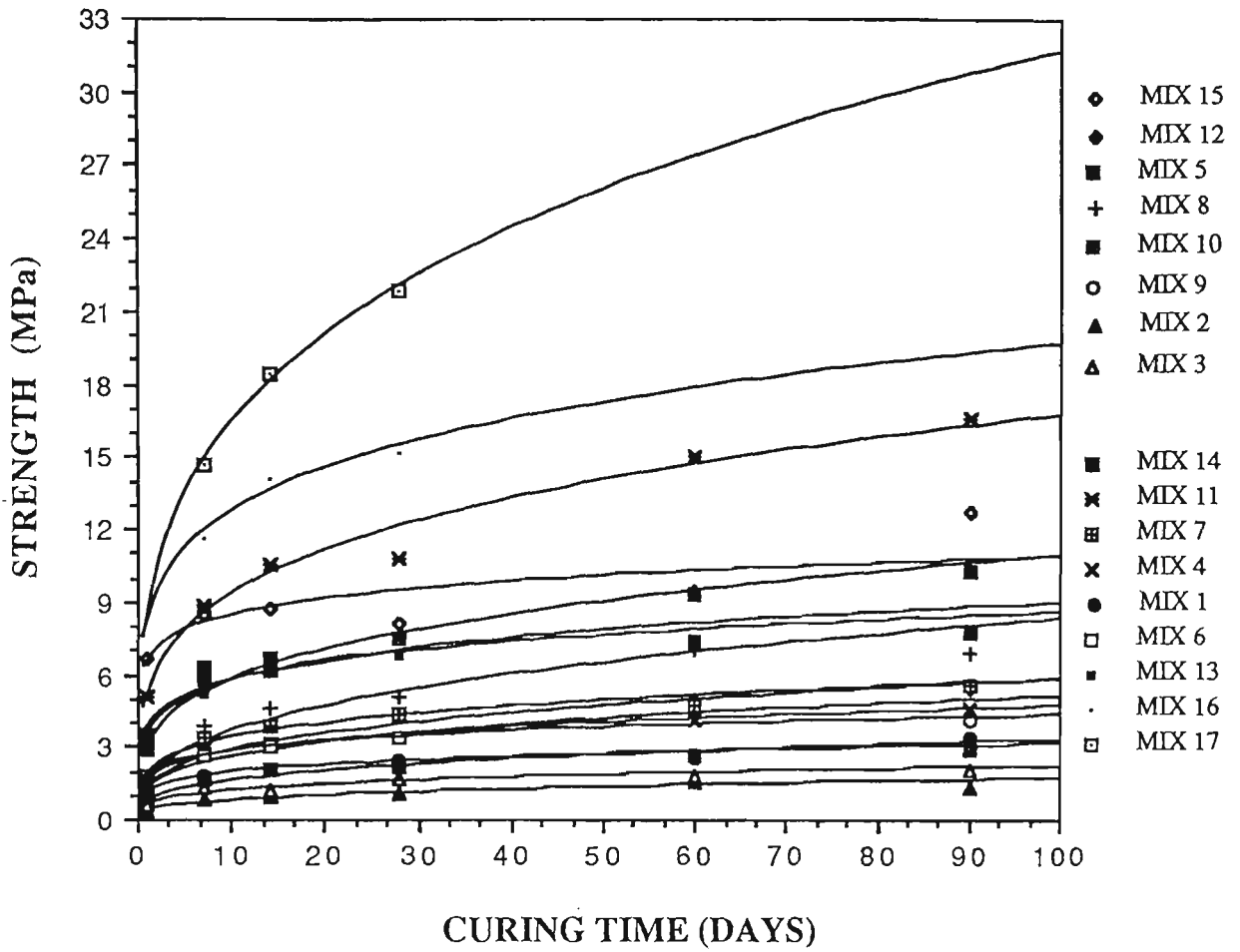


Figure 3.6 Plots of the measured strength against curing time for each mix.

and Helms, 1983; Thomas, 1986; Hii and Aziz, 1986; 1987a; 1987b; 1987c). However, it has been expected that after a critical value, a further increase in the curing time will not result in any significant change in the strength of a mix. It is apparent that the form of the curve is somewhat a typical one for concrete and it is a function of the cement chemistry of the material. The relationship between the strength S and curing time t of a mix may be described by the following equation:

$$S = A \cdot \exp(-B/f(t)) \quad (3.1)$$

where

A and B are unknown positive parameters;

$f(t)$ is a monotone increasing function of t .

In this case, constant A corresponds to the strength when the curing time tends to be infinitive, i.e. the final strength; and constant B describes the increasing rate of the strength with the curing time of a mix. For simplicity, $f(t)$ can be written as:

$$f(t)=t^n \quad (n>0) \quad (3.2)$$

Substituting eqn.(3.2) into eqn.(3.1) gives

$$S=A \cdot \exp(-B/t^n) \quad (3.3)$$

The values of constants A, B and n can be determined by optimising the fit of eqn.(3.3) to the measured data in Table 3.1 for each mix. This may have to involve a non-linear regression procedure, which is not so convenient in practice. Eqn.(3.3) can be rewritten as:

$$\ln S = \ln A - B/t^n \quad (3.4)$$

If n is a constant for any mix, the values of constants A and B can then be obtained by plotting $\ln S$ against $1/t^n$, different values of n have been tried for the data in Table 3.1. As shown in Figure 3.7, satisfactory fits can be obtained when n is equal to 0.5 though it may not be the optimum value. Figures 3.8 through 3.11 show the plot of $\ln S$ against $1/\sqrt{t}$ for different mixes. The values of constants A and B for each mix are included in Table 3.1, and the correlation coefficients for all the mixes are greater than 0.97. It is, therefore, concluded that the relationship between the strength and curing time of a mix can be accurately described by:

$$S=A \cdot \exp(-B/t^{0.5}) \quad (3.5)$$

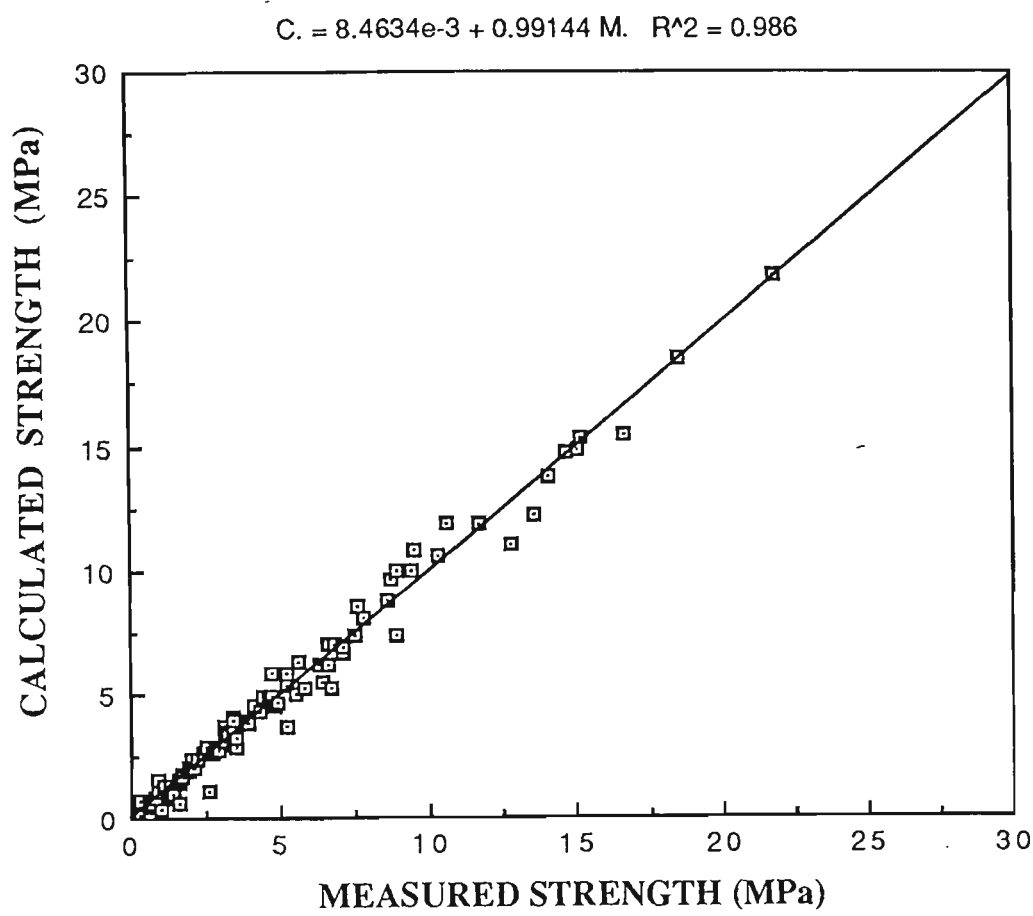


Figure 3.7 Comparison between calculated and measured strength.

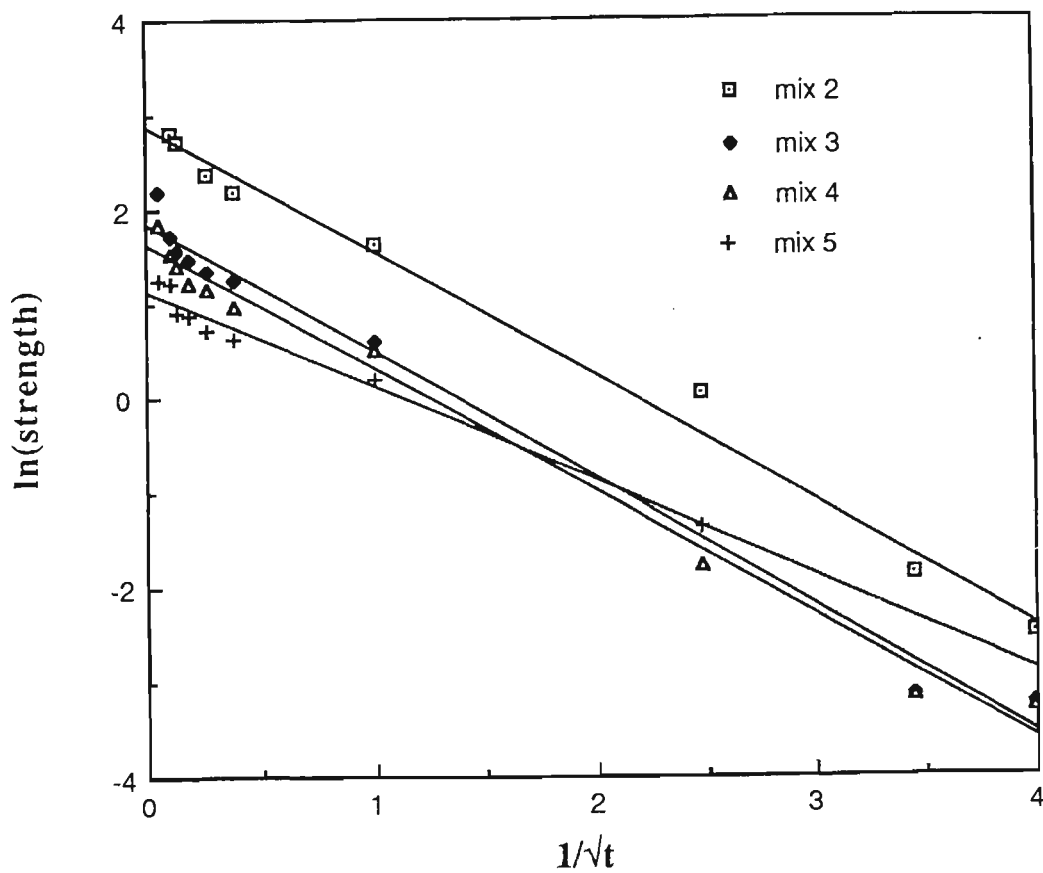


Figure 3.8 Plots of $\ln S$ against $1/\sqrt{t}$ for mixes 2 through 5.

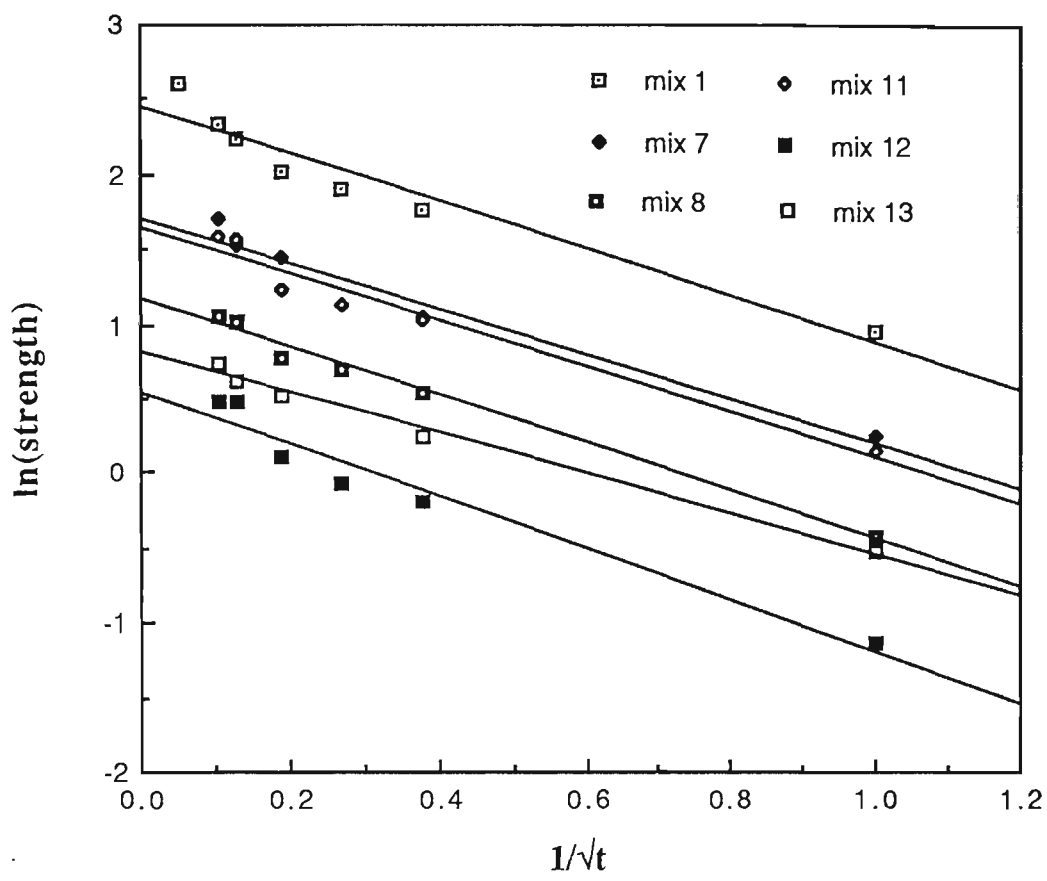


Figure 3.9 Plots of $\ln S$ against $1/\sqrt{t}$ for mixes 1, 7, 8, 11, 12 and 13.

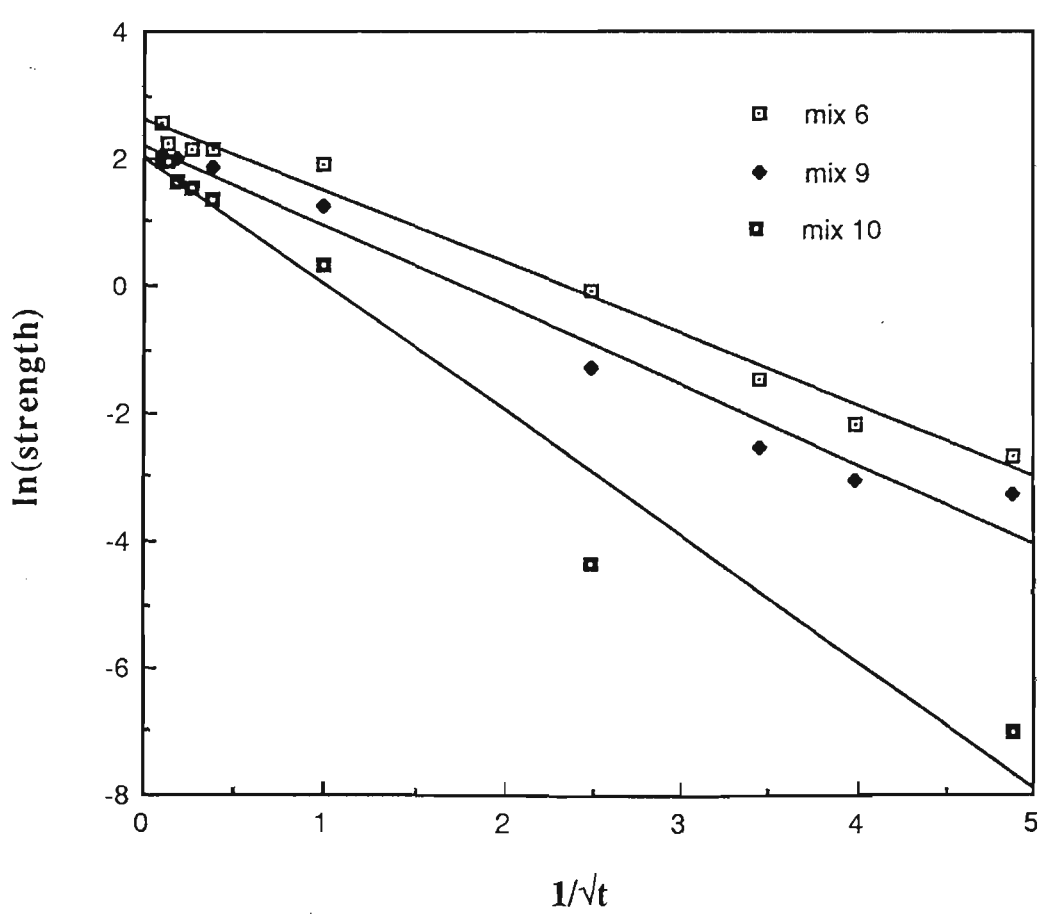


Figure 3.10 Plots of $\ln S$ against $1/\sqrt{t}$ for mixes 6, 9 and 10.

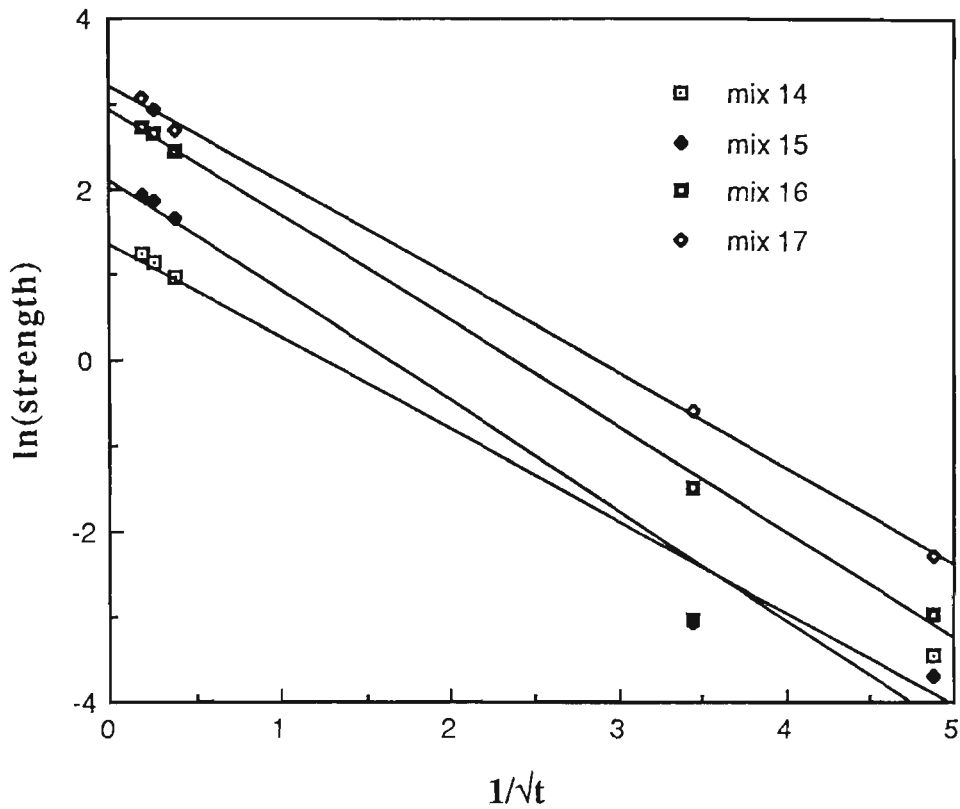


Figure 3.11 Plots of $\ln S$ against $1/\sqrt{t}$ for mixes 14 through 17.

Once the constants A and B in eqn.(3.5) are known, the strength S of a mix at any curing time t can be calculated. In this way, the relationship between the strength and the compositions of mixes at any given curing time can be further discussed as shown in Section 3.3.3.

3.3.3 Optimum design of CCWR material

The strength of a mix at any given curing time will depend on the compositions in the mix provided that other conditions, for examples, compaction, materials used and so on are unchanging. The variables which may affect the strength of CCWR material should be considered to be the mass percentages of water, calcium chloride accelerator CaCl_2 , OPC and coal washery refuse, which are

herein represented by X_1 , X_2 , X_3 and X_4 respectively. These variables, when summed up together, should satisfy the constraint:

$$X_1 + X_2 + X_3 + X_4 = 100 \quad (3.6)$$

Note that the ratio of the mass percents between CaCl_2 and OPC is a constant in the experiment, i.e.,

$$\frac{X_2}{X_3} = \text{constant}. \quad (3.7)$$

Therefore, there are only two independent variables:

$$R_1 = \frac{X_1}{X_3 + X_4} \quad (3.8)$$

$$R_2 = \frac{X_3}{X_4} \quad (3.9)$$

Obviously the increase in R_1 and R_2 means the increase of relative quantities of water content and OPC respectively. Once R_1 and R_2 are known, from eqns.(3.6) to (3.9) the mass percents of X_1 , X_2 , X_3 and X_4 can be calculated by the following equations:

$$X_1 = (R_2 + 1)R_1X_4$$

$$X_2 = 0.03X_3$$

$$X_3 = R_2X_4 \quad (3.10)$$

$$X_4[(1 + R_2)R_1 + 1.03R_2 + 1] = 100$$

The strength of a mix is therefore a function of R_1 and R_2 , which can only be determined empirically. For convenience, the form of the empirical function was chosen as:

$$S = k \cdot R_1^m R_2^n \quad (3.11)$$

where k , m and n are unknown parameters, which will be determined from the fit of eqn.(3.11) to measured data. As mentioned earlier, the strength of a mix at any given curing time can be calculated by eqn.(3.5). However, the strength at the curing time of 28 days is usually used as a standard. Therefore, the dependence of the strength at 28 days on the compositions of a mix will be discussed, and this is then compared with that at infinite curing time, the final strength. The data used for the calculations have been included in Table 3.1.

As eqn.(3.11) can be rewritten as:

$$\ln S = \ln k + m \cdot \ln R_1 + n \cdot \ln R_2 \quad (3.12)$$

the values of parameters k , m and n can then be obtained by linear regression. The strength of a mix at 28 day curing time and its final strength can be calculated by eqns.(3.13) and (3.14) respectively, the correlation coefficients of which are 0.984 and 0.980 respectively. It is obvious from Figure 3.12 that both the calculated and measured strengths are in good agreement.

$$S_{28d} = 2.776 \cdot R_1^{-2.313} R_2^{1.597} \quad (3.13)$$

$$S_{\text{final}} = 4.486 \cdot R_1^{-2.238} R_2^{1.596} \quad (3.14)$$

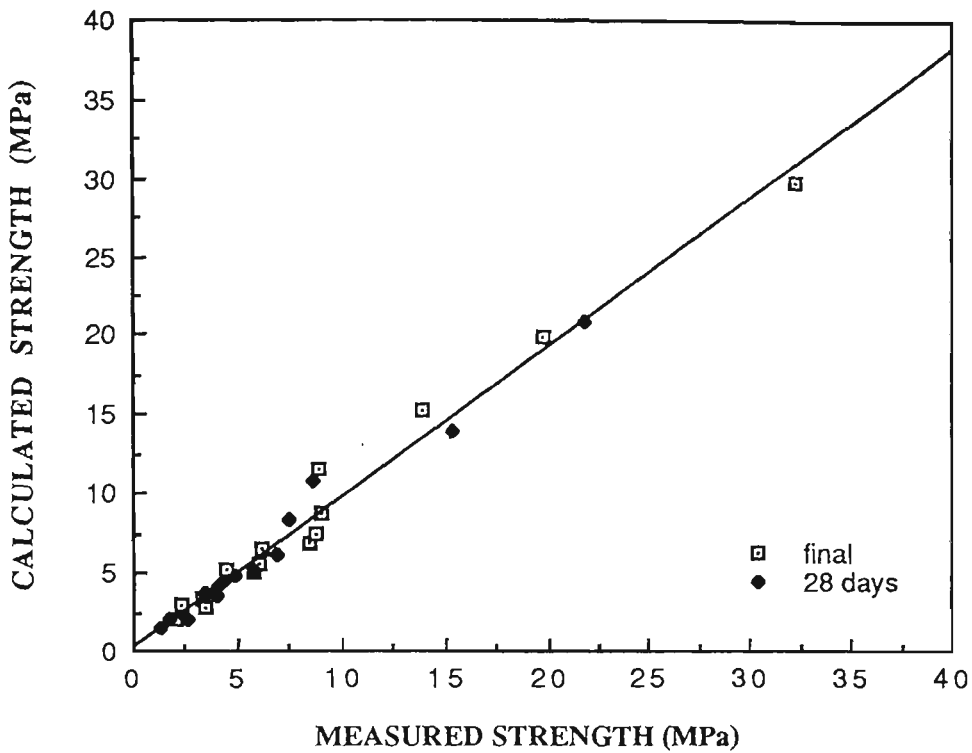


Figure 3.12 Comparison between the measured strength and the calculated (by eqns. (13) and (14)) strength.

The effect of the water content on the strength of a mix has been studied (Smith, 1967; Teychenne et al, 1975; Knissel and Helms, 1983; Loo and Weragama, 1985; Hii and Aziz, 1987c) and it has been found that an increase in the effective water results in a decrease in the strength. On the other hand, it has also been reported that a decrease in the aggregate to cement ratio may increase the strength of a mix (Smith, 1967; Loo and Ahmad, 1982). Actually, the effects of the compositions on the strength of a mix can be easily discussed from eqn.(3.13) or (3.14). As shown in Figures 3.13 and 3.14, an increase in strength of CCWR materials can be obtained either by decreasing the water content or increasing ratio of the mass percentage between OPC and coal washery refuse in mixes, which is similar to other concretes (Smith, 1967 and Loo and Weragama, 1985).

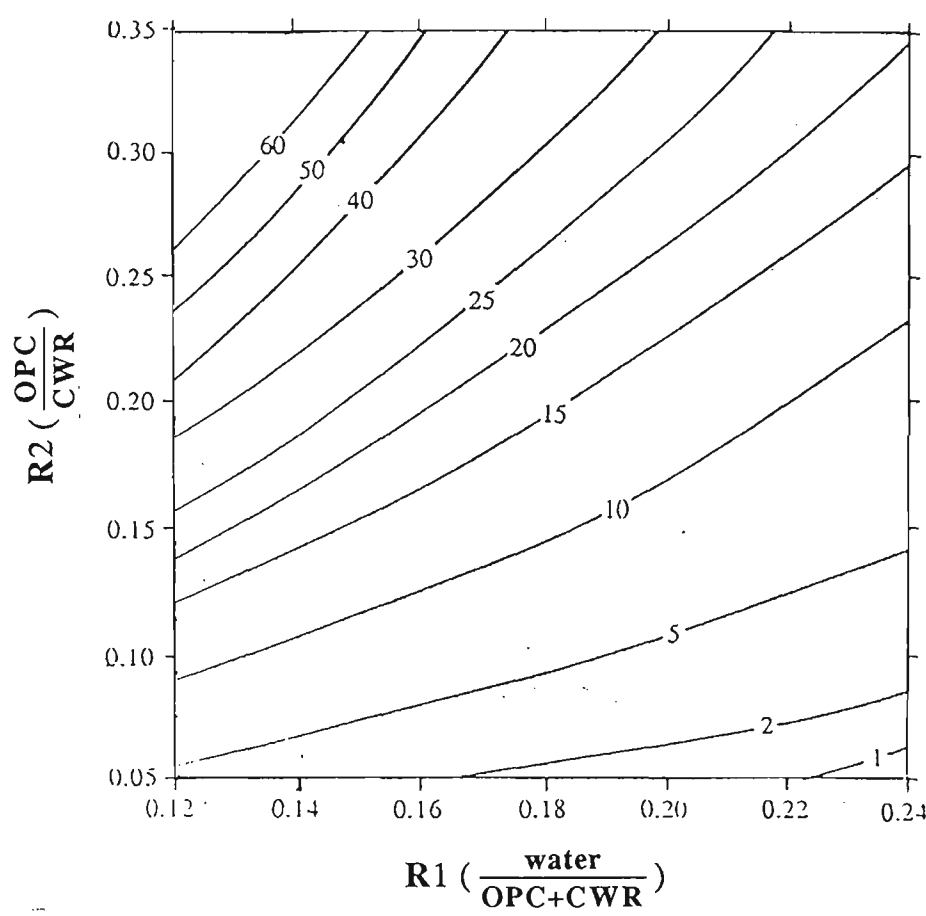


Figure 3.13 Final strength contour plots.

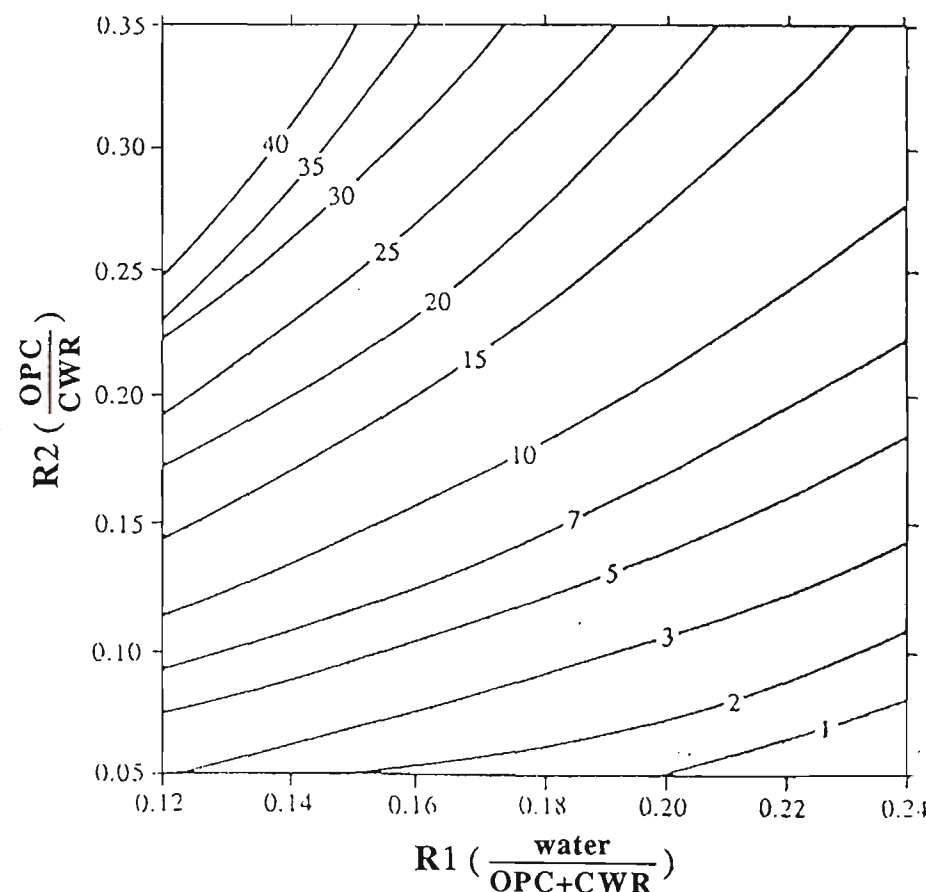


Figure 3.14 Contour plots for 28 day strength.

However, it should be pointed out that the "interaction" between R_1 and R_2 can not be ignored. For example, as shown in Figures 3.15 and 3.16, a decrease in R_1 can result in a significant change in the strength when R_2 is large but not much change when R_2 is small; and the effect of R_2 on strength is also dependent on the value of R_1 (see Figures 3.17 and 3.18).

3.4 APPLICATION OF THE EXPERIMENTAL DESIGN WITH MIXTURES

Response surface methodology was developed by Box and his colleagues (Box and Wilson, 1951; Box, 1954; Box and Youle, 1955; Box and Hunter, 1957) to explore relationships such as those between the yield of a chemical process and the pertinent process variables. In its usual form, response surface methodology exploits the relationship between a response variable and a set of input variables over a current region of interest. Since its introduction in the early 1950's, response surface methodology has become an acceptable and widely used set of concepts and techniques.

However, unlike the usual response surface problem where the concomitant variables represent quantitative amount, in the mixture problem the components represent proportions of a mixture or composition. These proportions must be non-negative and if expressed as fractions of the mixtures, they must sum to unity. For example, suppose there are n components in the system under study. If the proportion of the i 'th component in the mixture is represented by X_i , then:

$$X_i \geq 0 \quad (1 < i < n), \quad \sum_{i=1}^n X_i = 1 \quad (3.15)$$

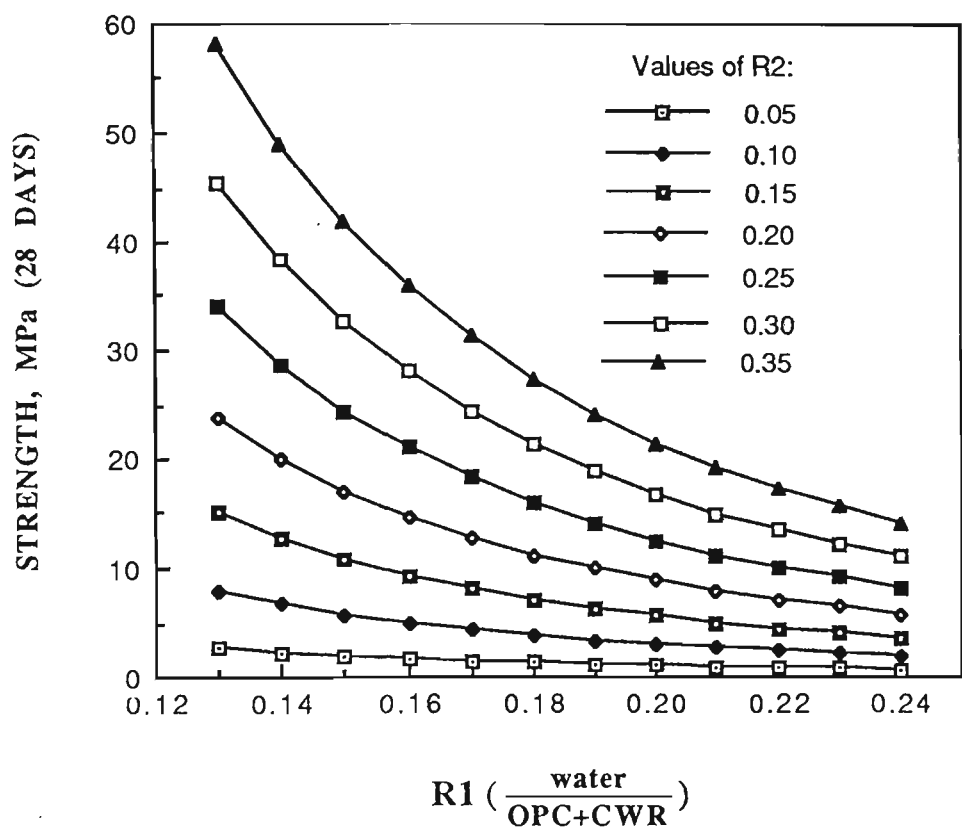


Figure 3.15 The dependence of the strength on R1 for different R2 (28 day strength).

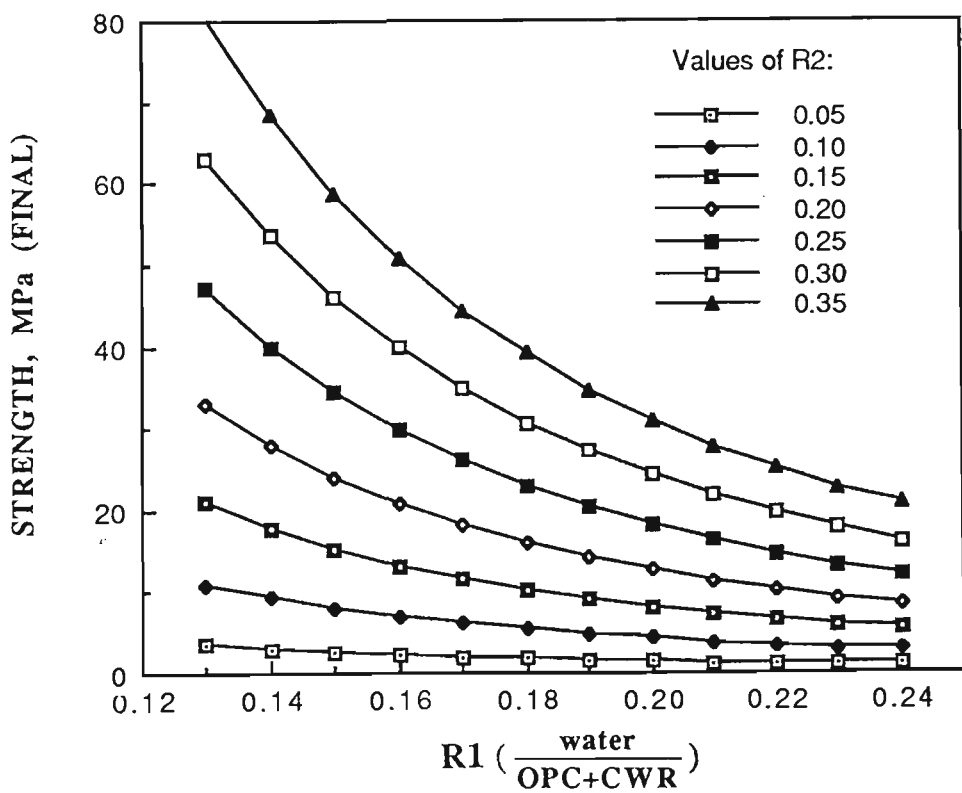


Figure 3.16 The dependence of the strength on R1 for different R2 (Final strength).

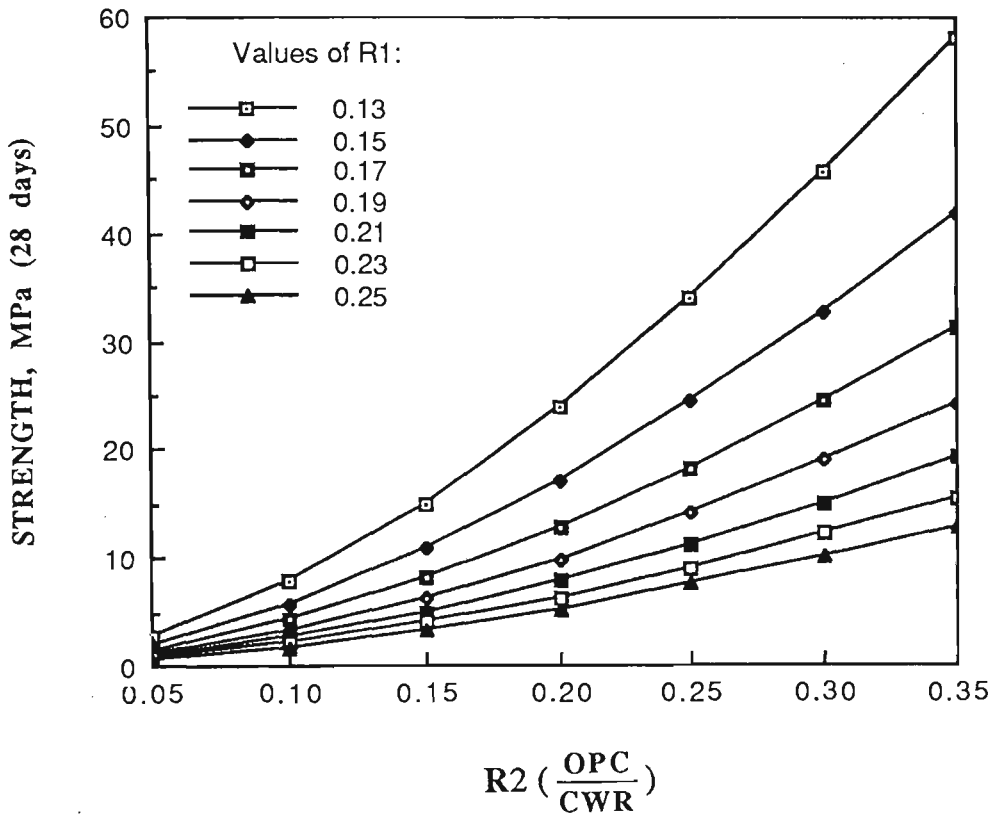


Figure 3.17 The dependence of the strength on R2 for different R1 (28 day strength).

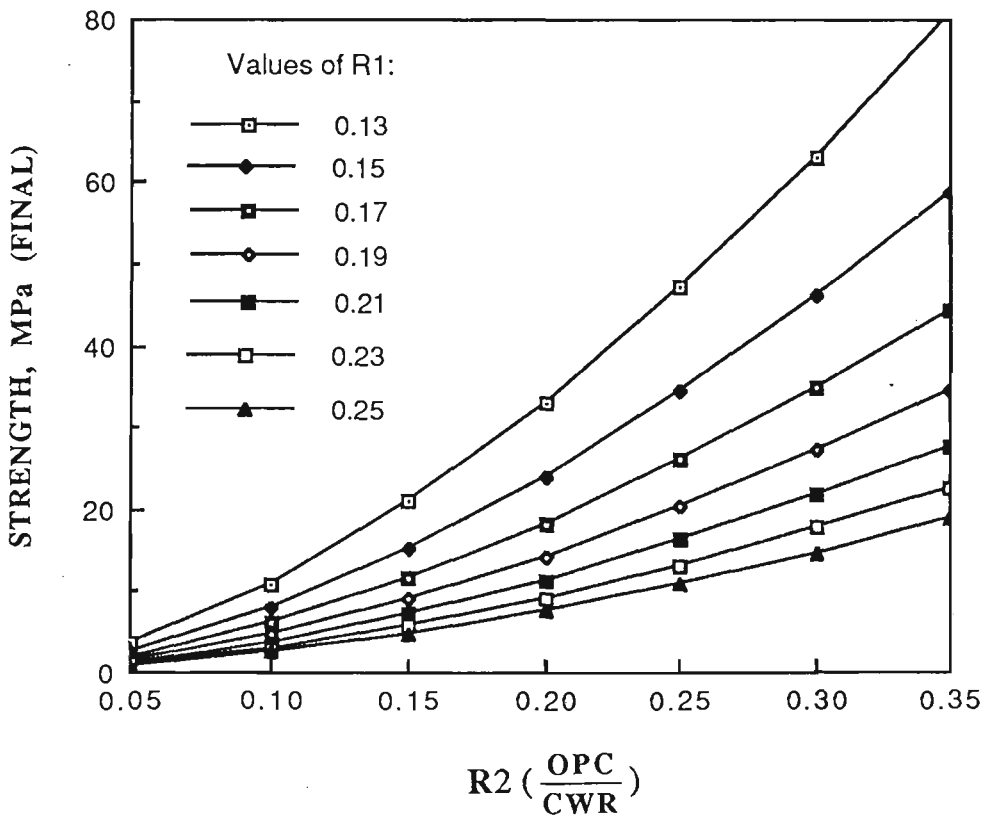


Figure 3.18 The dependence of the strength on R2 for different R1 (Final strength).

A mixture experiment is an experiment in which the response is only a function of the proportions of the components (constituents) present in the mixture and is not a function of total amount of the mixture. The general purpose of mixture experimentation is to make possible estimates through a response surface exploration of the properties of an inter-multicomponent system from only a limited number of observations. These observations are taken at preselected combination of the components (resulting in the mixture) in an attempt to determine which of the combination in some sense maximize the response.

Since the proportion X_i could be a unity, a mixture may be considered as entirely being consisted of only one component. Claringbold (1955) made use of the fact that the design region for mixture is the $(n-1)$ dimensional simplex. Rather than transforming components, Scheffé (1958) suggested modifying the usual polynomial model in the X_i 's to reflect the restrictions (3.15). Since then, as reviewed and summarized by Cornell (1981) great progress has been achieved and various experimental designs with mixtures have been proposed.

As discussed above, the design of CCWR materials is obviously one of the problems encountered in the experimental design with mixtures. To date the optimum design of CCWR materials is still based on the empirical approach. Considering the experimental cost and the time spent, one is naturally prompted to enquire whether there are any method which may cost you less and give you an immediate understanding of the effects of the compositions on the strength or other properties of mixes. It is postulated that the theory of experimental designs with mixtures can solve this problem. The present approach, though the experimental design has not been directly used, could be regarded as a successful example of the response surface methodology.

3.5 DEVELOPMENT OF A NEW YIELD FUNCTION FOR CCWR MATERIAL

The development of powerful finite element codes for analysing the stability of underground pack structures has very much stimulated the interest in constitutive laws for pack materials. At present, a considerable number of models such as the Drucker-Prager model (1952), and the Hoek and Brown model (1982) can be used to describe the strength and yield characteristics of pack materials under different loading conditions. Complex models such as those due to Pramono and Willam (1989) and Chen and Buyukozturk (1985) have also been developed. However, these models require complex experiments to determine the model parameters.

Based on the results of routine material strength tests (Hii and Aziz, 1987a), a logarithmic yield function which has been used by Tong and Wu (1985) to simulate the load-deformation behaviour of soft rocks is proposed for predicting the strength and yield characteristics of CCWR materials. The procedure for determining the parameters contained in the yield function is shown in Sections 3.5.1 and 3.5.2. It has been demonstrated that the proposed logarithmic yield function can predict the strength and yield characteristics of CCWR materials in a satisfactory manner.

3.5.1 General form of the yield function

The general form of the proposed yield function can be expressed as follows:

$$\sigma_1 = A + B \ln(\sigma_3 + C) \quad (3.16)$$

where

σ_1 = major principal stress;

σ_3 = minor principal stress; and

A, B, C = parameters to be considered by experiments.

3.5.2 Determination of parameters in the yield function

A numerical procedure has been developed to determine parameters A, B and C in the proposed yield function (eq.3.16). This procedure minimizes the error between the predicted and measured triaxial strength values. The error can be expressed as follows:

$$Q = \sum_{i=1}^N \left(\sigma_{1i}(\sigma_{3i}) - \sigma_{1i}^*(\sigma_{3i}) \right)^2 = F(A, B, C) \quad (3.17)$$

where

σ_{3i} = minor principal stress;

$\sigma_{1i}(\sigma_{3i})$ = predicted major principal stress under minor principal stress σ_{3i} condition;

$\sigma_{1i}^*(\sigma_{3i})$ = experimental major principal stress under minor principal stress σ_{3i} condition; and

N = number of triaxial tests.

To minimize the error Q, let

$$\frac{\partial Q}{\partial A} = \frac{\partial Q}{\partial B} = \frac{\partial Q}{\partial C} = 0 \quad (3.18)$$

Substitution of eq.3.16 into eq.3.18 produces:

$$NA + \left(\sum \ln(\sigma_{3i} + C) \right) B = \sum \sigma_{1i}^* \quad (3.19a)$$

$$\left(\sum \ln(\sigma_{3i} + C) \right) A + \left(\sum \ln^2(\sigma_{3i} + C) \right) B = \sum \ln(\sigma_{3i} + C) \sigma_{1i}^* \quad (3.19b)$$

$$\left(\sum \frac{1}{\sigma_{3i} + C} \right) A + \left(\sum \frac{\ln(\sigma_{3i} + C)}{\sigma_{3i} + C} \right) B = \sum \left(\frac{1}{\sigma_{3i} + C} \sigma_{1i}^* \right) \quad (3.19c)$$

From eqs.3.19a and 3.19b, parameters A and B can be expressed as:

$$A(C) = (B_1 A_{22} - B_2 A_{12}) \frac{1}{T_4} \quad (3.20a)$$

$$B(C) = (B_2 A_{11} - B_1 A_{12}) \frac{1}{T_4} \quad (3.20b)$$

where

$$A_{11} = N;$$

$$A_{12} = \sum \ln(\sigma_{3i} + C);$$

$$A_{22} = \sum \ln^2(\sigma_{3i} + C);$$

$$B_1 = \sum \sigma_{1i}^* ;$$

$$B_2 = \sum \ln(\sigma_{3i} + C) \sigma_{1i}^* ; \text{ and}$$

$$T_4 = (A_{11}A_{22} - A_{12}A_{21})^{-1}.$$

Substituting eq.3.20 into eq.3.19c and rewriting the equation, we can obtain:

$$F(C) = \left(\sum \frac{1}{\sigma_{3i} + C} \right) A(C) + \left(\sum \frac{\ln(\sigma_{3i} + C)}{\sigma_{3i} + C} \right) B(C) - \sum \left(\frac{1}{\sigma_{3i} + C} \sigma_{1i}^* \right) \quad (3.21)$$

By using a numerical procedure, the value of C can be evaluated from eq.3.21. Once C is determined, A and B can be computed using eq.3.20.

3.5.3 The procedure for the computation of parameters A , B and C

The procedure for the computation of parameters A , B and C is listed as follows (see Figure 3.19):

- (1) select $C_e > C_o$, which satisfies $F(C_o) \cdot F(C_e) < 0$;
- (2) let $D = C_e - C_o$, if $D < E_{ps}$, then GOTO (4);
- (3) let $C_m = C_o + (D / 2)$, if $F(C_o) \cdot F(C_m) < 0$, then
 $C_e = C_m$, otherwise $C_o = C_m$, then GOTO (2);
- (4) let $C = C_o + F(C_o) \cdot D / (F(C_o) - F(C_e))$; and
- (5) compute the values of parameters A and B using eq.3.20.

where E_{ps} denotes the allowable tolerance.

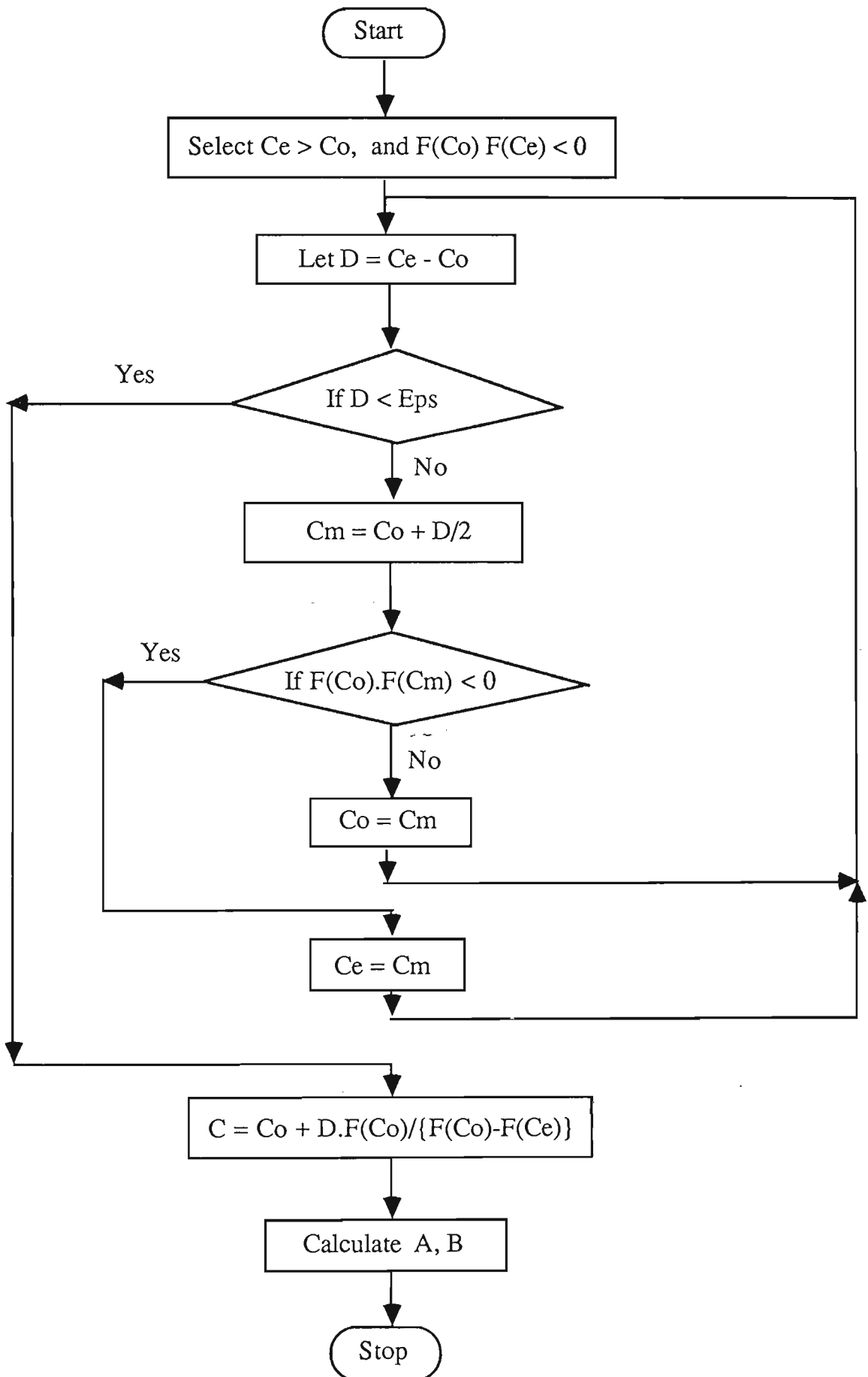


Figure 3.19 Flow chart for logarithmic yield function program.

CHAPTER FOUR

EXPERIMENTAL INVESTIGATIONS

CHAPTER 4

EXPERIMENTAL INVESTIGATIONS

4.0 INTRODUCTION

The main purpose of the experimental investigations is to develop a fill material, which utilizes CWR, for strata control in Australian underground coal mining operations. CWR is currently being developed as a fill material in many countries. Previous works by Knissel and Helms (1983), Atkins et al. (1984, 1986, 1987), Singh et al. (1985), Thomas (1986), Sleeman (1987), Zadeh et al. (1987), Bros (1987), Ruban and Shpirt (1987), Leininger et al. (1987), Senyur (1989), Thomas et al. (1989) and others have provided information on the properties and utilization of coal mining wastes with or without cement and various additives. However, only a few data on the mechanical properties and behaviour of CCWR material containing minus 10mm CWR have been published.

Experimental investigations have been undertaken to study the mechanical properties and behaviour of CCWR material. The mechanical properties evaluation of CCWR material is an important step in the development and utilization of CWR for strata control in Australian underground coal mining operations. In order to determine the mechanical properties of CCWR material, a computerized strength testing system capable of high speed data acquisition and further data processing is being developed (Hii and Standish, 1989, Hii and Aziz, 1989). The methodology and the strength testing system were tested prior to experimental investigations. These tests were designed to investigate and ensure that reliable results could be obtained from the strength testing system. A generalized approach to the analysis of

the deformation properties of CCWR material has been developed which permits an integrated analysis of geotechnical measurements in the development of CCWR material. The following sections detail the development of the experimental method used in the experimental programme.

Details of a set of standard quantities and conditions used in the preparation and the testing of CCWR material specimens are presented in this Chapter.

4.1 Material Used in the Experiments

Type A Portland cement, minus 10mm CWR and calcium chloride set accelerator were used in making the test specimens. Each of these materials will be described in details in the following sub-sections. Other materials used for the purpose of calibrating the flow-tube, used in the flow experiment, were four oil samples (details of the flow experiment are given in Section 4.6). The four oil samples were obtained from the Research and Development Department of Ampol. The gradings and physical properties of oil samples are presented in Table 4.1.

4.1.1 Sampling and collection of CWR

A selected CWR (from the coal washery, West Cliff Colliery, Appin, NSW, Australia) is the major constituent of the test specimens. A model of West Cliff coal washery is shown in Figure 4.1. Sampling of the coal washery refuse took place on seven consecutive weekdays. Samples were taken three to four times a day by stopping the refuse conveyor belt and taking the CWR from a suitable length by the full width of the conveyor belt as illustrated in Figure 4.2. Care was taken to retain any fine CWR by scraping or otherwise removing it from the conveyor belt and adding it to the sample. The sampling operations were conducted

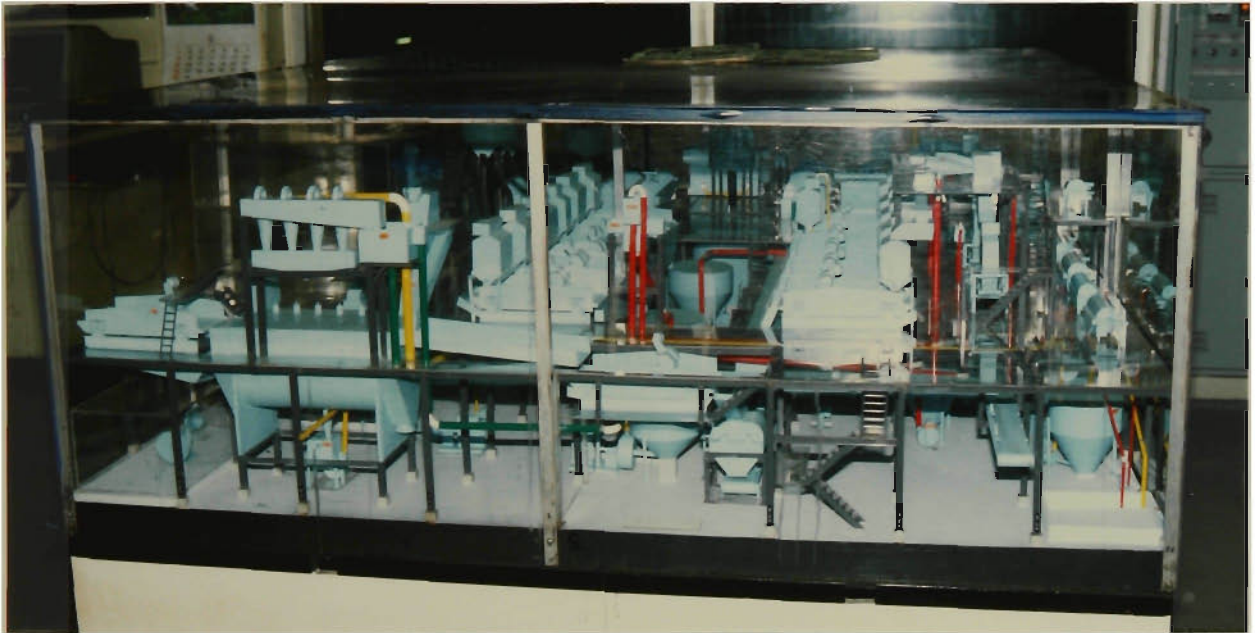


Figure 4.1 Model of West Cliff coal washery.



Figure 4.2 Collection of CWR sample.

with the aim to ensure that the samples obtained represent, as far as possible, the true nature and condition of the bulk of coal washery refuse from which they were drawn.

Table 4.1 Physical properties of oil samples.

Sample Type	Viscosity ♦ @ 100 °C (cSt)	Viscosity ♦ @ 40 °C (cSt)	Viscosity Index ⊗
80 SN	3.35	14.03	110
500 SN	10.35	88.55	98
160 BS	31.91	488.60	96
190/210 P	40.68	1339.00	39

♦ Tests conducted in accordance with ASTM D445.

⊗ Tests conducted in accordance with ASTM D567.

4.1.2 Processing of CWR

The sample-increments collected were re-combined to form bulk samples, then reduced by sample division to form the samples which were sieved through a standard 10mm sieve. The oversize CWR was passed through a small jaw crusher and the crushed CWR was re-screened. The oversize material was rejected (this constituted some 15.0% of the feed but could be reduced by more extensive crushing in practice). The processed CWR was then used for making the test specimens. The main purpose of processing the CWR was to produce a minus

10mm product which was necessary for the ultimate placement by pneumatic and high-density hydraulic conveying.

4.1.3 Grain size analysis of CWR using mechanical method

The grain size analysis was performed in accordance with AS 1289 C 6.1-1977 standard method of sieving analysis to determine the relative proportions of different grain sizes which made up a given mass of the CWR. It is realized that the sample is actually a statistical representation of the mass of the CWR. However, it is difficult to determine the individual sizes of CWR. It is, therefore, cautioned that the test can only bracket the various ranges of sizes. Figures 4.3 and 4.4 show typical grain shapes of West Cliff CWR.

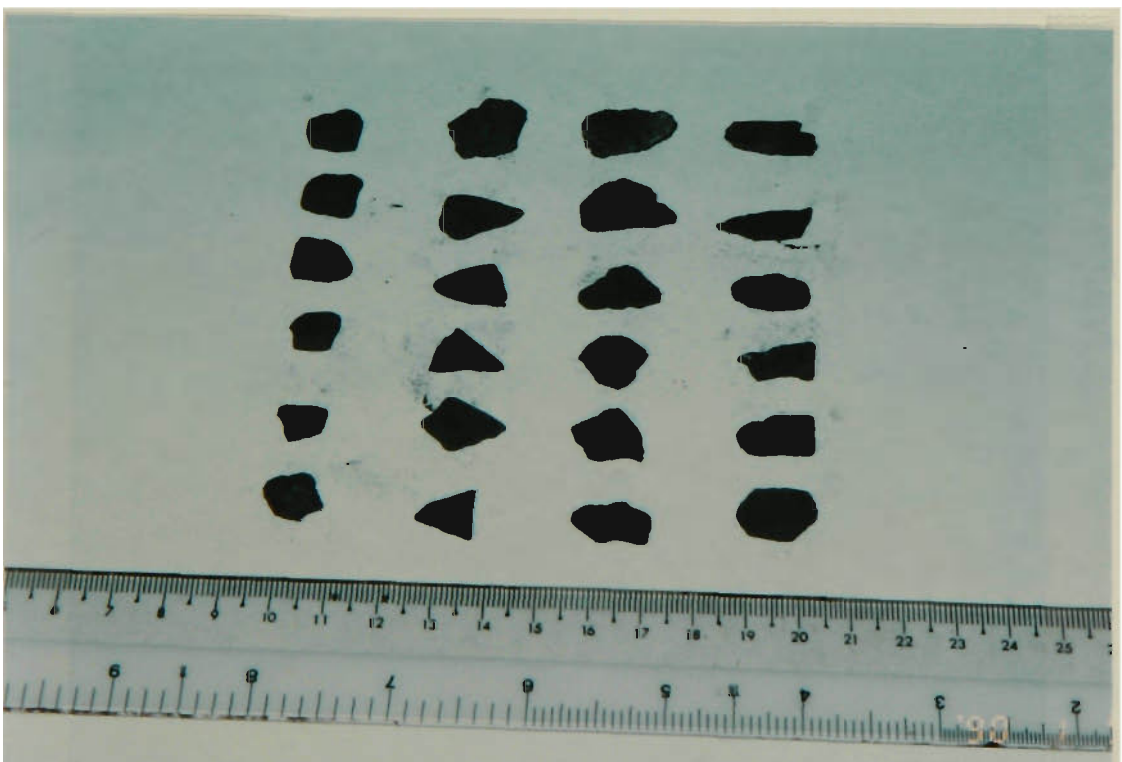


Figure 4.3 Typical grain shapes of West Cliff CWR

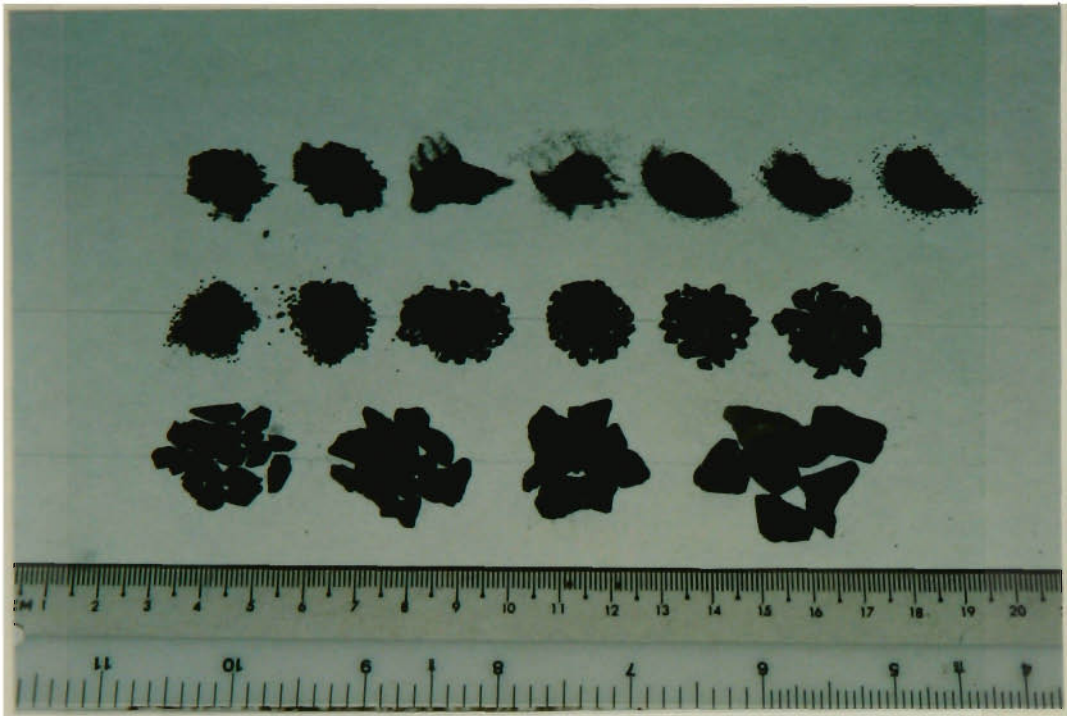


Figure 4.4 Grain shapes of West Cliff CWR.

Figure 4.5 shows the grain size distribution curves of the processed CWR. The relative density of the processed CWR was measured using Beckman Model 930 air comparison pycnometer and found to be 2.31. This value is comparable to that obtained by Thomas (1986) for a different sample where the relative density was found to be 2.54, also measured using Beckman Model 930 air comparison pycnometer.

4.1.4 X-ray diffraction analysis

Chemical composition analyses of West Cliff CWR were carried out with the help of the staff in the Departments of Geology and Chemistry, The University of Wollongong.

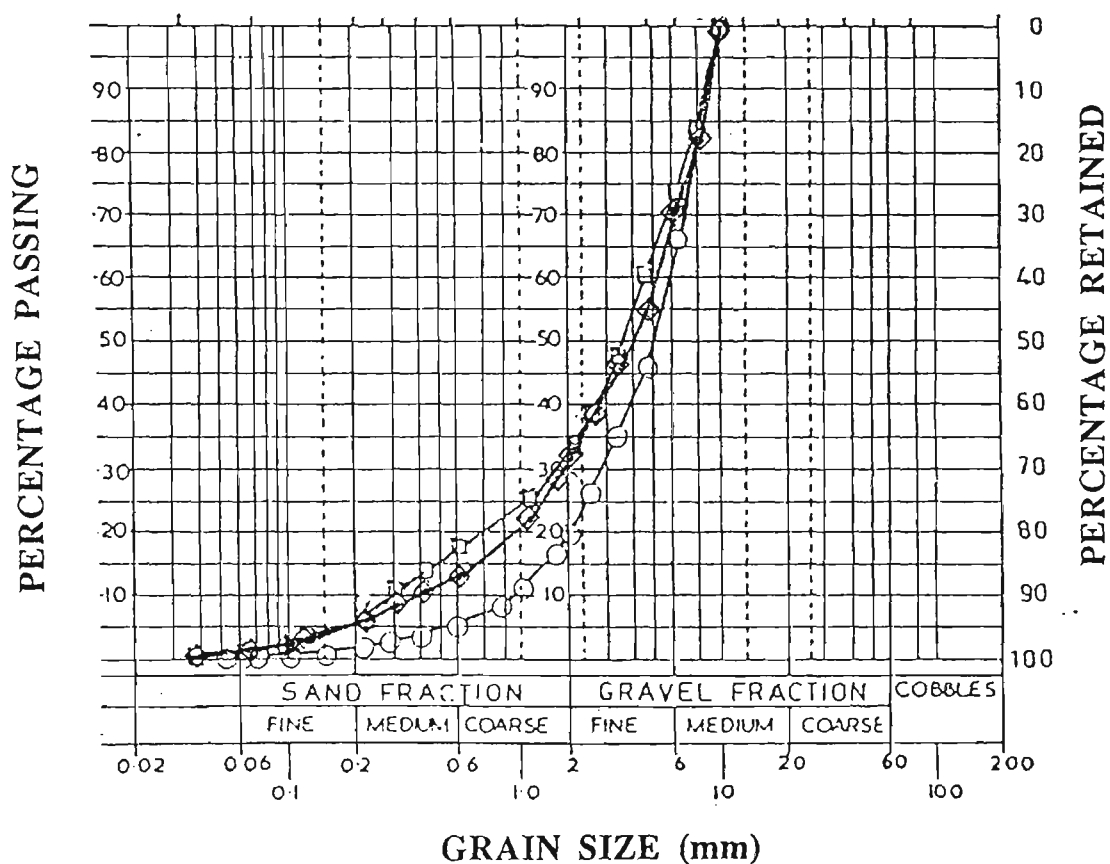


Figure 4.5 Grain size distribution curves of the processed coal washery refuse.

4.1.5 Ordinary Portland cement

Type A Portland cement used in the making of CCWR material specimens was supplied by Blue Circle Southern. An attempt has been made to find the moisture content of the Portland cement, however, the results revealed that the cement was very dry. The chemical and mineralogical compositions of Type A Portland cement is shown in Table 4.2.

Table 4.2 Chemical and mineralogical compositions of Type A Portland cement.

<u>Chemical Compositions</u>	
SiO ₂	22.2%
Al ₂ O ₃	4.8%
Fe ₂ O ₃	4.2%
CaO	64.9%
MgO	1.1%
SO ₃	2.9%
Loss on ignition	1.2%
Free CaO	1.1%
Insoluble residue	0.0%
Sulphuric Anhydrite	2.9%
<u>Mineralogical compositions</u>	
C ₃ S	64.0%
C ₂ S	10.0%
C ₃ A	6.0%
C ₄ AF	13.0%

4.1.6 Calcium chloride

The set accelerator used was 959 calcium chloride. The specification of 959 calcium chloride is detailed below.

959 calcium chloride, dried.

3-8 mesh.

$\text{CaCl}_2 = 110.98$

Assay 85.0% min.

Maximum limits of impurities.

Sulphate $\text{SO}_4 = 0.05\%$

Iron Fe = 0.02%

Merck Art 2382, a high grade calcium chloride-2-hydrat krist was also used, in a view to determine more accurately the mass percentage of the set accelerator used in the mix formulation. The specification of Merck Art 2382 calcium chloride-2-hydrat krist is detailed below.

$\text{CaCl}_2 \cdot 2\text{H}_2\text{O}$	min 99.5%
PH	4.5-6.5
So_4	max 0.005%
N	max 0.005%
Pb	max 0.0005%
Fe	max 0.0003%
Mg	max 0.005%
Sr	max 0.05%
Ba	max 0.003%
K	max 0.01%

(M = 147.02 g/mol)

4.2 OUTLINE OF THE EXPERIMENTAL PROGRAMME

The experimental programme was conducted in six series of tests which are listed chronologically as series I, II, III, IV, V and VI in Table 4.3. All pouring and batching details of CCWR material specimens are presented in Table 4.4. In addition, series VII experiments were conducted to determine the influence of water content on the flow properties of West Cliff CWR. Test procedures for the test series are detailed in Sections 4.3 through 4.9. Test procedures for test series I, II, III and IV have been reported in details (Hii and Aziz, 1986). Tests in series V were carried out generally to AS 1012.13/Amdt 1/1986-12-05 - Method for the Determination of Drying Shrinkage of Concrete.

Series I experiments were on unconfined compressive strength tests of CCWR material specimens with both lengths and diameters of 102.5mm. Series II, III and IV experiments were on indirect tensile strength tests, triaxial strength (confined compressive strength) tests and unconfined compressive strength tests respectively of CCWR material specimens with the standard NX size. Series V experiments were on the effect of water content on the drying shrinkage of CCWR material and are reported in section 4.7. Series VI experiments were on the influence of geometry on the strength and the elasticity of CCWR material models and are reported in section 4.8.

Test series I was designed to investigate the strength development with respect to time under uniaxial stress conditions of mixes of minus 10mm West Cliff CWR, calcium chloride set accelerator and Portland cement. The objective of this study was to determine the strength and characteristics of the formulated mixes and to access their suitability for application in strata control under Australian coal mining conditions.

Tests in series II, III and IV experiments were undertaken to develop a new yield function which can predict the strength and yield characteristics of CCWR material in a satisfactory manner. The proposed logarithmic yield function may be used to simulate the load deformation behaviour of CCWR material. Results generated from these three experiments can also provide valuable geotechnical data of CCWR material which are much needed for the design of CCWR pack structures.

Series V experiments were conducted to study the effect of water content on the drying shrinkage of CCWR material specimens. The objective of this study was to quantify the effect of water content, if any, on the drying shrinkage of CCWR material.

Series VI experiments, which were initiated after series I through V had been completed, were conducted to study the effect of geometry on the strength and elasticity of CCWR material. This is a relatively new development in pump packing material research. A special set of moulds were designed to complete these experiments.

Series VII experiments were conducted to determine the optimum water content for flowability of coal washery refuse. The study is detailed in Section 4.8.

All experimental results are evaluated in Chapter five.

Table 4.3 Summary of tests.

Test Series	Description of Tests	Experimental Measurements	Total No. of Tests
I	Unconfined compressive strength tests. (Specimens with both lengths and diameters of 102.5mm).	Force, axial and lateral displacements.	365
II	Indirect tensile strength tests. (The discs were 56mm in diameters and 29mm thick).	Force and displacement.	42
III	Triaxial tests. (Specimens with lengths and diameters of 113mm and 56mm).	Force and displacement.	44
IV	Unconfined compressive strength tests. (Specimens with lengths and diameters of 113mm and 56mm respectively).	Force, axial and lateral displacements.	30
V	Drying Shrinkage tests. (Prisms 75mm x 75mm x approximately 285mm long).	Length.	24
VI	Unconfined compression strength tests. (Specimens with a height of 150mm and diameters of 55.5mm, 75.5mm, 102.8mm, 149.5mm, 206mm, 242mm and 314.5mm)	Force, axial and lateral displacement.	19

Table 4.4(a) Batching and pouring details of various mixes of CCWR materials.

Mix	Date	COAL WASHERY REFUSE				PORTLAND CEMENT		CALCIUM CHLORIDE			Total Water Added (g)	Water Content (Wet basis) (%)	W/C Ratio	Air Temp. (°C)	Slump Test (mm)
		Moist Mass (g)	Dry Mass (g)	Water Content (%)	Mix Composition (%)	Dry Mass (g)	Mix Composition (%)	Moist Mass (g)	Solid Mass (g)	Liquid Contained (g)					
1	31-7-86	60000	57278	4.54	84.4	10588	15.6	317.7	270.0	47.65	11764	14.72	1.1	15.0	110
2	6-8-86	45000	43709	2.87	87.5	6244	12.5	220.4	187.3	33.05	7521	13.0	1.2	15.0	---
3	19-8-86	47000	45247	3.73	90.0	4525	10.0	159.7	135.7	23.96	7985	13.8	1.8	17.0	15
4	21-8-86	47799	46000	3.91	92.5	3730	7.5	131.6	111.9	19.75	7476	12.6	2.0	16.0	10
5	25-8-86	48000	45692	4.81	95.0	2285	5.0	80.6	68.5	12.10	6967	12.0	3.0	16.5	10
6	8-10-87	50000	47717	4.78	85.0	9706	15.0	297.2	252.6	44.60	7690	12.0	0.9	20.0	---
7	14-10-87	48000	46937	2.26	85.0	8283	15.0	292.3	248.5	43.9	13638	21.0	1.6	17.0	C

C denotes collapsed slump.

Table 4.4(b) Batching and pouring details of various mixes of CCWR materials.

Mix	Date	COAL WASHERY REFUSE			PORTLAND CEMENT			CALCIUM CHLORIDE			Total Water Added (g)	Water Content (Wet basis) (%)	W/C Ratio	Air Temp. (°C)	Slump Test (mm)
		Moist Mass (g)	Dry Mass (g)	Water Content (%)	Mix Composition (%)	Dry Mass (g)	Mix Composition (%)	Moist Mass (g)	Solid Mass (g)	Liquid Contained (g)					
8	21-10-87	50000	48876	2.30	90.0	5431	10.0	215.8	162.9	52.9	12877	19.1	2.4	20.0	C
9	28-10-87	50000	48957	2.13	90.0	5440	10.0	216.2	163.2	53.0	7440	12.0	1.4	23.0	0
10	9-11-87	57500	54797	4.93	87.5	7827	12.5	463.6	234.8	228.7	12421	16.5	1.6	22.0	85
11	3-11-87	45000	43555	3.32	87.5	6222	12.5	247.3	186.7	60.6	11811	19.1	1.9	30.0	C
12	5-11-87	50000	47388	5.51	92.5	3842	7.5	152.7	115.3	37.4	12044	19.0	3.1	22.5	C
13	24-11-87	50000	47801	4.60	92.5	3876	7.5	229.5	116.3	113.3	10234	16.5	2.6	24.5	75
14*	27-9-88	125171	120000	2.70	85.5	21176	14.5	1254.1	618.8	635.3	24987	15.0	1.2	24.0	65

C denotes collapsed slump.

*For series VI experiments.

4.3 EXPERIMENTAL EQUIPMENT

Measurements and the correct explication thereof are an essential part of any engineering research and development programme. The measurements must supply reliable information and their meanings must be correctly comprehended. Material property determination using laboratory tests plays a vital role in this research. The successful application of the science of solid mechanics to the practical problems of pack design requires the acquisition and reduction to usable form of large amounts of laboratory data.

In order to facilitate the development and utilization of CWR for strata reinforcement in underground coal mining operations, a computerized strength testing system capable of high speed data acquisition and further data processing has been developed. Computer programmes, written in BASIC, have been developed to control the measurement system and the data logging process, and to facilitate data processing, printing and plotting of test results all with less risk errors. One of the unique features of the language is the incorporation of block structures and the ability to create functions and procedures. BASIC can also handle interrupts within a program, which provides a powerful real-time capability. The mechanical measurement tests performed on this automated system have demonstrated that it is highly reliable in use.

4.3.1 Strength testing system

The servo-controlled strength testing system, Figure 4.6, consists of five units:

- (i) a reaction loading frame,
- (ii) an electronic control console,

- (iii) a hydraulic power pack,
- (iv) a LVDT strain measurement rig and/or strain gauges, and
- (v) a HP 3054A automatic data acquisition and control system.

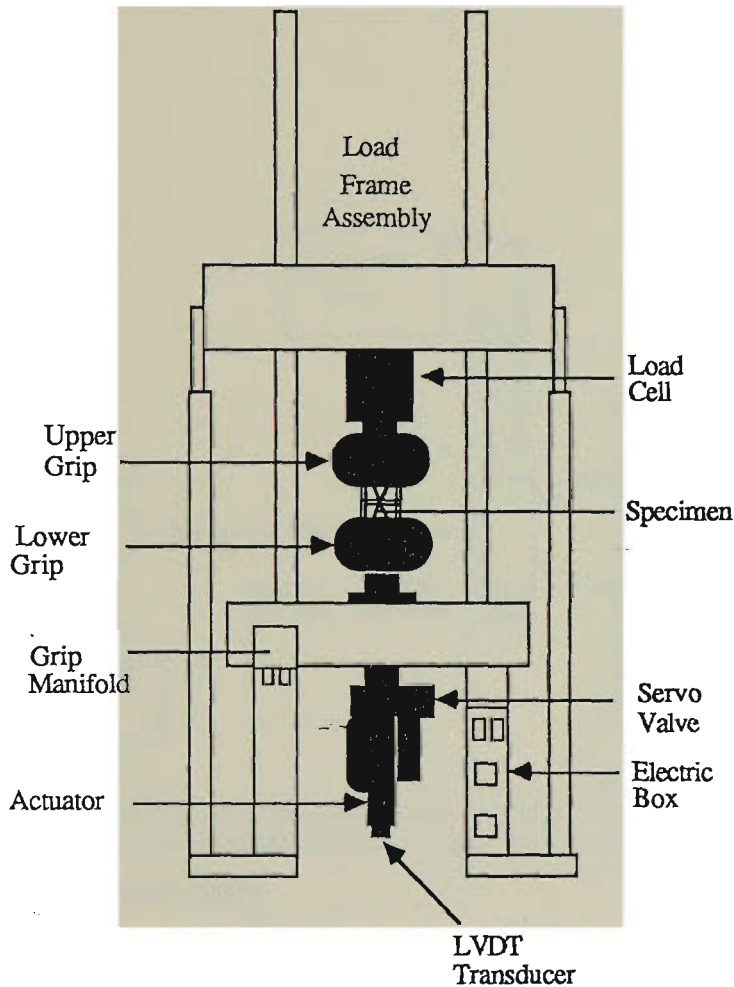


Figure 4.6 The servo controlled stiff testing machine.

4.3.2 Instron 8033 testing machine

An Instron 8033 servo-controlled stiff testing machine is used in this testing system. This machine is microprocessor controlled and a simple keyboard serves as the interface with the operator. Magnetic tape cassettes are used to load the test programmes. The Instron 8033 is capable of applying compressive and tensile loads of 500KN over a working stroke from minus 75mm to plus 75mm with an overall system stiffness greater than 1060 KN/mm. The control console provides the necessary feedback control to enable closed-loop servo-controlled

testing to be performed. The program controls the microprocessor to process data, and to control the flow of information to and from memory and input/output devices as shown in the block diagram in Figure 4.7.

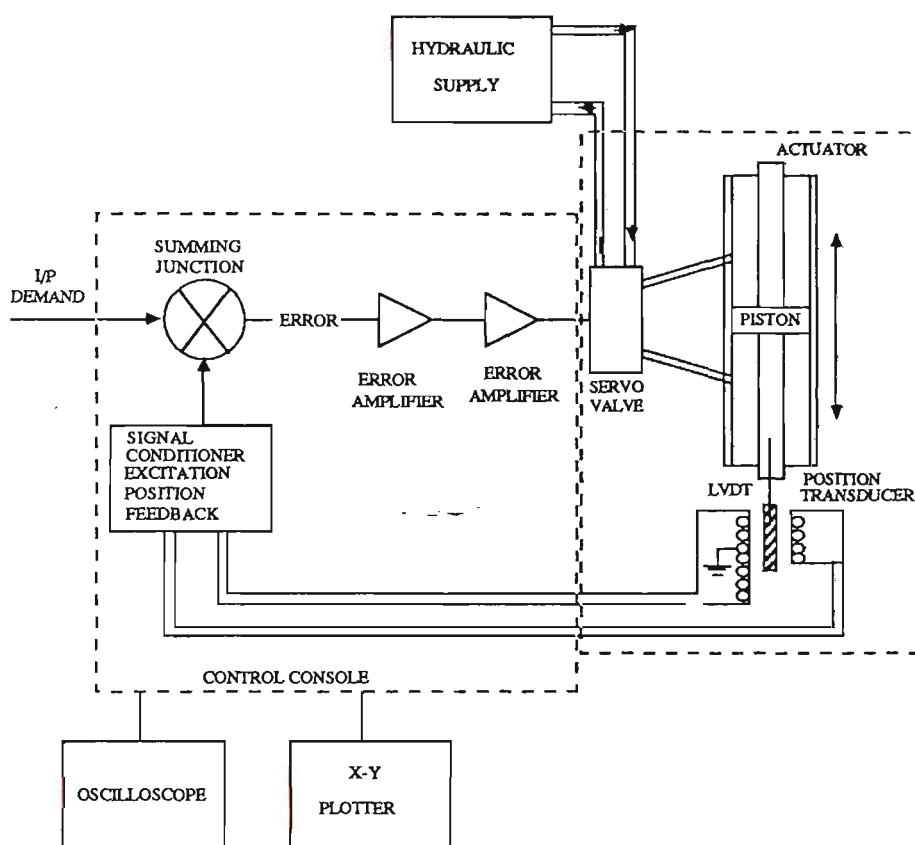


Figure 4.7 A closed loop servo block diagram.

The load cell, type 2518-110, which is employed in this machine has been tested for accuracy and linearity on a suitable calibration device, which in turn has been certified by the National Physical Laboratory to an accuracy better than 0.05%. The accuracy of each range of the cell has been found to equal or exceed 0.2% of cell rated output, or 0.5% of indicated load, whichever is greater.

4.3.3 Data acquisition system components

The data acquisition and control system for the monitoring of both axial and diametric strains of CCWR material specimens is shown in Figure 4.8 and consists of:

- (i) the HP 9826 microcomputer,
- (ii) the HP 3054A data acquisition and control system, and
- (iii) the HP 7DCDT series of displacement transducers (linear variable differential transformers (LVDT) and/or strain gauges).

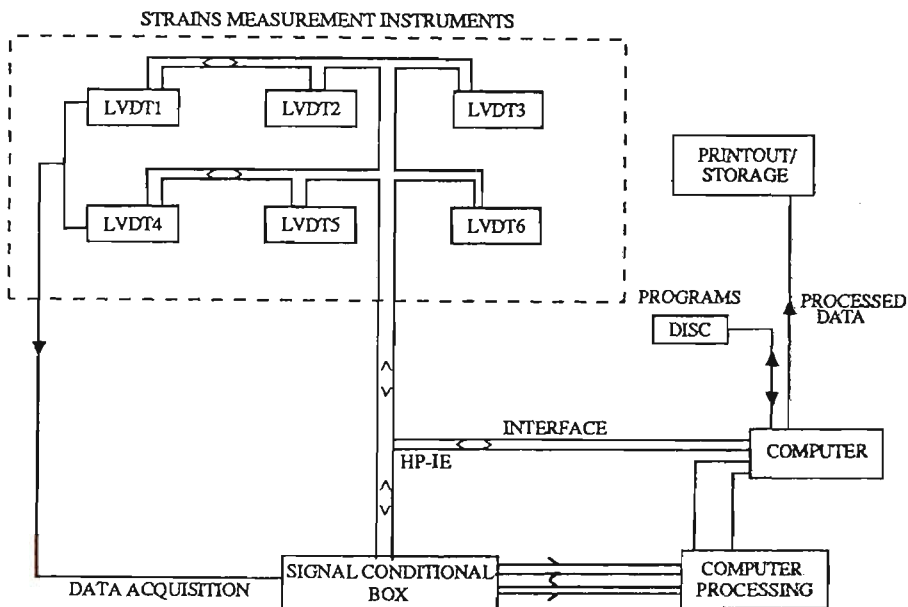


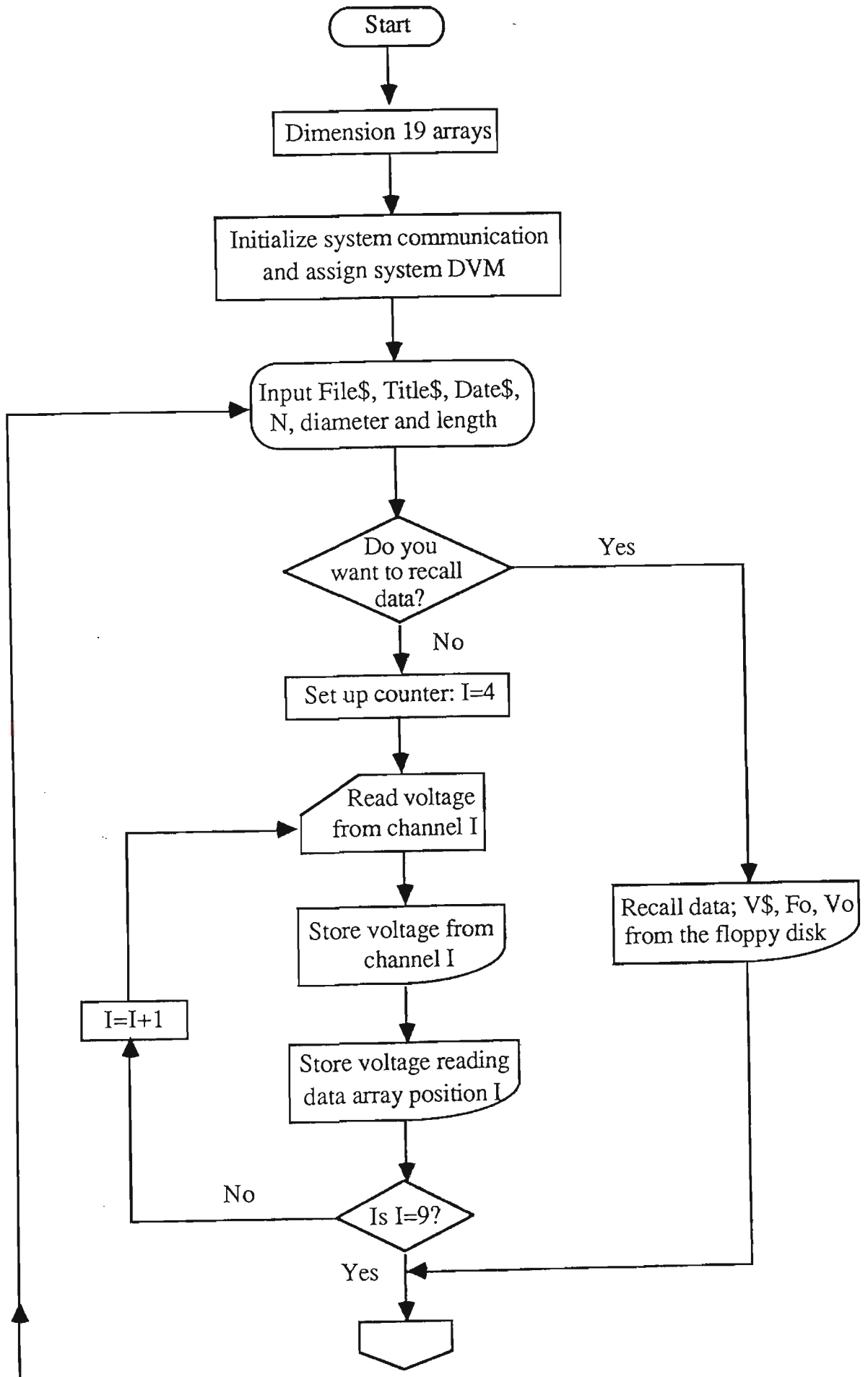
Figure 4.8 The interface of LVDT and HP data acquisition and control system.

The system also includes a control component with the function of monitoring and modifying the test in some pre-programmed manner. The LVDT transducers and strain gauges are used to convert displacements to electrical

signals. Generally, the transducer produces a change in either resistance, output voltage, or output current which is proportional to a physical change within the system being monitored. The HP 9826 microcomputer is the controller of the whole system. The HP 3054A, a computer based automatic data acquisition and control system, consists of a system mainframe 3497A and two voltmeters, the 3456A (for strain gauges) and the 3437A (for LVDT transducers). These instruments are interfaced via HP-IB cable to the 9826 computer.

The strength tests require the application of a compressive force to the test specimens and the measurement of one or more displacements. The need to record both axial and diametric displacements in conjunction with specimen loading to obtain strain data necessary to determine the elastic moduli (Young's modulus and Poisson's ratio) led to the design and application of the LVDT strain measurement rig. The HP 3054A automatic data acquisition and control system was used in conjunction with the LVDT strain measurement rig constructed using six LVDT transducers (three in the axial and three in the lateral direction). All LVDT transducers were calibrated to determine their linear displacement constants. These constants were included in the LVDT program to enable direct microstrain values to be obtained in the output. This LVDT strain measurement rig, is capable of measuring both axial and diametric strains to an accuracy of $\pm 0.5\%$ of reading.

Several computer programs have been developed by the author to control the data acquisition procedure for strain measurements. The LVDT program written in HP BASIC, is used to control the 3437A voltmeter to take readings in steps. Each LVDT transducer is sampled 30 times and the average is stored before switching to the next transducer. Figure 4.9 shows the flow chart for the LVDT program.



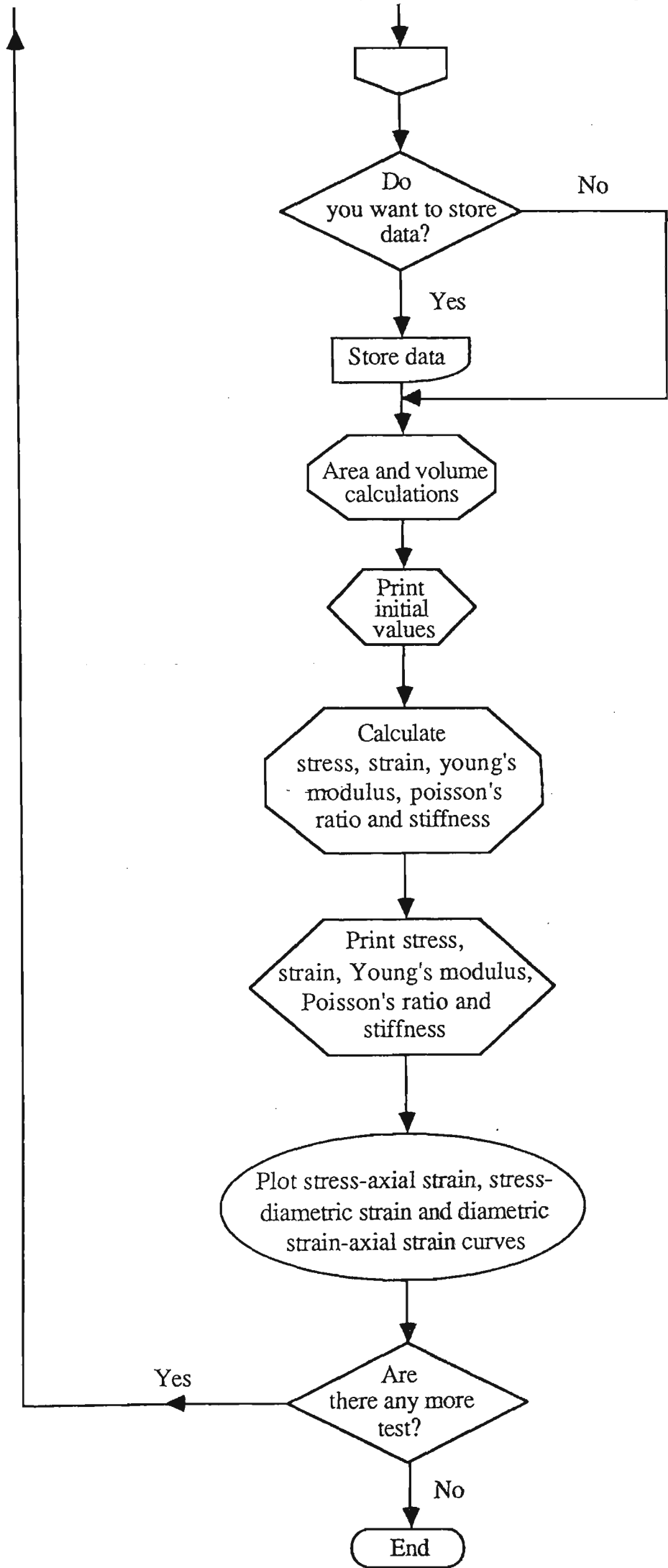


Figure 4.9 Flow chart for the LVDT program.

The recorded voltage signals are transferred to the HP 9826 microcomputer in a packed format, then converted to ASCII values. Subsequently these ASCII values are converted to microstrain values according to calibrated constants between voltage and displacement. Finally, an ASCII file is created to store the data on a disk. The data can be retrieved and recombined in a variety of ways depending on the needs, perhaps instantaneously or at any time, and processed, printed and plotted in any desirable form.

The strain gauging technique is also employed to obtain strain data of CCWR materials. The CCWR material specimens were instrumented with four foil-type (Showa N11-FA-30-120-11) strain gauges (two in the axial and two in the lateral direction). The gauges in both directions were wired in separate series circuits which enables automatic averaging of axial and transverse strain data. Each series of strain gauges was wired into a separate Wheatstone bridge configuration for zero balancing and subsequent strain monitoring.

During the test, the specimen was loaded in the testing machine at some preprogrammed loading rate (e.g. 0.0015mm/sec), and at the same time the load and strains were monitored. A strain program which is also written in HP BASIC controls the 3497A voltmeter to record readings in a step by step manner continually; strains are monitored by measuring the associated bridge output voltages, the magnitude of these output voltages are proportional to the specimen strain. Figure 4.10 diagrammatically shows the interface of strain gauges and the HP data acquisition and control system.

One of the unique features of HP BASIC language is the incorporation of block structures and the ability to create functions and procedures. The user can also create custom functions and procedures that extend the range of keywords

within the language as user needs dictate. HP BASIC can also handle interrupts within a program, which provides a powerful real-time capability.

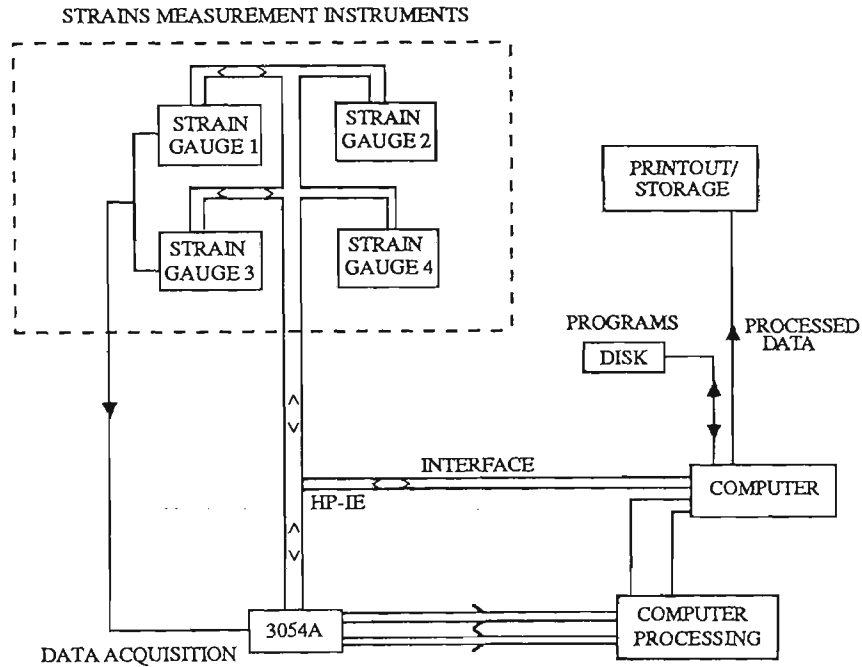


Figure 4.10 The interface of strain gauges and HP data acquisition and control system.

4.3.4 Device dependence of strain measurements of CCWR material specimens

Strain gauges and LVDT transducers are the two most widely used devices for measuring the strain properties of specimens during strength testing. Unfortunately, very little research has been undertaken to compare data obtained from both devices on the same material. For this reason a program of work is being attempted to correlate the strain property data obtained from both devices. The strain property measurements on CCWR material specimens indicate that the differences in data obtained from the two devices for the same material may, to a significant degree, be the result of device dependence. The findings are complicated

by the fact that end effects have more influence on the strain values obtained using LVDT transducers. Thus great care is needed when measuring strain properties to minimize device dependence.

4.3.5 Experimental Apparatus for Flow Tests of CWR

This consisted of a conical funnel and the flow-tube fixed to a specially fabricated steel frame as shown in Figure 4.11. The conical funnel from which the flow-tube extended was used to load the test materials. The tube is made of 3mm thick transparent perspex with an internal diameter of 50mm and length of 1.81m, and can be adjusted to any angle up to 55° .

The perspex tube made it possible to observe the actual flow of the material tested as it was discharged. Furthermore, for ease of cleaning, the tube is fully detachable from the frame. The base plate of the frame is made of 8mm thick steel for stability.

The bottom end of the perspex tube was machined flat so that a flat block of perspex could be manually pressed against it to form a watertight seal. After considering many possibilities, including mechanical hinges and various valve arrangements, this gate system was decided as the best method for a quick release of material in the tube. As well as being efficient, it also has simplicity and cost advantages.

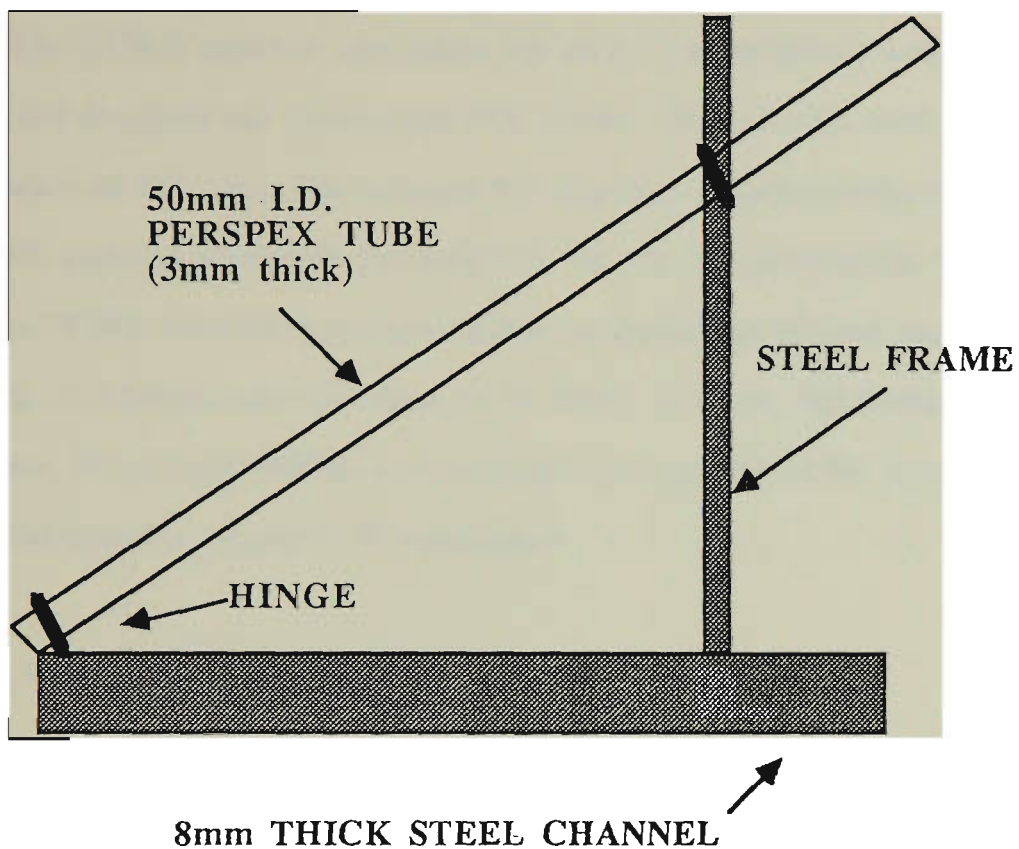


Figure 4.11 Schematic of the flow-tube experimental apparatus.

4.4 EXPERIMENTAL PROCEDURES

4.4.1 Test specimens identification coding

In the first group, specimen 10%-1.5HRS, for example, means the specimen had 10% of Portland cement and was tested 1.5 hours after pouring. In the second group, specimen 10%-1-1, for example, means the specimen had 10% of Portland cement, was tested after one day curing and was number one in a replicate set of three.

4.4.2 Design and construction of sample moulds

The CCWR material specimens for series I experiments were poured in specially designed and constructed PVC plastic tubing moulds with lengths and diameters of 102.5mm. The standard NX size triaxial jackets were used to pour CCWR material specimens for Series II, III and IV experiments. Figure 4.12 shows CCWR material specimen moulds. A special set of steel moulds with a height of 150mm and diameters of 55.5mm, 75.5mm, 102.8mm, 149.5mm, 206mm, 242mm and 300mm were designed and constructed for pouring CCWR material specimens for series VI experiments.

4.4.3 Sample preparation

A set of standard quantities and conditions have been used in the sample preparation. The following techniques were used for each of the 14 batches poured.



Figure 4.12 CCWR material specimen moulds.

4.4.4 Mixing of concrete

4.4.4.1 Batch size

The batch size was over-batched by 10% to ensure an excess of material after moulding the required specimens.

4.4.4.2 Mixer

The type of mixer used was a 0.2 cubic metre capacity, 'Bennett' motor-driven mixer.

4.4.4.3 Charging sequence

The mixer (see Figure 4.13) was charged with materials in the order set out below.

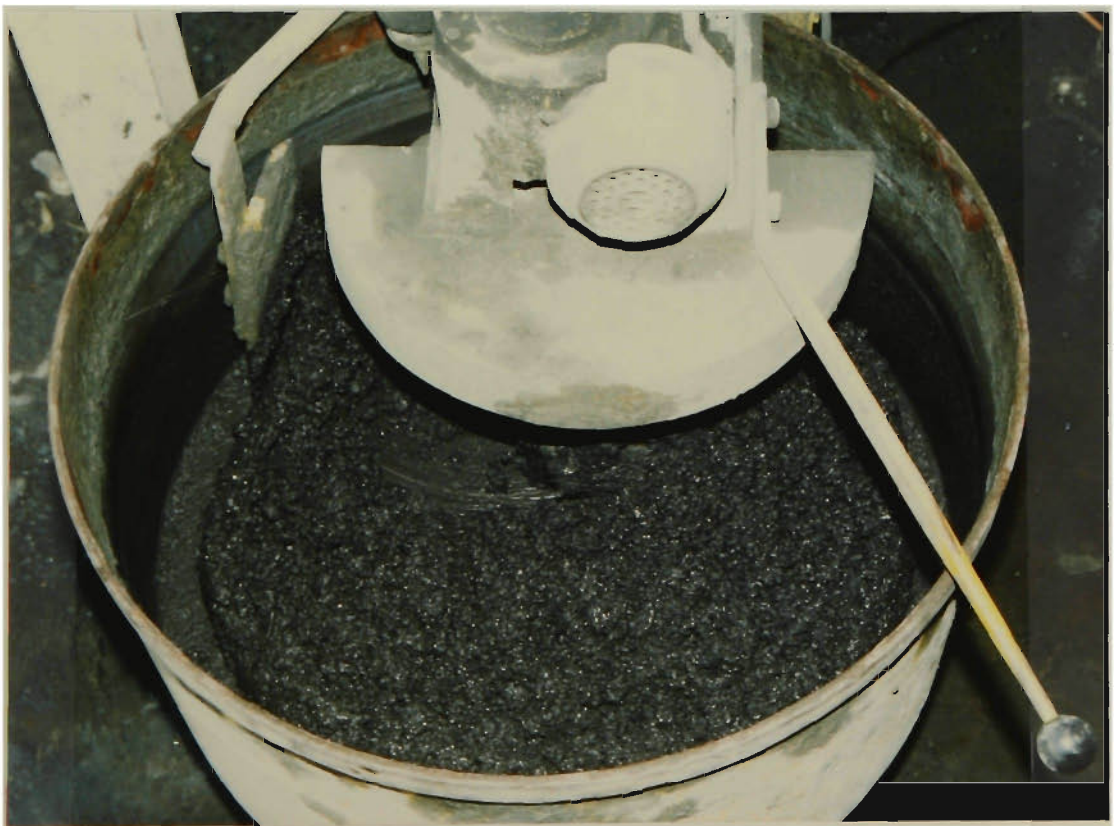


Figure 4.13 'Bennett' Mixer.

- (i) The inside of the mixer was moistened.
- (ii) The mixing drum was charged with moist CWR and part of the mixing water. Then it was left operating for two minutes.
- (iii) Portland cement was then added and the mixing time started. The balance of the mixing water was added promptly as required.
- (iv) Calcium chloride admixture which has been dissolved in part of the mixing water was added. The required level of this admixture has been determined from previous tests carried out by Thomas (1986).
- (v) Final water additions were made.
- (vi) Mixing was then continued for 15 minutes.

4.4.5 Pouring of CCWR material specimens

At the completion of mixing, slump test (see Figure 4.14) was performed within 2.5 minutes. This test was aimed at measuring the consistency of the mix. The mix was then sampled direct from the mixing pan, care being taken to avoid segregation. The following sequence was strictly followed in each case to allow assessment of any possible effects of non-uniformity.

1. Pour and vibrate 1.5H, 2H, 2.5H, 4.25H and 4.5H specimen.
2. Pour and vibrate 1-1, 7-1, 14-1, 28-1, 60-1 and 90-1 specimen.
3. Pour and vibrate 1-2, 7-2, 14-2, 28-2, 60-2 and 90-2 specimen.
4. Pour and vibrate 1-3, 7-3, 14-3, 28-3, 60-3 and 90-3 specimen.
5. Pour and vibrate the triaxial test specimens.



Figure 4.14 Slump test.

The workability of the mix determines the duration time of vibration to compact the specimen and the surface of the specimen mix will become relatively smooth when sufficient vibration has been applied. The duration of vibration of the specimens on the vibrating table (see Figure 4.15) known as 'ICAL Syntron Packer, Model VP65B', operating at a frequency of 50 Hz was approximately 5 seconds for batch one, 20 seconds for batches two, three, four, five, six, nine, ten and thirteen. Test specimens for batches seven, eight, eleven and twelve were not vibrated because of their relatively high fluidity. All the triaxial test specimens were vibrated for 25 seconds.



Figure 4.15 'ICAL Syntron Packer, Model VP65B'

According to Thomas (1986) vibration was thought to be necessary to produce adequate compaction of the test specimens which were much smaller than the actual pouring dimensions in practice.

It took 25 minutes to fill and vibrate all the test specimens. Another 15 minutes was needed to level the tops of the specimens. The duration of the preparation of specimens from start to finish was approximately one hour.

4.4.6 Curing of CCWR material specimens

At the completion of pouring and vibrating, CCWR material specimens were cured in plastic bags to prevent dehydration. After 24 hours from pouring,

CCWR material specimens were demoulded with ELE Press. The specimens were squared top and bottom and were later transferred to the humidity room for curing. All specimens were cured at 20 °C in the humidity room, the condition of which was the closest approximation to real mine situation.

4.4.7 Observations of the physical appearance of various CCWR material mixes

Descriptions of various CCWR material mixes given in Table 4.5 are reflected by the water content at pouring. They indicate the importance of water content on the mix consistency.

4.4.8 CCWR test specimen bulk density determination

The bulk density of CCWR specimen was determined at the time of compressive strength test and during the strength development period, and was done in accordance with ISRM suggested method. The bulk volume of the specimen was calculated from vernier caliper measurements. An average of several readings for each dimension, each accurate to 0.1mm was used in the calculation of the bulk volume.

$$\text{Bulk Density} = \frac{M_s + M_v}{V}$$

where, M_s = Grain mass.

M_v = Mass of Void.

V = Volume of grain + volume of void.

or V = Bulk volume.

Table 4.5 Descriptions of the physical appearance of various
CCWR material mixes.

Batch	Cement content	Water content	Remarks
1	15.6%	14.7%	Slightly wet
2	12.5%	13.0%	Slightly dry
3	10.0%	13.8%	Good consistency
4	7.5%	12.6%	Good consistency
5	5.0%	12.0%	Slightly dry
6	15.0%	12.0%	Very dry
7	15.0%	21.0%	Very wet
8	10.0%	19.1%	Very wet
9	10.0%	12.0%	Very dry
10	12.5%	16.5%	Good consistency
11	12.5%	19.1%	Very wet
12	7.5%	19.0%	Very wet
13	7.5%	16.5%	Good consistency

4.4.9 Determination of the grain mass M_s of CCWR specimens

The grain mass, M_s of CCWR specimen is defined as the equilibrium of constant mass of the specimen after oven drying at a temperature of 105 °C (the grain mass of CCWR specimens were determined in accordance with ISRM suggested standard methods). After compression testing, each specimen was dried to constant mass in an oven at a temperature of 105 °C. The dry density of CCWR specimen was then calculated using

$$\text{Dry Density} = \frac{M_s}{V}$$

where, M_s and V had been described in sub-section 4.4.8.

In this study, the porosity and grain density of CCWR specimen were also determined using saturated method.

4.4.10 Method for measuring the physical properties of CCWR specimens

Porosity, void ratio, specific gravity, bulk density and particle density of CCWR specimens were determined using volumetric method and done in accordance with ISRM suggested methods. The results from the measurement of these physical properties were also used to characterized the properties and the behaviour of CCWR material.

4.4.11 Method for determining the sound (sonic) velocity of CCWR specimens

The velocity of ultrasonic pulses travelling in the specimen depends on its density and elastic properties. The quality of the specimen can be related to its elastic stiffness. Therefore, the measurement of ultrasonic pulse velocity in the specimen can be used to indicate the quality of the specimen as well as to determine its elastic property. Also, the sonic velocity data of CCWR specimens obtained from this research can become a very useful and important parameter at the time of field installation and testing of future CCWR pack structures.

During curing and before compressive strength testing of the specimen, its sonic velocity was measured longitudinally using 'Pundit'. 'Pundit' is simple to operate and yet it can produce results with a high order of accuracy and stability. It generates low frequency ultrasonic pulses and measures the time taken for them to pass from one transducer to the other through the specimen interposed between them. A simplified 'Pundit' system diagram is shown in Figure 4.16.

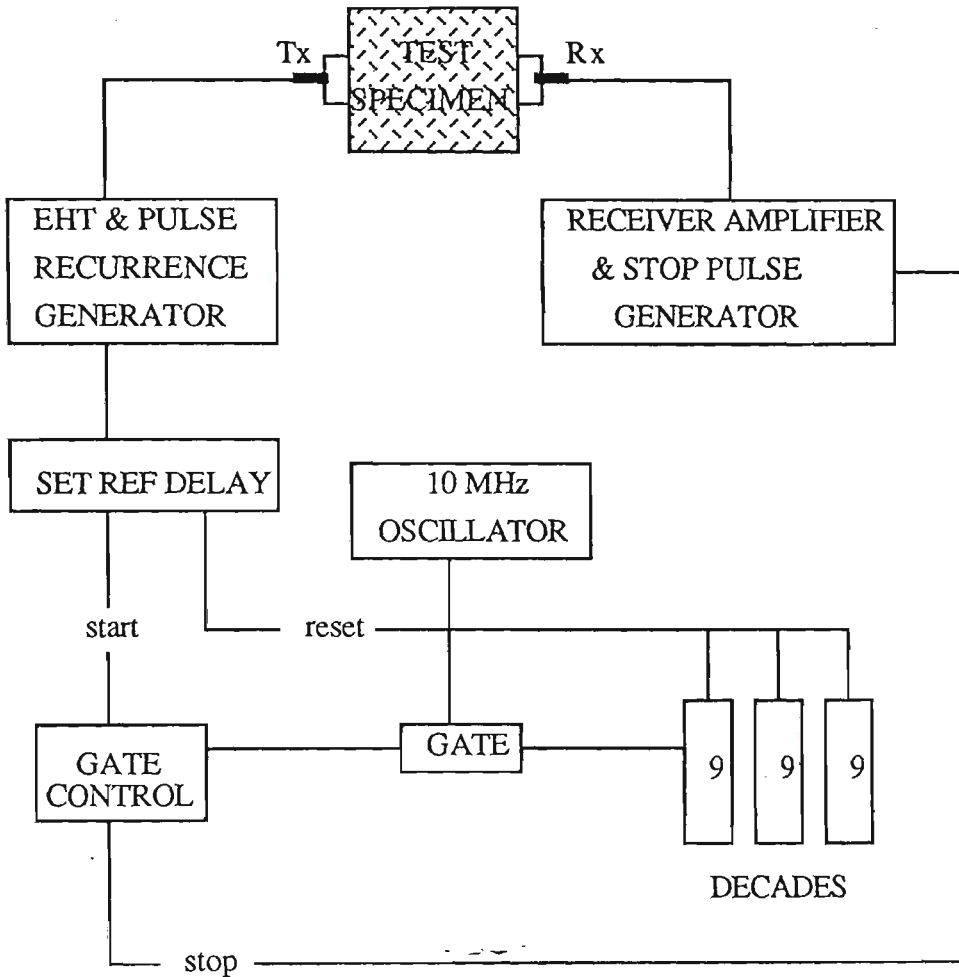


Figure 4.16 Simplified 'Pundit' system diagram.

The transit time was displayed in the form of three digits on three 'in-line' numerical indicator tubes. The range of time measurements used was 0.1 to 99.9 microsec in units of 0.1 microsec. The accuracy of the transit time measurement was generally not less than the direct reading values indicated on the display. An accuracy of not less than 0.5% could be achieved. Sonic velocity measurement results for CCWR material specimens are reported in Chapter 5. Specimen weights were recorded at the same time as sonic velocities were determined. Results from specimen weight and sonic velocity measurements of CCWR specimens have been reported in Hii and Aziz (1987a, 1987b).

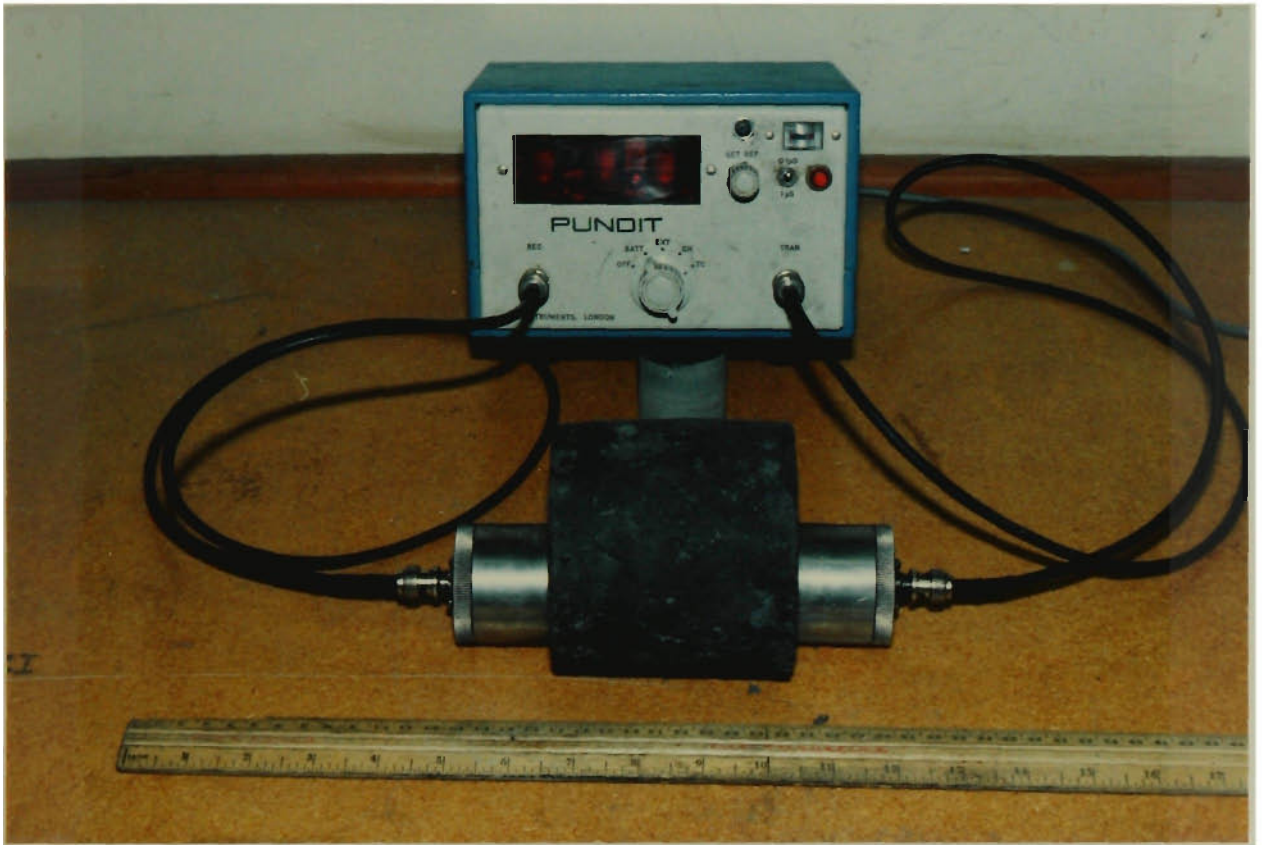


Figure 4.17 'Pundit' sonic velocity apparatus.

4.4.12 Strength test procedures

4.4.12.1 Unconfined compressive strength tests

The unconfined compressive strength tests (series I experiments) were conducted on CCWR specimens with both lengths and diameters of 102.5mm at ages of 1.5 hours, 2 hours, 2.5 hours, 4.25 hours, 4.5 hours, 1 day, 7 days, 14 days, 28 days, 60 days, 90 days and 365 days after casting. At least three specimens from each group were tested. These tests were performed to determine the ultimate compressive strength of the specimens. A strength testing system has been developed for testing the specimens (this strength testing system has been described in detail in Section 4.3).

The loading plates of the LVDT strain measurement rig were clamped to the Instron stiff testing machine and each specimen to be tested was centred between the loading plates as shown in Figure 4.18. A spherical seating was situated between the upper loading plate and the specimen to prevent unequal load distribution across the flat ends of the specimen. Three axial deflection LVDTs were adjusted to record similar initial deflections as were three lateral deflection LVDTs. Figure 4.19 shows the LVDT strain measurement rig. The initial electrical outputs were incorporated in the LVDT programme to compute axial and diametral strains from these starting points.

Axial load was applied at a constant rate of deflection (0.0015 mm/sec) until the complete failure of the specimen. Load values during testing together with electrical outputs from the transducers were recorded at regular load intervals until the complete load deformation curve was obtained.

The measured values were used for determining the compressive strength of the specimen given by:

$$\sigma_c = \frac{F}{A}$$

where σ_c is the ultimate compressive strength of the specimen (MPa),

F is the applied ultimate failure load (N), and

A is the cross-sectional area of the specimen (mm²).

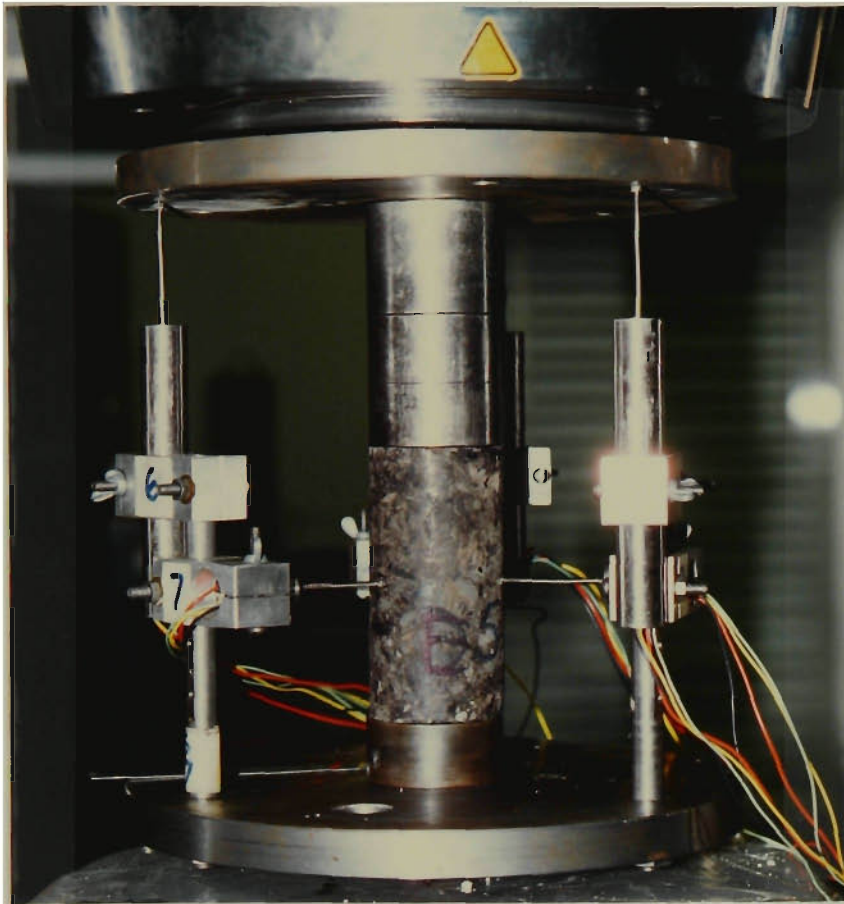


Figure 4.18 CCWR material specimen mounted in the LVDT strain measurement rig during the unconfined compressive strength test.

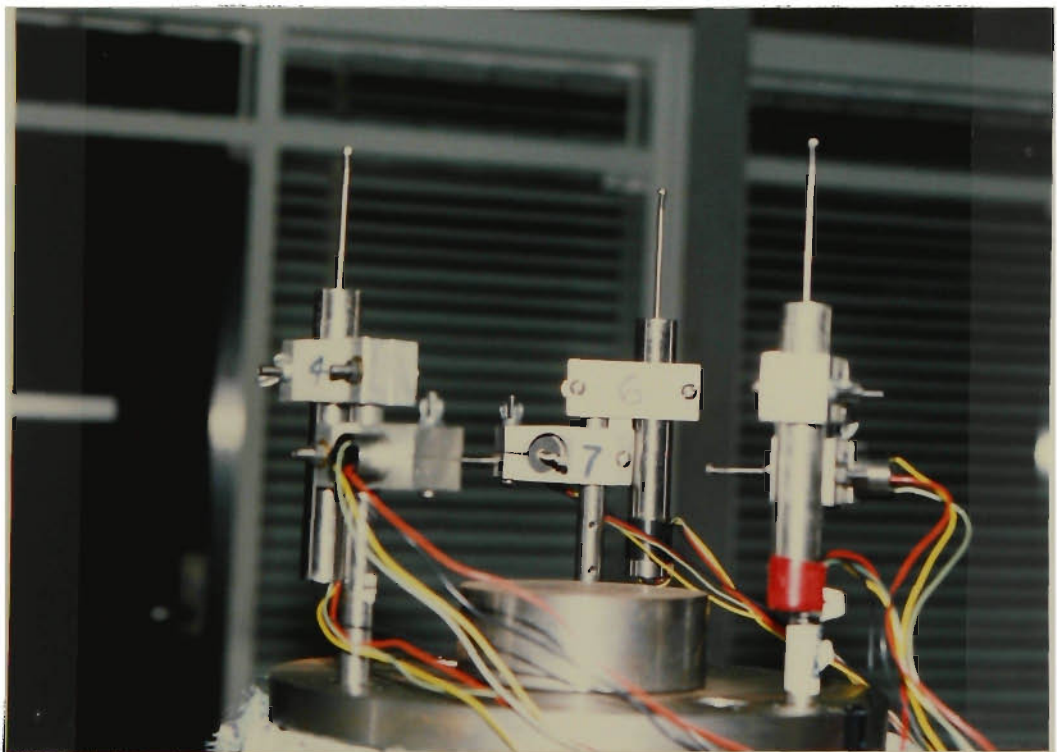


Figure 4.19 LVDT strain measurement rig.

Progressive and ultimate compressive strength were computed using the LVDT programme. Secant Young's modulus and Poisson's ratio of the specimen were also computed in this manner. Complete load deformation curves for all CCWR material specimens were obtained and these curves have been given in Hii and Aziz (1987a, 1987b). Results of compressive strength tests of CCWR specimens such as ultimate strength, secant Young's modulus, Poisson's ratio, maximum stiffness, post failure modulus and residual strength have been reported in detail in Hii and Aziz (1987a, 1987b). The specimen experimental data such as moist density, dry density, water content, sonic velocity value have also been reported in Hii and Aziz (1987a, 1987b).

4.4.12.2 Indirect tensile strength tests

The indirect tensile strength tests (series II experiments) were conducted in accordance with ISRM suggested methods. The indirect tensile test rig is shown in Figure 4.20. The tensile strength σ_t of the specimen was calculated by the following formula:

$$\sigma_t = \frac{0.636 P}{D t}$$

where σ_t is the indirect tensile strength (MPa),

P is the applied load at failure (N),

D is the diameter of test specimen (mm), and

t is the thickness of test specimen measured at the centre (mm).

The indirect tensile test results are reported in Chapter 5.



Figure 4.20 Indirect tensile strength (Brazilian) test rig.

4.4.12.3 Triaxial strength tests

Triaxial strength tests of CCWR specimens (series III experiments) were also conducted in accordance with ISRM suggested methods. Figure 4.21 illustrates a triaxial strength test. The triaxial and unconfined compressive strength tests (Series III and IV experiments) were conducted on specimens with lengths and diameters of 113mm and 56mm respectively. Series IV experiments (unconfined compressive strength tests) were carried out as set out in sub-section 4.4.12.1.

The conventional single point failure technique was used in all triaxial strength tests. A confining pressure was applied to the specimen and maintained constant at a selected level. The axial load was increased at a constant rate of deflection until the specimen failed at peak load. This peak load was then used to determine the cohesion strength C and the angle of friction ϕ parameters of the specimen. The experimental results of triaxial tests are reported in Chapter 5.

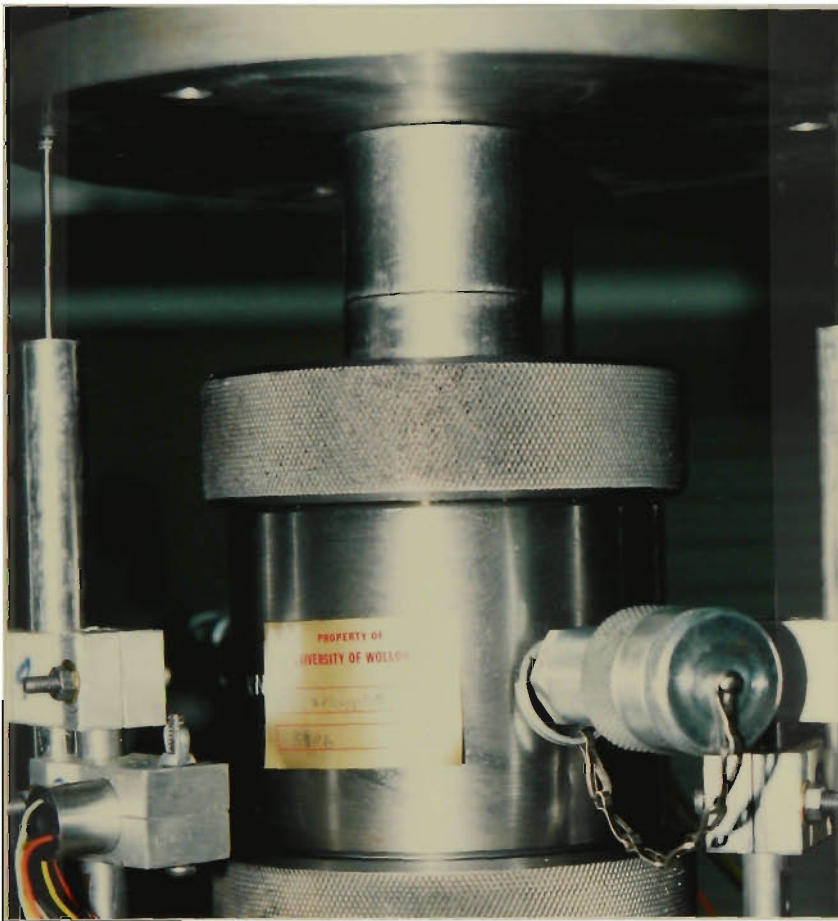


Figure 4.21 Triaxial cell applied to the LVDT strain rig.

4.4.13 Experimental technique for flow tests of CWR

In this study, test results from consistency measurements and flow tests were used to characterize the flow properties of CWR with different nominal water contents. A simple flow-tube technique was employed to quantify the flowability of CWR. This involved the flow of a fixed quantity of CWR through the flow-tube. The time for the fixed quantity of CWR to pass through the tube becomes a

measure of the consistence of CWR and this is known as the flow factor (FF). The flowability of CWR is then expressed as:

$$F = FF^{-1} \times 100$$

where F is the flowability and FF is the flow factor.

4.4.14 Testing procedures for flow tests of CCWR material

The initial flow tests were conducted to determine the slopes of the flow-tube for the test runs. The selected slopes of the flow-tube were 38.5°, 45° and 50°. The procedure employed in the flow tests of various oil samples was carried out in the order set out below:

- (i) The flow-tube was set at the desired angle, starting at 38.5°.
- (ii) The temperature of the oil sample and atmosphere was taken prior to each run.
- (iii) The flow-tube was closed at the bottom using the perspex gate and subsequently filled to the top, that is, until no more fluid could be added without spillage. This ensured that the same volume of fluid was used for each run.
- (iv) The bottom gate was then opened and timing simultaneously started. All timing was done using a hundredth (1/100 th) of a second AMF American Split-Taylor stopwatch.
- (v) Run was terminated when the fixed volume of fluid had passed through the flow-tube. The fixed volume of fluid was deemed to have passed through the flow-tube when the wave from the top of the flow-tube reached the bottom and discharge into the atmosphere.

- (vi) The time taken was recorded and the procedure repeated a further four times (a total of five runs).
- (vii) After five runs at 38.5° , the angle setting of the flow-tube was increased to 45° for five more runs using the same procedure, and finally to 50° . The flow-tube was then cleaned and dried ready for the next series of tests.

Test runs were conducted on CWR with nominal water contents of 2%, 5%, 10%, 15%, 20%, 25%, 25% and 30%. The procedure for the flow tests of CWR was identical to that of the oil samples except for some additional steps as described below:

- (i) CWR of a known water content was weighed out and hence the amount of water required to be added could be calculated.
- (ii) The temperature of the atmosphere and water to be added was recorded.
- (iii) The batch size was over-batched by 10% to ensure excess of material for the flow tests. The inside of the mixer was moistened. The mixing drum was charged with moist CWR and the mixing water. Mixing was then continued for 2.5 minutes. The type of mixer used was a 0.067 cubic metre capacity, planetary action mixer.
- (iv) At the completion of mixing, slump test was performed in accordance with AS 1012, part 3-1976. The slump test not only yielded valuable data, but also ensured that each mix received equal compaction prior to the flow test. The flow tests were then conducted on CWR as described before.

4.5 MECHANICAL PROPERTIES EVALUATION OF CCWR MATERIAL

This study is an integral part of a broad research programme on the development and utilization of CWR for strata reinforcement in underground coal mining operations. Because the information on the mechanical properties of CCWR material and the knowledge on the factors of influence are needed for economical use of this material, a comprehensive laboratory test programme has been devised to investigate the strength development of coal washery refuse as a function of various cement mixes over a 365 day period. The study also investigated the load deformation characteristics of CCWR material.

A set of standard quantities and conditions used in the preparations and testings of CCWR material specimens studied have been given in Sections 4.1 through 4.4. Results from sound velocity measurements, unconfined compressive strength tests, triaxial strength tests and indirect tensile strength tests and the measurement of physical properties such as porosity, void ratio, specific gravity, bulk density and particle density are used to characterize the properties and behaviour of CCWR material. The results and analyses of these tests and measurements are reported in Chapter 5.

4.6 EFFECT OF WATER CONTENT ON THE MECHANICAL PROPERTIES OF CCWR MATERIAL

In many cementitious mixtures, industrial by-products such as granulated blast furnace slag, fly ash, mine tailings and rice husk ash have been used successfully (Mehta and Pirtz, 1978; Munn, 1979; Blunk, 1979; Berry and Malhotra, 1980; Lerche and Renetzeder, 1984; Loo et al, 1984; Collepari, 1988; Mehta, 1989). More recently, the potential use of instant chilled steel slag as an

aggregate in concrete has been investigated (Montgomery and Wang, 1989). One method is to substitute these by-products for the more expensive commercial materials in proposed mixtures, either fully or partially.

In order to utilize CWR as a raw material for pump packing, it is necessary to study the influence of water content on the mechanical properties and behaviour of CCWR material because many problems are being experienced in obtaining a consistent mix owing to the variation in products from the coal washery. Two other reasons for this study are, firstly, a serious problem such as shrinkage cracking can arise frequently if the importance of water content is neglected, and secondly, realistic experimental data of CCWR material are needed in pack design.

Series I and V experiments were undertaken to investigate the influence of water content on the mechanical properties and behaviour of CCWR material. This study is also a research effort on the development of CCWR material with calcium chloride admixture to optimise particular physical properties with nominal water contents ranging from 12% to 21%.

All pouring and batching details of CCWR material specimens have been given in Table 4.4. Test procedures for test series I and V and materials used in making test specimens have been reported in details in Section 4.1 through 4.4. Tests in series V were carried out generally to AS 1012.13/Amdt 1/1986-12-05, Method for the Determination of Drying Shrinkage of Concrete.

The unconfined compressive strength, modulus of elasticity, sonic velocity, density and drying shrinkage of CCWR material were the primary properties investigated.

The results of this investigation are analysed and discussed in Chapter 5.

4.7 A NEW YIELD FUNCTION FOR CCWR MATERIAL

In order to develop an empirical yield criterion for CCWR material, series II, III and IV experiments were carried out. Series II, III and IV experiments consisted of tensile strength tests, triaxial strength tests and unconfined compressive strength tests respectively. These routine material tests were carried out in accordance with the ISRM Suggested Methods. Based on the results of these tests, a logarithmic yield function is proposed for predicting the strength and yield characteristics of CCWR material, and the parameters contained in the proposed yield function have been determined.

A procedure for the determination of the parameters have been discussed in Chapter 3. The logarithmic yield function program, written in FORTRAN, has been developed to facilitate data processing of test results and a listing of the fundamental FORTRAN code is given in Appendix I. The study has indicated that the proposed logarithmic yield function can predict the strength and yield characteristics of CCWR material in a satisfactory manner.

4.8 EFFECT OF WATER CONTENT ON THE FLOW PROPERTIES OF CWR

The objective of this study was to determine the optimum water content for flowability of West Cliff CWR (this has been reported in detail in Hii and Aziz, 1987c). A simple flow measuring device, called a flow-tube, was designed and constructed for this series of experiments. West Cliff CWR with different nominal water contents were mixed and tested using an inclined, open ended flow-tube technique. The flow-tube used consisted of a perspex tube topped with a receiving conical funnel and sealed at the discharge end by means of a flat block of perspex until filled with CWR.

A series of flow tests and supplementary consistency measurements (slump tests) were conducted to determine the influence of water content on the flow properties of CWR. In all, 130 flow tests and 24 slump tests were conducted to shed some light on the effect of water content on the flow characteristics of minus 10mm West Cliff CWR. The results and discussion of the flow and slump tests of CWR are presented in Chapter 5.

4.9 EFFECT OF GEOMETRY ON THE PROPERTIES AND BEHAVIOUR OF CCWR MATERIAL MODELS

Series VI experiments were conducted to investigate the influence of geometry on the mechanical properties and behaviour of CCWR material models. The study focuses on the effect of the width/height ratio on the strength of the material. The main purpose of this study is to ascertain the effect of end constraints on the strength of CCWR material models.

CCWR material models (scale 1:15) with a height of 150mm and diameters of 50mm, 75mm, 100mm, 150mm, 200mm, 250mm and 300mm were tested, simulating underground monolithic pack support with different widths in a coal seam of uniform height. After they were cast, the CCWR material models were cured at 20°C in the humidity room, condition of which was the closest approximation to real mine situation.

Unconfined compressive strength, modulus of elasticity and poisson's ratio were the primary properties investigated. The study also investigated the load deformation behaviour of CCWR material models under the test condition.

The experimental data of the mechanical properties and behaviour of CCWR material models are analysed and discussed in Chapter 5.

CHAPTER FIVE

EXPERIMENTAL RESULTS AND DISCUSSION

CHAPTER 5

EXPERIMENTAL RESULTS AND DISCUSSION

5.0 INTRODUCTION

The experimental results obtained from the experiments described in Chapter 4 are reported in this Chapter. The analysis, discussion and comparison of the experimental results will also be presented in this Chapter.

5.1 Effect of Crushing on the Grain Size Distribution of Minus 10mm CWR

An attempt was made to study the effect of crushing on the grain size distribution of CWR. The technique used was to perform sieve analyses on different CWR samples and the results obtained were then studied and compared.

Firstly, sieve analysis was performed on CWR which had not been processed. Secondly, at the completion of sieving, the sieved CWR was recombined and processed as described earlier. Thirdly, the processed minus 10mm CWR was used for the final sieve analysis.

The results obtained from these sieve analyses were then used to study the effect of crushing on the grain size distribution of CWR. This is presented in sub-section 5.1.1.

5.1.1 Discussion and conclusions drawn from sieve analyses

It was revealed that before processing of CWR, the gravel fraction and cobbles made up some 87.5% of its total weight. And after processing of CWR, about 80% of the processed CWR were lower medium gravel and fine gravel fractions.

Tables 5.1 and 5.2 show the grain size distribution of CWR before and after processing respectively. For brevity the experimental data of sieve analyses are presented in Tables AII1.1 through AII1.4 (in Appendix AII1). Sieve analyses were also conducted by Lama (Richmond et al, 1985) using wet screening and the results are conveniently given in Tables AII1.5 through AII1.14.

According to Lama (Richmond et al, 1985), the results indicate that the percentage of large particles which are greater than plus 12.7mm varies between 39.0% and 71.0% by weight and with the mean value of about 58.9%. In addition, the minus 0.106mm fractions form only about 8.8% and this suggests that the finer fractions form a very small part of the total. The practical significance of this singular aspect is that this could create problems if the hydraulic transportation system is used to convey this material for pack applications.

The curves in Figures 5.1 and 5.2 show that crushing of CWR did not really affect its grains with sizes 1.0mm and under. It was also noted, however, that crushing of CWR shifted AB portion of the curve in Figure 5.1 to the left. This indicated an increase in the weight percentage of particles with sizes bigger than 1.0mm. Also noted was that processing of CWR generated some 0.1 per cent of the coarse silt fraction.

Table 5.1 The grain size distribution of CWR before processing.

Total Weight (%)	Weight Percentage (%)	General Remarks
87.5	42.0	Coarse gravel fraction and cobbles.
	30.0	Medium gravel fraction.
	15.0	Fine gravel fraction.
12.5	6.0	Coarse sand fraction.
	4.5	Medium sand fraction.
	2.0	Fine sand fraction.

Table 5.2 The grain size distribution of the processed CWR.

Total Weight (%)	Weight Percentage (%)	General Remarks
80.0	35.0	Lower medium gravel fraction.
	45.0	Fine gravel fraction.
19.92	15.0	Coarse sand fraction
	3.75	Medium sand fraction
	1.17	Fine sand fraction
0.08	0.08	Coarse silt fraction

The shape of West Cliff CWR ranges from longish to flat with different degrees of roundness as shown in Figures 4.3 and 4.4 (Chapter 4). The length to thickness ratios range from 1:1 to 4:1 and the length to width ratios range from 1:1 to 3.6:1. The maximum grain size has been limited to minus 10mm.

West Cliff CWR is composed of sand grains, some may be the size of a pea, and other may be much finer. Some grains are so fine that individuals cannot be distinguished. The colour of CWR is light to dark grey. CWR is very porous, it is also usually soft and can be easily carved into shapes.

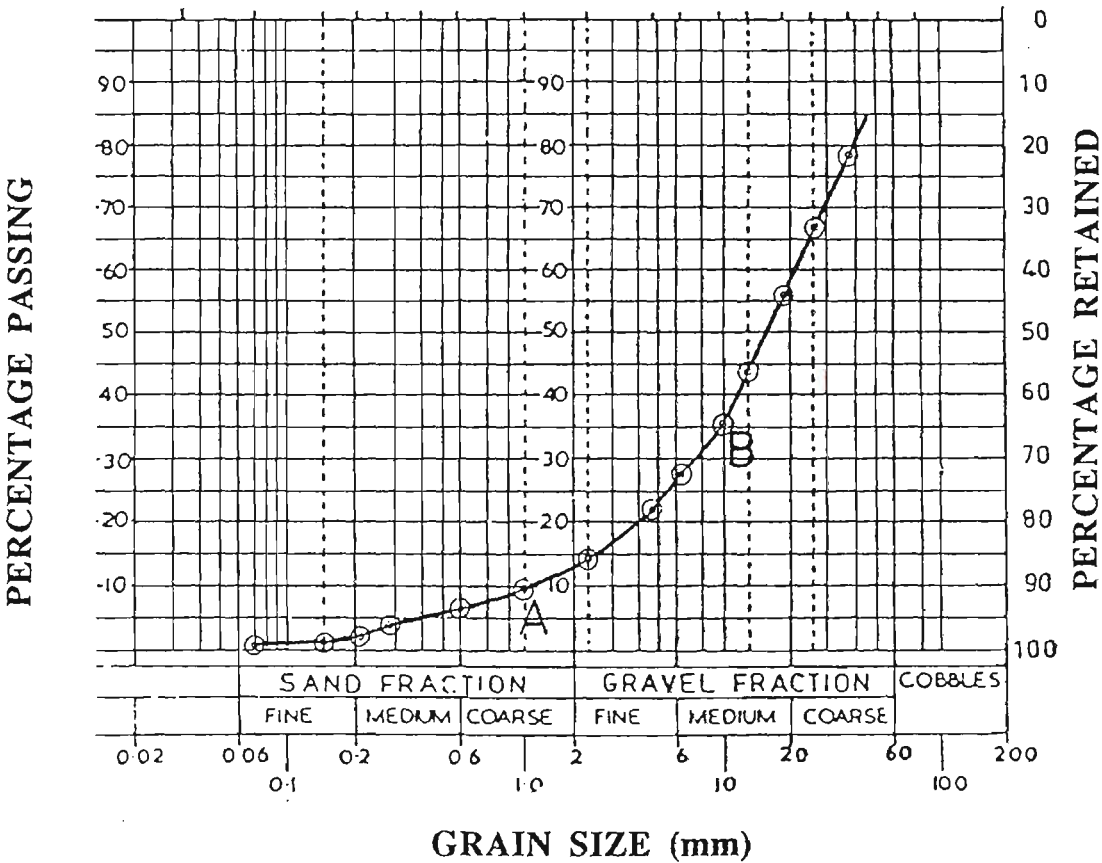


Figure 5.1 The grain size distribution curve of CWR before processing.

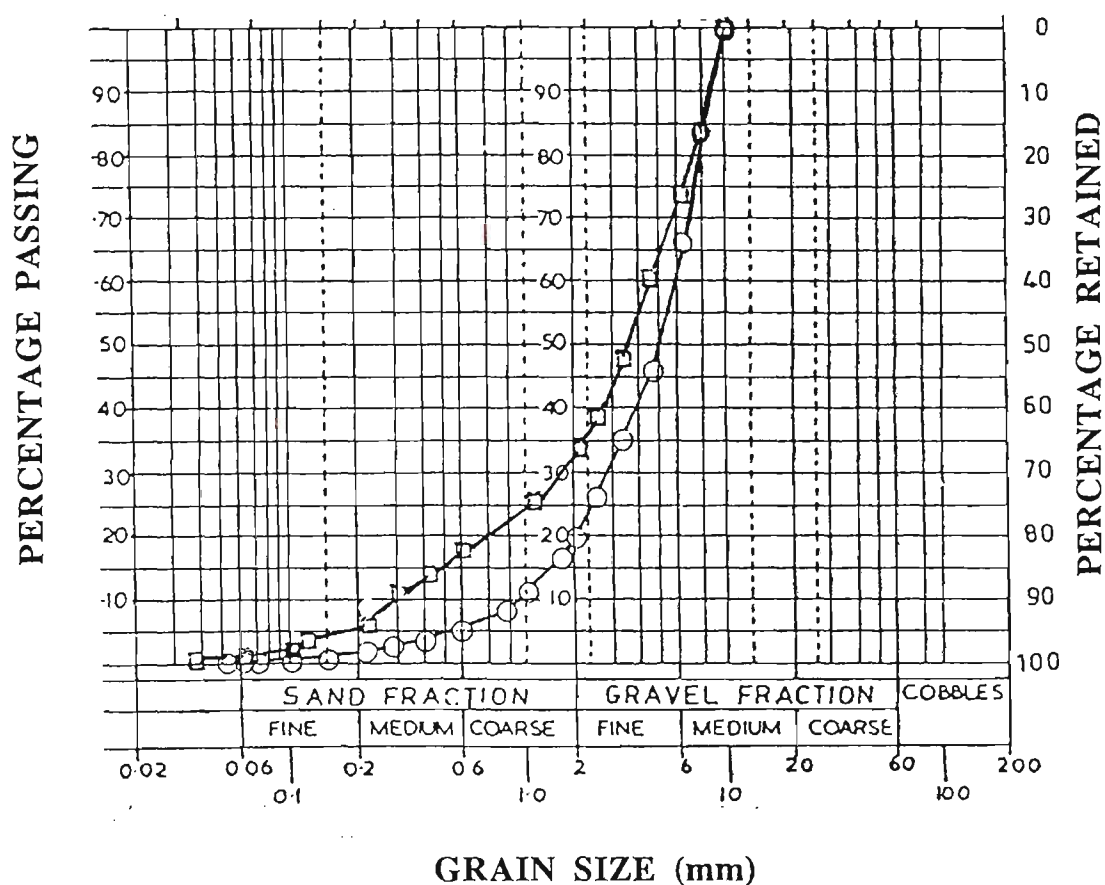


Figure 5.2 The grain size distribution curve of CWR after processing.

5.2 RESULTS FROM X-RAY DIFFRACTION ANALYSES AND DISCUSSION

The results of x-ray diffraction analyses of West Cliff CWR are given in Table 5.3. Silicon oxide, aluminium oxide and iron oxide compounds are the three major compounds found in West Cliff CWR. They are on average 60.0% of silicon oxide, 21.0% aluminium oxide and 5.0% iron oxide which constitute some 86.0% of the total composition of West Cliff CWR.

The results indicate that West Cliff CWR may be classified as a siliceous or pozzolanic material. It is very obvious by comparing Tables 5.3 and 5.4 that the chemical composition of West Cliff CWR are very similar to that of the fine

discards of the United Kingdom. However, it is also apparent that West Cliff CWR (60.0% SiO₂) contains a comparatively higher percentage of silicon oxide than that of the fine discards of the United Kingdom (maximum 46.0% SiO₂). It is indicative that West Cliff CWR which contains silicon oxide, aluminium oxide, calcium oxide and magnesium oxide exhibits pozzolanic characteristics.

Chemical composition analyses of coal preparation wastes conducted in the USSR have indicated that coal preparation wastes generated from different coalfields exhibit a significant variation in their chemical compositions. Chemical compositions of coal preparation wastes from four main coalfields of the Soviet Union are presented in Table 5.5. It is obvious from Table 5.5 that the chemical composition of coal preparation wastes differs markedly from one location to the next and even within the limit of any particular coalfields. According to Ruban and Shpirt (1987) for each individual coal washery plant the variation in chemical composition between samples collected on any particular day is rather small. It can be noted from Table 5.3 that the variation in chemical composition between samples of West Cliff CWR is also small.

The most important clay mineral constituents of West Cliff CWR are 50% to 60% of kaolinite, 35% to 40% of illite and 5% to 10% of montmorillonite (montmorillonite is of course the well known troublesome clay). The major minerals found in West Cliff CWR include well crystallized quartz, degraded muscovite and calcite.

The following metals also exist in West Cliff CWR:

Sample D - 130 ppm of rubidium, 222 ppm of strontium, 276 ppm of zirconium, 17 ppm of niobium, 17 ppm of lead, 23 ppm of

thorium, 35 ppm of yttrium, 37 ppm of nickel, 63 ppm of copper, 52 ppm of zinc and 35 ppm of gallium.

Sample E - 148 ppm of rubidium, 182 ppm of strontium, 289 ppm of zirconium, 17 ppm of niobium, 18 ppm of lead, 21 ppm of thorium, 32 ppm of yttrium, 43 ppm of nickel, 70 ppm of copper, 86 ppm of zinc and 36 ppm of gallium.

Table 5.3 Chemical compositions of West Cliff CWR.

SAMPLE	A	B	C	D	E	F	G
Silicon as SiO ₂	67.17	64.69	65.81	65.93	67.62	43.3	43.2
Aluminium as Al ₂ O ₃	24.54	22.65	22.70	22.43	23.87	14.7	14.9
Iron as Fe ₂ O ₃	4.19	6.51	5.68	5.75	3.56	3.7	3.9
Potassium as K ₂ O	2.93	3.08	3.09	2.97	3.23	1.9	1.9
Calcium as CaO	1.09	1.74	1.45	1.98	1.28	2.2	2.3
Magnesium as MgO	0.76	0.92	1.24	1.34	1.26	1.0	1.1
Titanium as TiO ₂	1.01	1.05	1.07	1.02	1.02	0.67	0.67
Manganese as MnO	0.10	0.14	0.10	0.12	0.06	0.06	0.07
Phosphorus as P ₂ O ₅	0.05	0.26	0.19	0.28	0.15	0.13	0.14
Sodium as Na ₂ O	-	-	-	-	-	0.1	0.08
Ignition loss	21.9	25.3	25.3	-	-	32.1	31.7
Total	101.9	101.0	101.3	101.8	102.0	99.9	100.0

Note that all values given in Table 5.3 are expressed in percentage.

Table 5.4 Average major geomechanical compounds in fine discards (UK).
(after Taylor, 1984)

	Minimum	Maximum
SiO ₂	10.74	46.19
Al ₂ O ₃	5.45	29.91
Fe ₂ O ₃	2.14	8.70
MnO	N.D.	N.D.
MgO	0.05	2.38
CaO	0.19	7.21
Na ₂ O	0.10	0.82
K ₂ O	0.74	4.40
TiO ₂	0.46	1.06
S	0.44	7.85
P ₂ O ₅	0.03	0.18

N.D. denotes not determined.

All values presented in Table 5.4 are expressed in percentage.

Table 5.5 Chemical composition of coal preparation wastes for
four main coalfields of the Soviet Union.

(after Ruban and Shpirt, 1987)

Content	Coalfields (method of preparation)							
	Donbass		Kuzbass		Karaganda		Pechora	Ekibastuz
	grav.	float.	grav.	float.	grav.	float.	grav.	grav. [®]
SiO ₂	50-62	51-58	57-78	50-67	53-63	54-56	61-65	53-64
Al ₂ O ₃	17-31	18-32	14-26	14-31	23-35	23-28	20-24	27-39
Fe ₂ O ₃	3-16	4-12	2-10	2-9	4-7	6-13	6-8	0.2-5
CaO	0.3-5	2-4	1-7	1-10	1-6	1-5	1-2	0.4-2
MgO	0.8-2	1-2	0.3-3	0.7-3	0.3-1	1-2	2-4	0.4-1

[®]Wastes of open cut mining operations and coal preparation pilot plant.

5.3 MECHANICAL PROPERTIES EVALUATION OF CCWR MATERIAL

In this study an attempt has been made to present a brief analysis of the current state of work dealing with experimental studies of deformation properties of CCWR material as affected by uniaxial compression and confining pressure. An examination is also made of the CCWR material characteristics in relation to strata behaviour.

5.3.1 Unconfined compressive strength test results

The complete load deformation curves for all CCWR specimens have been reported in Hii and Aziz (1987a, 1987b). Photographs for each specimen taken before and after the compressive strength testing have also been shown in Hii and Aziz (1987a, 1987b). The calculated compressive strength test results, specimen experimental data are presented in Appendix AII4. The results of compressive strength testing are summarised in Tables 5.6(a) and 5.6(b).

The results of the uniaxial compressive strength tests in relation to the curing time of the specimens of different mix formulations (mixes 1 to 5) are presented in Figure 5.3. Mixes 2 to 5 exhibit good early strength followed by rapid strength development from 1.5 to 5 hours. Figure 5.4 graphically illustrates this property. The increase in maximum compressive strength for Mixes 2 to 5 during the initial 24 hours curing time is shown in Figure 5.5. This increase is quite pronounced.

It should be noted that specimens of mix 1 could not be tested under 24 hours curing time. This is due to the fact that specimens could not be demoulded before this time because of the high fluidity caused by the relatively high water content of 14.7%. Increases in the compressive strength from 1 to 7 days curing time are still quite rapid although the rate is slightly lower than described for up to 24 hours curing time. Thereafter, the increase in strength is not significant for mixes 3 to 5. This could be explained by the high water to cement ratios of 1.76, 2.0 and 3.0 for mixes 3, 4 and 5 consecutively. Mix 1 displays a moderate strength increase from 7 to 90 days curing time while mix 2 displays a high strength increase.

Table 5.6(a) Summary of results of compressive strength tests.

Portland Cement (%)	Water Content (%)	Slump (mm)	Compressive Strength (MPa)													
			0.25H	0.5H	0.75H	1H	1.5H	2H	4H	1 Day	7 Days	14 Days	28 Days	60 Days	90 Days	365 Days
25*	16.3					0.104		0.551			14.690	18.500	21.80			
20*	15.96					0.051		0.229			11.70	14.10	15.19			
15	21.0	C								1.289	2.870	3.111	4.248	4.623	5.443	
15*	17.6					0.025		0.046			5.170	6.530	6.780			
15	14.7	110								2.589	5.774	6.620	7.539	9.325	10.282	13.559
15	12.0	0	0.037	0.033	0.042	0.068	0.111	0.231	0.892	6.714	8.552	8.682	8.126	9.493	12.773	
12.5	19.1	C								1.152	2.800	3.117	3.394	4.803	4.157	
12.5	16.5	85				0.009			0.013	1.365	3.895	4.670	5.134	7.029	6.875	
12.5	13.0	0					0.082	0.151	1.021	5.138	8.859	10.612	10.838	15.073	16.599	

* (after Thomas, 1986).

C denotes collapsed slump.

Table 5.6(b) Summary of results of compressive strength tests.

Portland Cement (%)	Water Content (%)	Slump (mm)	Compressive Strength (MPa)													
			0.25H	0.5H	0.75H	1H	1.5H	2H	4H	1 Day	7 Days	14 Days	28 Days	60 Days	90 Days	365 Days
10	19.1	C								0.659	1.703	2.011	2.183	2.724	2.886	
10*	16.2					0.032		0.048			2.650	3.070	3.410			
10	13.8	15					0.039	0.042		1.799	3.449	3.882	4.344	4.699	5.631	8.875
10	12.0	10			0.041	0.036	0.047	0.078	0.271	3.495	6.305	6.232	7.474	7.433	7.795	
7.5	19.0	C								0.321	0.823	0.924	1.112	1.616	1.617	
7.5	16.5	75								0.594	1.289	1.213	1.680	1.864	2.097	
7.5	12.6	10					0.038	0.042	0.166	1.629	2.664	3.152	3.379	4.105	4.625	6.356
5.0	12.0	10							0.255	1.208	1.876	2.041	2.432	2.493	3.388	3.439

* (after Thomas, 1986).

C denotes collapsed slump.

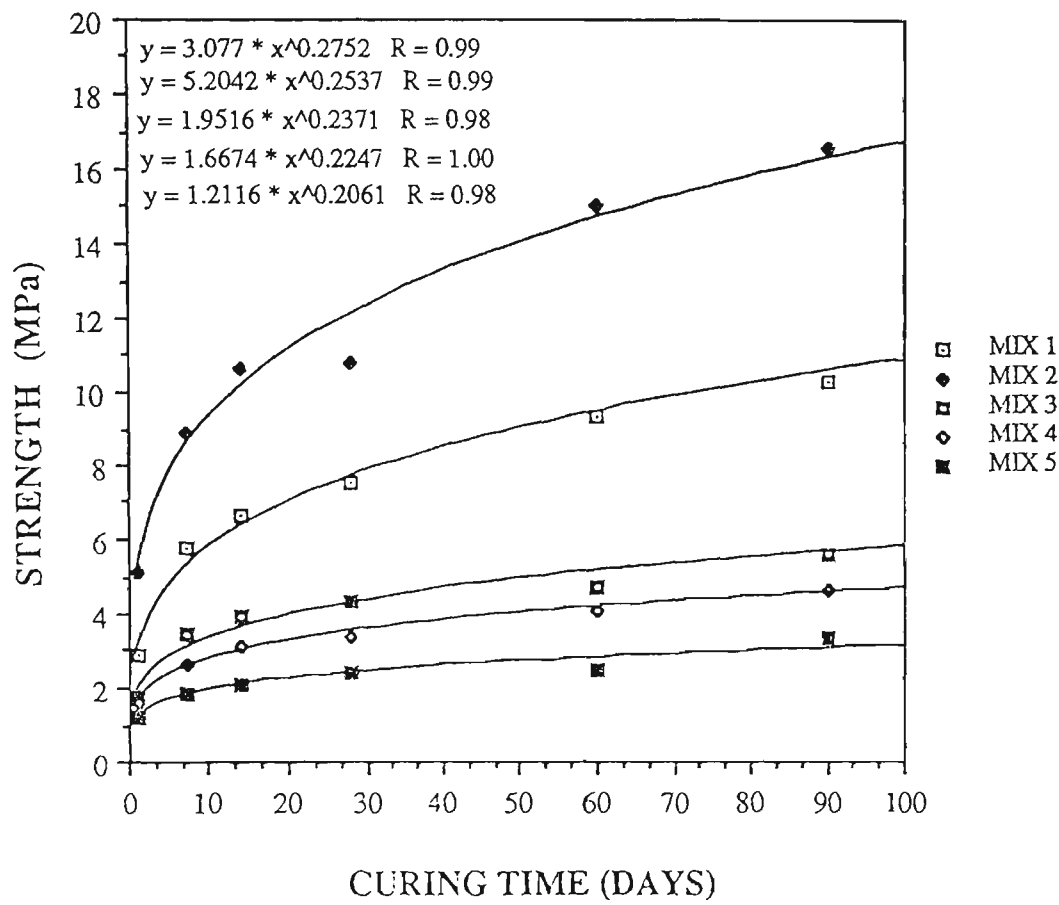


Figure 5.3 Plots of the measured strength against curing time for mixes 1 to 5.

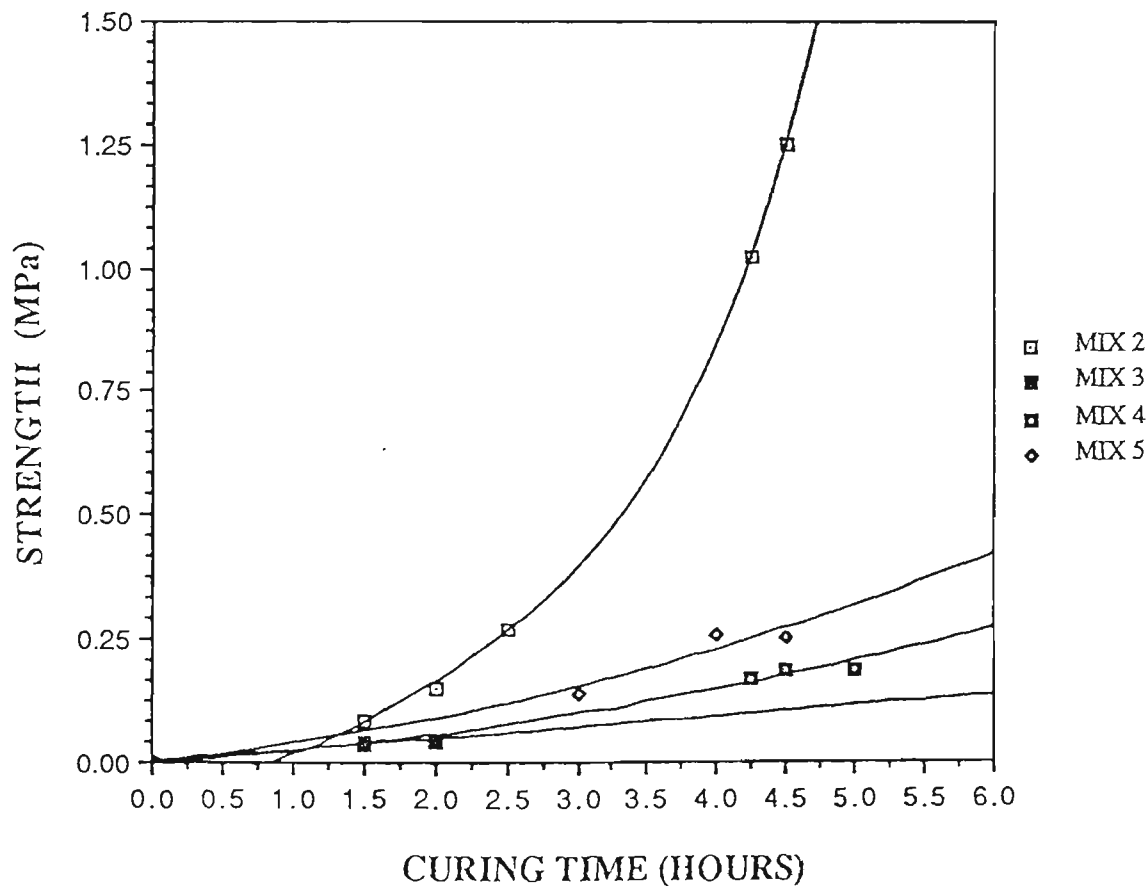


Figure 5.4 Stress-curing time curves of various mixes of CCWR specimens for up to 5 hours curing time.

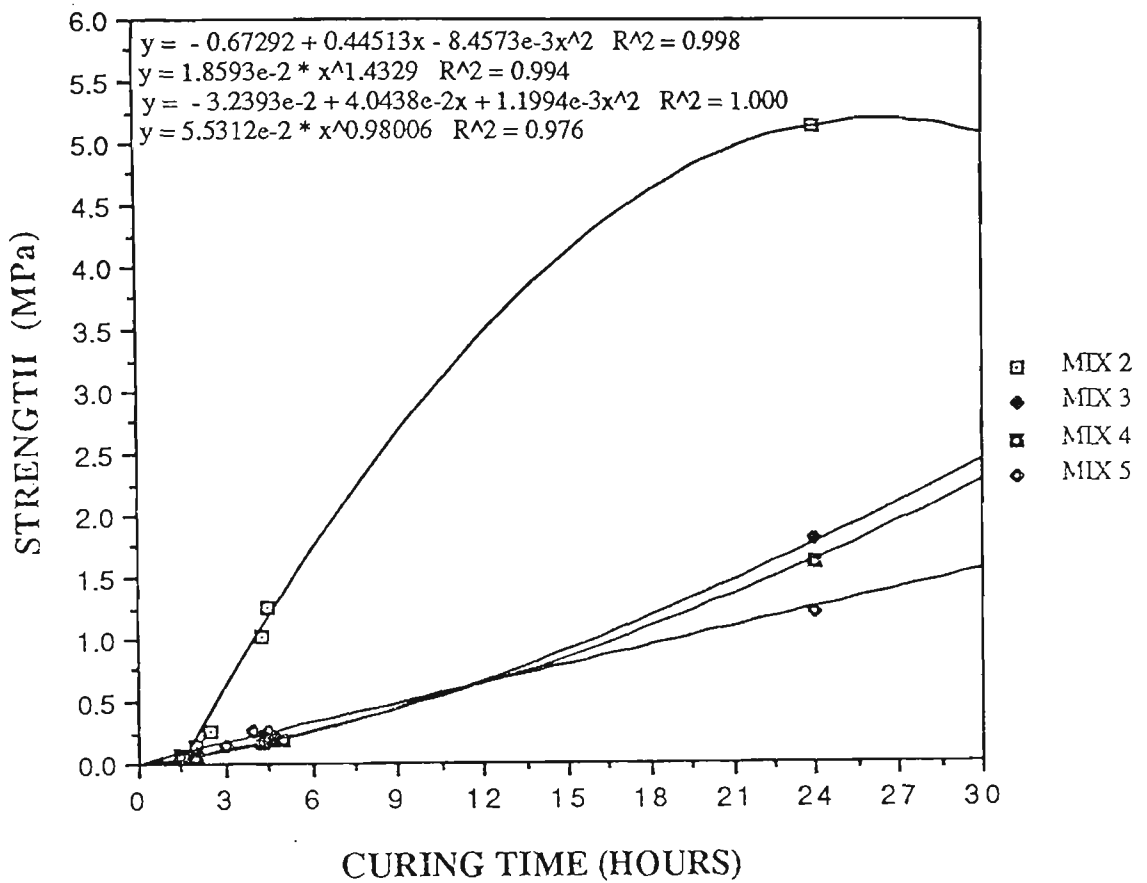


Figure 5.5 Stress-curing time curves of mixes 2 to 5 of CCWR specimens for up to 24 hours curing time.

The form of the curve is a function of a very complicated cement chemistry of the material. The load deformation relationships of the specimens of mixes 1 and 2 which have been shown in Appendices A and B (Hii and Aziz, 1987a) indicate that the specimens with a curing time of up to 90 days display a plastic form. At the curing of 1 day and after, the rate of increase in strength is more rapid and leads to a more significant peak strength. At the time the peak strength is reached there is a sharp drop in strength and this is a characteristic of a relatively brittle material.

The results indicate that the specimens of mix 2 exhibit stiffer and more brittle characteristics than those of mix 1. The higher strength development pattern of mix 2 than that of mix 1 can be explained by examining Table 4.4(a). It can be

seen from Table 4.4(a) (in Section 4.2, Chapter 4) that the water to cement ratios are very similar being 1.1 for mix 1 and 1.2 for mix 2; the higher fluidity of mix 1 on pouring coupled with the slightly lower water to cement ratio may have resulted in this behaviour. Also, the higher mass percentage of calcium chloride admixture (2.55% in mix 1 and 3.0% in mix 2) used in mix 2 and a longer duration of vibration (5 seconds for mix 1 and 20 seconds for mix 2) could contribute to its higher maximum strengths. Error in the preparation of mix 2 resulting in a higher cement percentage than desired could also explain these anomalies, although this is quite unlikely to occur.

The post failure modulus and residual strength results of CCWR specimens for mixes 1 to 5 are presented in Appendix AII5. The results indicate that the specimens exhibit low residual strengths.

5.3.2 Triaxial strength test results

Results of triaxial strength tests carried out on different mix compositions are presented in Tables 5.7 through 5.11. The results of the triaxial strength tests are summarised in Table 5.12. The stress-strain relationships of mixes of CCWR specimens under different confining stresses are presented in Figures 5.6 through 5.10. The results show that the plastic behaviour of the material under confining pressure is not only dominant for specimens with short curing time (7 days), but is also evident for specimens with longer curing times. This is not like the brittle mode of failure experienced for specimens under uniaxial compressive tests. Therefore the effect of confining stress is the major contributory factor for such a change in failure mode.

Table 5.7 Results of triaxial tests for CCWR material specimens
(mixes one through three).

Mix	Specimen	Confining Pressure (MPa)	Strength (MPa)	Wet density (t/m ³)	Water content (%)
1	A1	0	8.699	1.900	11.27
	A2	0	8.680	1.880	11.33
	A7	0	9.796	1.911	10.60
	A4	1.39	16.238	1.873	9.10
	A5	3.75	20.668	1.914	9.20
	A6	5.56	24.589	1.868	10.00
	A3	6.95	28.728	1.920	10.60
2	B5	0	13.122	1.999	8.17
	B6	0	13.379	2.001	8.07
	B7	0	12.768	2.008	8.26
	B4	2.09	22.729	2.039	7.87
	B3	4.17	28.624	2.203	7.90
	B2	5.56	32.831	2.044	7.90
	B1	6.95	35.833	1.994	7.90
3	C1	0	4.295	1.949	10.46
	C5	0	4.190	1.918	10.44
	C4	1.39	11.364	1.893	9.26
	C2	2.09	13.567	1.941	10.30

Table 5.8 Results of triaxial tests for CCWR material specimens
(mixes four and five).

Mix	Specimen	Confining Pressure (MPa)	Strength (MPa)	Wet density (t/m ³)	Water content (%)
4	D5	0	3.515	2.050	8.22
	D6	0	3.034	1.898	8.95
	D3	0.10	3.095	1.921	---
	D1	0.20	5.135	1.909	7.50
	D2	0.40	5.640	1.923	9.50
5	E5	0	1.902	1.729	8.27
	E6	0	1.897	1.984	9.26
	E1	0.17	3.078	1.992	8.96
	E4	0.35	4.083	1.950	9.13
	E2	0.52	5.196	1.970	9.08
	E3	0.86	6.666	1.958	9.18

Table 5.9 Results of triaxial tests for CCWR material specimens
(mixes seven and eight).

Mix	Specimen	Confining Pressure (MPa)	Strength (MPa)	Water content (%)
7	G1	0	2.995	20.33
	G2	0	3.289	19.89
	G3	0	3.126	20.72
	G4	0.137	4.060	19.24
	G5	0.274	4.022	20.11
	G6	0.411	4.720	21.31
	G7	0.548	5.522	19.50
	G8	0.689	5.717	21.72
8	H1	0	1.728	16.42
	H2	0	1.786	16.87
	H3	0	1.612	16.71
	H4	0.137	2.421	17.64
	H5	0.274	3.241	16.67
	H6	0.411	3.504	18.05
	H7	0.548	4.276	17.90
	H8	0.689	5.047	17.27

Table 5.10 Results of triaxial tests for CCWR material specimens
(mixes ten and eleven).

Mix	Specimen	Confining Pressure (MPa)	Strength (MPa)	Water content (%)
10	J1	0	5.303	12.58
	J2	0	5.522	11.75
	J3	0	5.359	12.04
	J4	0.137	4.779	13.36
	J5	0.274	5.765	12.39
	J6	0.411	6.496	12.72
	J7	0.548	7.511	13.19
	J8	0.689	8.404	13.25
11	K1	0	3.295	14.21
	K2	0	3.185	14.43
	K3	0	3.307	15.21
	K4	0.137	3.472	15.95
	K5	0.274	4.423	16.35
	K6	0.411	5.067	15.38
	K7	0.548	5.231	15.87
	K8	0.689	5.729	16.32

Table 5.11 Results of triaxial tests for CCWR material specimens
(mixes twelve and thirteen).

Mix	Specimen	Confining Pressure (MPa)	Strength (MPa)	Water content (%)
12	L1	0	0.974	17.28
	L2	0	1.000	17.24
	L3	0	0.971	16.36
	L4	0.137	1.538	16.31
	L5	0.274	2.116	16.53
	L6	0.411	2.603	16.79
	L7	0.548	3.133	16.71
	L8	0.689	3.695	16.51
13	M1	0	1.848	11.91
	M2	0	1.976	12.59
	M3	0	1.790	12.17
	M4	0.274	3.886	12.56
	M5	0.689	5.704	12.67

Table 5.12 Summary of triaxial test results for CCWR specimens.

Mix	Material friction angle (o)	Cohesive strength (MPa)	Unconfined compressive (MPa)	Tensile strength (MPa)
15.0%C-21.0%W	28	0.625	3.123	0.608
15.6%C-14.7%W	14	1.400	9.058	---
12.5%C-19.1%W	22	0.740	3.262	0.629
12.5%C-16.5%W	20	1.100	5.395	0.840
12.5%C-13.0%W	16	2.600	13.090	---
10.0%C-19.1%W	30	0.420	1.709	0.394
10.0%C-16.5%W	29	0.400	1.871	0.403
7.5%C-19.1%W	32	0.225	0.982	0.170
7.5%C-16.5%W	29	0.400	1.871	0.403
7.5%C-12.6%W	36	0.600	3.275	0.422
5.0%C-13.0%W	41	0.350	1.900	0.191

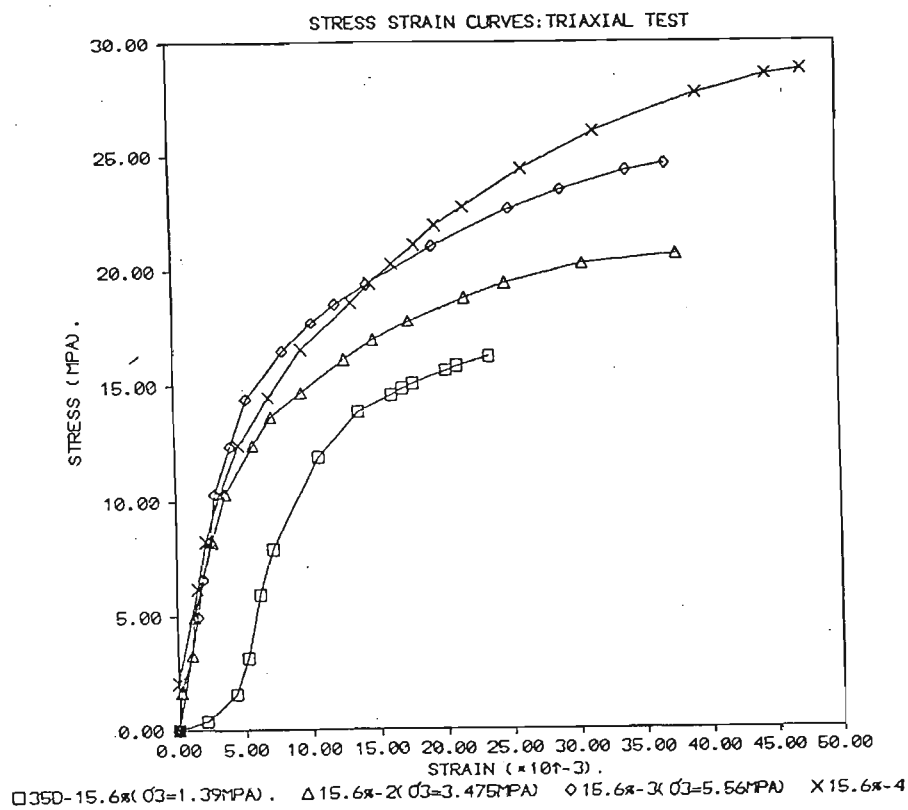


Figure 5.6 Triaxial strength test results for CCWR specimens at different confining pressure (15.6% cement, mix 1).

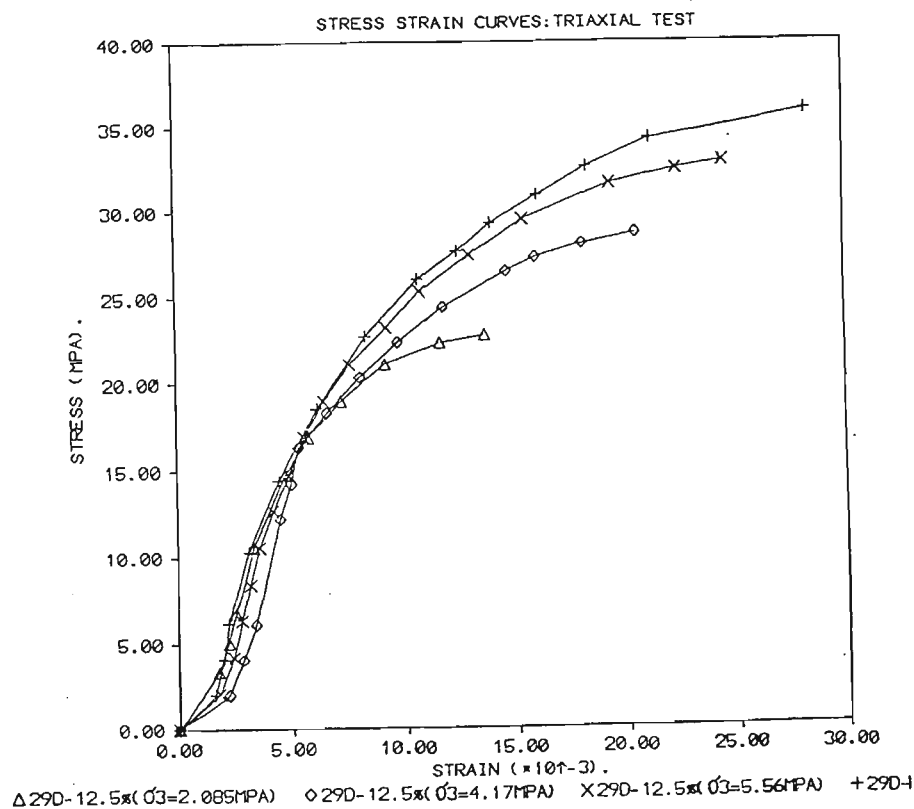


Figure 5.7 Triaxial strength test results for CCWR specimens at different confining pressure (12.5% cement, mix 2).

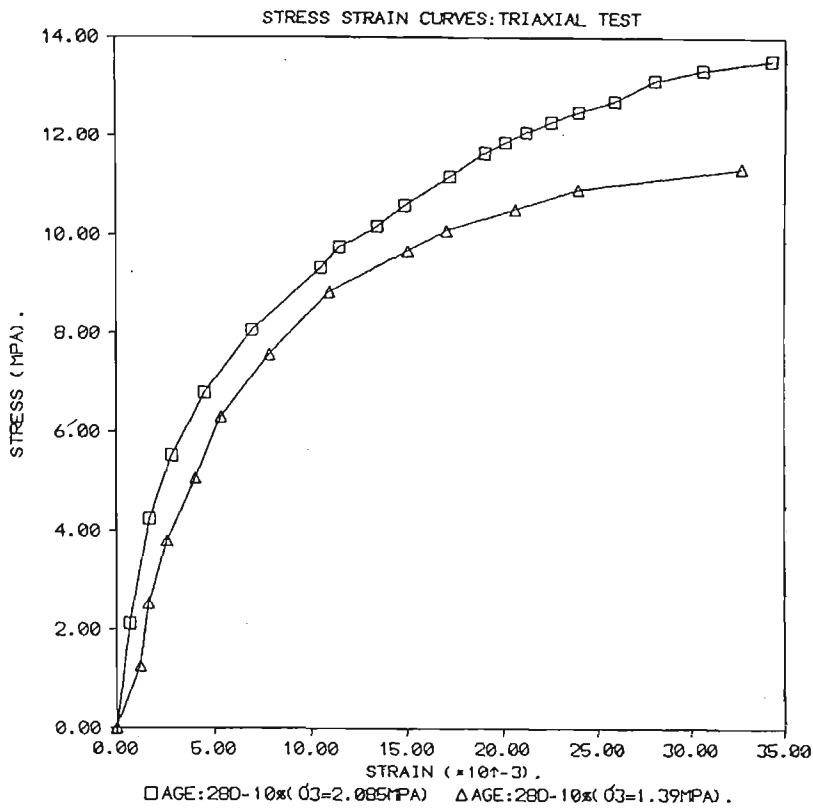


Figure 5.8 Triaxial strength test results for CCWR specimens at different confining pressure (10.0% cement, mix 3).

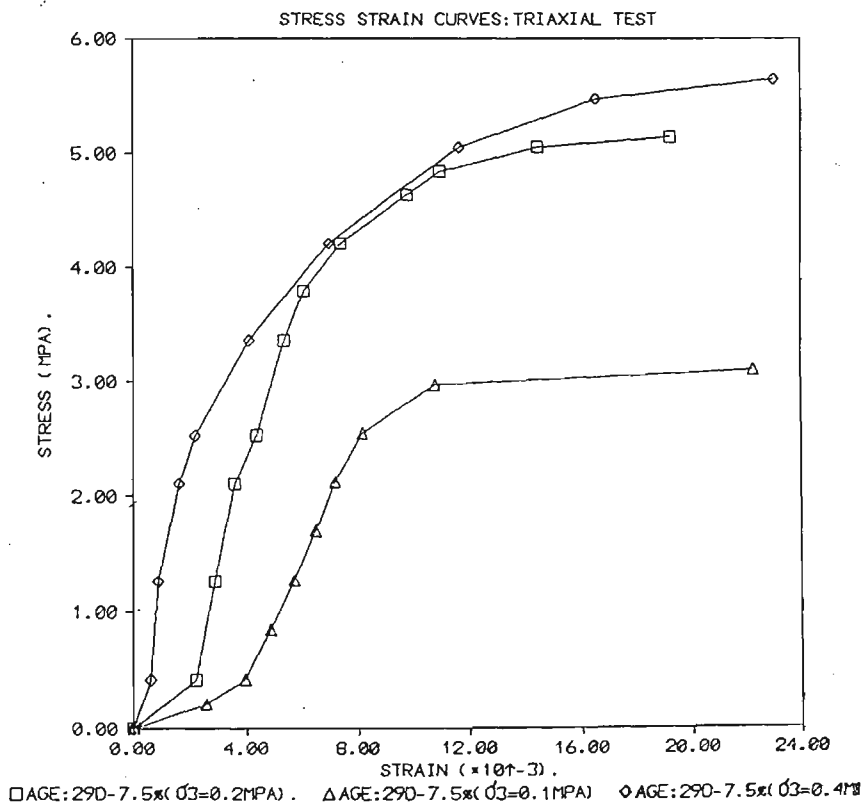


Figure 5.9 Triaxial strength test results for CCWR specimens at different confining pressure (7.5% cement, mix 4).

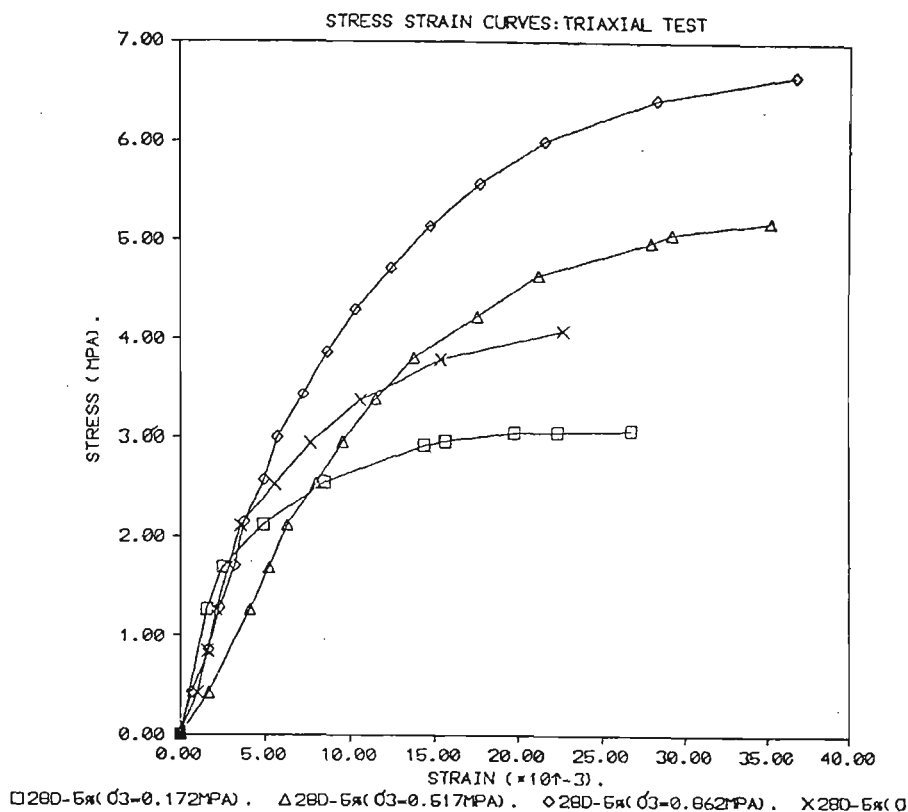


Figure 5.10 Triaxial strength test results for CCWR specimens at different confining pressure (5.0% cement, mix 5).

Under triaxial stress conditions the post-failure stress-strain curves (Figures 5.6 through 5.10) show that the test specimens behave in a brittle-ductile manner. The residual strength values constitute a high proportion of the peak strength values. In field application, the CCWR pack will initially be confined by the forms. As the pack is loaded it may expand laterally and confinement will be offered by adjacent packs. This means that a higher degree of resistance to closure will still be offered by the packs.

Figures 5.11 through 5.21 show the peak strength Mohr's envelopes for different mix compositions. Figures 5.22 and 5.23 show the peak strength envelope of CCWR specimens. Mixes 3 to 5 display an expected increase in the friction angle ϕ and a decrease in the cohesive strength C for a subsequent decrease in the mix cement percentage. Mix 1 exhibits a lower cohesive strength than mix 2 and this explains the lower strength development pattern of mix 1 than mix 2 as described in Section 5.3.1.

Figure 5.11 Peak strength Mohr's envelopes for 15.0%C-21.0%W mix.

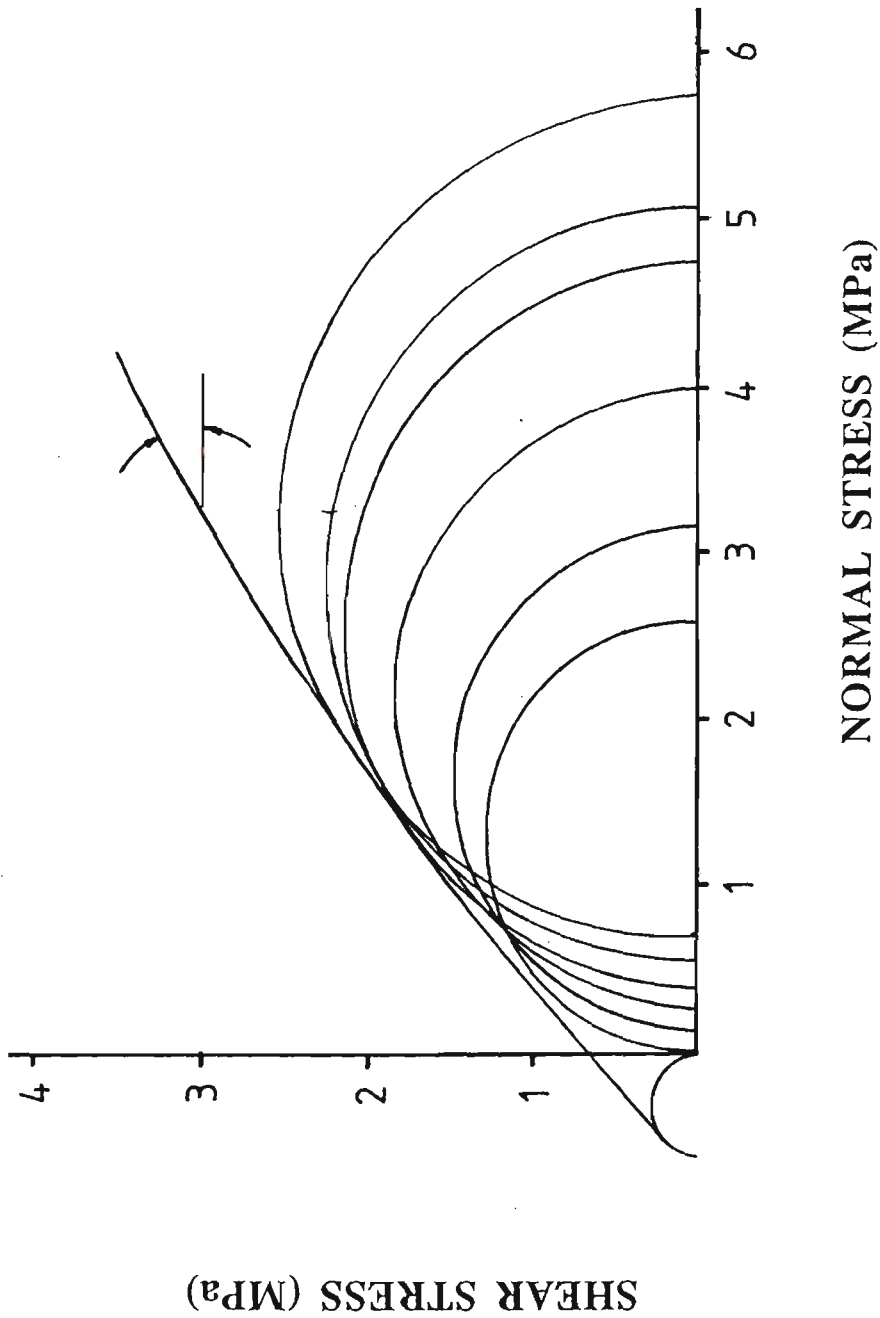


Figure 5.12 Peak strength Mohr's envelopes for 15.0%C-14.7%W mix.

$C = 1.4 \text{ Mpa.}$
 $\sigma_c = 9.1 \text{ MPa.}$
 $\phi = 14^\circ$

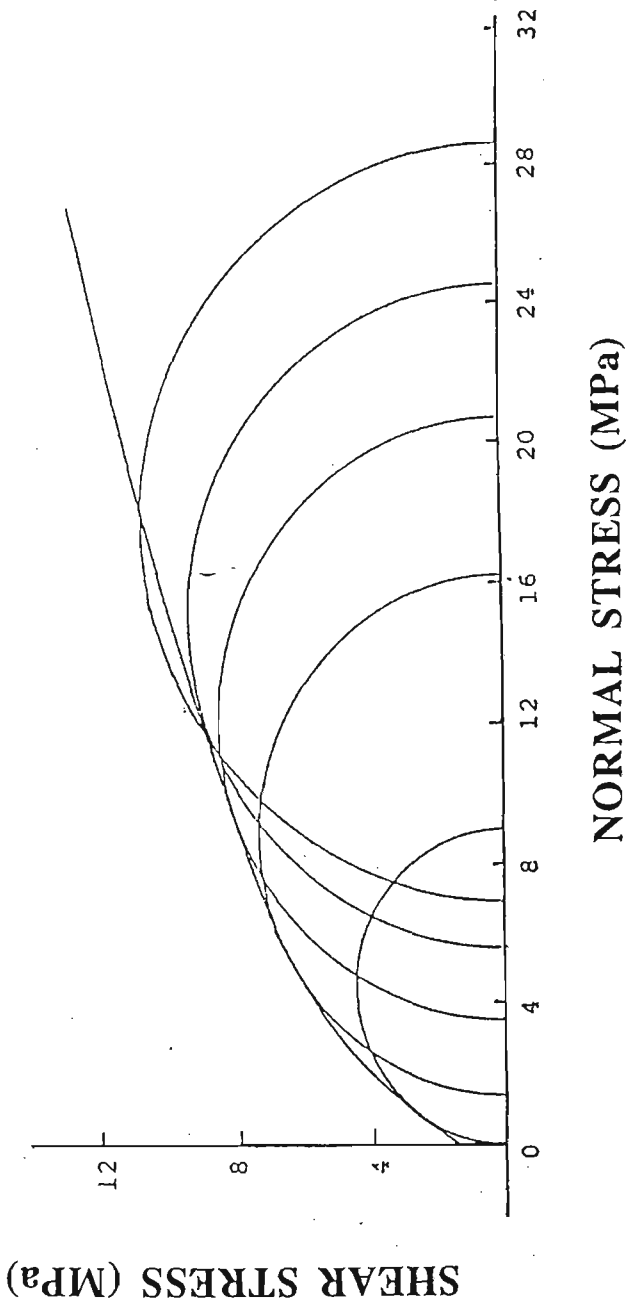
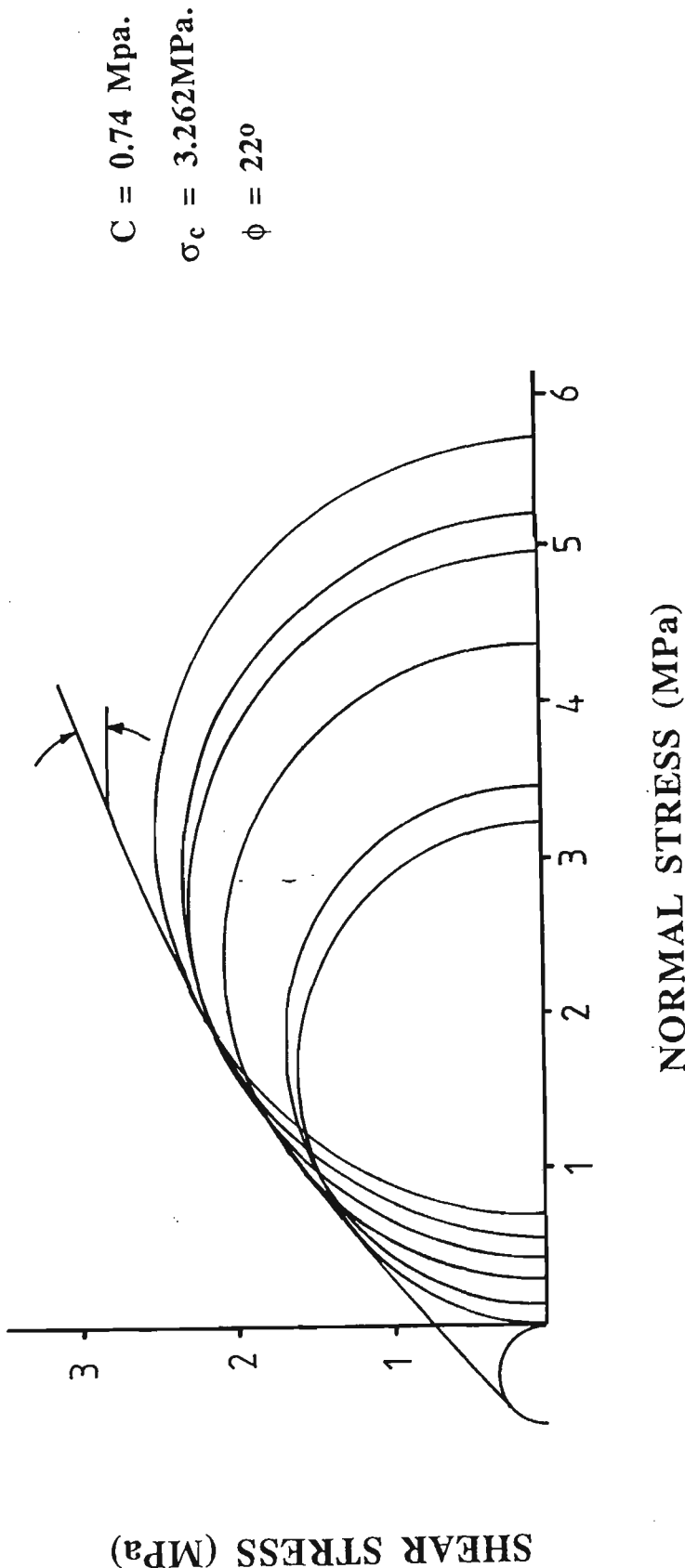


Figure 5.13 Peak strength Mohr's envelopes for 12.5%C-19.1%W mix.



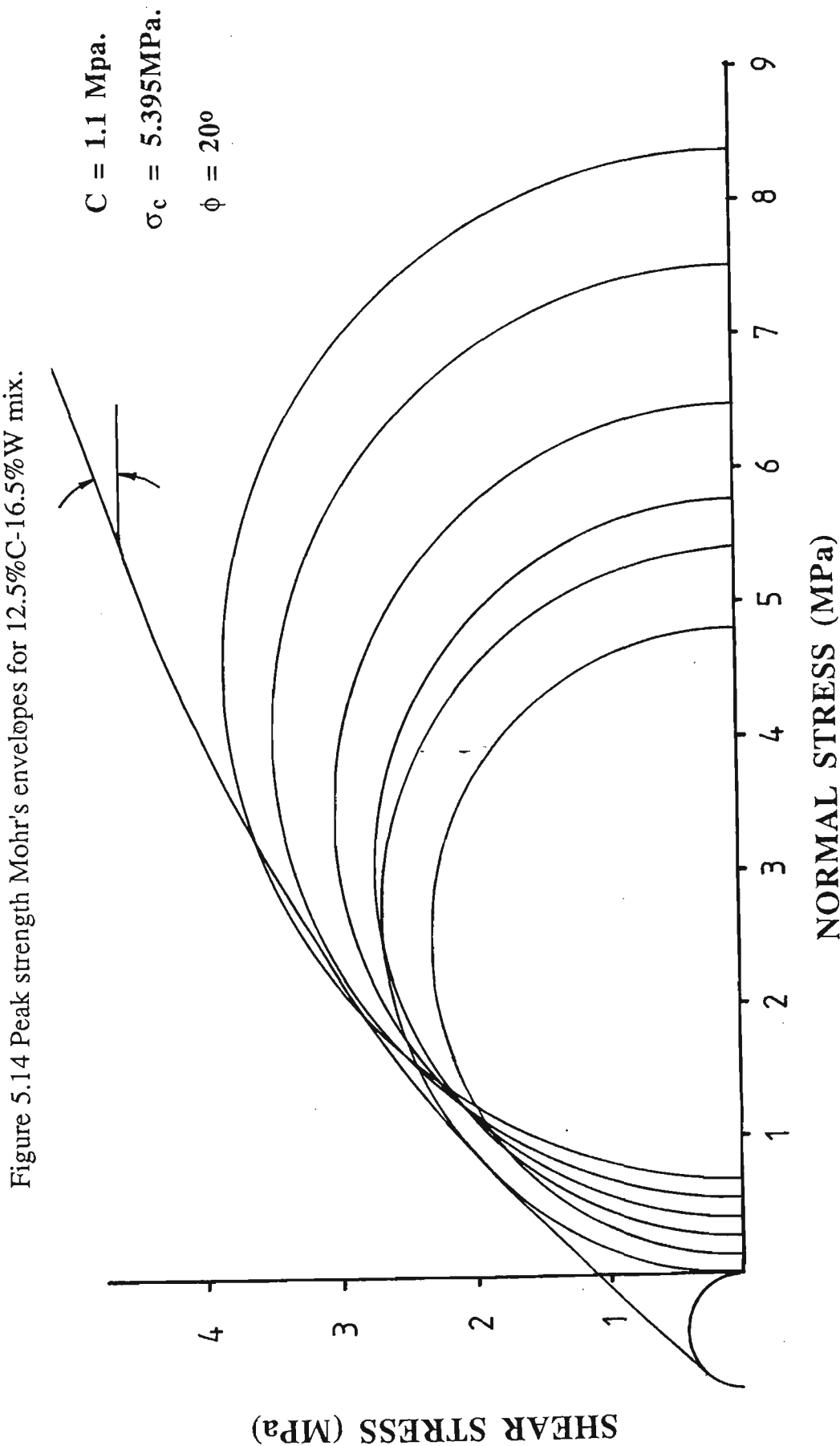


Figure 5.15 Peak strength Mohr's envelopes for 12.5%C-13.0%W mix.

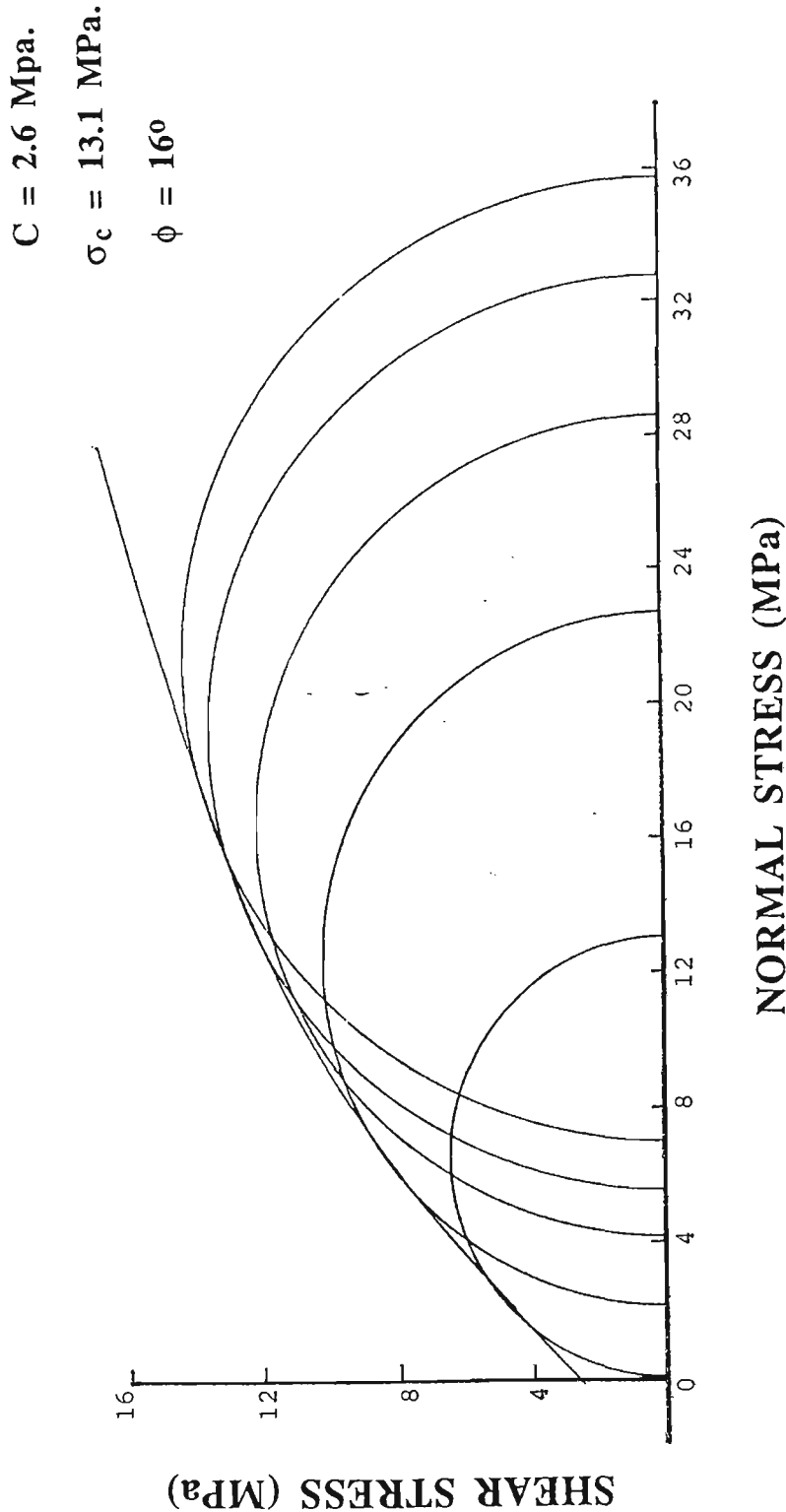


Figure 5.16 Peak strength Mohr's envelopes for 10.0%C-19.1%W mix.

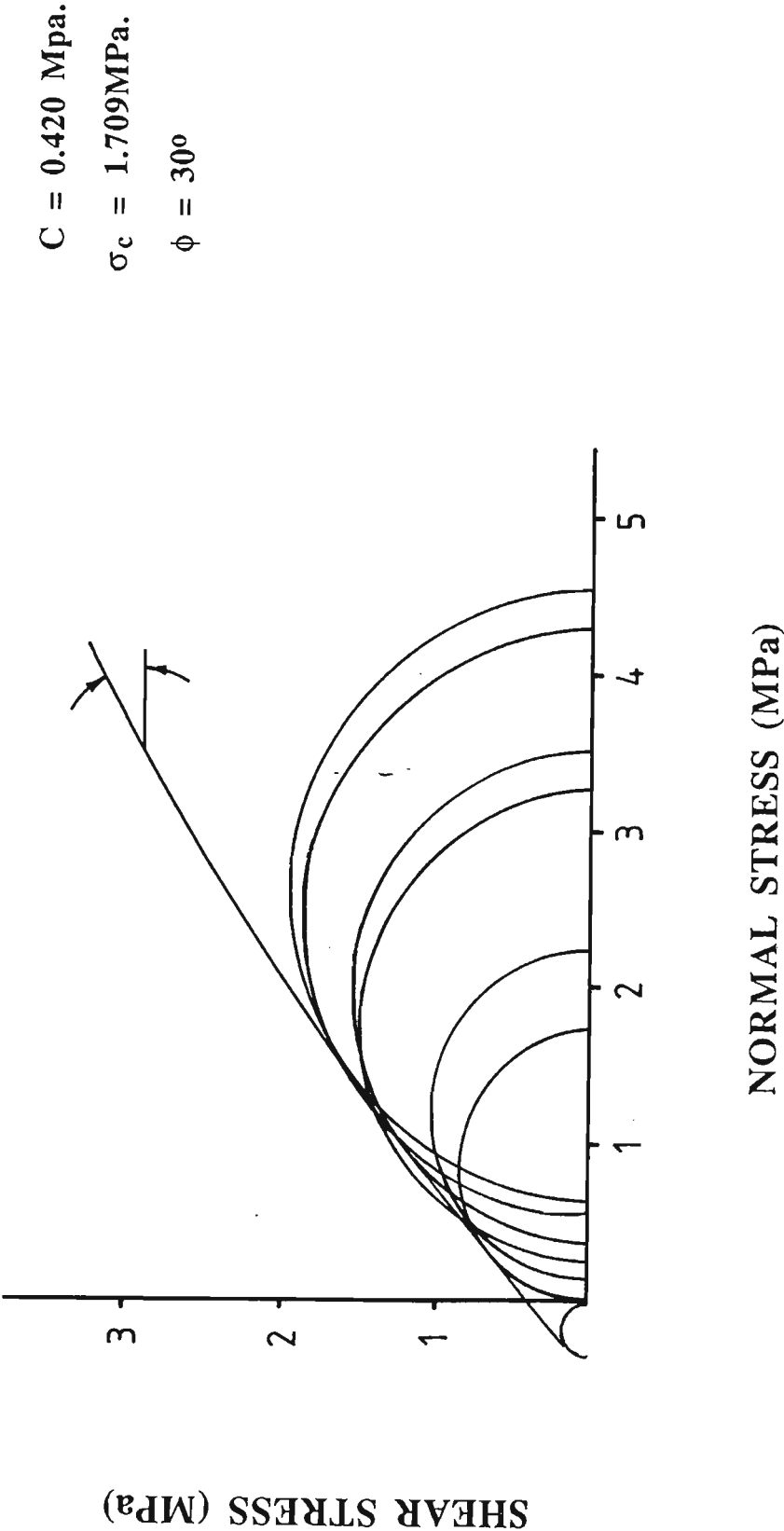


Figure 5.17 Peak strength Mohr's envelopes for 10.0%C-16.5%W mix.

$C = 0.8 \text{ Mpa.}$
 $\sigma_c = 4.24 \text{ MPa.}$
 $\phi = 28^\circ$

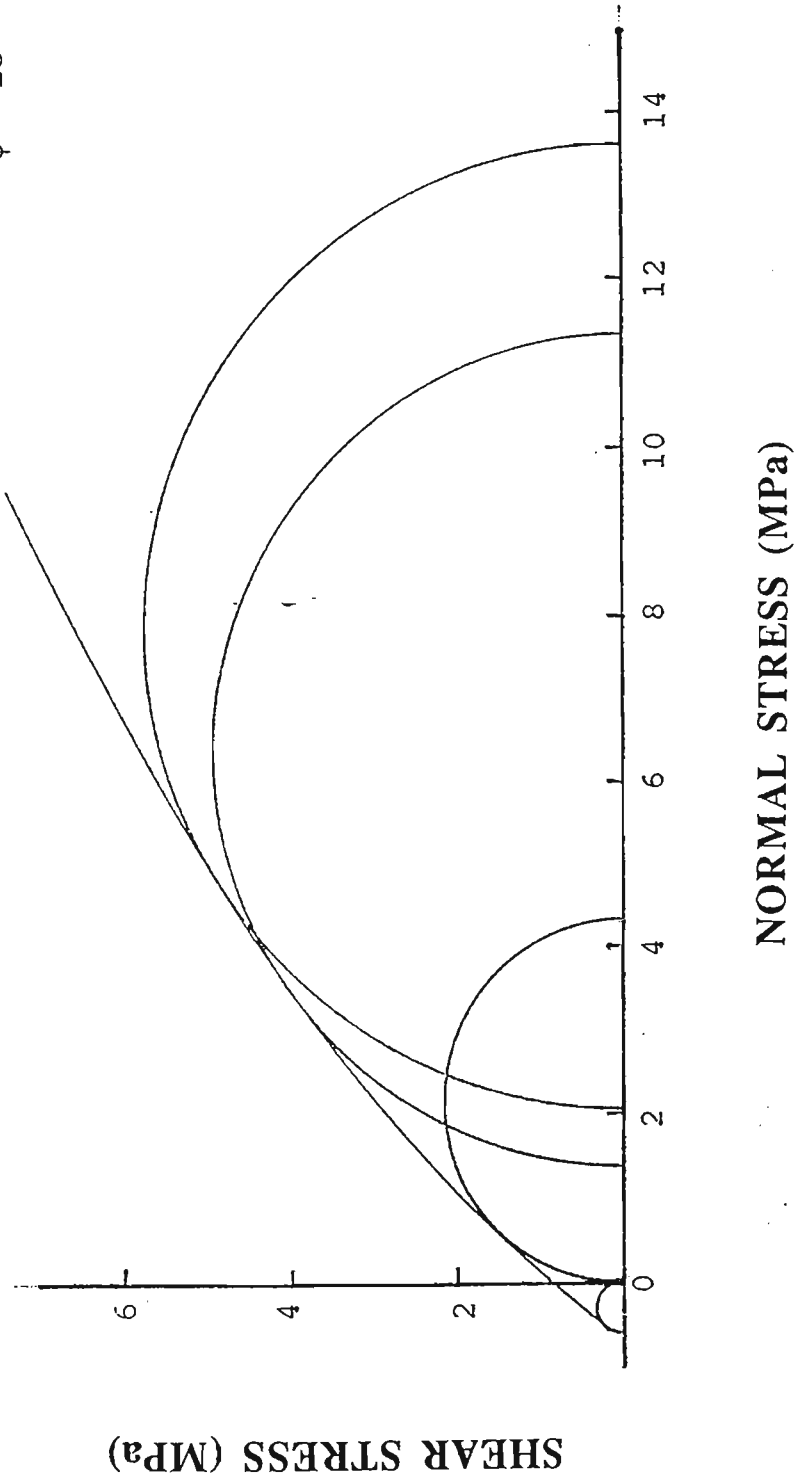


Figure 5.18 Peak strength Mohr's envelopes for 7.5%C-19.1%W mix.

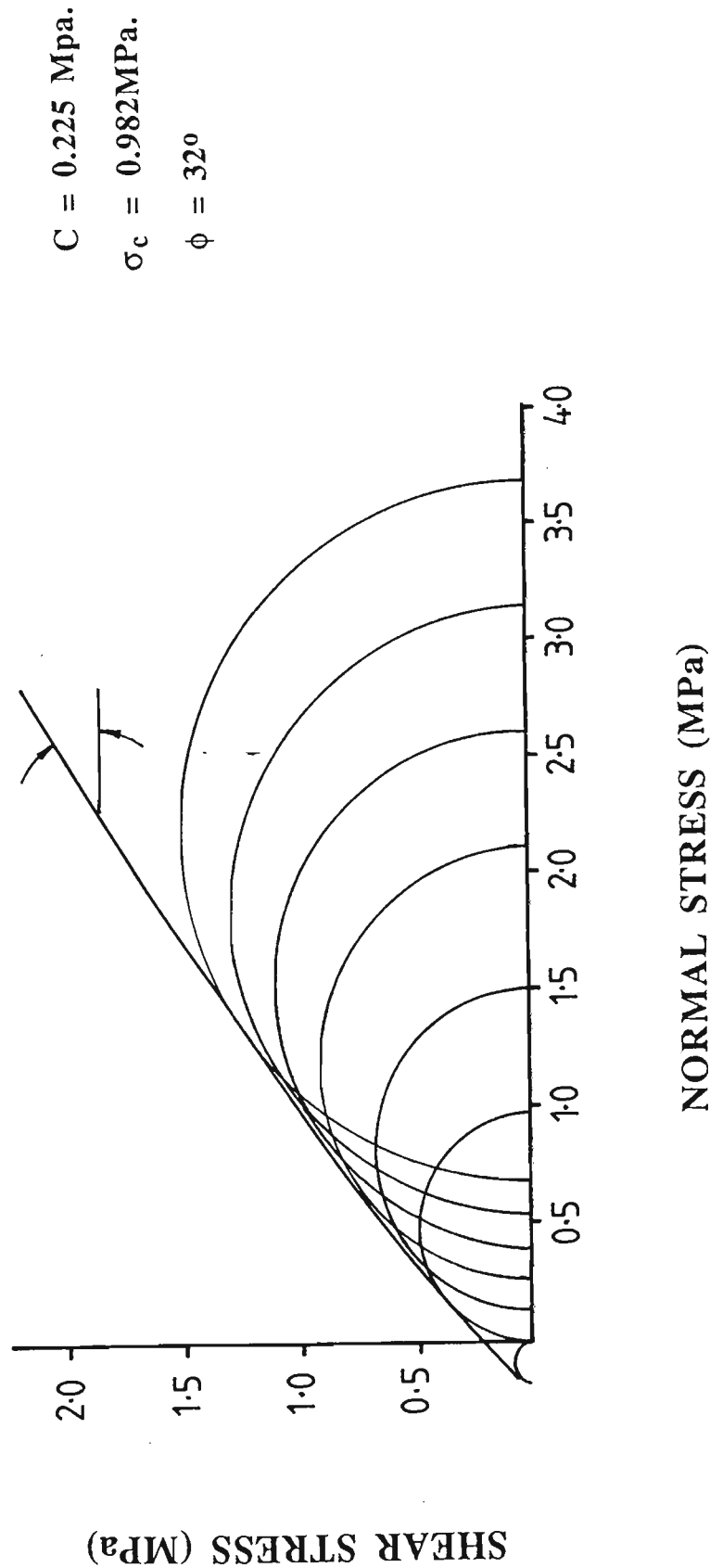
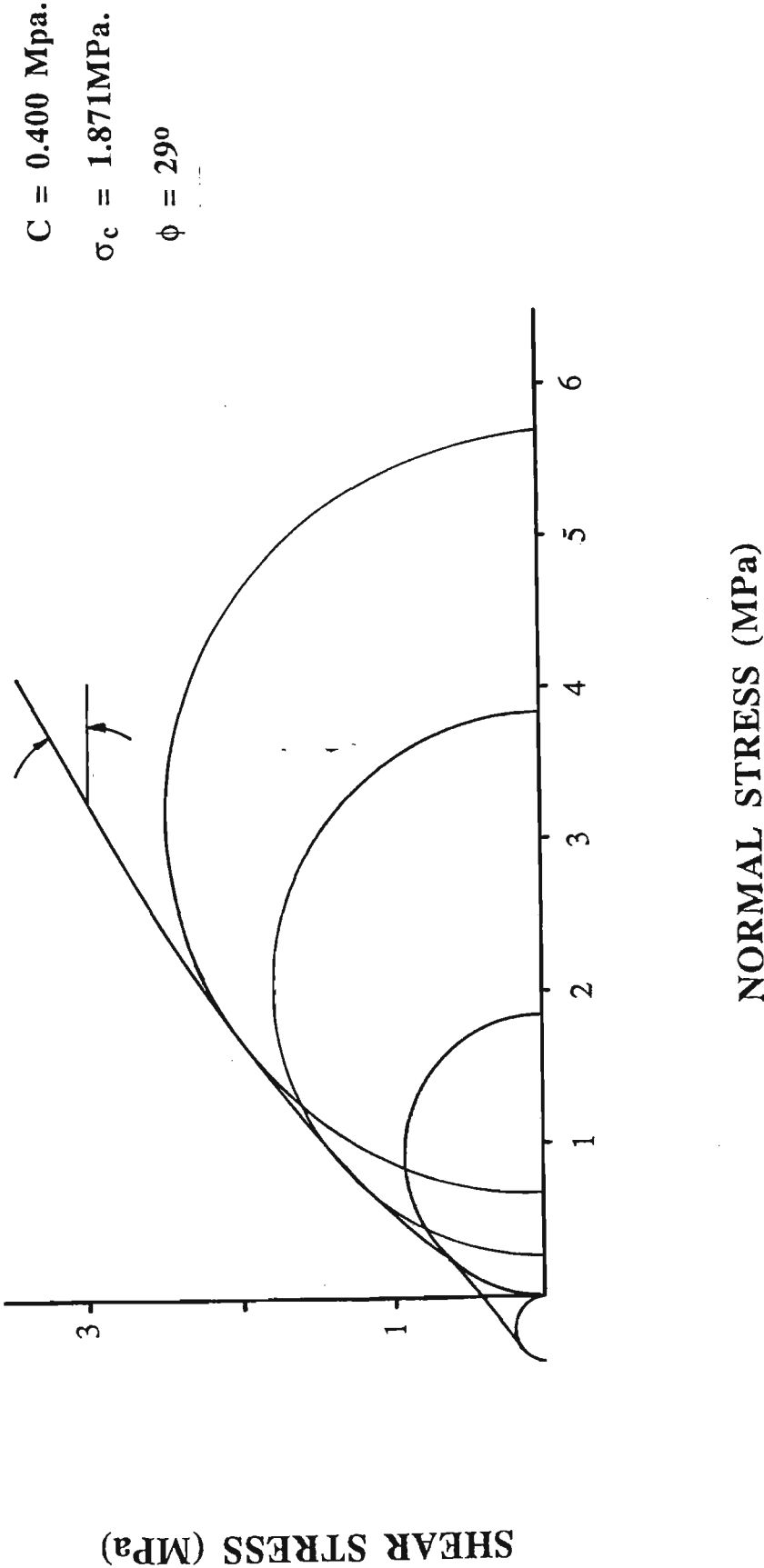


Figure 5.19 Peak strength Mohr's envelopes for 7.5%C-16.5%W mix.



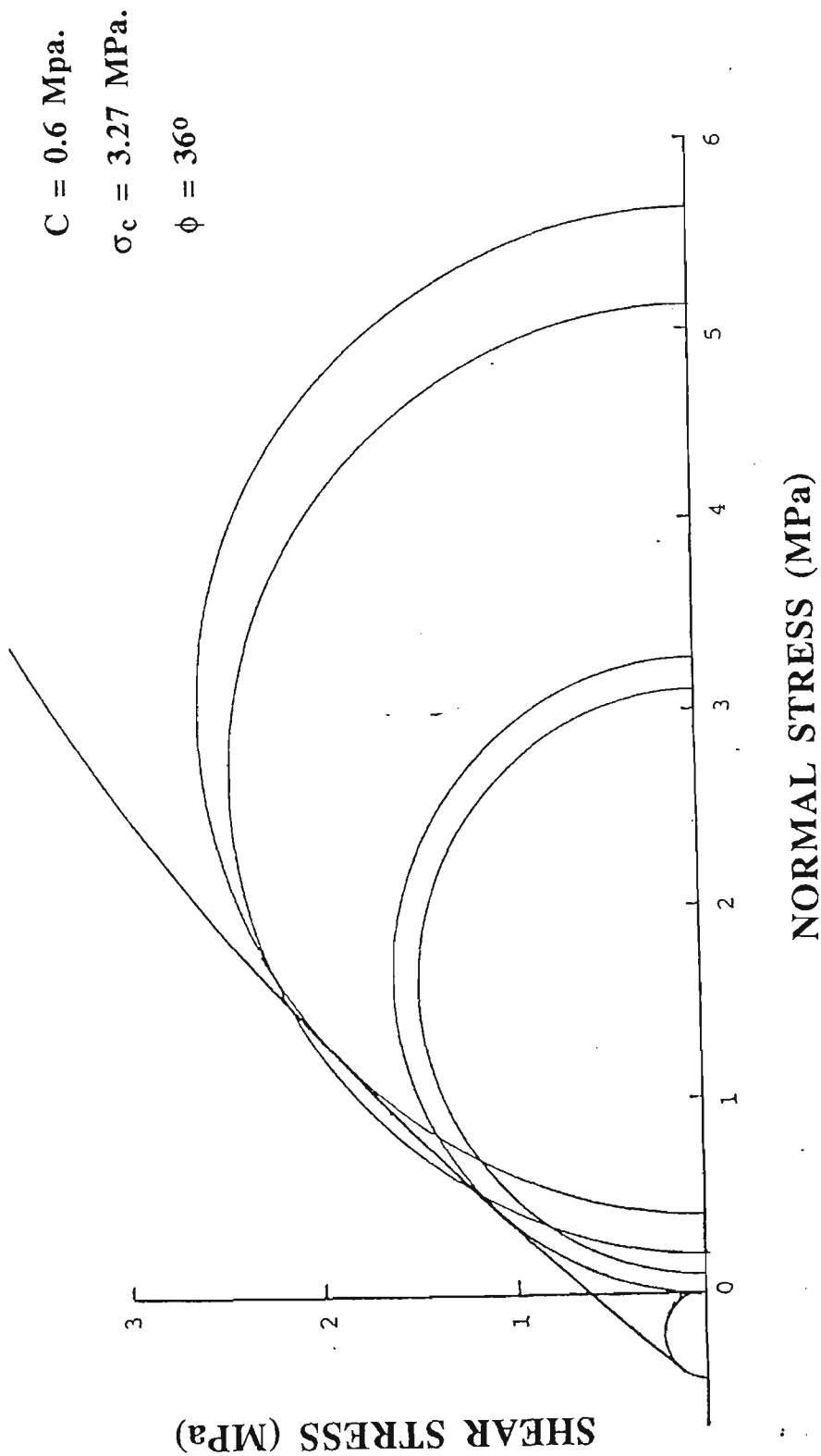
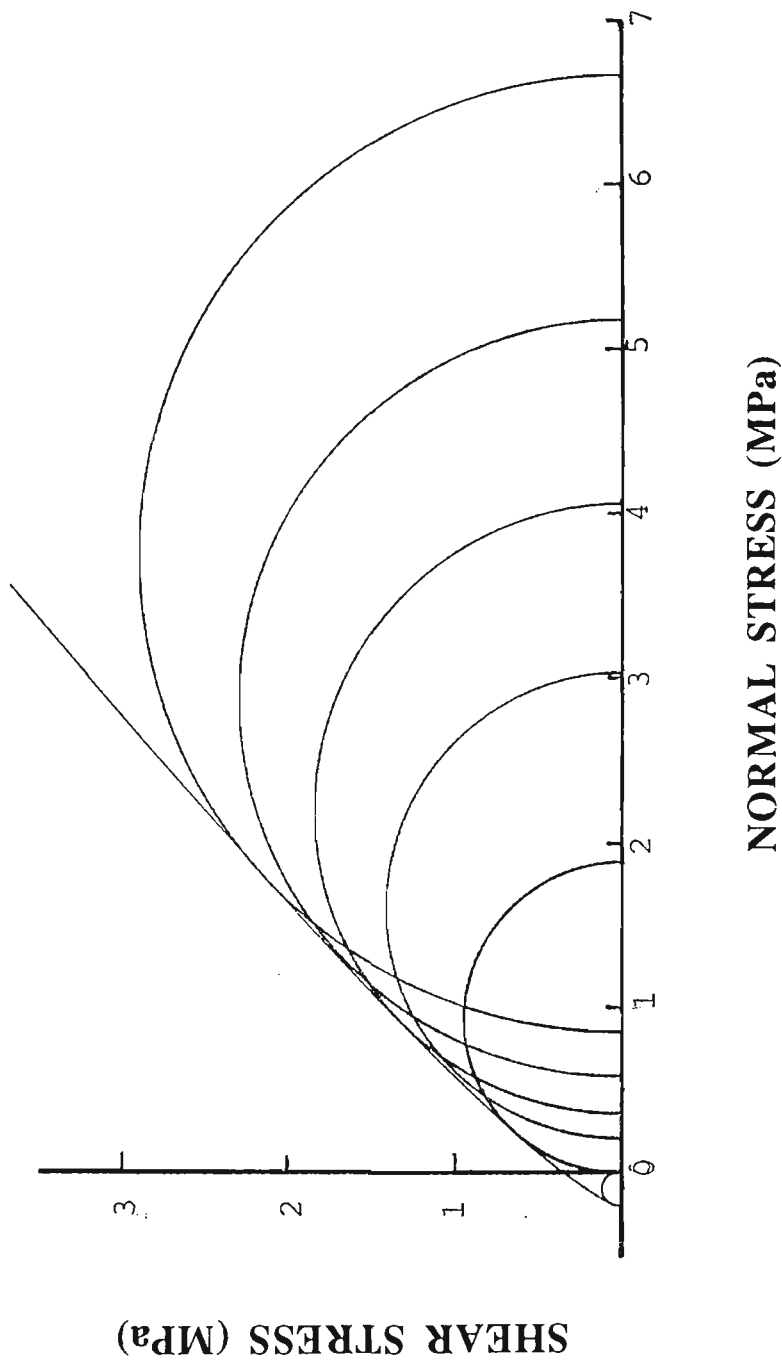


Figure 5.20 Peak strength Mohr's envelopes for 7.5%C-12.6%W mix.

Figure 5.21 Peak strength Mohr's envelopes for 5.0%C-13.0%W mix.



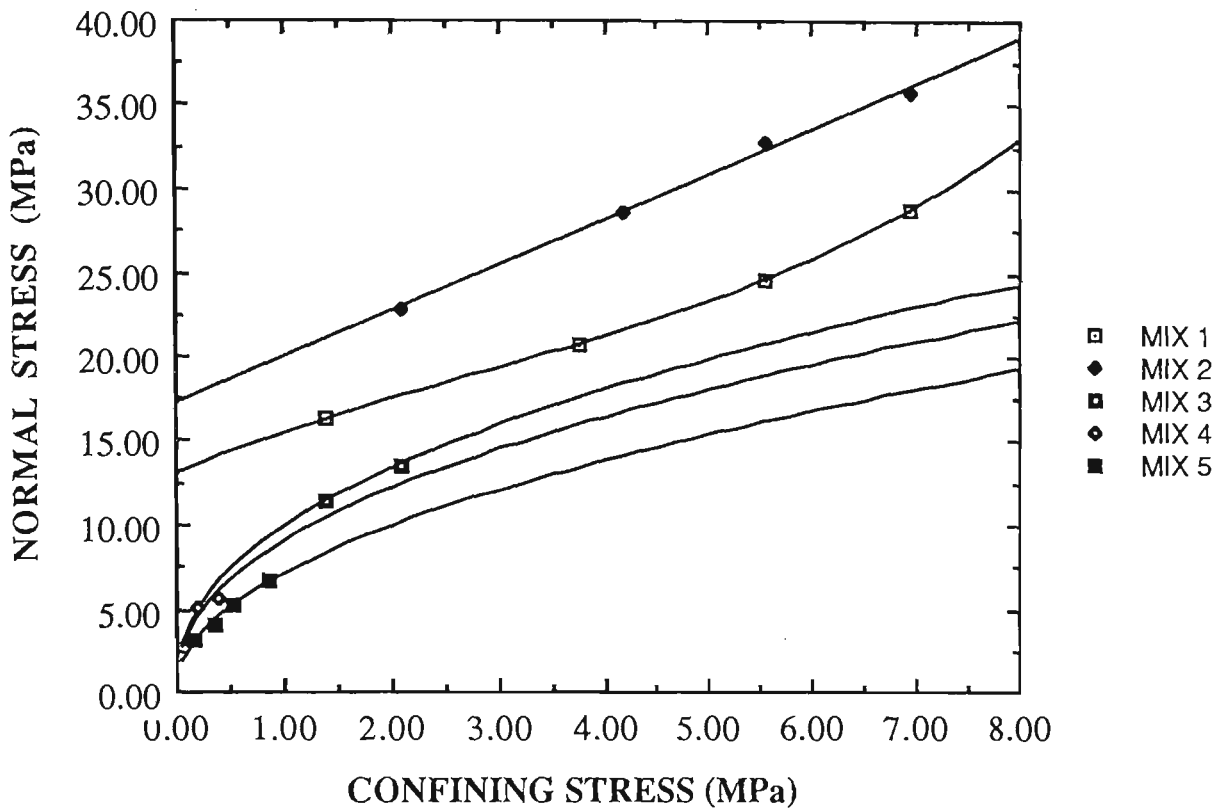


Figure 5.22 Peak strength envelope of CCWR specimens for mixes 1 to 5.

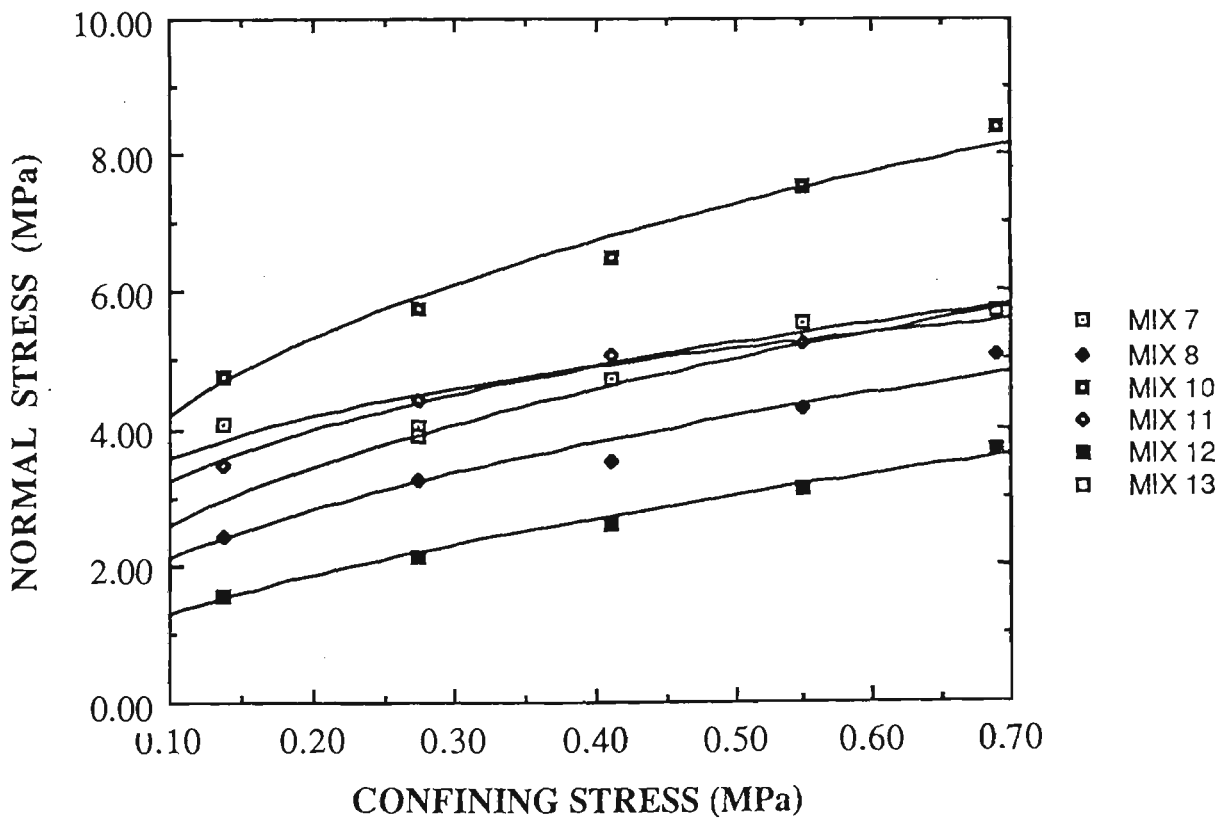


Figure 5.23 Peak strength envelope of CCWR specimens for mixes 7, 8, 10, 11, 12 and 13.

5.3.3 Brazilian test results

Brazilian test results of different mix compositions are given in Tables 5.13 through to 5.16. The tensile strength of CCWR specimens reflects that of the compressive strength. As would be expected the CCWR material is weaker in tension than in compression. A rule of thumb is that the tensile strength of the material is usually one tenth of its compressive strength.

The tensile properties of CCWR specimens are therefore slightly better than might be expected. After 28 days curing time the tensile strengths for mixes 3 and 4 are approximately 15.0% and 13.0% of the compressive strength respectively. In practice, a large portion of a pack will be in compression, particularly the centre which will be confined by the outer material. The performance of the material therefore will not be significantly affected by its tensile property.

5.3.4 Sonic velocity values measured during curing

Sonic velocity values are presented in Tables AII2.1 through to AII2.13 (in Appendix AII2). All velocities show a marked increase from 1 day curing time to 90 days curing time. This indicates stiffness increases in the specimens. Calculated values of stiffness, Young's modulus and Poisson's ratio for the tested specimens support this proposal.

The results show a slight but consistent increase with increased cement content. The results also indicate that the degree of compaction of the specimen may influence its sonic velocity value. When comparing specimens of mixes 1 and 2 (5 seconds vibration for mix 1 and 20 seconds vibration for mix 2), specimens of mix 2 exhibit higher velocity values.

Table 5.13 Results of Brazilian tests for CCWR material specimens
(mixes three through five).

Mix	Specimen	Tensile strength (MPa)	Wet density (t/m ³)	Water content (%)
3	CB1	0.697	1.934	9.54
	CB2	0.575	1.963	11.34
	CB3	0.669	1.951	10.91
	CB4	0.441	1.949	11.40
	CB5	0.760	1.940	---
Mean tensile strength = 0.628 MPa				
4	DB1	0.446	1.907	10.93
	DB2	0.365	1.942	10.83
	DB3	0.440	1.944	9.79
	DB4	0.436	1.992	10.60
Mean tensile strength = 0.422 MPa				
5	EB1	0.154	1.972	10.59
	EB2	0.188	1.990	10.40
	EB3	0.232	1.960	10.12
Mean tensile strength = 0.191 MPa				

Sonic velocity and curing time relationships of CCWR specimens are illustrated in Figures AII6.1 and AII6.2. Scatter plots of sonic velocity against unconfined compressive strength of CCWR specimens for different mix formulations are illustrated in Figures AII6.3 and AII6.4. As expected the sonic velocity value of the specimen increases with a corresponding increase in its strength. This trend is consistent for all CCWR mixes. The sonic velocity and strength relationships of each mix is given in Appendix AII6. The results generated in this study may be used to predict the in-situ strength of CCWR material.

5.3.5 Moist weight values measured during curing

Specimen moist weight values are presented in Tables AII3.1 through to AII3.13 (in Appendix AII3). These values were recorded to indicate the degree of dehydration of the individual specimen. The values presented show a general decreasing trend.

5.3.6 Observations and analyses of CCWR specimen behaviour

5.3.6.1 Physical properties of CCWR specimens

The relative density of coal washery refuse solids was found to be 2.31 and this value is slightly lower than that obtained by Thomas (2.54) (Thomas, 1986). The physical properties of representative CCWR specimens are summarised in Table 5.17. The results indicate that mix 1 has a relatively higher porosity (26.0% for mix 1 and 18.6% for mix 2) and void ratio (0.35 for mix 1 and 0.23% for mix 2) than mix 2. This can further explain the higher maximum strengths of mix 2 than mix 1 as described in Section 5.3.1.

Table 5.17 Physical properties of CCWR specimens for different mixes.

Mix	Porosity	Void Ratio	Specific Gravity	ρ_{wet} (t/m ³)	ρ_{dry} (t/m ³)	ρ_s (t/m ³)
15%C-12%W	11.516	0.114	2.054	2.049	1.941	2.193
15.6%C-14.7%W	25.990	0.351	1.930	1.928	1.681	2.272
15%C-21%W	24.728	0.247	1.960	1.955	1.709	2.271
12.5%C-13%W	18.580	0.228	2.033	2.031	1.853	2.276
12.5%C-16.5%W	20.303	0.202	2.013	2.007	1.807	2.268
12.5%C-19.1%W	23.030	0.229	1.952	1.947	1.729	2.246
10%C-12%W	14.494	0.145	2.083	2.077	1.935	2.264
10%C-13.8%W	23.990	0.316	1.966	1.963	1.733	2.280
10%C-19%W	25.898	0.259	1.961	1.956	1.698	2.291
7.5%C-12.6%W	23.600	0.309	1.979	1.977	1.752	2.293
7.5%C-16.5%W	24.995	0.248	2.011	2.006	1.757	2.343
7.5%C-19%W	28.311	0.282	1.976	1.971	1.690	2.358
5%C-12%W	21.480	0.274	1.972	1.969	1.776	2.261

5.3.6.2 Specimen failure modes

Failure due to unconfined compressive testing of CCWR specimens can be described in two phases:

- (1) Small axial cracks appeared just before the maximum compressive strength was reached (see Figure 5.24). These cracks indicated tensile cleavage.
- (2) As strain increased these cracks widened and large slabs of the specimen surface broke away leaving a typical hour glass failure shape (see Figure 5.25). This indicated a concentration of shear stress along some diagonal plane within the material and this caused it to fail in shear.

Another failure mode observed is the shear cone with splitting above (see Figure 5.26).

5.3.7 Discussion of results

The results presented in Sections 5.3.1 through 5.3.6 and the associated analyses are discussed in this Section. Comparisons between five CCWR mixes will be made in relation to pack strength requirements. An examination is also made of the CCWR material characteristics in relation to strata behaviour.

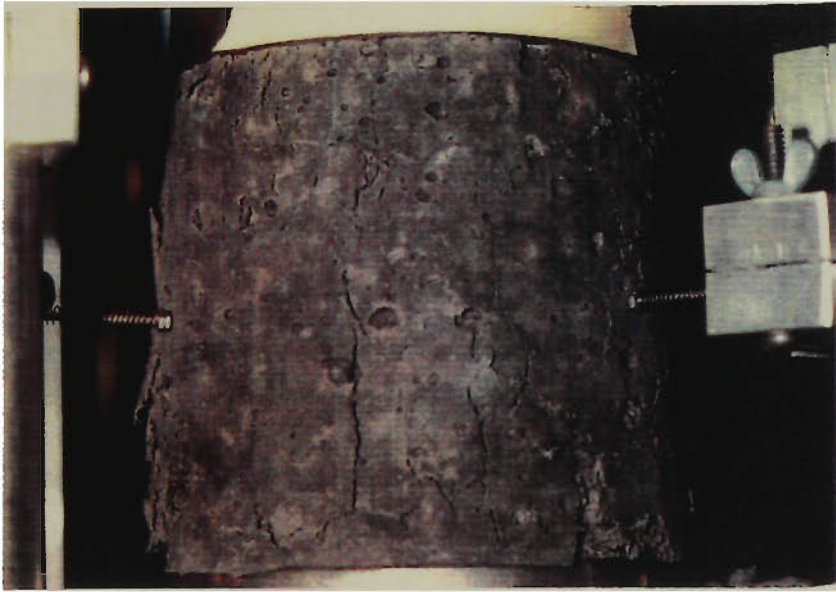


Figure 5.24 Small axial cracks appeared just before the maximum compressive strength was reached - indicating tensile cleavage failure.



Figure 5.25 A typical hour glass failure shape.



Figure 5.26 Shear cone with splitting above.

5.3.7.1 Mechanical properties of CCWR specimens

Mix 1 (15.6% cement)

The high fluidity of mix 1 on pouring did not permit early strength testing of the specimens (1 hour and 2 hours). The results for 1 day curing time specimens reveal a strength value of 2.589 MPa which is nearly two times the strength requirement described in Section 2.6 in Chapter 2.

Specimen strengths of 5.774 MPa after 7 days curing, 6.620 MPa after 90 days curing indicate very favourable pack properties. Young's modulus values of 0.386 GPa after 1 day increasing to 1.658 GPa after 90 days indicate satisfactory

stiffness property of the material. For bulk transport of pack material a value of 1.95 t/m^3 may be used for design purposes.

The mode of failure of specimens in compression is as described in Section 5.3.6.2. The failure behaviour of the specimens indicates the cohesive strength of 1.4 MPa is satisfactory.

Mix 2 (12.5% cement)

The ultimate compressive strengths of mix 2 specimens are higher than those of mix 1. The strength of 0.082 MPa after 1.5 hours is suitable for deshuttering purposes while the strength of 1.021 MPa after 4.25 hours is about two times the value recommended in the United Kingdom. This mix formulation gives a high strength of 16.599 MPa after 90 days. A Young's modulus of 2.847 GPa after 90 days gives a satisfactory elastic modulus property of the material.

The mix has a superior cohesive strength of 2.6 MPa (1.86 times the cohesive strength of mix 1) and this reflects its high strength development pattern. The mode of failure behaviour of specimens is typical shear cone with splitting above. The failure behaviour of the specimens indicates the mix composition has a comparatively good cohesive property.

Mix 3 (10.0% cement)

The compressive strength test results show that the early strengths of the specimens of mix 3 are relatively low. This could extend deshuttering time in practice. However, the material can be self-supporting if pumped into strong pack bags or forms. The strength values after 1 day curing are favourable with the design

criteria in the United Kingdom but the final strength of only 5.631 MPa after 90 day curing would appear to be insufficient for Australian pack requirements.

The mode of failure consists of a general crumbling by the development of multiple cracks at mid-height of the specimens. The failure surfaces of the specimens appeared to be powdery indicating a low cohesive property of the material.

Mix 4 (7.5% cement) and Mix 5 (5.0% cement)

Mixes 4 and 5 exhibit relatively low compressive strengths. The compressive strength values are lower than those required for the pack design. The final maximum strengths of 4.625 MPa for mix 4 and 3.388 MPa for mix 5 after 90 days curing are much lower than needed for effective strata control.

The mode of failure for both mixes manifests as slabs crumbling and breaking away from the walls of the specimens. Again, the failure surfaces of the specimens appeared to be powdery. This reflects the low cohesive strengths of the materials (0.6 MPa for mix 4 and 0.35 for mix 5).

5.3.7.2 CCWR pack characteristics in relation to strata behaviour

An attempt is made to understand the implications of the mechanical properties of CCWR material in the underground environment. The longwall strata behaviour and the generation of pack load has been described in some details in Section 3.1.5. However, an accurate assessment of the initial and ultimate strength requirements of the pack in the underground environment would be complex. Nevertheless, the initial strengths of 0.082 MPa in 1.5 hours, 0.151 MPa in 2.0 hours, 0.267 MPa in 2.5 hours, 1.251 MPa in 4.5 hours, 5.138 MPa in 24 hours

and the long term strength of 16.599 MPa in 90 days for mix 2 indicate that the mechanical properties of CCWR material are close to those required. It is indicative that this material can offer a good early resistance, however, its strength should continue to develop in spite of accommodating the irresistible movement of the strata and possibly a degree of failure.

If the major displacement of the strata takes place within the first few days of installation of CCWR pack, it may remain substantially unfailed. Contrary to this, the pack may fail considerably, however, the initial confinement of the pack by the retaining bags or forms and later by other packs can ensure a good residual strength for the pack. However, at this present period of research accurate prediction of the effect on strata behaviour, in general, by use of the pack material properties can not be quantified.

5.4 EFFECT OF WATER CONTENT ON THE MECHANICAL PROPERTIES OF CCWR MATERIAL

The results of unconfined compressive strength tests are summarized in Tables 5.18 and 5.19. The effect of water content on the unconfined compressive strength of CCWR material is illustrated in Figures 5.27 through 5.30. Generally, unconfined compressive strength decreases as water content of CCWR material decreases, its slump value also increases and this is shown in Tables 5.18 and 5.19. The results indicate that the strength of CCWR material of any mix proportion can be severely affected by the degree of consistency of the mix. The practical implications of this singular aspect is that the consistency of the mix be such that CCWR material can be transported and placed sufficiently easily without segregation.

Table 5.18 Effect of water content on the unconfined compressive strength of CCWR materials at different curing times.

Portland Cement (%)	Water Content (%)	Slump (mm)	Compressive Strength (MPa)						
			1 Day	7 Days	14 Days	28 Days	60 Days	90 Days	365 Days
15	21.0	C	1.289	2.870	3.111	4.248	4.623	5.443	
15*	17.6			5.170	6.530	6.780			13.559
15	14.7	110	2.589	5.774	6.620	7.539	9.325	10.282	
15	12.0	0	6.714	8.552	8.682	8.126	9.493	12.773	
12.5	19.1	C	1.152	2.800	3.117	3.394	4.803	4.157	
12.5	16.5	85	1.365	3.895	4.670	5.134	7.029	6.875	
12.5	13.0	0	5.138	8.859	10.612	10.838	15.073	16.599	

* (after Thomas, 1986).

C denotes collapsed slump.

Table 5.19 Effect of water content on the unconfined compressive strength of CCWR materials at different curing times.

Portland Cement (%)	Water Content (%)	Slump (mm)	Compressive Strength (MPa)						
			1 Day	7 Days	14 Days	28 Days	60 Days	90 Days	365 Days
10.0	19.1	C	0.659	1.703	2.011	2.183	2.724	2.886	
10.0*	16.2			2.650	3.070	3.410			8.875
10.0	13.8	15	1.799	3.449	3.882	4.344	4.699	5.631	
10.0	12.0	10	3.495	6.305	6.232	7.474	7.433	7.795	
7.5	19.0	C	0.321	0.823	0.924	1.112	1.616	1.617	
7.5	16.5	75	0.594	1.289	1.213	1.680	1.864	2.097	
7.5*	12.5	10	1.629	2.664	3.152	3.379	4.105	4.625	6.356
5.0	12.0	10	1.208	1.876	2.041	2.432	2.493	3.388	3.439

* (after Thomas, 1986).

C denotes collapsed slump.

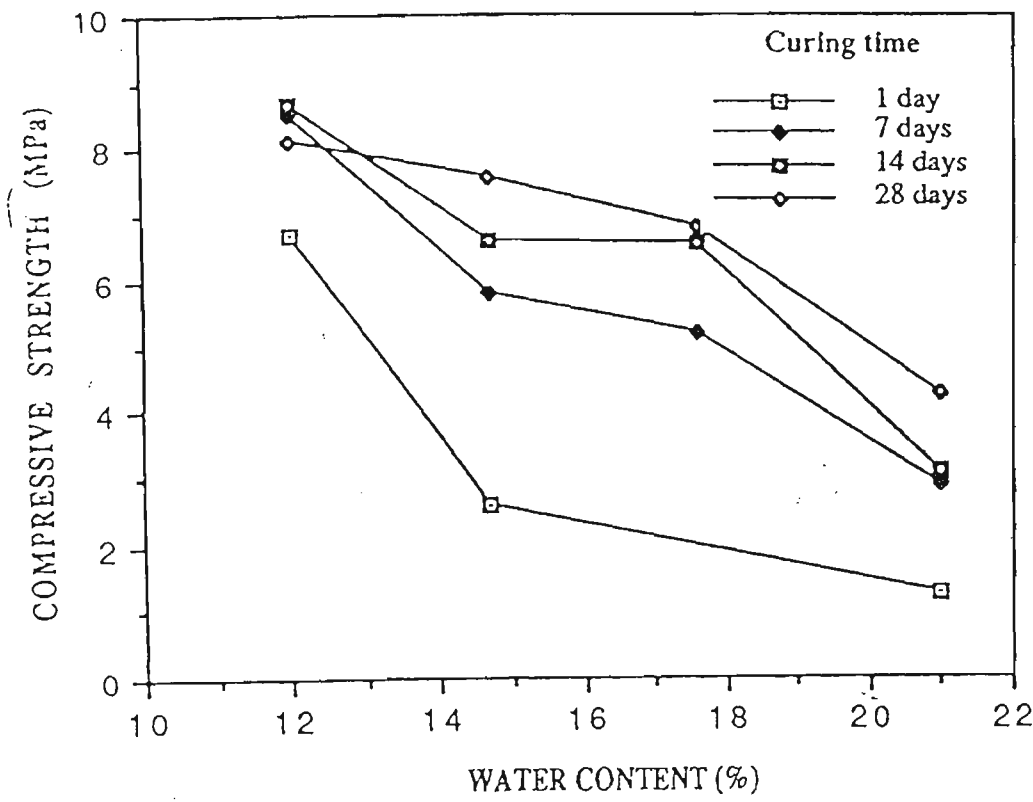


Figure 5.27 Effect of nominal water content on the strength of CCWR specimens at different curing time (15% OPC).

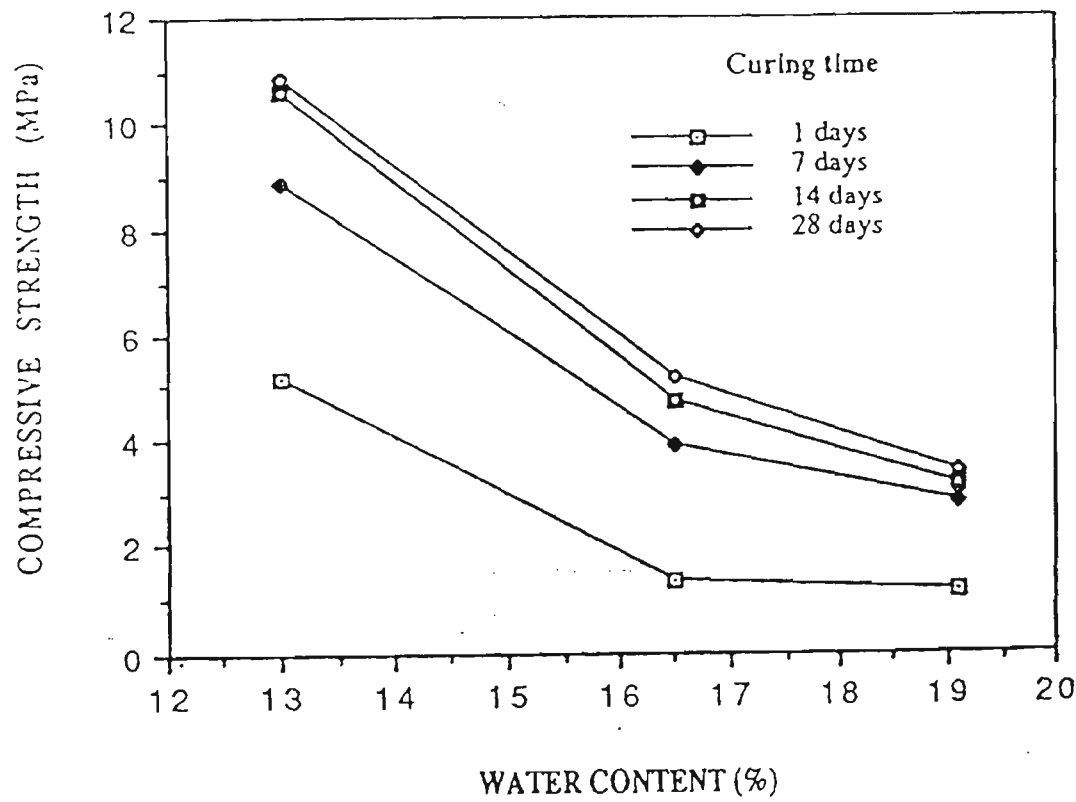


Figure 5.28 Effect of nominal water content on the strength of CCWR specimens at different curing time (12.5% OPC).

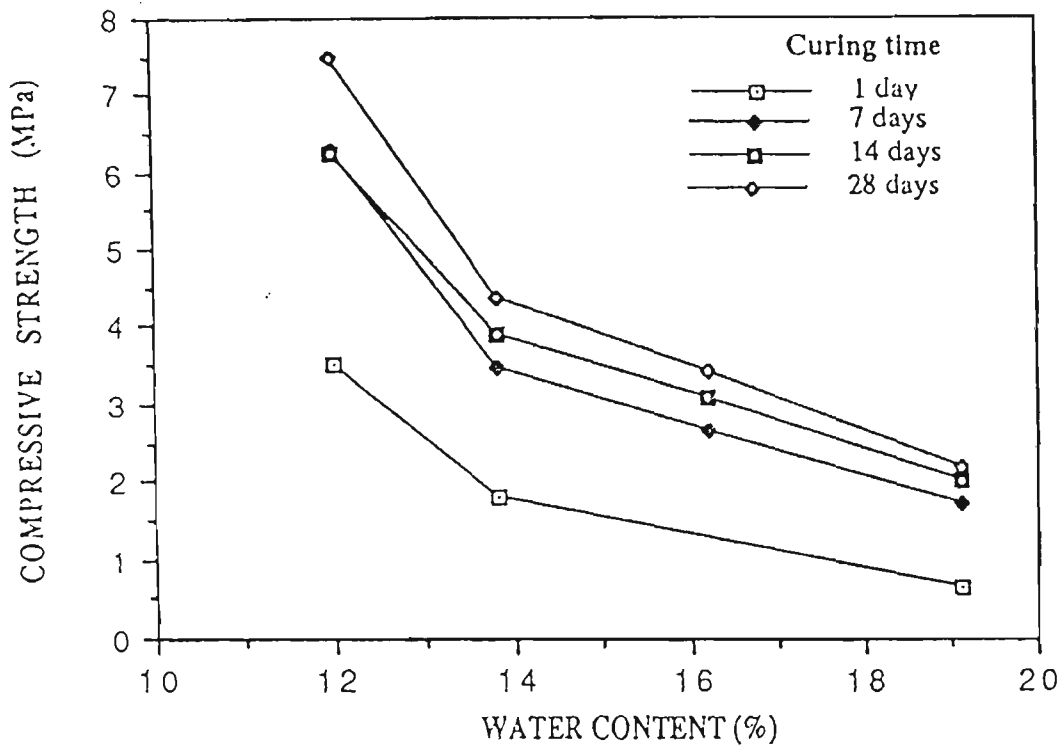


Figure 5.29 Effect of nominal water content on the strength of CCWR specimens at different curing time (10% OPC).

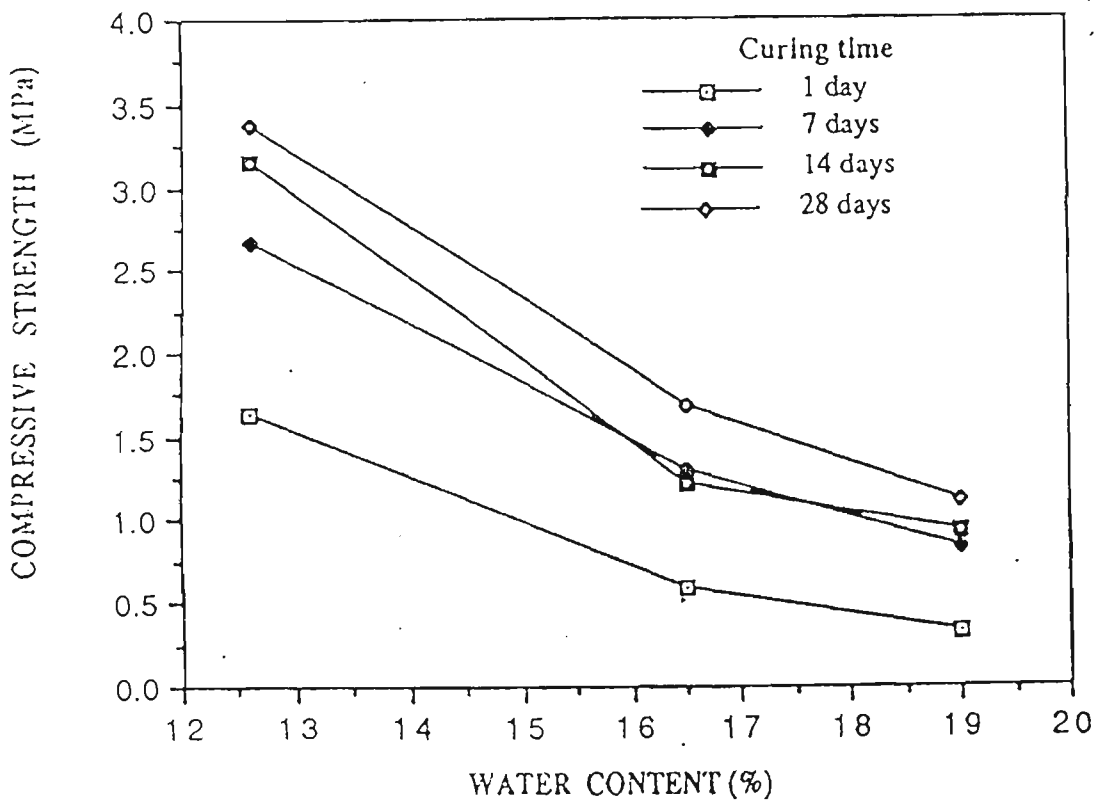


Figure 5.30 Effect of nominal water content on the strength of CCWR specimens at different curing time (7.5% OPC).

Wet mixes which contained high nominal water contents of 19.0% and 21.0% were proven to be very prone to segregation. Partial mechanical separation of the coarse and fine constituents of the mixes were also noted. Bleeding also occurred, which resulted in the mix water rising to the surface of the freshly poured test specimens. Consequently, both segregation and bleeding can lead to non-homogeneous CCWR concrete. However, although the strength of dry mixes with nominal water contents of 12.0%, 12.6% and 13.0% appeared to be sufficiently high, they would require more mixing water for sufficient workability and cohesion. The importance of water content, therefore, with regard to its effect on the strength and workability of the CCWR material is emphasised.

5.4.1 Effect of water content on the drying shrinkage of CCWR material

The drying shrinkage of each specimen, and the average drying shrinkage, at each drying period, namely after air drying of 2, 3, 4, 8 and 16 weeks, expressed to the nearest 10 microstrain are presented in Tables 5.20 through 5.27. Drying shrinkage of CCWR material varies from 684 microstrain for 12.5% Portland cement mix (with moisture content of 19.1% dry basis) at two weeks to 2740 microstrain for 7.5% Portland cement mix (with moisture content of 19.0% dry basis) at 16 weeks. Figure 5.31 illustrates the effect of water content on the drying shrinkage of CCWR specimens.

It is evident from the tests that the drying shrinkage of wet mixes is larger than that of dry mixes. In general, moisture content affects the drying shrinkage of CCWR material as it reduces the volume of the restraining CWR. However, results indicate that drying shrinkage is insignificant in all mixes. Generally, small shrinkage means small microcracking and small crack connectivity, therefore, lower permeability and moisture absorption are expected.

Table 5.20 Drying shrinkage values for 15.0%C-12.0%W specimens.

Curing time (week)	Drying shrinkage values (mm)					Average drying shrinkage (microstrain)
	Specimen			\bar{s}	σ_{n-1}	
	1	2	3			
2	0.362	0.362	0.348	0.357	0.008	1390
3	0.478	0.474	0.464	0.472	0.007	1890
4	0.530	0.530	0.517	0.526	0.008	2100
8	0.517	0.516	0.504	0.512	0.007	2050
16	0.524	0.523	0.511	0.519	0.007	2080

Note: Gauge length = 250mm.

Table 5.21 Drying shrinkage values for 15.0%C-21.0%W specimens.

Curing time (week)	Drying shrinkage values (mm)					Average drying shrinkage (microstrain)
	Specimen			\bar{s}	σ_{n-1}	
	1	2	3			
2	0.343	0.336	0.321	0.334	0.011	1330
3	0.602	0.579	0.566	0.583	0.018	2330
4	0.714	0.689	0.683	0.695	0.016	2780
8	0.714	0.694	0.691	0.701	0.015	2800
16	0.714	0.688	0.688	0.697	0.015	2800

Note: Gauge length = 250mm.

Table 5.22 Drying shrinkage values for 12.5%C-16.5%W specimens.

Curing time (week)	Drying shrinkage values (mm)					Average drying shrinkage (microstrain)
	Specimen			\bar{s}	σ_{n-1}	
	1	2	3			
2	0.242	0.236	0.233	0.237	0.005	948
3	0.443	0.437	0.433	0.438	0.005	1750
4	0.534	0.529	0.523	0.529	0.006	2120
8	0.607	0.607	0.605	0.606	0.001	2420
16	0.615	0.617	0.616	0.616	0.001	2460

Note: Gauge length = 250mm.

Table 5.23 Drying shrinkage values for 12.5%C-19.1%W specimens.

Curing time (week)	Drying shrinkage values (mm)					Average drying shrinkage (microstrain)
	Specimen			\bar{s}	σ_{n-1}	
	1	2	3			
2	0.171	0.167	0.176	0.171	0.005	684
3	0.316	0.306	0.322	0.315	0.008	1260
4	0.465	0.441	0.468	0.458	0.015	1830
8	0.575	0.545	0.584	0.568	0.020	2270
16	0.626	0.591	0.638	0.618	0.024	2470

Note: Gauge length = 250mm.

Table 5.24 Drying shrinkage values for 10.0%C-12.0%W specimens.

Curing time (week)	Drying shrinkage values (mm)					Average drying shrinkage (microstrain)
	Specimen			\bar{s}	σ_{n-1}	
	1	2	3			
2	0.256	0.249	0.257	0.254	0.004	1020
3	0.303	0.295	0.303	0.300	0.005	1200
4	0.384	0.374	0.387	0.378	0.007	1510
8	0.471	0.641 [*]	0.465	0.468	0.004	1870
16	0.511	0.700 [*]	0.517	0.514	0.004	2056

Note: Gauge length = 250mm.

* Drying shrinkage value abnormally high and not included in the average.

Table 5.25 Drying shrinkage values for 10.0%C-19.1%W specimens.

Curing time (week)	Drying shrinkage values (mm)					Average drying shrinkage (microstrain)
	Specimen			\bar{s}	σ_{n-1}	
	1	2	3			
2	0.229	0.218	0.235	0.227	0.008	910
3	0.459	0.449	0.479	0.462	0.015	1850
4	0.429	0.421	0.446	0.432	0.013	1730
8	0.517	0.507	0.535	0.520	0.014	2080
16	0.559	0.548	0.580	0.562	0.016	2250

Note: Gauge length = 250mm.

Table 5.26 Drying shrinkage values for 7.5%C-16.5%W specimens.

Curing time (week)	Drying shrinkage values (mm)					Average drying shrinkage (microstrain)
	Specimen			\bar{s}	σ_{n-1}	
	1	2	3			
2	0.248	0.265	0.252	0.255	0.009	1020
3	0.487	0.511	0.487	0.495	0.014	1980
4	0.574	0.599	0.576	0.583	0.014	2330
8	0.586	0.601	0.583	0.590	0.010	2360

Note: Gauge length = 250mm.

Table 5.27 Drying shrinkage values for 7.5%C-19.0%W specimens.

Curing time (week)	Drying shrinkage values (mm)					Average drying shrinkage (microstrain)
	Specimen			\bar{s}	σ_{n-1}	
	1	2	3			
2	0.276	0.250	0.234	0.253	0.021	1010
3	0.623	0.572	0.563	0.586	0.033	2340
4	0.681	0.622	0.630	0.644	0.032	2580
8	0.717	0.659	0.673	0.683	0.030	2730
16	0.717	0.664	0.673	0.685	0.028	2740

Note: Gauge length = 250mm.

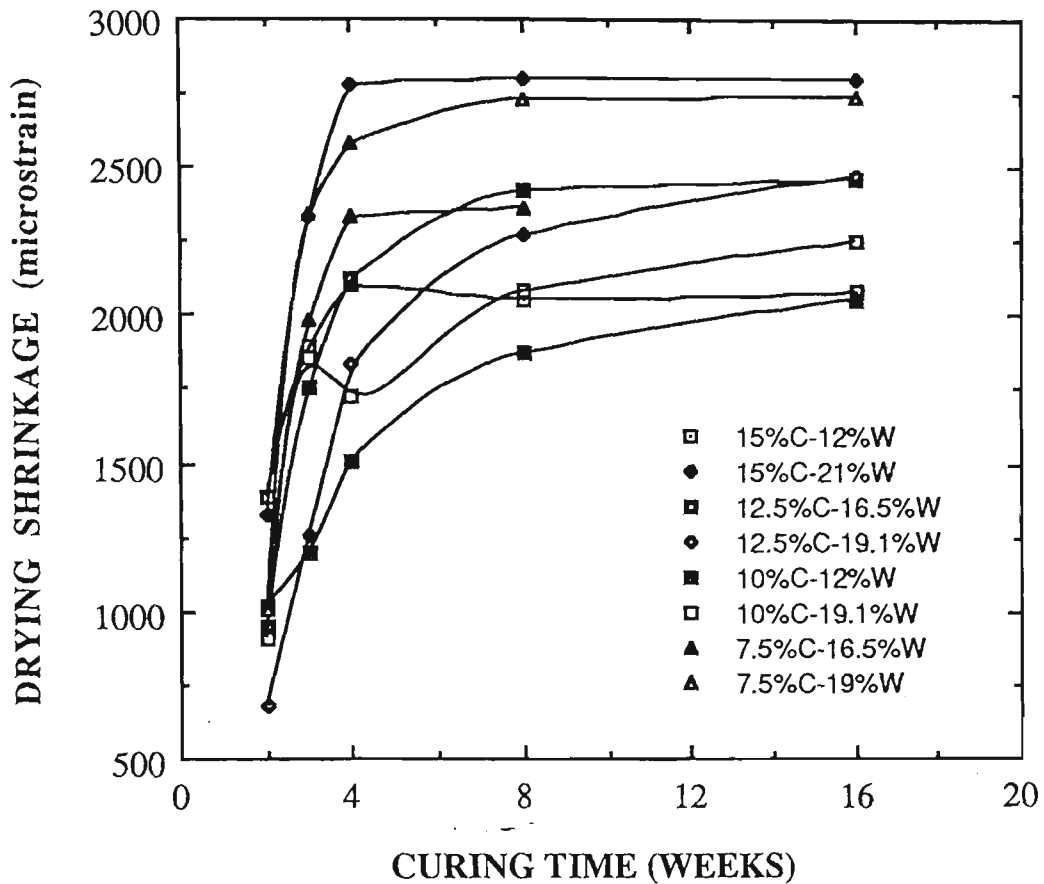


Figure 5.31 The effect of water content on the drying shrinkage of CCWR specimens.

5.5 A NEW YIELD FUNCTION FOR CCWR MATERIAL

A variety of laboratory tests such as indirect tensile tests, triaxial strength tests and unconfined compressive strength tests of CCWR specimens have been carried out. Results of these routine material strength tests have been tabulated in Tables 5.7 through 5.16. Table 5.28 shows the stress components at failure of various CCWR materials generated by using the logarithmic yield function program.

Table 5.28 Comparisons of predicted and measured values for various CCWR materials.

Mix	Minor Stress σ_3 (MPa)	Measured Values σ_{1m} (MPa)	Predicted Values σ_{1p} (MPa)	Error σ_{1e} (MPa)
1	0.00	9.06	10.36	-1.30
	1.39	16.24	14.37	1.86
	3.75	20.67	20.73	-1.06
	5.56	24.59	25.26	-0.67
	6.95	28.73	28.55	0.17
2	0.00	13.09	14.16	-1.07
	2.09	22.73	21.44	1.29
	4.17	28.62	28.24	0.39
	5.56	32.83	32.55	0.28
	6.95	35.83	36.71	-0.87
3	-0.68	0.00	-0.06	0.06
	0.00	4.24	4.40	-0.16
	1.39	11.36	11.11	0.26
	2.09	13.57	13.72	-0.16
4	-0.44	0.00	0.02	-0.02
	0.00	3.28	3.08	0.20
	0.10	3.10	3.76	-0.67
	0.20	5.14	4.45	0.69
	0.40	5.64	5.81	-0.17
5	-0.19	0.00	0.50	-0.50
	0.00	1.90	1.72	0.18
	0.17	3.08	2.79	0.29
	0.35	4.08	3.91	0.17
	0.52	5.20	4.96	0.23
	0.86	6.67	7.04	-0.38

Based on the data tabulated in Table 5.28, the empirical logarithmic yield functions were determined as:

$$\sigma_1 = -226.88 + 73.83 \ln (24.8 + \sigma_3), \text{ for mix 1;}$$

$$\sigma_1 = -358.54 + 109.24 \ln (30.32 + \sigma_3), \text{ for mix 2;}$$

$$\sigma_1 = -15.64 + 17.91 \ln (3.06 + \sigma_3), \text{ for mix 3;}$$

$$\sigma_1 = -857.33 + 241.76 \ln (35.12 + \sigma_3), \text{ for mix 4; and}$$

$$\sigma_1 = -381.01 + 127.46 \ln (20.14 + \sigma_3), \text{ for mix 5;}$$

Figures 5.32 to 5.34 illustrate plots of the predicted results generated from the proposed yield functions and the experimental results. It is noted that the predicted triaxial strength values are very close to those measured by simple triaxial tests.

Results generated from this study have shown that the proposed yield function can predict the strength and yield characteristics of the CCWR material in a satisfactory manner.

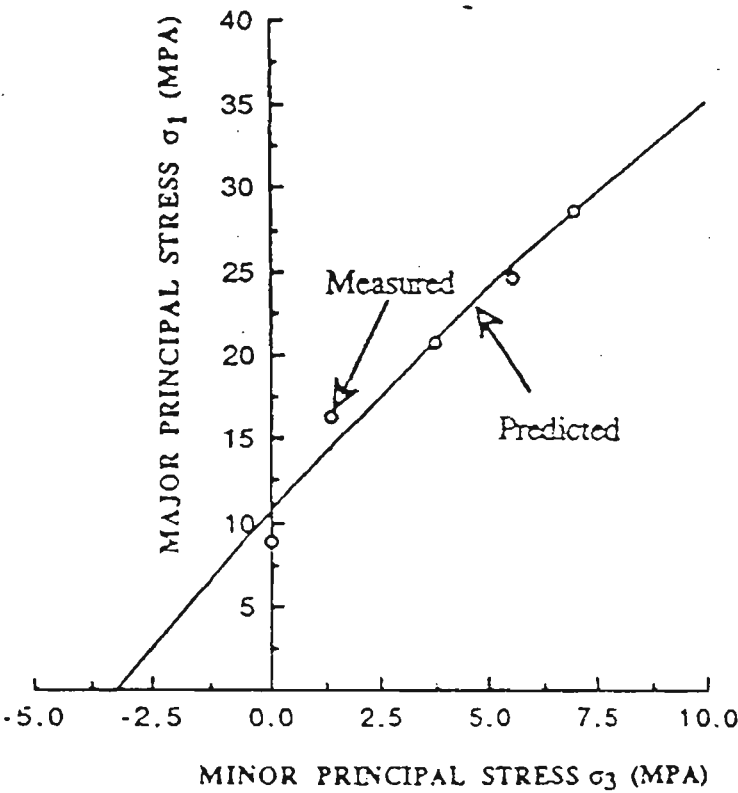


Figure 5.32 Measured and predicted triaxial strengths of CCWR mix 1.

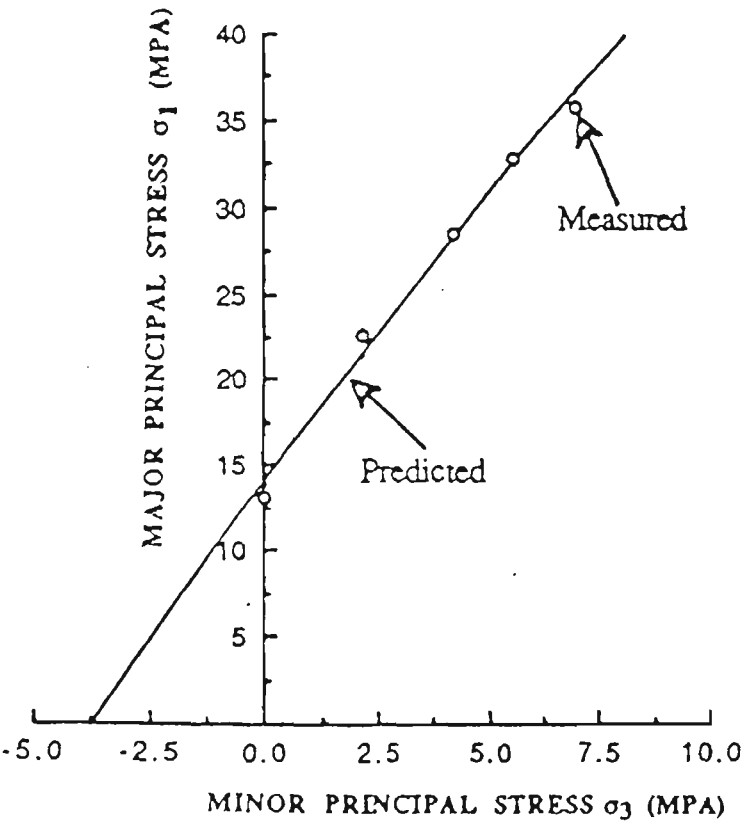


Figure 5.33 Measured and predicted triaxial strengths of CCWR mix 2.

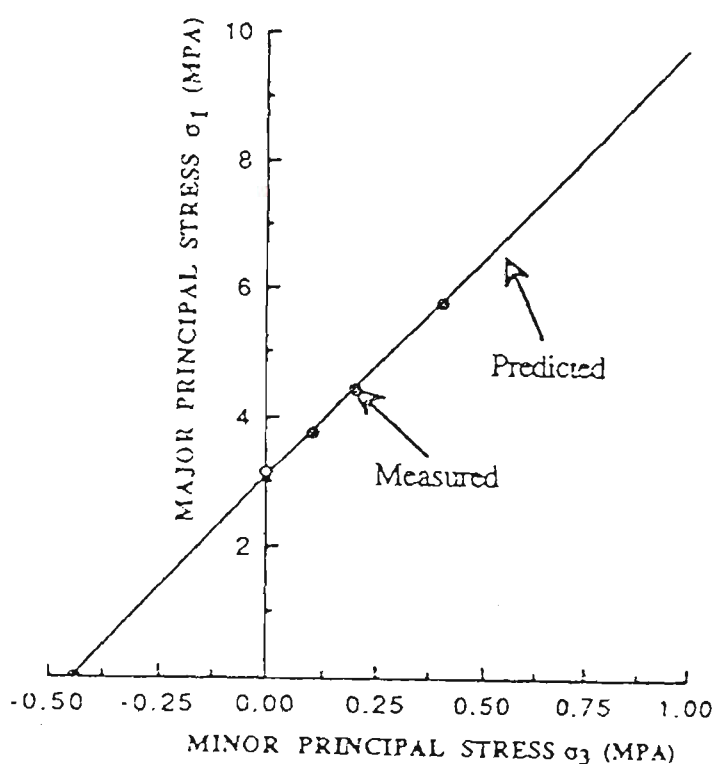


Figure 5.34 Measured and predicted triaxial strengths of CCWR mix 4.

5.6 EFFECT OF WATER CONTENT ON THE FLOW PROPERTIES OF CWR

5.6.1 Slump test results

The relationship between water content and slump values is given in Table 5.29. The effect of water content on the slump values of CWR is presented in Figure 5.35. It is apparent that variation in water content of CWR results in variable slumps. CWR with a nominal water content of 2.0% exhibits a high shear slump value of 130.0mm. This is an indication of the lack of cohesion in the material. At 5.0% water content, a zero slump was measured indicating a material of stiff consistency. As water content was increased from 5.0% to 15.0%, a relatively small increase in the slump value was observed.

Table 5.29 Slump test results of CWR.

Water Content (%)	Slump Values (mm)	Temp. of Water (°C)	Temp. of Atmosphere (°C)	Remarks
1.9	50	17.0	18.0	Shear slump was observed, a dry mix.
a. 2.0	130	17.0	18.0	Shear slump was observed, a dry mix.
b. 2.0	135	17.0	18.0	Shear slump was observed, a dry mix.
3.0	--	17.0	18.0	No slump value can be measured as the mix stuck to the wall of slump cone.
a. 5.0	0	17.0	18.0	A very stiff mix was observed.
b. 5.0	0	17.0	18.0	A very stiff mix was observed.
c. 5.0	0	17.0	18.0	Again a very stiff mix was observed.
7.5	0	17.0	18.0	Again a very stiff mix was observed.
a. 10.0	10	17.0	18.0	True slump was observed. Particles of the mix appeared to be coated with water.
b. 10.0	15	17.0	18.0	True slump was observed.
c. 10.0	10	17.0	18.0	Again true slump was observed.
a. 15.0	15	17.0	18.0	True slump was observed. A mix of good consistence.
b. 15.0	20	17.0	18.0	True slump was observed.
a. 20.0	145	16.5	18.0	Shear slump was observed. The mix was saturated with water.
b. 20.0	170	17.0	18.0	Shear slump was observed.
c. 20.0	185	17.0	18.0	Shear slump was observed.
a. 25.0	150	17.0	18.0	Collapsed slump was observed. Evidence of some free water.
b. 25.0	210	17.0	18.0	Collapsed slump was observed.
a. 30.0	233	17.0	18.0	Laterally collapsed slump was observed. The mix was over-saturated with water.
b. 30.0	200	17.0	18.0	Laterally collapsed slump was observed.

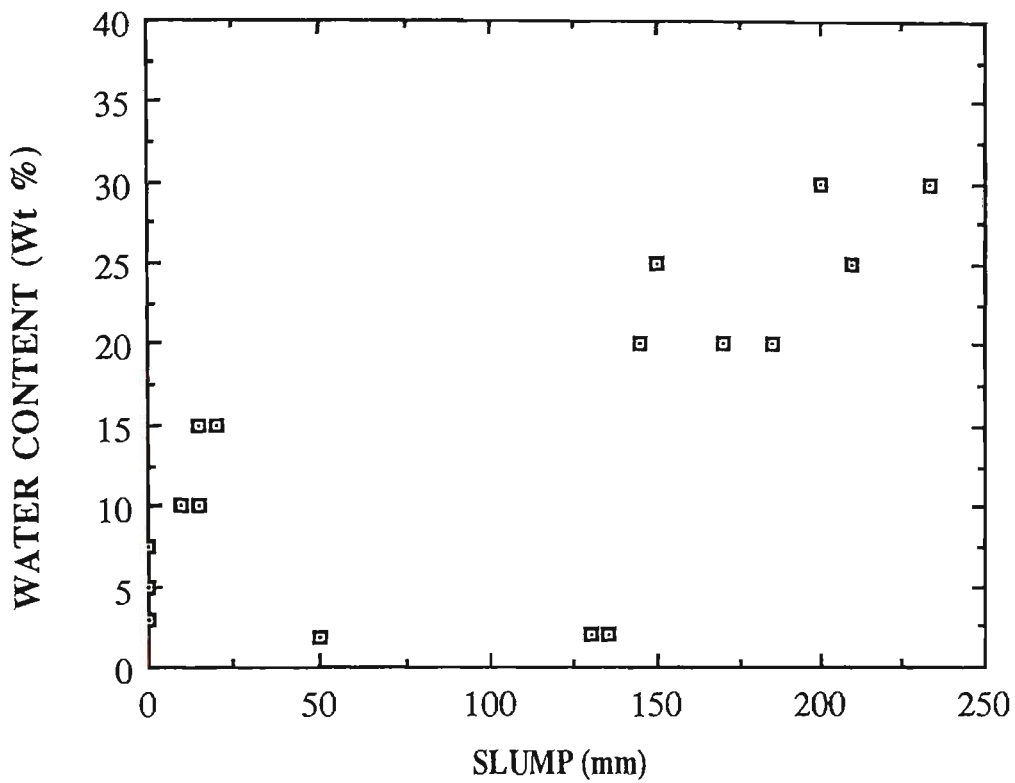


Figure 5.35 Effect of water content on the slump values of CWR.

It is important to note that in the rather dry range no variation can be detected between materials of different workability. From 15.0% to 20.0% water content the slump is more sensitive to variations in workability. However, for CWR with water content in the range between 20.0% and 30.0%, widely different values of slump were obtained for different samples with the same water content.

It is noted that from 5.0% to 30.0% water content the slump value of CWR shows a near linear relationship to water content. As water content of CWR increases, its slump value also increases, but not proportionately. This does agree with the finding of Lerche and Renetzeder (1984).

5.6.2 Flow test results

For the first series of flow tests, in which CWR was used, the average values of flowability for each slope (38.5° , 45.0° and 50.0°) are plotted against water content in Figures AII7.1 through AII7.3 (in Appendix AII7), respectively, indicating the effect of water content on the flowability of CWR. A comparison of the flowability of CWR for all mixes at different slopes is shown in Figure 5.36. The individual flow factor (FF) measurement of flow tests are shown in Tables AII7.1 through AII7.7.

For brevity the individual flow factor (FF) measurement of flow tests of different oil samples is not presented in this thesis. However, the kinematic viscosity-flow factor graphs for different oil samples are plotted in Figures AII7.4 through AII7.6.

Flow tests of different oil samples were conducted with a view to calibrating the flow-tube. The technique employed is to pass each oil sample with a known kinematic viscosity (cST) through measurement of time. The practical significant of this lies in the fact that, provided that accurate time measurement of the discharge is maintained, flow factors of oil samples and CWR with different nominal water content will be directly comparable.

5.6.3 Discussion of flow test results

The effect of water content on the flowability of CWR is shown in Figure 5.37. Test results show that CWR with a low water content of 2.0% have high flowability and this is reflected by an equally high slump value of 130.0mm. CWR was observed to develop into a very stiff material as the water content was increased to 5.0% (slump value = 0). Consequently, there was a notable decrease in the

flowability of CWR at test slopes of 45° and 50° , and an even more significant decrease observed at 38.5° . In practice, CWR with a water content of 5% will require a certain amount of energy to initiate the flow, but once its shear strength is exceeded it will flow with minimal energy, and this is a characteristic of a so called Bingham fluid.

At 10% water content, CWR exhibits good flowability. There was a marked decrease in the flowability of CWR as its water content was increased to 15.0%. This appeared to be a very cohesive material with a low slump of 15.0mm, exhibiting minimum flowability. The importance of the 15.0% water content in relation to the flow properties of CWR is emphasized.

The increase in flowability for CWR with water content from 15.0% to 30.0% is quite pronounced and this is reflected by a corresponding overall increase in slump values. Furthermore, the flowability value within this range of water content shows a linear relationship to both water content and slump value. The comparisons of CWR with different water contents with regard to flowability and slump value should indicate the overall typical effect of water content on its flow properties.

Atkins et al. (1987) reported that the degree of saturation (water content) is one of the most important factors governing the pumpability or flowability of CWR, as the variation in water content influences the quantity of the material to be pumped. They further stressed that solids concentration and void ratio also influenced the pumpability of CWR, the most important factors being particle size of the solids, water content and solid concentrations. The author's findings are in complete agreement with these statements. It is important to note that chemical composition of CWR, and in particular the presence of relatively cohesive

compounds like clay minerals, is of decisive importance to its flow characteristics. These findings agree with those of Lerche and Renetzeder (1984).

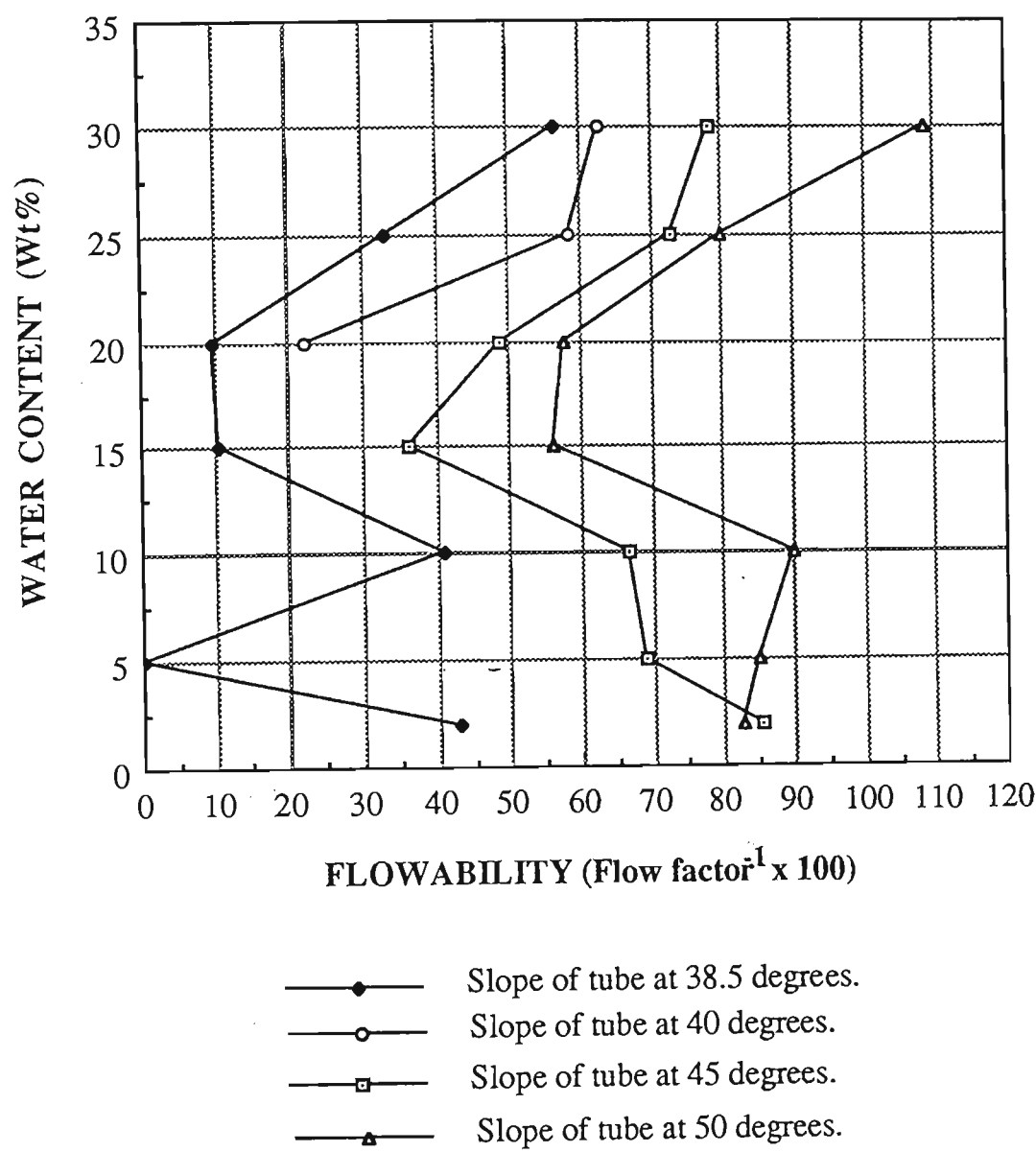


Figure 5.36 A Comparison of the flowability of CWR for all mixes at different slopes.

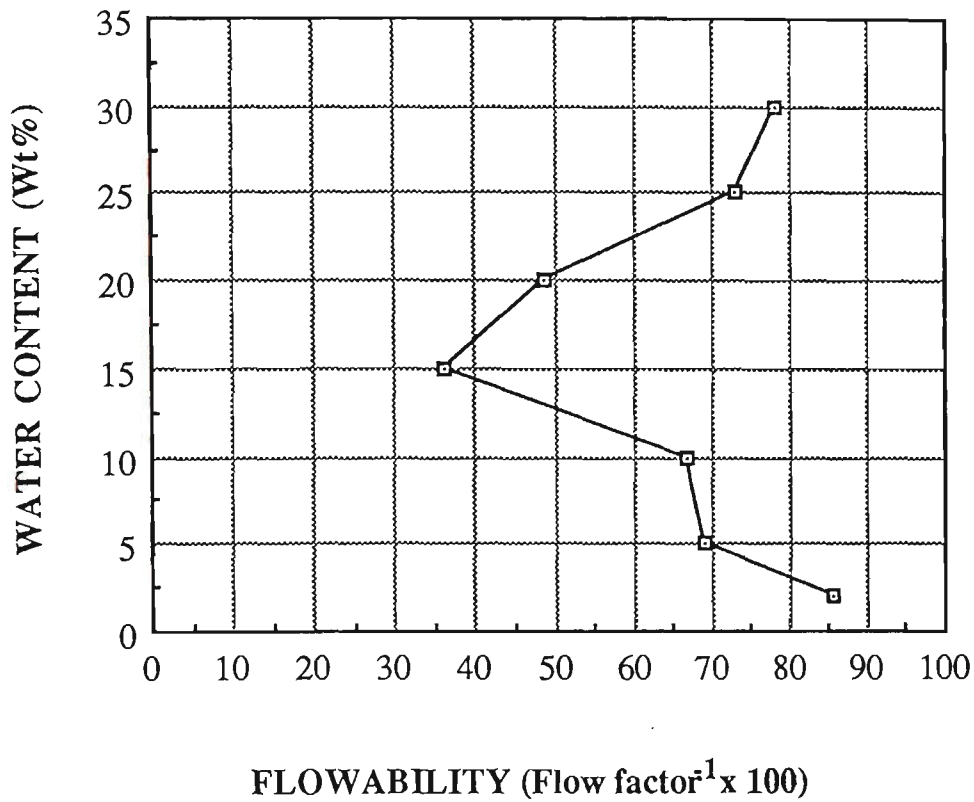


Figure 5.37 Effect of water content on the flowability of CWR.

5.7 EFFECT OF GEOMETRY ON THE PROPERTIES AND BEHAVIOUR OF CCWR MATERIAL MODELS

Results of unconfined compressive strength tests for series VI experiments are presented in Tables 5.30 through 5.33. Table 5.34 shows the summary of results of series VI experiments. Figures 5.38 through 5.42 show the effect of geometry on the properties and behaviour of CCWR material models. The results indicate that the geometry has a significant effect on both the mechanical properties and load deformation behaviour of CCWR material models.

Table 5.30 Results of compressive strength testing for series VI experiments (Effect of geometry on the strength and elasticity properties of CCWR material models).

Specimen Diameter	Max. Load (KN)	Max. Strength (MPa)	Axial Modulus (GPa)	Poisson's Ratio	H/D	Moist Density (Kg/m ³)	Stiffness (KN/mm)
55.5mm-2	24.000	11.982	6.667	0.26	2.92	1902.9	40.00
55.5mm-3	23.600	11.783	6.497	0.19	2.93	1904.2	40.57
Mean	23.800	11.883	6.582	0.23	2.93	1903.6	40.29
75.5mm-1	59.000	12.933	8.520	0.21	1.95	1898.7	105.17
75.5mm-2	54.750	12.006	7.387	---	1.97	1852.8	90.91
75.5mm-3	56.250	12.285	8.098	0.26	1.92	1867.2	89.39
Mean	56.667	12.408	8.002	0.24	1.95	1873.6	95.16

Table 5.31 Results of compressive strength testing for series VI experiments (Effect of geometry on the strength and elasticity properties of CCWR material models).

Specimen Diameter	Max. Load (KN)	Max. Strength (MPa)	Axial Modulus (GPa)	Poisson's Ratio	H/D	Moist Density (Kg/m ³)	Stiffness (KN/mm)
102.8mm-1	102.000	12.289	9.407	0.25	1.44	1919.6	135.00
-2	99.500	12.667	7.627	0.21	1.48	1908.7	91.66
-3	100.000	12.048	8.505	---	1.41	1915.1	137.93
Mean	100.500	12.335	8.513	0.23	1.44	1914.5	121.53
149.5mm-1	216.000	12.305	7.643	---	1.01	1894.7	192.00
-2	200.000	11.394	6.389	0.20	0.95	1884.6	172.40
-3	205.520	11.708	8.368	0.23	0.97	1890.0	208.00
-4	196.000	11.166	---	---	0.99	1892.4	150.78
Mean	204.380	11.643	7.467	0.21	0.98	1890.3	180.80

Table 5.32 Results of compressive strength testing for series VI experiments (Effect of geometry on the strength and elasticity properties of CCWR material models).

Specimen Diameter	Max. Load (KN)	Max. Strength (MPa)	Axial Modulus (GPa)	Poisson's Ratio	H/D	Moist Density (Kg/m ³)	Stiffness (KN/mm)
206.0mm-1	412.000	12.362	5.484	0.14	0.72	1910.7	230.30
-2	430.000	12.902	6.240	0.17	0.72	1908.2	248.92
-3	400.000	12.002	6.212	0.17	0.72	1913.6	261.33
Mean	414.000	12.422	5.979	0.16	0.72	1910.8	246.85
242.0mm-1	744.000	16.175	4.796	0.11	0.62	1916.4	280.00
-2	716.000	15.567	4.694	0.11	0.61	1921.5	289.66
Mean	730.000	15.871	4.745	0.11	0.61	1919.0	284.83

Table 5.33 Results of compressive strength testing for series VI experiments (Effect of geometry on the strength and elasticity properties of CCWR material models).

Specimen Diameter	Max. Load (KN)	Max. Strength (MPa)	Axial Modulus (GPa)	Poisson's Ratio	H/D	Moist Density (Kg/m ³)	Stiffness (KN/mm)
314.5mm-1	1240.000	15.962	3.301	0.07	0.47	1891.5	333.30
-2	1225.000	15.769	3.512	0.09	0.47	1900.5	335.00
Mean	1232.500	15.866	3.407	0.08	0.47	1896.0	334.15

Table 5.34 Summary of results of compressive strength testing for series VI experiments (Effect of geometry on the strength and elasticity properties of CCWR material models).

Specimen Diameter	Max. Load (KN)	Max. Strength (MPa)	Axial Modulus (GPa)	Poisson's Ratio	H/D	Moist Density (Kg/m ³)	Stiffness (KN/mm)
55.5mm	23.800	11.883	6.582	0.24	2.93	1900.6	40.29
75.5mm	56.667	12.408	8.002	0.24	1.95	1873.6	95.16
102.8mm	100.500	12.335	8.513	0.23	1.44	1914.5	121.53
149.5mm	204.380	11.643	7.467	0.21	0.98	1890.3	180.80
206.0mm	414.000	12.422	5.979	0.16	0.72	1910.8	246.85
242.0mm	730.000	15.871	4.745	0.11	0.61	1919.0	284.83
314.5mm	1232.500	15.866	3.407	0.08	0.47	1896.0	334.15

5.7.1 Effect of geometry on the strength of CCWR material models

Figure 5.38 shows the effect of geometry on the unconfined compressive strength of CCWR material models. It can be noted from Figure 5.38 that generally the unconfined compressive strength of the model decreases with the increase in the height to diameter (H/D) ratio. The increase in model diameters from 55.5mm through to 206.0mm results in a small increase in the strength of the model. However, the increase in model diameters from 206.0mm through to 242.0mm gives a marked increase in the strength of the model.

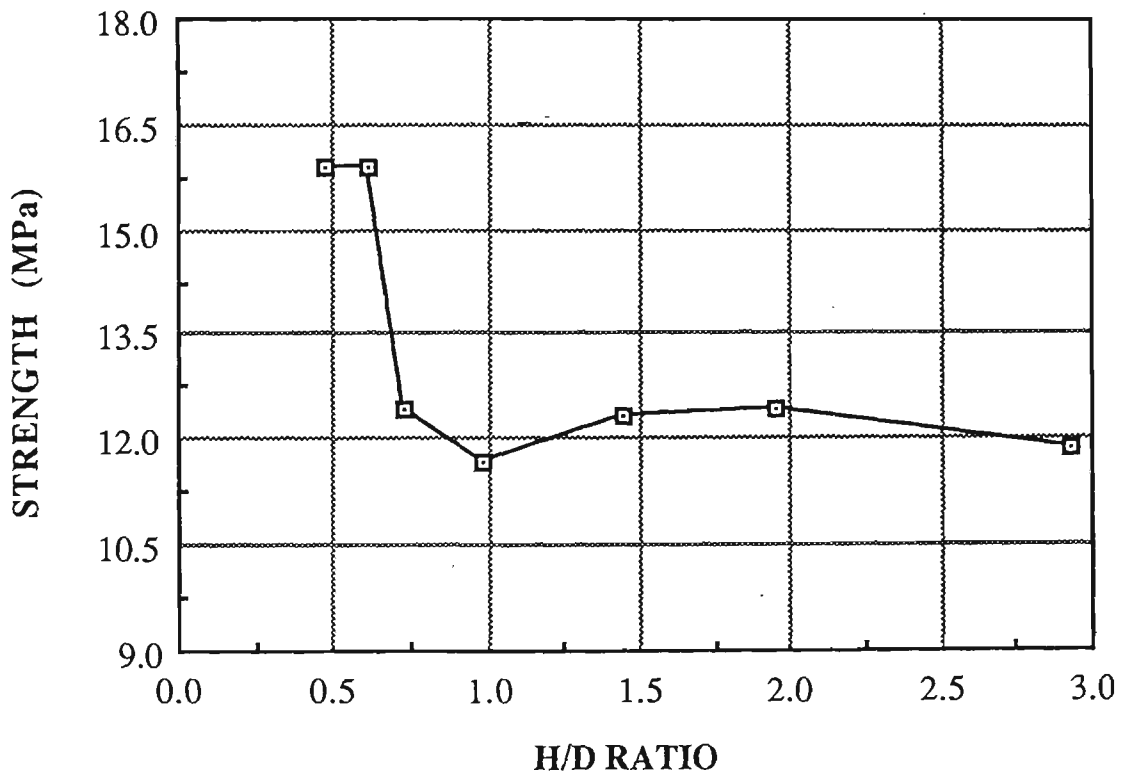


Figure 5.38 Effect of geometry on the unconfined compressive strength of CCWR material models.

5.7.2 Effect of geometry on the axial modulus of CCWR material models

Figure 5.39 illustrates the effect of geometry on the axial modulus of CCWR material models. The increase from 0.47 through to 1.44 in height to diameter ratios of models gives a significant increase in the axial modulus of the models. A further increase (from 1.44 through to 2.93) in the height to diameter ratio of the model results in a decrease in the axial modulus of the model. The optimum geometry for maximum axial modulus is the model with a height to diameter ratio of 1.44.

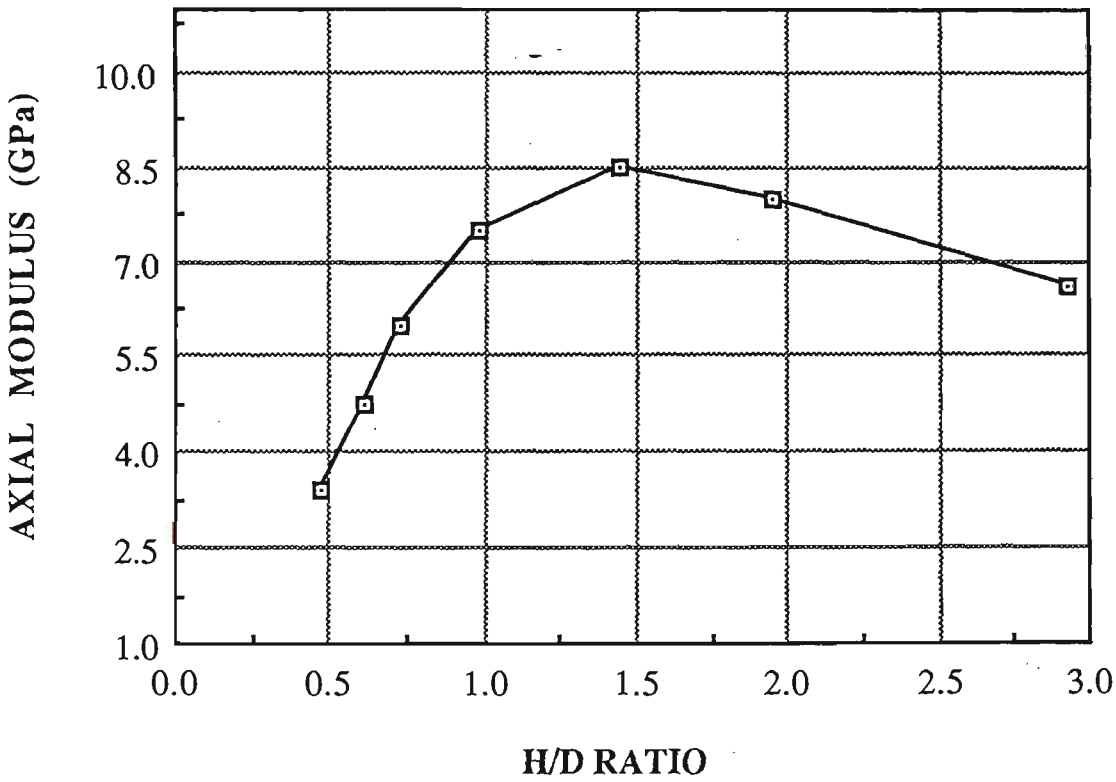


Figure 5.39 Effect of geometry on the axial modulus of CCWR material models.

5.7.3 Effect of geometry on the Poisson's ratio of CCWR material models

The effect of geometry on the Poisson's ratio of CCWR material models is illustrated in Figure 5.40. It is obvious from Figure 5.40 that the increase from 0.47 through to 1.44 in height to diameter ratios of models give a marked increase in the Poisson's ratio of the models. The Poisson's ratio of the models with height to diameter ratios of 1.44 through to 2.93 remains relatively constant.

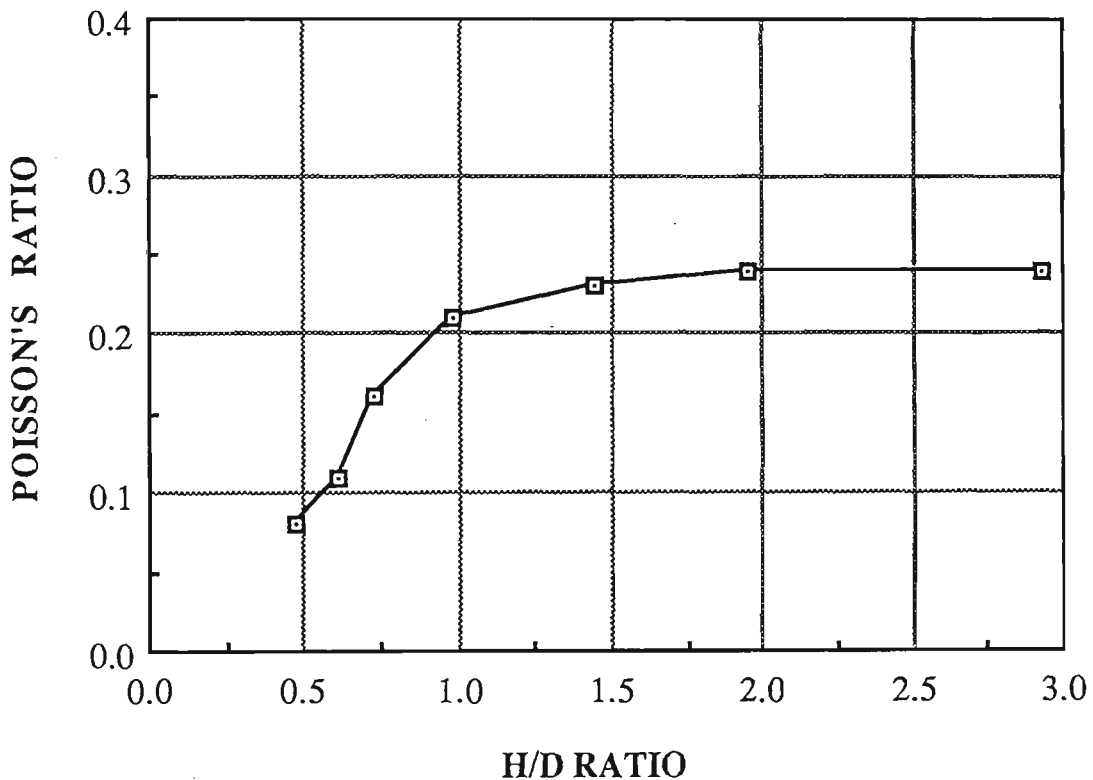


Figure 5.40 Effect of geometry on the Poisson's ratio of CCWR material models.

5.7.4 Effect of geometry on the stiffness of CCWR material models

The effect of geometry on the stiffness of CCWR material models is illustrated in Figure 5.41. Generally, the stiffness of CCWR material model decreases with the increase in its height to diameter ratio.

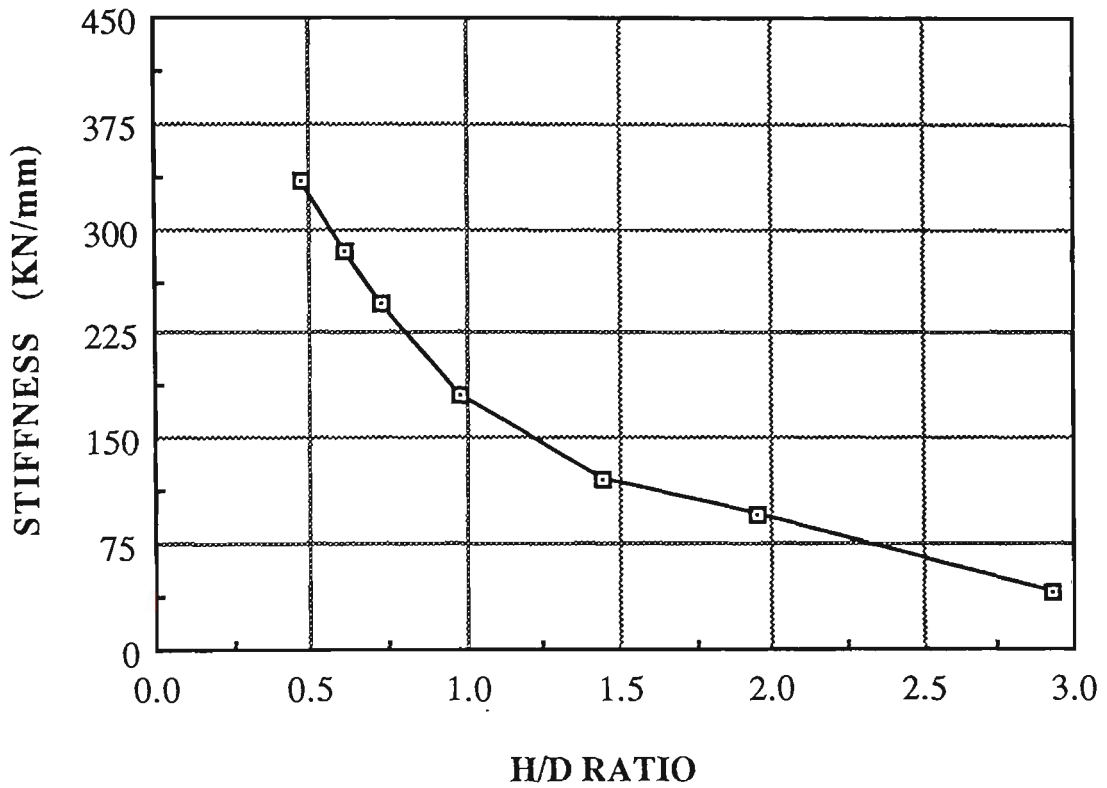


Figure 5.41 Effect of geometry on the stiffness of CCWR material models.

5.7.5 Discussion of test results

Generally, the measured strength of the model increases with the increase in its diameter. It is indicative that the model with a lower height to diameter ratio exhibits a corresponding greater end constraint effect. Due to the end constraint phenomenon, confining pressures were created around the core of CCWR material models and this increased the strength of the models. The findings from the study are in good agreement with that reported by Vutukuri et al. (1974).

Figures 5.42 through 5.48 illustrate the observed shapes of CCWR material models at complete failures and clearly show the effect of geometry on the

load deformation behaviour of CCWR material models. Complete collapse failures which were observed for models with high height to diameter ratios of 1.44, 1.95 and 2.93 can be described in two phases:

- (i) tensional cracks appeared as the maximum compressive strength was reached (brittle shear failure pattern); and
- (ii) as the strain increased these cracks widened and large slabs of the model surface broke away leaving a typical hour glass failure shape, and a concentration of shear stress along some diagonal plane within the model was observed (this caused the model to fail in shear).

Another failure mode observed, for models with height to diameter ratios of 0.47, 0.61 and 0.72, is the shear cone with splitting above (see Figures 5.49 through 5.51). For models with height to diameter ratios of 0.47 and 0.61, distinct fractured regions or yielded zones were observed at surfaces of models but no collapse occurred. It is clear that these yielded zones offer some degree of confinement to inner cores of models. This confinement phenomenon contributes to the higher strength of the model.

It is particularly interesting to note that there is a marked increase in the strength of CCWR material models with diameter to height ratios of 0.61. This increase in the strength of CCWR material models becomes comparatively small for models with even lower height to diameter ratios than 0.61. The practical significance of this singular aspect is that, in CCWR pack design for roof support in a real mine situation, the width to height ratio of the pack can neither be too low nor too high and there exists an optimal width to height ratio of the pack.

For roof support in a real mine situation, if the width to height ratio of CCWR pack is lower than 1.6, there is a danger of inadequate roof support which can lead to complete failure of the pack support and the roof. On the other hand, if the width to height ratio of CCWR pack is too high, resulting in a very stiff pack which can cause floor heave and roadway closure problem, this may involve unacceptable cost penalties. Of course, a more detailed study on this aspect is a vast subject on its own, therefore, more comprehensive investigations on the end constraint effect on insitu CCWR pack and triaxial strength properties of CCWR materials are essential. Some studies on these aspects have been carried out by the author. The results of these findings have been reported separately in Wu et al. (1989), Hii et al. (1990a) and Zhang and Hii (1990a, 1990b).



Figure 5.42 CCWR models with distinct shear plane at complete failures
(diameter=55.5mm).

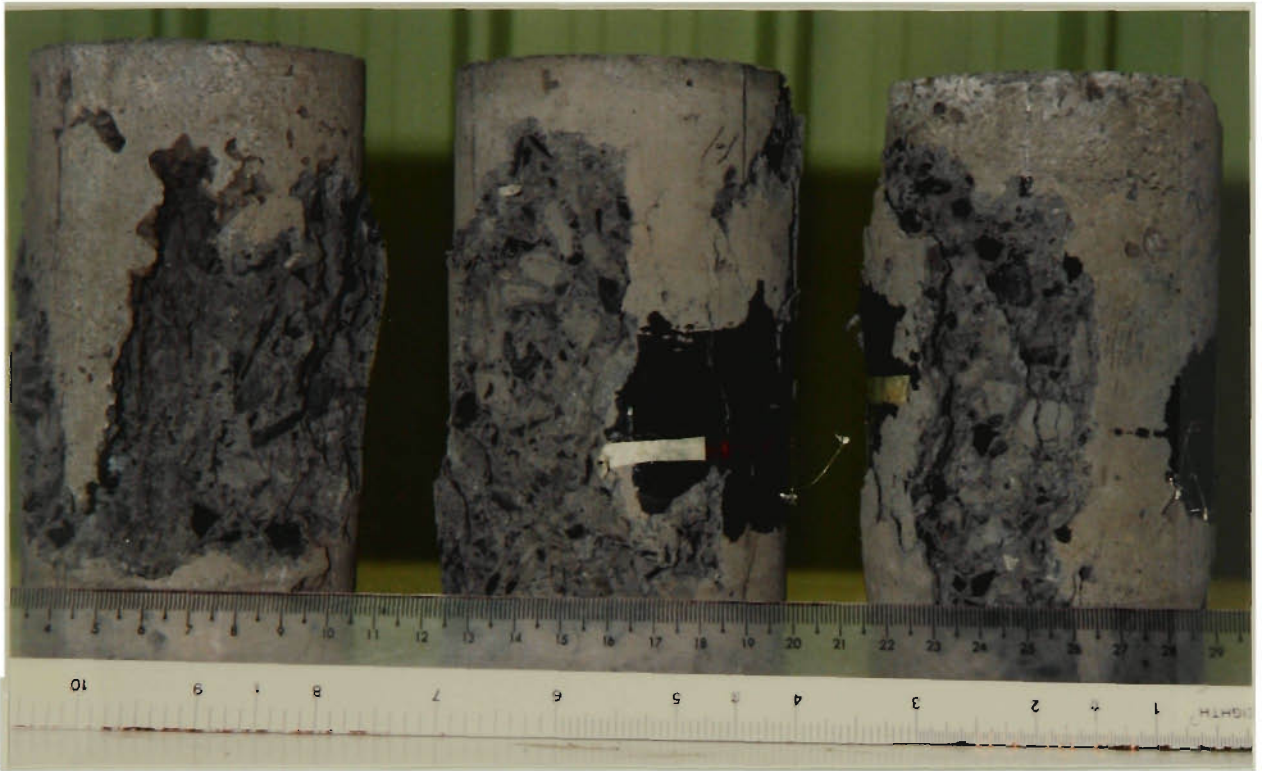


Figure 5.43 CCWR models at complete failures (diameter=75.5mm).

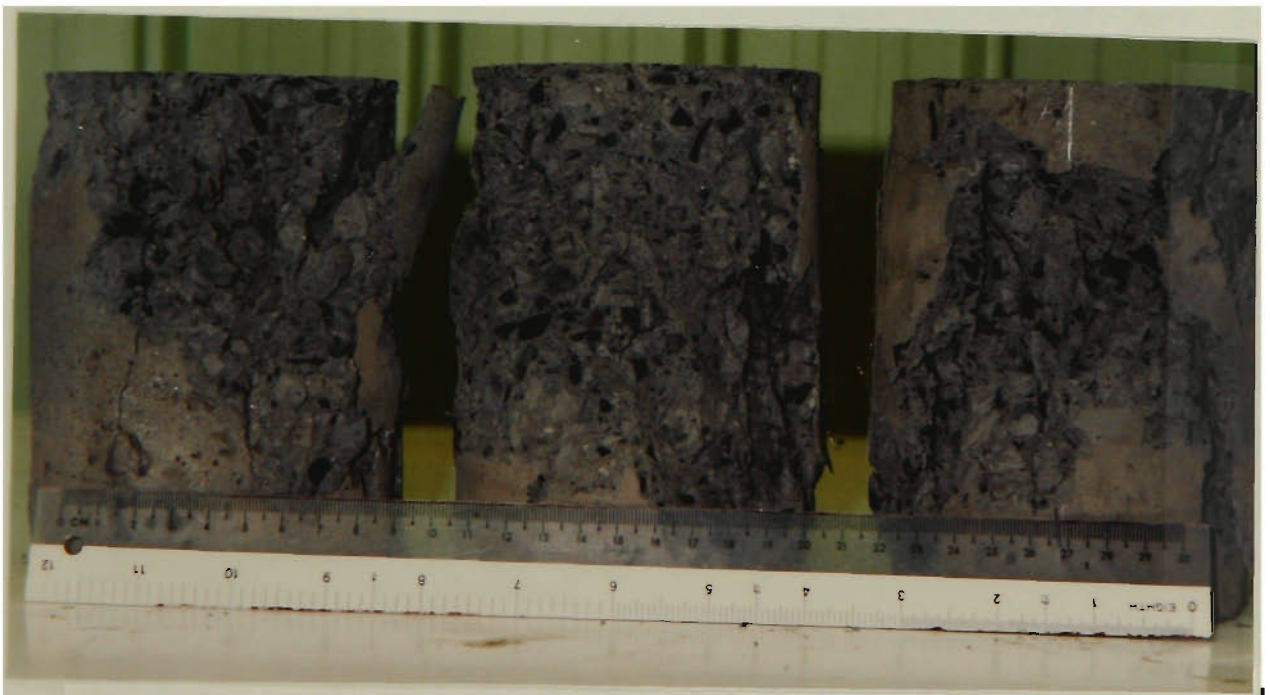


Figure 5.44 CCWR models at complete failures (diameter=102.8mm).



Figure 5.45 CCWR models at complete failures (diameter=149.5mm).



Figure 5.46 CCWR models at complete failures (diameter=206mm).

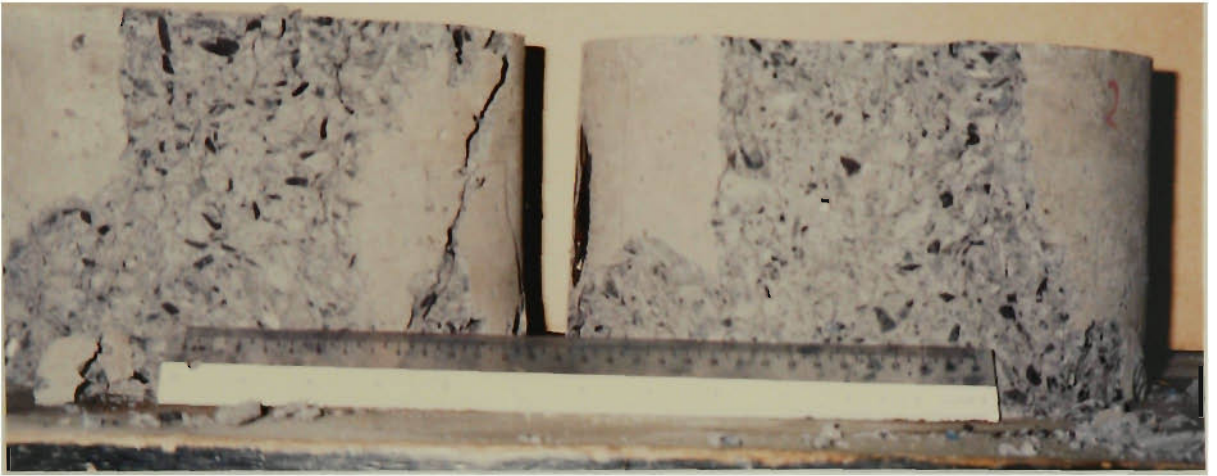


Figure 5.47 CCWR models at complete failures (diameter=242mm).

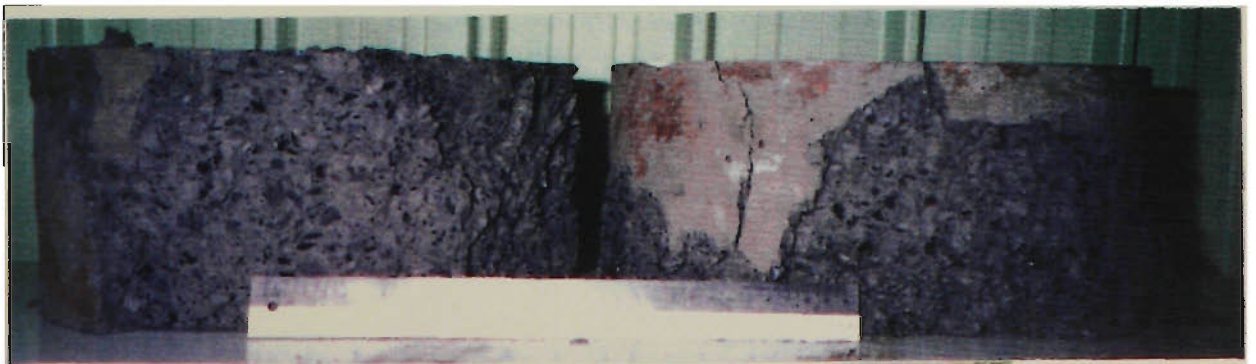
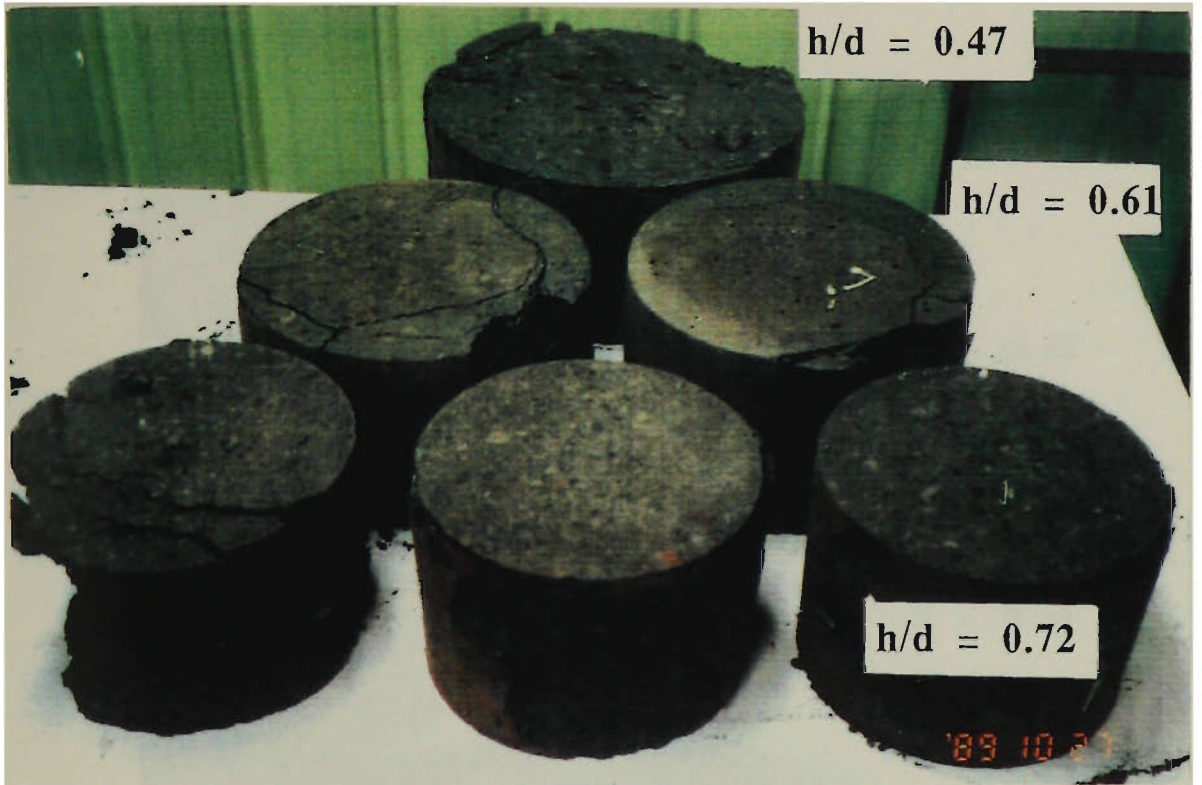


Figure 5.48 CCWR models at complete failures (diameter=314.5mm).

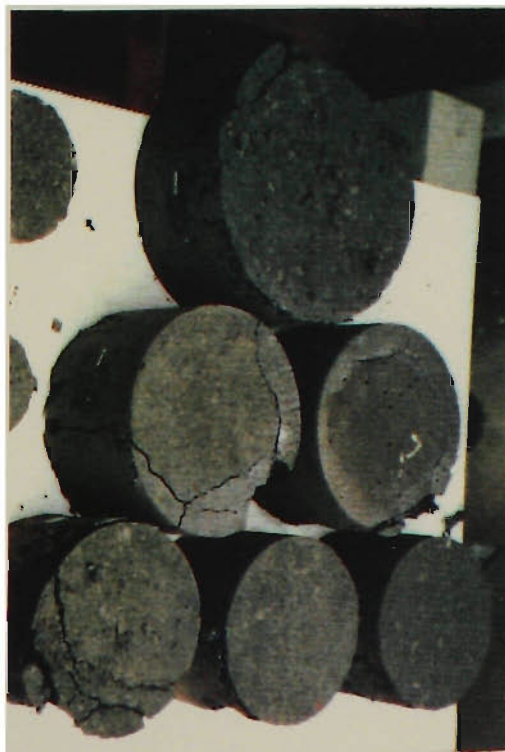
END ELEVATION B



END ELEVATION C

ELEVATION A

Figure 5.49 Various CCWR models at complete failures (Elevation A).



$h/d = 0.47$

$h/d = 0.61$

$h/d = 0.72$

Figure 5.50 Various CCWR models at complete failures (End elevation B).

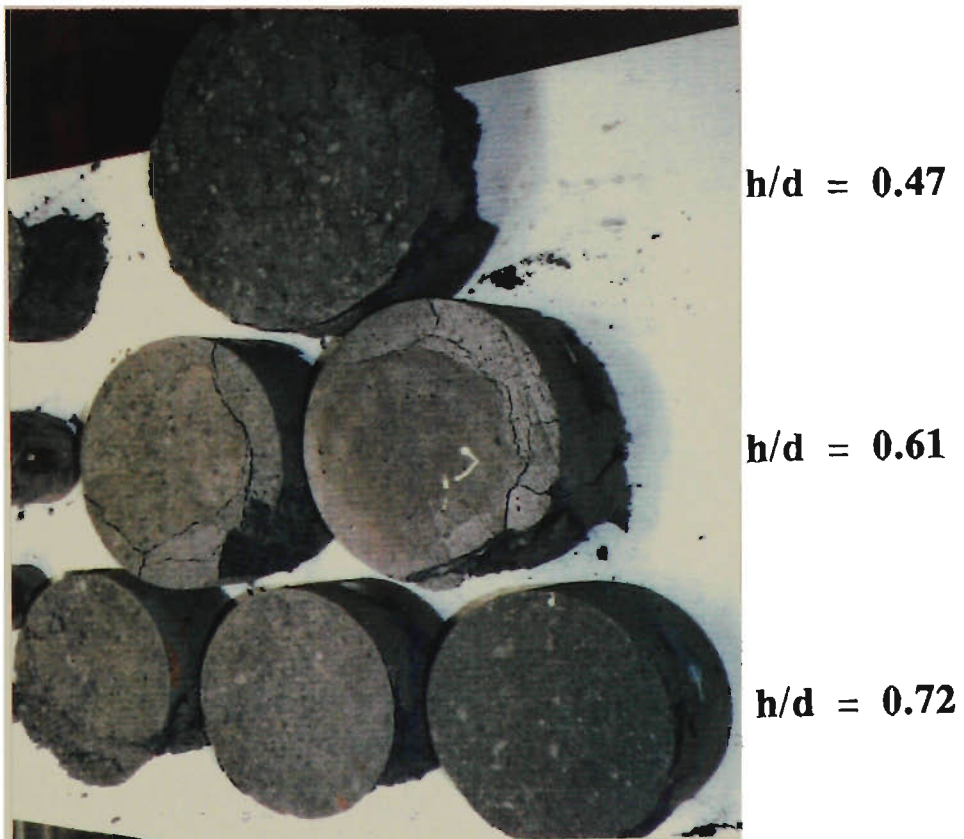


Figure 5.51 Various CCWR models at complete failures (End elevation C).

CHAPTER SIX

ALTERNATIVE METHOD OF IMPROVING GATEROAD STABILITY USING YIELD PILLAR TECHNIQUE

CHAPTER 6

ALTERNATIVE METHOD OF IMPROVING GATEROAD STABILITY USING YIELD PILLAR TECHNIQUE

6.0 INTRODUCTION

In the previous Chapters emphasis has been placed on the development and use of artificial roof supports such as pump packs, Monier 'Big Bag' chocks and wooden chocks for strata control in underground coal mines. According to Hebblewhite (1988), whilst there should be no major constraints apart from the cost constraint (capital cost for installing the pump packing system) to construct center packwalls in roadways away from the goaf abutment, there are serious limitations imposed by the physical properties of flyash and cement based packwalls and failures of the packwalls under the influence of the goaf abutment are inevitable.

The results of this study have shown that CCWR material can be used as a support material, although further work needs to be conducted to investigate the pumpability of this material. While the reinforced Monier 'Big Bag' chocks compared favourably with the wooden chocks the steel mesh reinforcement of the 'Big Bag' chocks can be very costly and even then serious shortcomings such as floor heave and roadway closure still exist. An alternative method of improving gateroad stability using yield pillar technique was therefore investigated.

A yield pillar technique analysed by the finite element method appears suitable for simulation of excavation of roadways under different virgin stress conditions. Comparison of stability of yield and conventional pillars in several

examples substantiates the feasibility of the technique and indicates that yield pillars are potentially capable of eliminating roof falls and floor heave in adjacent entries and crosscuts, and pillar bumps. A procedure using finite element method has been established for the design of yield pillar under various geological conditions (Hii and Wu, 1989).

It is well known that the concept of yielding pillar can be successfully used in solving ground control problems (Serata, 1982, Mark et al, 1988, Newman, 1988, Hii and Wu, 1989, Tsang et al, 1989). The procedure developed in this study may also be used as a tool for pack design. Recall that both the yielding pillar and artificial yielding pillar (pump pack) are designed to yield and absorb vertical closure without bulging and weakening the pillar. The concept utilizes the self support capacity and ultimately the strain hardening and softening characteristics of the surrounding rocks to create a stress relief environment. The application of the stress control method in yielding pillar design is presented in this Chapter. It is emphasized that the findings from the study are applicable to pump pack design.

Another objective of this study is to stimulate further investigation into yielding pillars which are increasingly gaining acceptance as a technique for improving ground control in underground coal mines. It is clear that much additional work will be required before a complete understanding of the yield pillar phenomenon is achieved, hence suggestions for continued work are highlighted.

6.1 REVIEW OF PAST WORK

The mining industry over the last two decades, has seen a major increase in the usage of computers in most phases of its operations. Computer literacy has become an important requirement in the mining profession. In recent years, most mines have been operating in deeper and more difficult conditions than before,

resulting in low productivity and extremely difficult working conditions with high roof and side stresses. In order to alleviate these problems, the yield pillar technique has been developed and used successfully in overseas mines, deep mines in the U.S.A. and Canada in particular (Serata, 1982, Serata et al, 1986, 1987, Shephard, 1986, Ruston, 1986, Mark et al, 1988, Tsang et al, 1989). Peng's group at West Virginia University, Morgantown, West Virginia, U.S.A., has recently been conducting a case study on the application of the yield pillar under strong roof and strong floor condition. The comprehensive research with the yield pillar experiment in 315 Panel to establish the ideal pillar size has led to the successful application of this technology to the maingate of Longwall 12 at West Cliff Colliery (Anon. 1989).

Such applied research is not always possible in the current state of the industry, considering the high costs involved in the experiment and the often marginal economic nature of underground mining operations. Therefore, attempts to establish the ideal pillar sizes for the introduction of yield pillars under different virgin stress field conditions have given rise to the use of a computerised mine structural analysis which has the potential capacity to calculate the distribution of overburden stresses caused by mining and the resulting loadings on any given portion of the underground mine. In recent years, computer modelling has been increasingly recognized as an important asset in the design and analysis of underground rock structures (Hebblewhite, 1982, Beckett and Madrid, 1986, Kripakov, 1987, Zhou and Zhang, 1989, Schmidt and Wu, 1989, Hii and Wu, 1989). The computational power of today's computers together with sophisticated software have enabled the application of the computer modelling technique to provide an approximate solution to complicated rock mechanics problems not readily solved by other means. Generally, safety and productivity may be increased and the costs reduced if an analysis is performed.

6.1.1 Stress Control Methods

The function of strata control in underground mines is to improve roadway stability. Two prominent forms of strata control are the active roadway support and the roadway strata control utilising stress control methods.

Common types of active roadway supports comprise rock bolting (roof bolting and cable bolting), cementitious and resin injection, steel and timber prop support, steel arching, steel meshing, timber chock support, monolithic cementitious support (Australian big bag chock) and steel-fibre-reinforced concrete cribbing (block and donut cribbing). The main function of these supports is to increase the strength of the pressure arch acting above the opening.

Over the last two decades, yield pillars have been used to produce and control the redistribution of stresses around mine openings (Serata, 1982, Serata et al, 1986, 1987, Newman, 1988, Tsang et al, 1989, Hii and Wu, 1989). The yield pillar technique is the principal tool of stress control methods, and the control required to achieve a desired stress condition as mentioned by Serata (1982) is highly site-specific, varying with geological conditions, material properties, initial stress fields, ground water conditions, discontinuity planes and other geological anomalies. Serata (1982) has grouped the current field practice into the following six categories of stress control techniques:

- (i) Stress Relief Technique;
- (ii) Parallel Room Technique;
- (iii) Time-Control Technique;
- (iv) Compounded Time-Control Technique;
- (v) Multiple-Level Technique; and
- (vi) Large Room Technique.

Detailed descriptions of all the six stress control techniques have been reported in Serata (1982).

The stress control technology which has found extensive use in salt and potash mines has been expanded to a wide variety of underground mine openings in various weak grounds including coal mines through more than two decades of field experience. In Australia, pillar systems utilising yield pillar technology is now finding application in underground coal mines but only on an extremely limited scale. The main reasons for the limited application have been the lack of general appreciation of the rock mechanics principles involved in yielding pillar technology and the mining legislation which controls the size of the pillars in underground coal mines (Marshall and Lama, 1986). However, this technology is becoming widely used in deep underground mines for stabilizing openings in weak and complex grounds.

Recently three stress control methods such as pillar extraction on the advance, stress relief headings and yield pillar technique have been used in Australian underground coal mines. It has been demonstrated in practice that these stress control techniques can reduce the extent of lateral stress acting within the pressure arch by decreasing the lateral constraint in the roof strata.

6.2 Theoretical Considerations of Stress Control Design

Openings in underground coal mines excavated by room and pillar method experience the highest concentration of shear stress which is potentially destructive, and according to Serata et al. (1986) this is due to the formation of a stress envelope around each individual opening as shown in Figure 6.1. This high concentration of shear stress may cause roof and floor failures if the strength of the surrounding

rocks is lower than the shear stress. Stress control method can be used to relocate these destructive stress envelopes away from the individual room boundaries and this may be achieved by grouping the room closely as also illustrated in Figure 6.1. However, this must be done by first excavating the two side rooms follow by the middle room (Serata et al, 1986)

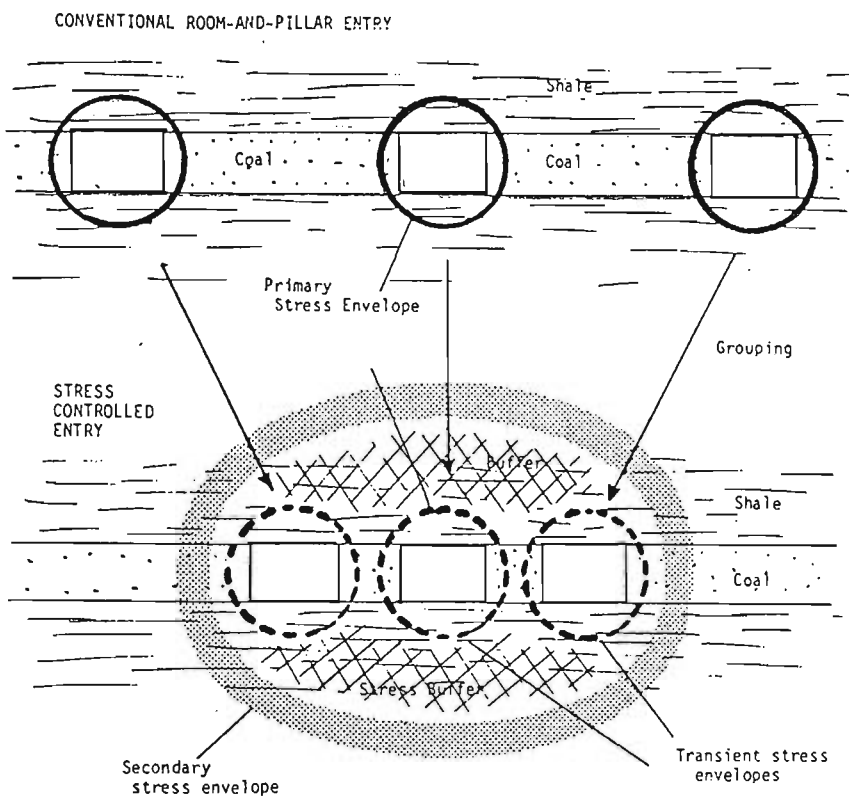


Figure 6.1. Principle of stress control method which is illustrated by three-room "stress-controlled" entry and this is formed by grouping three isolated conventional rooms very close together, and hence transforming three primary destructive stress envelopes into a single secondary protective stress envelope.

(after Serata et al, 1986)

Since the protective stress envelope is formed as a direct and natural reaction to both the overburden and lateral tectonic stresses it takes the entire burden of those stresses, and as mentioned by Serata et al. (1986) the yielding pillars which accommodates the deformation do not actually fail as they are protected and stress relieved by the formation of the so called protective stress envelope. An important feature of this stress control technique is that the immediate roof and floor which are located inside the protective stress envelope are also stress relieved, and they form a natural protective lining for the final protective stress envelope.

As mentioned earlier, the design of a stress controlled entry in an underground coal mine can be highly site-specific and two major factors are to be considered for any given coal seam. Firstly, there is the operation factor such as the desired number of rooms to be grouped into a single entry and the desired width of individual rooms within the entry. Secondly, the so called "live" geomechanical factor which is both time dependent and site specific, and this comprises the virgin stress fields and the material properties of coal and the surrounding rocks (Serata et al, 1986).

It is important to note that in a steady state, the rate of hardening is balanced by that of softening and therefore the strength enhancement due to hardening is essentially nil (Hambley, 1989). However, the stress relief due to the development of a pressure arch as mentioned above does undeniably occur, hence, the idea of protecting openings using the concept of a pressure arch is valid.

6.3 EFFECT OF VIRGIN STRESS FIELDS ON THE FEASIBILITY STUDY OF YIELD PILLAR TECHNIQUE

In general, a yield pillar is designed to yield or crush in a controlled fashion throughout its width and to provide locally resilient support in the mine excavation while operating in a plastic mode, at a factor of safety less than unity. Contrary to the traditional concept of pillar design, in yield pillar design a relatively small pillar is designed to yield as soon as it is being developed, and its original load is transferred to the adjacent pillars (Tsang et al, 1989).

In Australia, yield pillars have been used in West Cliff Colliery, NSW, and it has been demonstrated that they can improve entry stability and control floor heave problems (Anon. 1989). However, the existing yield pillar design is mostly based on trials and errors, and the mechanisms and limitations of yield pillar technique are still not well understood.

It is well known that the duration of yielding of coal and rocks before collapse depends on the initial loading condition material properties, and as long as the rate of yielding is in the safe range, the overall stability condition for the entry-pillar system may be maintained for the required service life time. The design of yield pillars therefore must take into account the overall stability of the surrounding geology and the orientation and direction of stress. For safe mining operations, a yield pillar must satisfy two basic requirements (Tsang et al, 1989): firstly, it should yield totally after development so that its load can be transferred, and secondly, it should sustain and maintain good working conditions in the adjacent entries for the intended service life period.

If the yield pillar satisfies both the abovementioned requirements it is defined as a stable or functional yield pillar, however, if it only satisfies the first

requirement it is considered to be an unstable or unfunctionable yield pillar. It should be noted that a yield pillar is less stable than a stiff pillar but by considering the overall stability condition, a yield pillar may provide the best results and also it may be the only alternative design for certain geological conditions.

In this study, the mechanisms of yield pillar were discussed. This Section presents an application of the finite element method to investigate the feasibility of using the yield pillar technique under different virgin stress field conditions in Australian underground mining operations. A given portion of an underground mine in the Southern Coalfields, NSW, Australia is specified as a grid and the program then calculates the two dimensional ground stresses and deformations resulting from the formation of both the yield pillar and the conventional pillar.

6.3.1 Method of analysis

The finite element method is employed for the computation of stresses in pillars under various virgin stress fields. The factor of safety of the pillar is evaluated according to the ratio of the computed stress and the strength of rocks.

6.3.2 Computation of stresses in pillars

Stresses in pillars are computed by using an excavation model (Brown and Booker, 1984, Schmidt , Wu and Lu, 1989), in which the loading or the unloading history of stresses during the formation of pillars can be simulated. Figure 6.2 shows the formation of Pillar A, that is, by excavating Roadways 1 and 2. Stresses in Pillar A are computed as:

$$\sigma_A = \sigma_{A0} + \Delta\sigma_A \quad (6.1)$$

where

σ_A is the redistributed stress in the pillar;

σ_{A0} is the virgin stress determined by in-situ stress measurement; and

$\Delta\sigma_A$ is the increment of stress in the pillar due to the excavation of roadways 1 and 2 and it can be computed by the finite element procedure, the details of which is presented in the following.

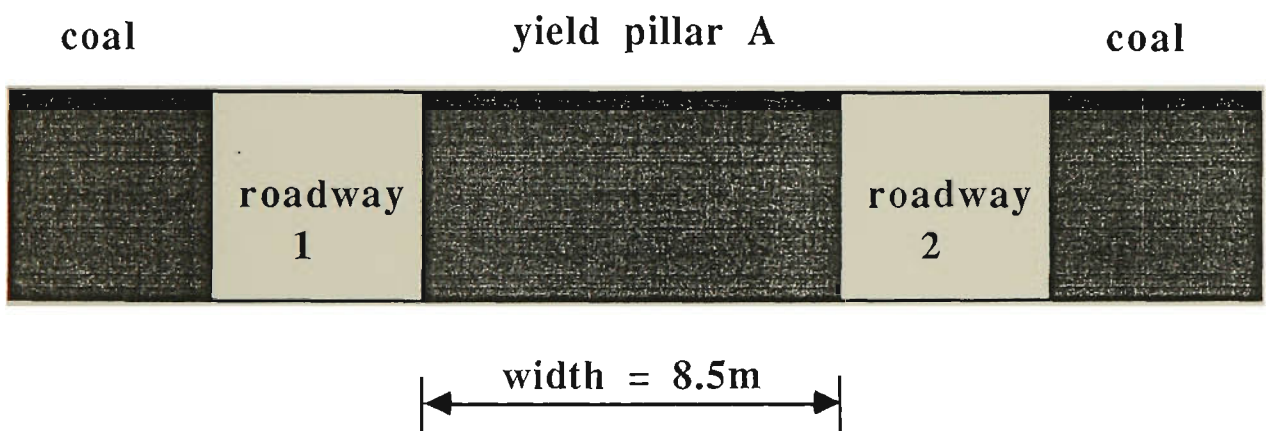


Figure 6.2 Formation of Pillar A.

The finite element formulae used for the computation of pillar stress can be obtained from the virtual work principle. Consider a domain Ω with a boundary Γ the virtual work equation governing the behaviour of the domain can be expressed in an incremental form as:

$$\int_{\Omega} \delta \epsilon^T \Delta \sigma d\Omega = \int_{\Omega} \delta u^T \Delta b_v d\Omega + \int_{\Gamma} \delta u^T \Delta p d\Gamma \quad (6.2)$$

where

δu and $\delta \epsilon$ are the virtual displacements and the corresponding strain in domain Ω ; Δb_v denotes the increment of body force; and Δp denotes the increment of boundary traction.

To solve eq.(6.2) numerically, the domain Ω is discretized into a number of elements Ω_e connected at the nodes. Consequently, the boundary Γ is also divided into a number of boundary element Γ_e . In each element, the displacement field is approximated by:

$$\{\Delta u\} = [N] \{\Delta a\} \quad (6.3)$$

where

$[N]$ is the matrix of specified shape functions; and $\{\Delta a\}$ is the vector of nodal displacement increments.

From eq.(6.3) both the strain and stress increments can be expressed in terms of nodal displacement increment $\{\Delta a\}$ as:

$$\{\Delta \epsilon\} = [B] \{\Delta a\} \quad (6.4)$$

$$\{\Delta \sigma\} = [D]_{ep} [B] \{\Delta a\} \text{ or } \{\Delta \sigma\} = [D] [B] \{\Delta a\} + \{\Delta \sigma_0\} \quad (6.5)$$

where

$[D]$, $[D]_{ep}$ are the elasticity matrix and elastic-plastic matrix respectively; $[B]$ is the derivative matrix of $[N]$;

$\{\Delta\sigma_o\}$ is the initial stress increment.

The substitution of eqs. (6.3), (6.4) and (6.5) into eq. (6.2) produces:

$$\begin{aligned} \{\Delta a\}^T \int_{\Omega} [B]^T [D] [B] d\Omega \{\Delta a\} &= \{\Delta a\}^T \int_{\Omega} [N]^T \{\Delta b_v\} d\Omega - \{\Delta a\}^T \int_{\Omega} [B]^T \{\Delta\sigma_o\} d\Omega \\ &+ \{\Delta a\}^T \int_{\Gamma} [B]^T \{\Delta p\} d\Gamma \end{aligned} \quad (6.6)$$

Due to the arbitrary, $\{\Delta a\}^T$ in eq. (6.6) can be deleted. And then by abbreviating the notation, there results:

$$[K] \{\Delta a\} = [\Delta F_v] - [\Delta F_o] + [\Delta F_{\tau}] \quad (6.7)$$

with

$$[K] = \int_{\Omega} [B]^T [D] [B] d\Omega$$

$$[\Delta F_v] = \int_{\Omega} [N]^T \{\Delta b_v\} d\Omega$$

$$[\Delta F_o] = \int_{\Omega} [B]^T \{\Delta\sigma_o\} d\Omega$$

$$[\Delta F_{\tau}] = \int_{\Omega} [N]^T \{\Delta p\} d\Omega$$

where

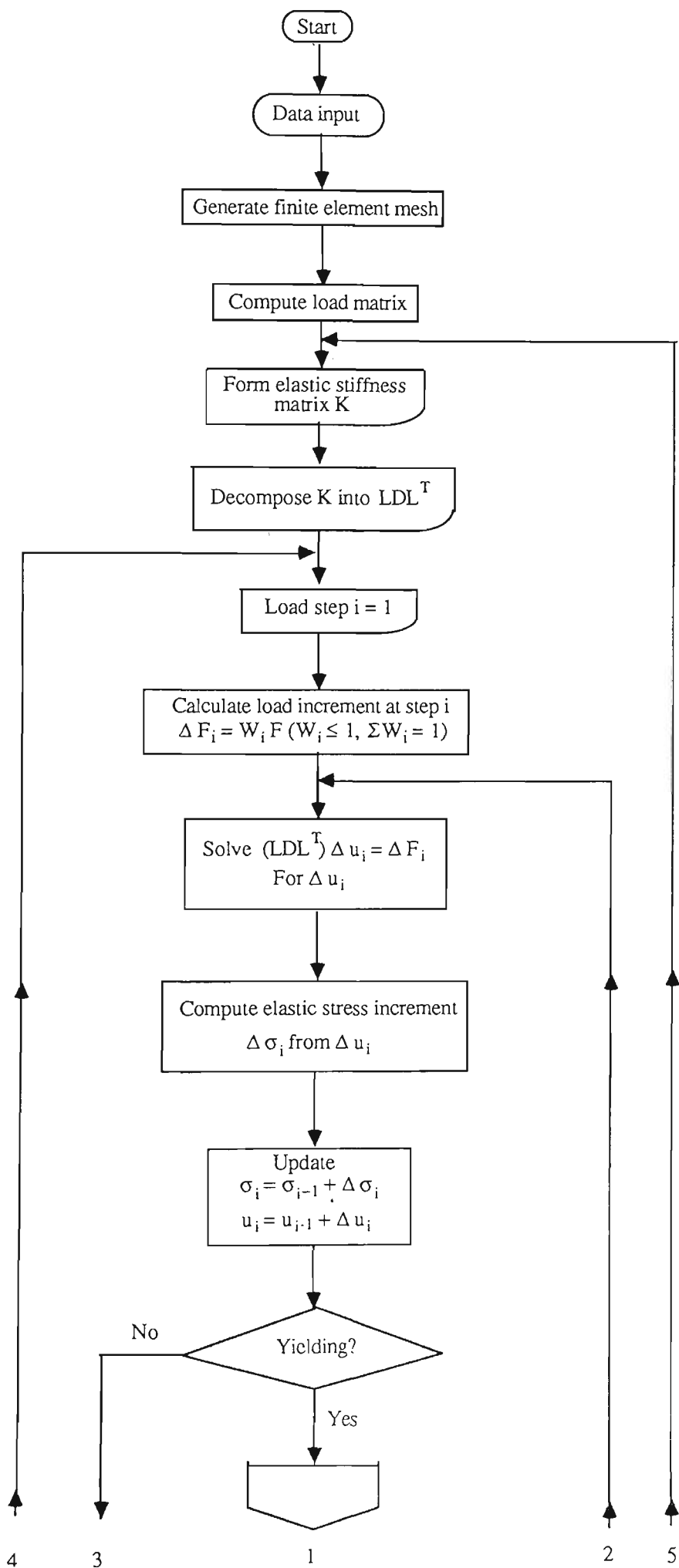
$[K]$ is the stiffness matrix;

$[\Delta F_v]$ is the nodal force due to the increment of the body force;

$[\Delta F_o]$ denotes the iterative term of the nodal force; and

$[\Delta F_\tau]$ denotes the boundary traction, which, in the current computation model is the stress relaxation at the excavation boundary due to the excavation of Roadways 1 and 2.

Eq. (6.7) is a nonlinear equation because $[\Delta F_o]$ depends on $\Delta\sigma_o$, and $\Delta\sigma_o$, in turn, depends on σ . Therefore an iterative procedure is used for the computation. Figure 6.3 shows the flow chart of the computation procedures.



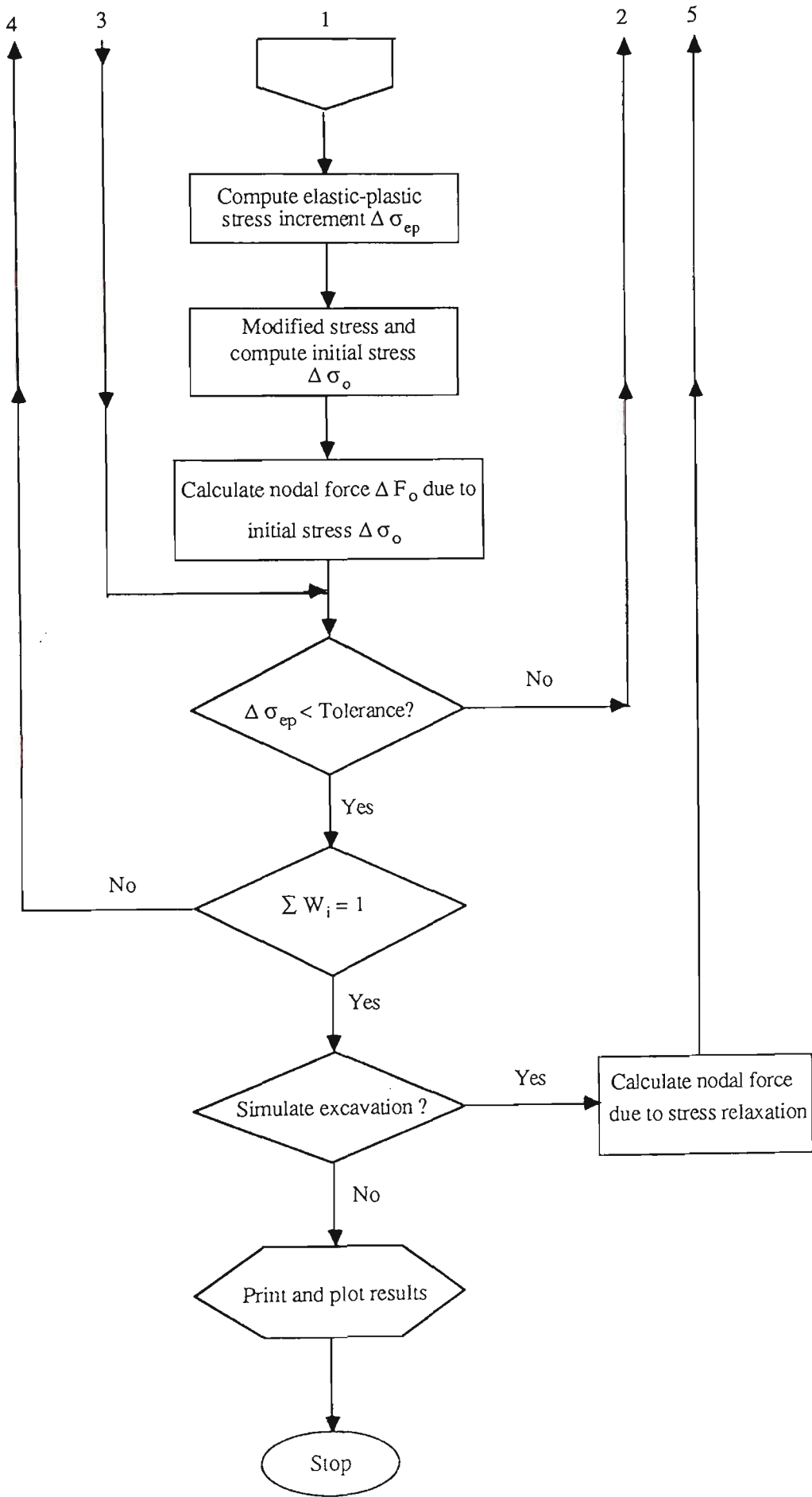


Figure 6.3 Flow chart of the iterative scheme.

6.3.3 Determination of the factor of safety

Once the stress in any point of the pillar is obtained, the factor of safety at that point can be evaluated as the ratio of the strength and the stress, that is,

$$SF = \frac{\sigma_s(\sigma_3)}{\sigma_1} \quad (6.3)$$

where SF is the safety factor; $\sigma_s(\sigma_3)$ is the strength of the rock, which is the function of σ_3 ; σ_1 denotes the major principal stress; and σ_3 denotes the minor principal stress.

6.3.4 Scheme of analysis

Two illustrative examples are designed to investigate the feasibility of using yield pillar under different virgin stress fields.

Illustrative example 1 considers the stability of a yield pillar under various virgin stress fields. The width of the pillar adopted is 8.5m, and the finite element mesh generated is shown in Figure 6.4.

Illustrative example 2 considers the stability of a conventional pillar under the same virgin stress field as in example 1. The width of the pillar is taken as 30m.

In both examples, five cases of virgin stress field are considered, and this is tabulated in Table 6.1. Table 6.2 shows the properties of rocks used in the analysis of the illustrative examples.

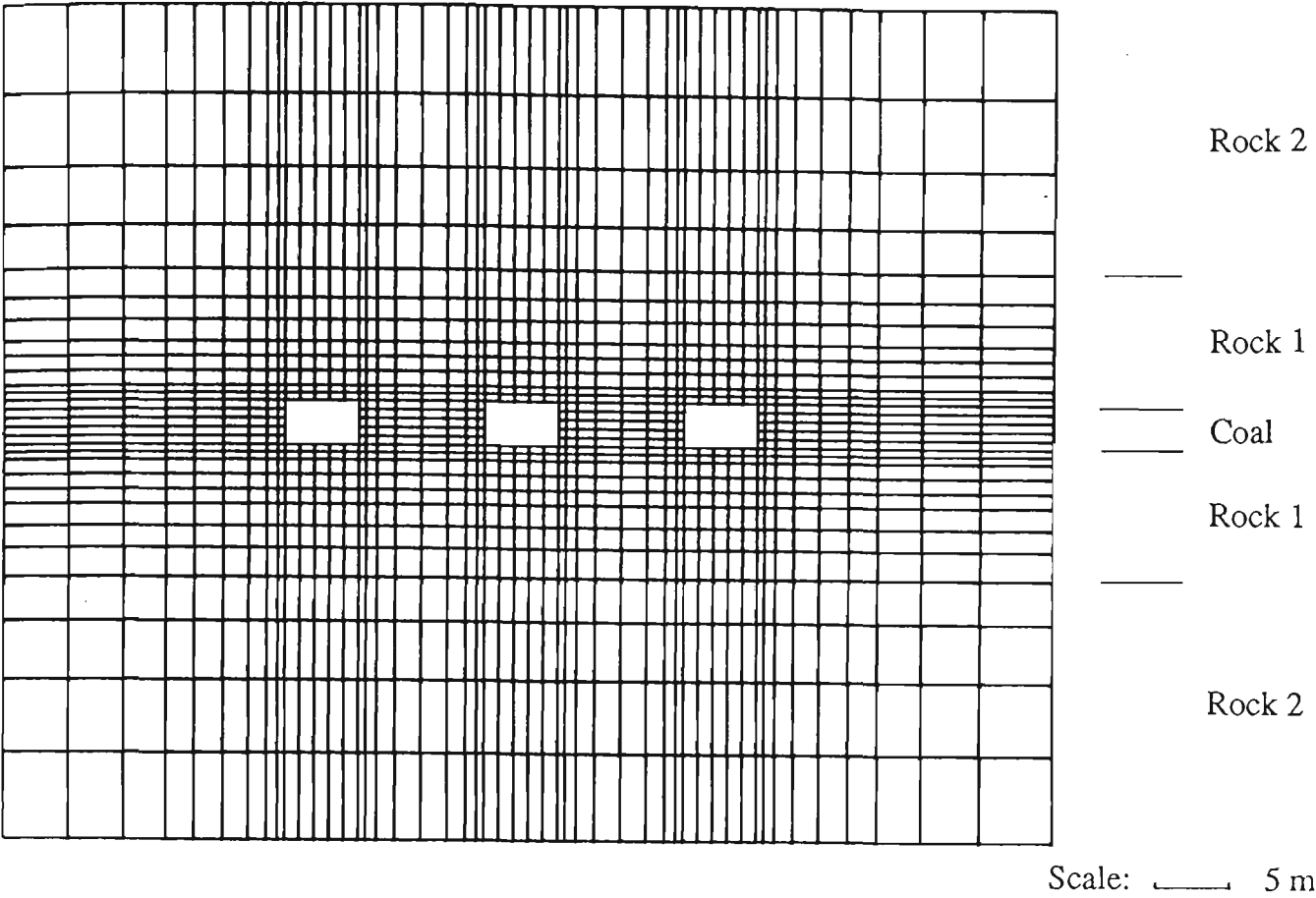


Figure 6.4 Finite element mesh for yield pillar scheme.

Table 6.1 Virgin stress fields.

Case	1	2	3	4	5
Horizontal stress σ_{oh} (MPa)	-5	-10	-15	-20	-25
Vertical stress σ_{ov} (MPa)	-10	-10	-10	-10	-10
Ratio k $\sigma_{oh} / \sigma_{ov}$	0.5	1	1.5	2.0	2.5

Table 6.2 Properties of rocks.

Parameters	Young's modulus (MPa)	Poisson's ratio	Cohesive strength (MPa)	Angle of friction ($^{\circ}$)	Tensile strength (MPa)	Residual cohesive strength (MPa)	Residual angle of friction ($^{\circ}$)
Coal	1000	0.3	0.4	35	0.01	0.15	28
Rock 1	2000	0.25	1.5	37	0.1	0.6	30
Rock 2	3000	0.25	3.0	37	0.2	1.2	30

6.4 RESULTS AND DISCUSSION

Figures 6.5 and 6.6 show the principal stress distribution for both the yield pillar and the conventional pillar under Case 5. It is indicative that the horizontal stress relaxation occurs in the entire yield pillar. In the conventional pillar, however, the horizontal stress relaxation only occurs in the two sides of the pillar. The computed maximum stress at the centre of the conventional pillar is the horizontal stress, and no significant horizontal stress relaxation takes place.

Figure 6.7 illustrates the distribution of horizontal and vertical stresses along the cross sections of both the yield pillar and the conventional pillar under Case 5. It is evident that a significant relaxation of horizontal stresses occurs approximately 4m from the edge of the pillars. The results indicate that the average deviator stress of the yield pillar is smaller than that of the conventional pillars.

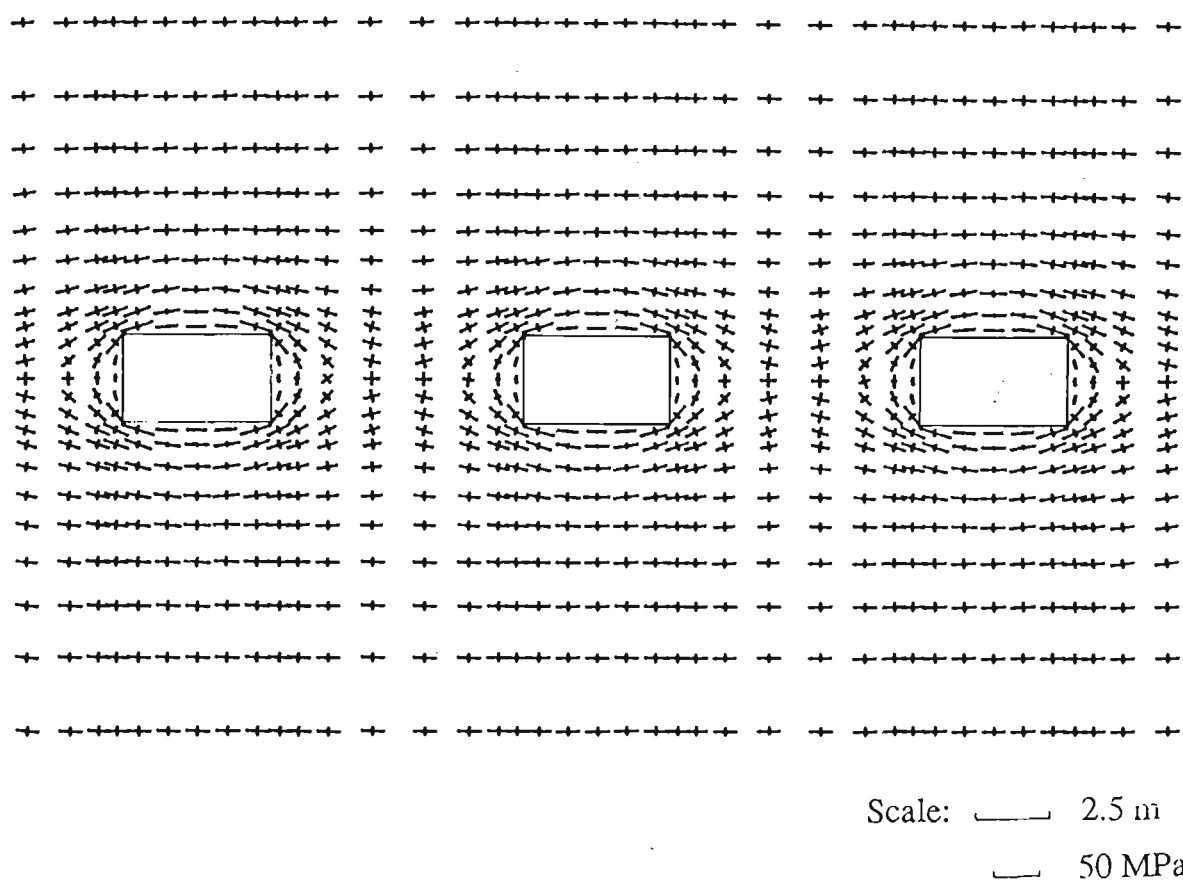


Figure 6.5 Principal stress field in the yield pillar scheme.

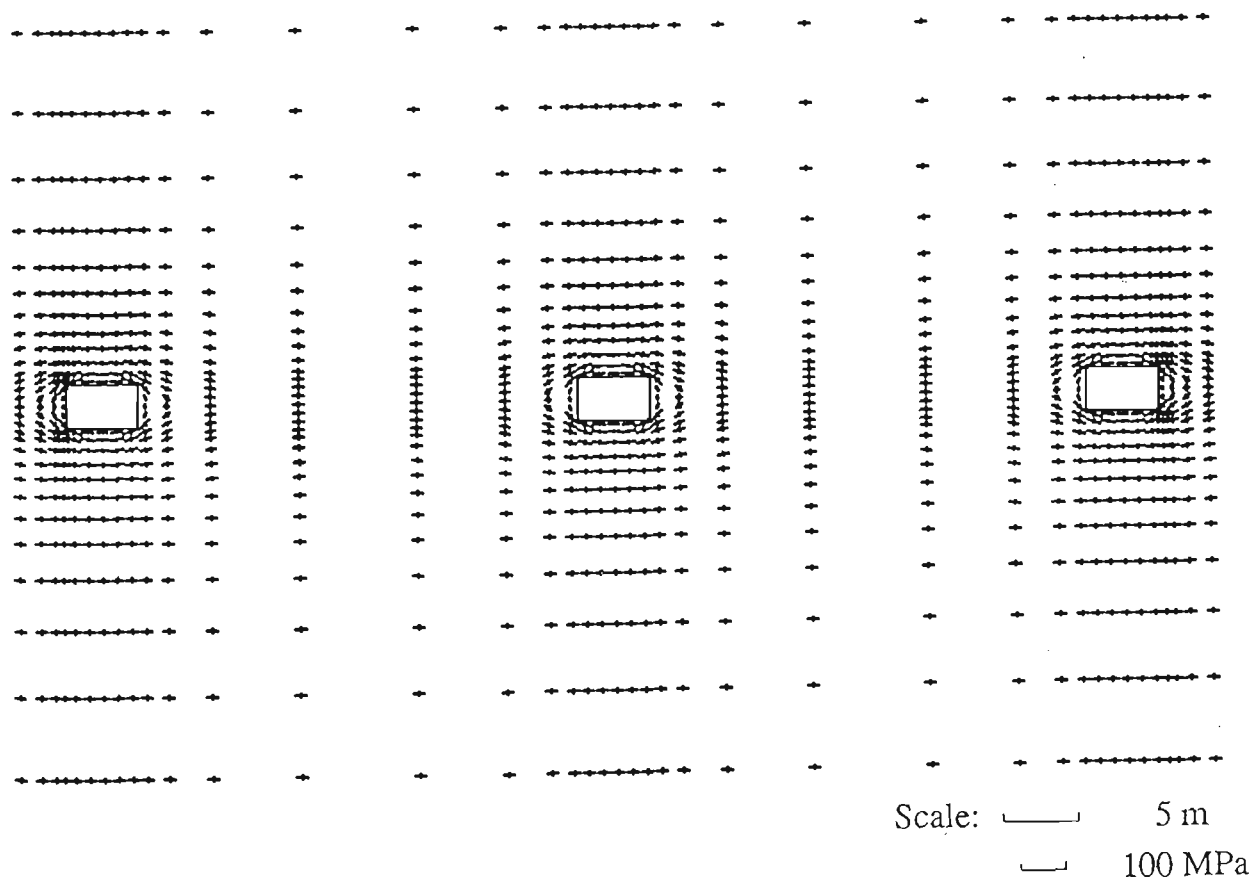


Figure 6.6 Principal stress field in the conventional pillar scheme.

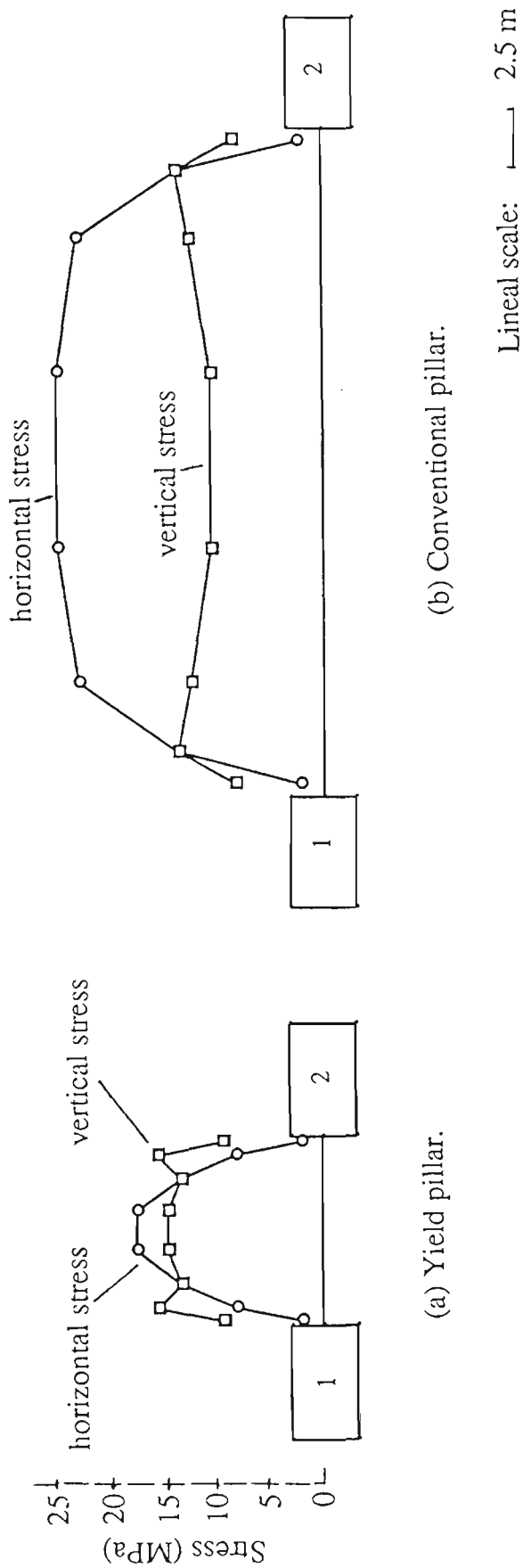


Figure 6.7 Distribution of stress along a cross-section of pillar.

Figure 6.8 shows the average safety factor of the cross section of the pillar versus the ratio of the vertical virgin stress and the horizontal virgin stress. It is clear that, in the case of high horizontal virgin stress fields, k is greater than 1.6, the yield pillar is more stable than the conventional pillar even though the width of the yield pillar is much smaller. However, in the case of low horizontal virgin stress fields, the conventional pillar exhibits comparatively greater stability than the yield pillar.

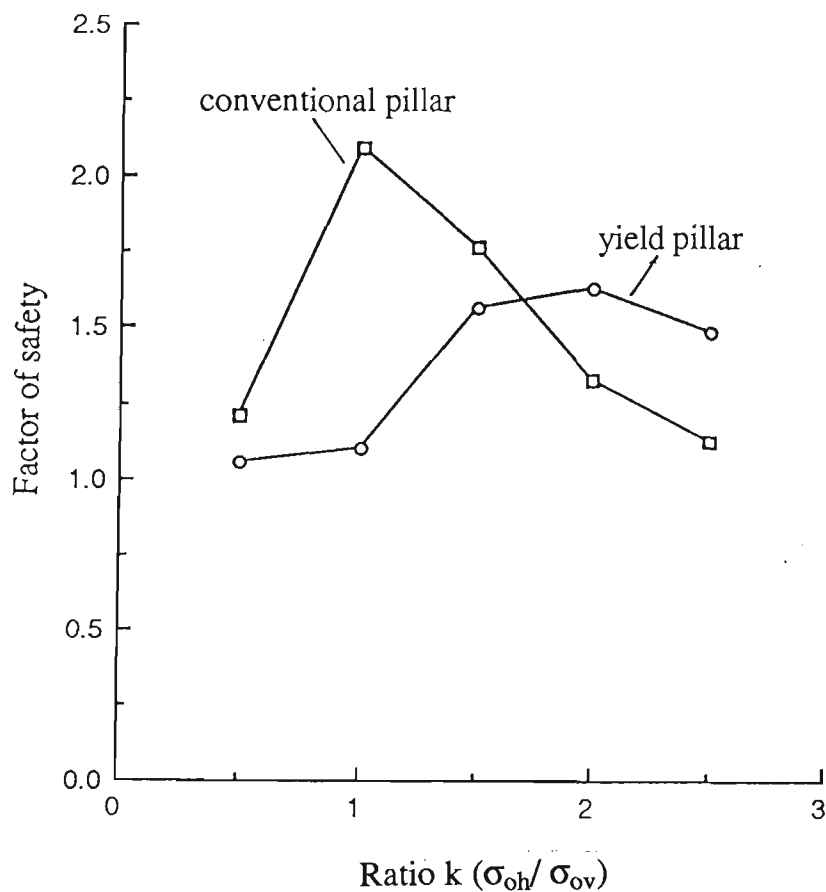


Figure 6.8 Safety factor versus k ($\sigma_{oh} / \sigma_{ov}$)

6.5 CONCLUSIONS

The finite element method may be successfully employed to investigate the feasibility of using the yield pillar technique under different virgin stress field conditions. It is demonstrated that when k , the ratio of the horizontal virgin stress and the vertical virgin stress, is greater than 1.6, the yield pillar technique can be successfully used, and a greater pillar stability is achievable. On the other hand, if the ratio k is not greater than 1.6, a decrease in the pillar width will give a lower safety factor of the pillar.

It is suggested that there exists an optimal pillar width for a particular ratio of k . The pillar design using the optimal pillar width will exhibit the highest safety factor of the pillar.

Further work should include:

- (i) an experimental research to verify the numerical results, and
- (ii) the development of nomographs, from which the optimal width of the pillar can be determined for a particular ratio k .

CHAPTER SEVEN

CONCLUSIONS

CHAPTER 7

CONCLUSIONS

From a review of strata control theories and overseas successes in achieving effective strata control using monolithic pump packing techniques it can be concluded that a study into the introduction of pump packing technology to Australian coal mining operations is warranted.

It can be inferred from the literature survey that the selection of any type of packing material for use in the Australian coal mines would obviously be influenced by the availability of the product at a competitive price and its function as a support material. Given the existing environmental constraints imposed on the coal mine operators, the utilization of CWR as a packing material is an attractive proposition.

In the likely event of high tonnage demand for packing material, the processed CWR can be piped down from the surface to the packing site, where it will be readily mixed with other ingredients and pumped into the pack form or bag.

In general, pump packs are designed to yield and thus control convergence, and are often built to an optimum size to save manpower and material costs. In addition, as German experience has shown, pump packs greater than a critical width lead to floor heave as the packs do not yield under load (Lewis and Stace, 1981).

Extensive field trials and studies over the years have established the following criteria for pack strengths (Whittaker et al, 1977, Issac et al, 1982, Smart et al, 1982a, 1982b, Buddery, 1984, Clark and Newson, 1985, Smart, 1986, Isaac and Payne, 1986). The strength of 0.1 MPa for deshuttering purposes, and initial strengths of 0.4 - 0.5 MPa in 4 hours, and 1 - 1.4 MPa in 24 hours are desirable. A more important criterion is that the pack should be able to develop strength as quickly as possible, and the final strength should be in the order of 6 -10 MPa.

It is important to note that the above criteria for pack strength apply especially for the United Kingdom conditions. Therefore, it is in the opinion of the author that the pack strength for Australian conditions should be higher in order to accommodate the excessive load of the massive sandstone roof (Hii and Aziz, 1986a). However, the required pack strength for Australian underground coal mines should be quantified from field trials and in-situ monitoring programmes.

The planning of an efficient pump packing system requires a high level of prediction, both of geological conditions and those likely to be caused by mining. It is noted that the continued effective control of the roof strata in the vicinity of a roadway can only be achieved when the pack supports are capable of sustaining the variations which arise from the changing mine layout, the ground stress conditions and the variations in the geological conditions.

An attempt has been made to emphasise the importance of understanding the tectonic forces which prevail in mining. Consequently, an improvement in this understanding can help to effectively control these forces by the selective use of pump packing systems.

The integrated methods of colliery waste disposal for ground control as proposed by Atkins et al. (1986) are of particular interest to the coal mining

industry. The pump packing system using CCWR material undoubtedly will have a large contribution to make to the Australian mining industry in the foreseeable future.

The experimental investigation has shown that the use of CCWR pack material is a major step in the development of a cost-effective pack. The laboratory study has greatly improved understanding of the mechanical properties and behaviour of the pack material produced.

Laboratory tests performed on the experimentally formulated CCWR specimens of varying mix compositions have shown great promise towards monolithic pack material applications. However, results indicate that water content and calcium chloride admixture must be very closely controlled to ensure optimum pack quality, as confirmed by overseas studies in similar research work (Lerche and Renetzeder, 1984, Zadeh et al, 1987).

It is shown that the relationship between the strength S and curing time t of a CCWR material mix can be described by the following equation:

$$S=A \cdot \exp(-B/t^{0.5}) \quad (3.5)$$

The response surface methodology is shown to be valid for the analysis of test results presented and it is suggested to be used as a general method in the study of the optimum design of CCWR materials. For CCWR materials the unconfined compressive strength can be calculated from the compositions of a mix using equations (3.14) and (3.15).

As expected an increase in the strength of CCWR materials can be attained either by decreasing the water content or increasing the quantity of OPC used in the mixtures.

It has been demonstrated that the proposed logarithmic yield function can predict the strength and yield characteristics of CCWR materials in a satisfactory manner. The general form of the proposed yield function can be expressed as follows:

$$\sigma_1 = A + B \ln(\sigma_3 + C) \quad (3.16)$$

The following conclusions can be drawn from the present investigation concerning the effect of water content on the mechanical properties of CCWR material containing calcium chloride admixture:

- (i) For any length of curing time up to 28 days, the strength of CCWR material markedly decreases as the water content increases.
- (ii) The decrease in ultimate unconfined compressive strength due to an increase in water content for CCWR material test specimens at lower curing time spans is quite significant. The practical significance of this aspect is that the water content must be very closely controlled to ensure high early strength of CCWR concrete which is rather essential for successful monolithic pack applications.
- (iii) Test results indicate that the drying shrinkage of CCWR material is insignificant in all mixes.

- (iv) The importance of water content with regard to its effect on strength, workability and other related mechanical properties of CCWR material is emphasised.

The initial test results of the study have revealed the effect of water content on flow properties of CWR. The importance of the effect of water content and other related parameters on the flow characteristics of CWR has been emphasised by the author and various researchers (Lerche and Renetzeder, 1984; Verkerk, 1986 and Atkins et al, 1987). Based on the results of this investigation the following statements appear justified:

- (i) CWR with a nominal water content in the region of 15.0% exhibits undesirable flow characteristics, and this is manifested by its relatively low flowability behaviour.
- (ii) Within the range from 15.0% to 30.0% water content, the flowability of CWR shows a linearly increasing relationship to both water content and slump value.
- (iii) The presence of very fine grains (less than 0.2mm), amounting to about 1.25 weight percentage, appeared to be remarkably beneficial under all flow conditions of the study. They were observed to form a very thin film at the inner wall of the flow-tube. Lerche and Renetzeder (1984) have shown similar finding to that described above. Because of their practical significance, this would bear further confirmation for other flow and pumping conditions of interest.

The results indicate that geometry has a significant effect on both the mechanical properties and load deformation characteristics of CCWR material models. The measured strength of the model increases with the increase in its diameter. It is indicative that the model with a higher width to height ratio exhibits a corresponding greater end constraint effect. Due to the end constraint phenomenon, confining pressures were created around the core of CCWR material models and this increased the strength of the models. Of course, a more detailed study on this aspect is a vast subject on its own, therefore, more investigations on the end constraint effect on insitu CCWR pack and triaxial strength properties of CCWR materials are essential.

It is envisaged that the results obtained can serve as a realistic basis for numerical analysis of underground pack under variable geological and stress conditions. The experimental data of the material models generated from this study may also be used as a guide in the pack design in underground coal mining operations.

The finite element method may be successfully employed to investigate the feasibility of using the yield pillar technique under different virgin stress field conditions. It is demonstrated that when k , the ratio of the horizontal virgin stress and the vertical virgin stress, is greater than 1.6, the yield pillar technique can be successfully used, and a greater pillar stability is achievable. On the other hand, if the ratio k is not greater than 1.6, a decrease in the pillar width will give a lower safety factor of the pillar.

It is suggested that there exists an optimal pillar width for a particular ratio of k . The pillar design using the optimal pillar width will exhibit the highest safety factor of the pillar.

RECOMMENDATIONS FOR FURTHER RESEARCH:

- (i) Permeabilities are among the most important characteristics of materials as, for example, ventilation applications. Furthermore, permeabilities are, to some degree, a function of water/cement ratio and strength. The measurements of permeabilities are therefore suggested.
- (ii) Quantitative rheological measurements for pumpability is recommended.
- (iii) More tests are required before meaningful flow properties of CWR can be quantified. A detailed evaluation of the conveying characteristics of CWR in an adequately sized test rig, such as the one at the University of Wollongong, is suggested.
- (iv) Field data from insitu stress measurements are much needed for the calibration and refinement of the finite element model. An experimental research to verify the numerical results is also recommended.
- (v) Development of nomographs, from which the optimal width of the yield pillar can be determined for a particular ratio k .

BIBLIOGRAPHY

BIBLIOGRAPHY

Anon., (1989), The Longwall 12 at West Cliff Set to Go, The KCC Conveyor, Kembla Coal and Coke Pty. Ltd., Wollongong, N.S.W., Australia, Vol. 4, No. 1, Jan.-Feb., pp. 1-2.

Arnold, P.C. and Reed, A.R., (1986), On the Machine Dependence of Flow Property Measurements on Bulk Solids, 2nd International Conference on Bulk Materials Storage Handling and Transportation, Wollongong, N.S.W., Australia, 7th-9th July, pp. 98-101.

AS 1013, Part 3-1976, Method for the Determination of Properties Related to the Consistence of Concrete, Standards Association of Australia, SAA Publication.

AS 1289 C 6.1-1977, Standard Method of Sieving Analysis, Standards Association of Australia, SAA Publication.

AS 1012.13/Amdt 1/1986-12-05, Method for the Determination of Drying Shrinkage of Concrete, Standards Association of Australia, SAA Publication.

ASTM C 230-80, Standard Specification for Flow Table for Use in Tests of Hydraulic Cement, Annual Book of ASTM Standard, Cement, Lime, Gypsum, Section 4, Vol. 04.01, 1983, 6 Pages.

Atkins, A.S., Atkin, J.C., Singh, R.N. and Zadeh, A.M.H., (1986), An Alternative Method of Surface Disposal and Stabilization of Coal Mine Tailings, Geotechnology and Geohydrological Aspects of Waste Management, Fort Collins, pp. 277-286.

Atkins, A.S., Aziz, N.I., Singh, R.N. and Bridgewood, E.W., (1986), Integrated Methods of Colliery Waste Disposal for Ground Control and Safety, The AusIMM Illawarra Branch, Ground Movement and Control Related to Coal Mining Symposium, Wollongong, Australia, August, pp. 263-268.

Atkins, A.S., Hughes, D., Parkin, D. and Singh, R.N., (1984), Utilization of Colliery Tailings in Mining Activities, Paper 18, 1st Symposium on the Reclamation, Treatment and Utilization of Coal Mining Wastes, Durham, England, September, pp. 18.1-18.11.

Atkins, A.S., Singh, R.N., Barkhordarian, R.N. and Zadeh, A.H., (1987), Pumpability of Coal Mine Tailings for Underground Disposal and for Regional Support, Second International Symposium on the Reclamation, Treatment and Utilization of Coal Mining Wastes, Edited by Rainbow, A.K.B., Elsevier, 7th-11th. September, Nottingham University, pp. 401-414.

Australian Standards for Civil Engineering Students, (1982), Published by the Standards Association of Australia, North Sydney.

Aziz, N.I., (1983), The Performance of Powered Support System at Longwall Coal Seam LW2, West Cliff Colliery, Report MI 83/2, Department of Civil and Mining Engineering, The University of Wollongong, N.S.W., Australia, 76 Pages (Unpublished Report).

Babcock, C.O., (1987), Compressive Strength, Burst Proneness, and Failure Modes of Model Coal Pillars Related to the End Constraint and Geometry, 28th US Symposium on Rock Mechanics, Tucson, USA, 29th June-1st July, pp. 173-180.

- Barracrough, W., (1984), Strata Control in Longwall Mining with Particular Reference to the Performance of Powered Supports at Longwall LW5, Corrimal Colliery, Undergraduate Thesis, Department of Civil and Mining Engineering, The University of Wollongong, N.S.W., Australia.
- Batten, M.B., (1985), The Application of Monolithic Pump Packs to Colliery Support, Undergraduate Thesis, Department of Civil and Mining Engineering, The University of Wollongong, N.S.W., Australia.
- Beckett, L.A. and Madrid, R.S., (1986), Practical Application of MULSIM/BM for Improved Mine Design, 3rd Conf. on the Use of Computers in the Coal Industry, West Virginia University, Morgantown, West Virginia, U.S.A., 28th-30th July, pp. 209-219.
- Beckwith, T.G., Buck, N.L. and Marangoni, R.D, (1982), Mechanical Measurements, 3rd edn., Addison-Wesley.
- Bentley, J.P., (1983), Principles of Measurement Systems, Longman.
- Berry, E.E. and Malhotra V.M., (1980), Fly Ash for Use in Concrete, A Critical Review, ACI Journal, March-April, pp. 59-72.
- Bexon, R., (1986), Monolithic Packing, Mining Engineer, Vol. 296, No. 296, May, pp. 512-519.
- Biron, C. and Arioglu, E., (1983), Design of Supports in Mines, John Wiley and Sons, pp. 171-232.

- Blight, G.E. and Clarke, I.E., (1983), Design and Properties of Stiff Fill for Lateral Support of Pillars, Proceedings of the International Symposium on Mining with Backfill, Lulea, 7th-9th, June, pp. 303-308.
- Blunk, G., (1979), Utilisation of Blast Furnace Slag and Steelmaking Slag in the Federal Republic of Germany, The AusIMM., Illawarra Branch, Utilisation of Steelplant Slags Symposium, February, pp. 35-39.
- Bollinger, J.G. and Duffie, N.A., (1988), Computer Control of Machines and Processes, Addison-Wesley.
- Bowles, J.E., (1978), Engineering Properties of Soils and Their Measurement, 2nd Edition, McGraw-Hill International Book Company, pp. 35-46.
- Broadhead, W.S., (1988), Practical and Economic Feasibility of Transporting Coal Washery Refuse into Underground Coal Mines, Undergraduate Thesis, Department of Mechanical Engineering, The University of Wollongong, N.S.W., Australia, November, 129 Pages.
- Bros, B., (1987), Geotechnical Aspects of Fine Coal Waste Disposal in Lower Silesia, Poland, Second International Symposium on the Reclamation, Treatment and Utilization of Coal Mining Wastes, Edited by Rainbow, A.K.B., Elsevier, 7th-11th September, Nottingham University, pp. 381-392.
- Brown, P.T. and Booker, J.R., (1984), Simulating Excavation by Finite Element Methods, The ninth Aust. Conf. on the Mech. of Structures and Materials, The University of Sydney, 29th-31th August, pp. 44-47.

- Brown, E.T., (1981), Rock Characterization Testing and Monitoring, ISRM Suggested Methods, Pergamon Press, pp. 81-116.
- Box, G.E.P., (1954), The Exploration and Exploitation of Response Surfaces: Some General Considerations and Examples, *Biometrics*, Vol. 10, pp. 16-60.
- Box, G.E.P. and Hunter, J.S., (1957), Multi-factors Designs for Exploring Response Surfaces, *Annals of Mathematical Statistics*, Vol. 28, pp.195-241.
- Box, G.E.P. and Wilson, K.B., (1951), On the Experimental Attainment of Optimum Conditions, *J. of Royal Statistical Society*, B13, pp. 1-45.
- Box, G.E.P. and Youle, P.V., (1955), The Exploration and Exploitation of Response Surfaces: An Example of the Link Between the Fitted Surface and the Basic Mechanism of the System, *Biometrics*, Vol. 11, pp. 287-323.
- Buddery, P.S., (1984), Grout Pack Strength Characteristics in Longwall Gate Roadways, *Mining Science and Technology*, Vol. 1, pp. 165-172.
- Buddery, P.S. and Ashika, S.T., (1982), Evaluation of Monolithic Packing Systems with Special Reference to the Aquapak Trials at Ellistown Colliery, Research Report, Department of Mining Engineering, The University of Nottingham, UK, January (Unpublished Report).
- Buddery, P.S., Hassani, F.P. and Singh, R.N., (1984), A Study of Aquapak Behaviour with Reference to Strata Control Requirements, *The Coal Journal*. November, pp. 55-56.

- Buschmann, N., (1987), Testing of Packing Materials Made of Waste Products, Gluckauf, Translation Vol. 123 No. 20, 22nd October, pp.557-561.
- Cain, P. and Stokes, A.W., (1987), Monolithic Packing in the Undersea Coalfield of Cape Breton, Nova Scotia, Mining Engineer, No. 313, Vol. 147, October, pp. 168-174.
- Callis, A.V. and Newson, S.R., (1987), Progress into Roadway Reinforcement Techniques in the UK, Mining Engineer, No. 314, Vol. 147, pp. 233-242.
- Cambourn, G.R., (1984), Comparison of Support Performance on Two Longwalls at South Bulli Colliery, Undergraduate Thesis, Department of Civil and Mining Engineering, The University of Wollongong, N.S.W., Australia.
- Chen, E.S. and Buyukozturk, O., (1985), Constitutive Model for Concrete in Cyclic Compression, Engrg. Mech., ASCE, 111(6), pp. 797-814.
- Chlumechy, N. and Smith, R., (1986), Donut Cribbing a New Heavy-Duty Roof Support Concept, Proceedings Fifth Conference on Ground Control in Mining, 11th-13th., June, pp. 29-43.
- Choi, D.S., (1989), Theoretical Analysis of Breaking Strength of Mine Pillars and Test Specimens, 30th US Symposium on Rock Mechanics, Morgantown, WV, USA, pp. 953-962.
- Claringbold, P.J., (1955), Use of the Simplex Design in the Studies of Joint Action of Related Hormones, Biometrics, Vol. 11, pp. 174-185.

- Clark, C.A. and Newson, S.R., (1985), A Review of Monolithic Pumped Packing Systems, *Mining Engineer*, Vol. 144, No. 282, March, pp. 491-495.
- Collepari, M., (1988), International Workshop on the Use of Fly Ash, Slag, Silica Fume and Other Siliceous Materials in Concrete, July, 4th-6th, The Regent Hotel Sydney, Australia.
- Collier, L., (1984), Further Developments of Monolithic Packing in the Warwickshire Coalfield, *Mining Engineer*, Vol. 143, No. 271, April, pp. 475-483.
- Cornell, J.A., (1981), *Experiments with Mixtures: Designs, Models and Analysis of Mixture Data*, New York, John Wiley and Sons.
- Deutschman, A.D., Michels, W.J. and Wilson, C.E., (1975), *Machine Design Theory and Practice*, Macmillan Publishing Co., Inc., pp. 409-417.
- Didcoct, D.A., (1982), Research, Development, and Use of Steel-Fibre-Reinforced Concrete Cribbing for Mine Roof Support, *Proceedings Second Conference on Ground Control in Mining*, 19th-21st July, pp. 202-208.
- Drucker, D.C. and Prager, W., (1952). "Soil Mechanics and Plastic Analysis or Limit Design", *Quarterly of Appl. Math.*, Vol. 10, No. 2, pp. 157-165.
- Materials Testing Division, *ELE International Catalogue*, A Mowlem Technology Company.

- Evans, D.W. and Colaizzi, G.J., (1982), Control of Mine Subsidence Utilizing Coal Ash as a Backfill Material, Proceedings Second Conference on Ground Control in Mining, 19th-21st July, pp. 222-228.
- Faddick, R.R., (1978), Flow Properties of Energy Slurries, Proc. of the 3rd. Int. Tech. Conf. on Slurry Transportation, 29th-31st March, Las Vegas, Nevada, pp. 93-97.
- Farmer, I.W. and Robertson, J.T., (1975), The Effect of Pack Construction on Roadway Stability behind Working Faces, The Mining Engineer, Vol. 134, Nos. 166-167, August/September, pp. 599-606.
- Foseco: Technik Catalogues on Tekpak and Tekpak XX.
- Franklin, J.A. and Dusseault, M.B., (1989), Rock Engineering, McGraw-Hill, pp. 539-562.
- Freeman, P.N., (1982), The Design and Installation of 52's Face at Newdigate Colliery, Mining Engineer, Vol.141, No. 247, April, pp. 609-613.
- Garland, B., (1984), Strata Control in Longwall Mining with Particular Reference to the Work Face Appin Colliery, Undergraduate Thesis, Department of Civil and Mining Engineering, The University of Wollongong, N.S.W., Australia, pp. 1-17.
- Glynn, E.E., (1987), Elastic Moduli of Rock: A Comparison of In-Situ Vs. Laboratory Values, 28th US Symposium on Rock Mechanics, Tucson, USA, 29th June-1st July, pp. 223-230.

Harlech, (1925), Hydraulic Stowing of Mines, The Science and Art of Mining, Vol 36, pp. 104, 118, 134, 148, 359.

- Gomez, B., (1989), Advanced Instrumentation Monitors Smelter Emissions, Engineers Australia, Vol. 61, No. 8, 5th May, pp. 35.
- Gomez, B., (1989), BHP Exports Instruments Developed for CIM, Engineers Australia, Vol. 61, No. 8, 5th May, pp. 34-35.
- Grosvenor, P.J., (1986), Experimental Investigations into the Material Properties of Monolithic Pump Packing Systems with Special Reference to Cemented Coal Washery Refuse, Undergraduate Thesis, Department of Civil and Mining Engineering, The University of Wollongong, N.S.W., Australia.
- Hambley, D.F., (1989), Pillar Design for Mines in Saltrock - 1, Mining Science and Technology, 9, pp. 111-123.
- Hebblewhite, B.K., (1982), The Use of Modelling Techniques for Mine Design, The Aust. J. of Coal Mining Tech. and Research, No. 1, pp. 1-19.
- Hebblewhite, B., (1983), Alternative Longwall Panel Layouts for Use in Australian Coal Mines, Paper 3, Proceedings of Longwall Mining Design, Development and Extraction Seminar, Sydney, NSW, Australia.
- Hebblewhite, B., (1988), Evaluation of Cementitious Support for Increased Recovery of Coal Reserves, Commonwealth of Australia National Energy Research, Development and Demonstration Program, End of Grant Report Number 858, Australian Coal Industry Research Laboratories, October, 267 Pages.
- Heidarieh Zadeh, A.M., Barkhordarian A., Singh, R.N., Atkins, A.S. and Hughes, D., (1986), Studies of Cost Effective and Environmentally Acceptable

- Methods of Coal Mine Tailings Disposal, 3rd Interim Report (SERC Research Contract No. GR/D-06902), Department of Mining Engineering, University of Nottingham in Collaboration with the Department of Mining Engineering, North Staffordshire Polytechnic, Stoke-on-Trent, September, 20 Pages.
- Highton, W. and Cooper, J.M., (1984), Development of Monolithic Packing Systems within Western Area, Mining Engineer, Vol. 143, No. 273, June, pp. 623-628.
- Hoek, E. and Wood, D.F., (1988), Rock Support, Mining Magazine, October, pp. 282-287.
- Hii, J.K. and Aziz, N.I., (1986a), The State of the Art of Pump Packing in Coal Mining, Research Report No.1, Department of Civil and Mining Engineering, The University of Wollongong, N.S.W., Australia, May, 76 Pages.
- Hii, J.K. and Aziz, N.I., (1986b), An Evaluation of the Mechanical Properties of Cemented West Cliff Washery Refuse, Research Report No.2, Department of Civil and Mining Engineering, The University of Wollongong, N.S.W., Australia, September, 30 Pages.
- Hii, J.K. and Aziz, N.I., (1987a), Mechanical Evaluation of Cement and Coal Washery Refuse Material, Research Report No.3, Vol.1, Department of Civil and Mining Engineering, The University of Wollongong, N.S.W., Australia, January, 262 Pages.
- Hii, J.K. and Aziz, N.I., (1987b), Mechanical Evaluation of Cement and Coal Washery Refuse Material, Research Report No.3, Vol.2, Department of Civil

and Mining Engineering, The University of Wollongong, N.S.W., Australia, January, 263 Pages.

Hii, J.K. and Aziz, N.I., (1987c), Influence of Water Content on the Flow Properties of Mine Tailings, Research Report No.4, Department of Civil and Mining Engineering, The University of Wollongong, N.S.W., Australia, July, 28 Pages.

Hii, J.K. and Aziz, N.I., (1987d), Influence of Water Content on the Mechanical Properties of Cement and Coal Washery Refuse Material, Research Report No.5, Department of Civil and Mining Engineering, The University of Wollongong, N.S.W., Australia, December, 16 Pages.

Hii, J.K. and Aziz, N.I., (1989a), Microcomputer Automation of the Strength Testing System for Use in a Rock Mechanics Laboratory, Australasian Instrumentation and Measurement Conference, The Institution of Engineers Australia, Adelaide, South Australia, 14th-16th November, pp. 51-55.

Hii, J.K. and Aziz, N.I., (1989b), Influence of Water Content on the Mechanical Properties of CCWR Concrete, First Conference on Concrete and Structures, Kuala Lumpur, Malaysia, 3rd and 4th October, pp. 47-50.

Hii, J.K. and Aziz, N.I., (1990), Properties and Behaviour of Cement and Coal Washery Refuse Concrete, Concrete for the Nineties, International Conference on the Use of Fly Ash, Slag, Silica Fume and Other Siliceous Materials in Concrete, Leura (Blue Mountains), New South Wales, Australia, 3rd-5th September, 15 Pages.

- Hii, J.K. and Standish, P., (1989), Data Acquisition Systems for Rock Mechanics Applications, Computer Systems in the Australian Mining Industry, The University of Wollongong, N.S.W., Australia, September, pp.133-139.
- Hii, J.K., and Wu, Y.H., (1989), Effect of Virgin Stress Fields on the Feasibility of Using Yield Pillar Technique, Computer Systems in the Australian Mining Industry, The University of Wollongong, N.S.W., Australia, September, pp. 107-111.
- Hii, J.K. and Yu, A.B., (1989), The Design of CCWR Concrete, First Conference on Concrete and Structures, Kuala Lumpur, Malaysia, 3rd-4th October, pp.51-56.
- Hii, J.K., Aziz, N.I., Zhang S. and Wu, Y.H., (1990a), Influence of Geometry on Strength and Elasticity of Cement and Coal Washery Refuse Material Models, 3rd International Symposium on the Reclamation, Treatment and Utilization of Coal Mining Wastes, The Kelvin Conference Centre, Wolfson Hall, The University of Glasgow, UK, 3rd-7th September, 7 Pages.
- Hii, J.K., Aziz, N.I., Zhang, S. and Wu, Y.H., (1990b), Development and Utilization of Coal Washery Refuse for Strata Reinforcement in Underground Coal Mining Operations, 3rd International Symposium on the Reclamation, Treatment and Utilization of Coal Mining Wastes, The Kelvin Conference Centre, Wolfson Hall, The University of Glasgow, UK, 3rd-7th September, 9 Pages.
- Hii, J.K., Zhang, S. and Wu, Y.H., (1990), Evaluation of the Triaxial Strength of Cement and Coal Washery Refuse Concrete, The Twelfth Australasian Conference on the Mechanics of Structures and Materials, 24th-26th September,

Heinrich, F., (1971), Technical Experience with Gateroad Side Pack from Anhydrite and Blitzdammer, Gluckauf, Vol 107 No.2, pp. 51-63.

Hoek, E., (1982), Analysis of Slope Stability in Very Heavily Jointed or Weathered Rock Masses, 3rd International Conference on Stability in Surface Mining, Vol 3, Edited by Brawner, C.O., Published by the Society of Mining Engineers of the American Institute of Mining, Metallurgical, and Petroleum Engineers, Inc., New York, pp. 375-406.

- Organised by School of Civil Engineering, Queensland University of Technology, Australia, in Press.
- Hodgkinson, D.R., (1977), Pump Packing Systems at Florence Colliery, *Mining Engineer*, Vol. 136, No. 195, August, pp. 707-716.
- Operating and Service Manual, Vol. 3, Hewlett Packard Company, U.S.A., 1979.
- Huang, Z.B., Zhang, Y.G. and Hii, J.K., (1989), On the Matrices Wear and Self-sharpening of Impregnated Diamond Drill Bits, Second Large Open Pit Mining Conference, The AusIMM Latrobe Valley Branch, Melbourne, Victoria, Australia, April, pp.25-29.
- Hughson, R., Tuminski, A. and Holla, L., (1987), A Review of Stowing and Packing Practices in Coal Mining, *The AusIMM Bulletin and Proceedings*, Australia, Vol. 292, No. 9, pp. 79-86.
- Hunke, H., (1983), Cost Effectiveness of Centralised and Decentralised Pack Material Supply Systems, *Gluckauf*, Translation Vol. 9, No. 119, 12th May, pp. 167-171.
- Hurlbut, B.J., (1985), Experimental and Computational Investigation of Strain-Softening in Concrete, Thesis Presented to the University of Colorado, Boulder, Colorado, in Partial Fulfilment of the Requirement for the Degree of Master of Science, USA.
- Iannacchione, A.T., (1989), Numerical Simulation of Coal Pillar Loading with the Aid of a Strain-softening Finite Difference Model, 30th US Symposium on Rock Mechanics, Morgantown, WV, USA, pp. 775-782.

Instron Instruments and Systems for Advanced Materials Testing, Handbook for Model 8033 Materials Testing Machine.

Isaac, A.K. and Payne, A.R., (1986), Influence of Pack Design Upon Gateroad Deformation in Soft Floor Conditions, The AusIMM Illawarra Branch, Ground Movement and Control Related to Coal Mining Symposium, Wollongong, Australia, August, pp. 253-262.

Isaac, A.K., Smart, B.D.G. and Roberts, D., (1982), The Reuse of Gateroads Serving Retreat Faces at Betws Colliery, Mining Engineer, Vol. 141, No. 249, June, pp. 727-737.

Jackson, J.B., (1980), Reducing Run of Mine Dirt, Colliery Guardian, Vol. 228, No. 9, September, pp. 435-441.

James, A.M., (1986), New Materials Technology Applied to Longwall Mining, The AusIMM Illawarra Branch, Ground Movement and Control Related to Coal Mining Symposium, Wollongong, Australia, August, pp. 240-246.

Jones, C., (1989), Aust Smoke Detectors for British Rail, Engineers Australia, Vol. 61, No. 8, 5th May, pp. 37.

Jones, C, (1989), Mass Spectrometer Invented at UNSW, Engineers Australia, Vol. 61, No. 8, 5th May, pp. 38.

Kellet, W.H. and Mills, P.S., (1980), Advancements in Monolithic Packing Materials Developed by MRDE, Colliery Guardian, Vol. 228, No. 9, September, pp. 240-241.

- Keren, L. and Kainian, S., (1983), Influence of Tailings Particles on Physical and Mechanical Properties of Fill, Proceedings of the International Symposium on Mining with Backfill, Lulea, 7th-9th June, pp. 21-30.
- Kimura, T., (1987), Experimental and Theoretical Studies on Strain Softening Behaviour of Rocks, 28th US Symposium on Rock Mechanics, Tucson, USA, 29th June-1st July, pp. 197-202.
- Klek, S.R., (1982), An Investigation into Pneumatic Handling of Cement for Littleton Colliery, Mining Engineer, Vol. 142, No. 254, pp. 259-263.
- Knissel, W. and Helms, W., (1983), Strength of Cemented Rockfill from Washery Refuse, Results from Laboratory Investigations, Proceedings of the International Symposium on Mining with Backfill, Lulea, 7th-9th, June, pp. 31-38.
- Kripakov, N.P., (1987). Numerical Modeling in Mine Structure Design, Underground Mining Methods and Tech., Edited by Szwilski, A.B. and Richards, M.J., Elsevier Sci. Publishers B.V., Amsterdam, pp. 441-455.
- Kuo, B.C., (1987), Automatic Control Systems, 5th edn., Prentice Hall.
- Lama, R.D., (1988), Developments in Underground Coal Mining Technology and Their Implications, The AusIMM Illawarra Branch, 21st Century Higher Production Coal Mining Systems, Their Implications, Wollongong, N.S.W., Australia, April, pp. 7-17.

- Lama, R.D. and Vutukuri, V.S., (1978), Handbook on Mechanical Properties of Rocks, Vols. 2-4 Series of Rock and Soil Mechanics, Trans Tech Publications, Germany.
- Lee, G.E., (1985), The Washability Analysis of ROM Coal from West Cliff Washplant Reject for December, Report No. 04/5693, ACIRL, N.S.W., Australia, 6 Pages (Unpublished Report).
- Lehmann, B.G. and Krahe, J., (1987), Light-Weight Supports with material Backfilling to Consolidate a Lateral Road, Gluckauf, Translation Vol. 123, No. 21, 5th November, pp 578-580.
- Leininger, D., Leonhard, J. Erdmann, W. and Schieder, T, (1987), Research on Suitability of Coal Preparation Refuse in Civil Engineering in Federal Republic of Germany, Second International Symposium on the Reclamation, Treatment and Utilization of Coal Mining Wastes, Edited by Rainbow, A.K.B., Elsevier, 7th-11th September, Nottingham University, pp. 55-68.
- Lerche, R. and Renetzeder, H., (1984), The Development of "Pumped Fill" at Grund Mine, A successful New Approach to Back-filling Using High-density Hydraulic Conveying, Preussag AG Metall, Federal Republic of Germany, Presented at the 9th. Int. Conf. on the Hydraulic Transport of Solids in Pipes, Rome, Italy, 17th-19th October, 24 Pages.
- Lewis, S. and Stace, L.R., (1981), A Rationale of Roadside Packing, Mining Engineer, No. 235, Vol. 140, April, pp. 717-721.

- Loo, Y.C. and Ahmad, S.F., (1982), A Comparative Study of Four Popular Concrete Mix Design Methods, AIT, Bangkok, Thailand, Research Report No. 151, 23 pages.
- Loo, Y.C., Nimityongskul, P. and Karasudhi, P., (1984), Economical Rice Husk Ash Concrete, Building Research and Practice, the CIB Journal, July/August, Vol. 12, No. 4, pp. 233-238.
- Loo, Y.C. and Weragama, W.K.B., (1985), Mix Design of Rice Husk Ash Concrete, Journal of CIB, the Internal Council for Building Research Studies and Documentation, Kent, UK, Vol. 13, No.6, Nov./Dec., pp. 361-367.
- Lydon, F.D., (1972), Concrete Mix Design, Applied Science Publishers Ltd. London, 139 Pages.
- Mark, C., Listak, J. and Bieniawski, Z.T., (1988), Yielding Coal Pillars - Field Measurements and Analysis of Design Methods, Key Questions in Rock Mechanics: Proceedings of the 29th U.S. Symposium, Edited by Cundall, P.A., Sterling, R.L. and Starfield, A.M., University of Minnesota, Minneapolis, USA, 13th-15th June, pp. 261-270.
- Marshall, P. and Lama, R.D., (1986), Changes in Underground Coal Mining Technology - An Australian Outlook, 13th Congress of the Council of Mining and Metallurgical Institutions, Singapore, 11th-16th May, pp. 91-101.
- McCarthy, K., (1974), Experiences in Roadside Packing with the Low Pressure Jet Stower at Daw Mill Mine, The Mining Engineer, November, pp. 59-65.

- McCarthy, K. and Robinson, A., (1981), Pump Packing Experiences at Newdigate and Daw Mill Collieries, *Mining Engineer*, Vol. 140, No. 236, May, pp. 831-836.
- Mehta, P.K., (1989), Pozzolanic and Cementitious By-Products in Concrete - Another Look, Third CANMET/ACI Int. Conf., Fly Ash, Silica Fume, Slag and Natural Pozzolans in Concrete, Editor V.M. Malhotra, Vol. 1, June, pp. 1-43.
- Mehta, P.K. and Pirtz, D., (1978), Use of Rice Hull Ash to Reduce Temperature in High-strength Mass Concrete, *ACI Journal*, Vol. 75, No.2, pp. 60-63.
- Mifflin, A.D., (1986), Pump Packing Developments of Rowhurst 304s Face at Hem Heath Colliery, *Mining Engineer*, Vol. 145, No.292, January, pp. 307-310.
- Monier Construction Products Catalogues, Monier Resources, Australia.
- Montgomery, D.G. and Wang, G.C., (1989), Instant Chilled Steel (I.C.S.) Slag as an Aggregate in Concrete, Third CANMET/ACI Int. Conf., Fly Ash, Silica Fume, Slag and Natural Pozzolans in Concrete, Supplementary Paper, Editor V.M. Malhotra, June, 3 Pages.
- Morgan, D.R. and Bruere, G.M., (1975), Workshop on The Use of Chemical Admixtures in Concrete, The University of New South Wales, Sydney, Australia, 1st-2nd December, pp. 29-184.

- Munn, R.L., (1979), Blast Furnace Slag as an Aggregate in Concrete, The AusIMM., Illawarra Branch, Utilisation of Steelplant Slags Symposium, N.S.W., Australia, February, pp. 41-50.
- Nadai, A., (1963), Theory of Flow and Fracture of Solids, Monographs Engineering Societies, Vol. 2, McGraw-Hill Book Company, Inc., pp. 357-377.
- Nandy, S.K. and Szwilski, A.B., (1987), Disposal and Utilization of Mineral Wastes as a Mine Backfill, Underground Mining Methods and Technology, edited by Szwilski, A.B. and Richards, M.J. Elsevier Science Publishers, B.V., Amsterdam, Netherlands, pp. 401-414.
- Neville, A.M., (1981), Properties of Concrete, 3rd Edition, Pitman.
- Newman, D.A., (1988), Yield Pillar Behaviour in Deep Mines, Proceedings 6th Annual Workshop Generic Mineral Technology Center Mine Systems Design and Ground Control, Fairbanks, Alaska, 31st July-2nd August, Edited by Topuz, E. and Richard Lucas, J., pp. 21-29.
- Newson, S.R., (1983), Strata Control - Present Problems, Future Plans, Mining Engineer, Vol. 143, No. 266, November, pp. 229-235.
- Nixon, D.W. and Mills, P.S., (1981), Pump Packing Developments a Hem Heath Colliery, Mining Engineer, Vol. 140, March, pp. 645-651.
- Nguyen, V.U., Aziz, N.I., Hii, J.K. and Fabjanczyk, M.W., (1986), An Experimental Investigation on Cable Reinforcement, The AusIMM Illawarra Branch, Ground Movement and Control Related to Coal Mining Symposium, Wollongong, Australia, August, pp. 93-101.

- NSW Government, (1983), Coal Reject Disposal in the Southern Coalfields, Coal Reject Disposal Sub-Committee, Report to the Coal Resource Development Committee (NSW Department of Mineral Resources: Sydney), May, pp. 1-47.
- Ostermann, W., Jacobi, H., Sander, K.H. and Diederich, T., (1988), Re-introduction of Pneumatic Stowing at the Friedrich Heinrich Colliery, Gluckauf, Journal for Technology and Economics in the Mining Industry, Vol. 124, No.21, 3rd. November, pp. 476-481.
- Peng, S.S., (1986), Coal Mine Ground Control, 2nd. Edition, John Wiley and Sons.
- Peng, S.S. and Chiang, H.S., (1984), Longwall Mining, John Wiley and Sons.
- Plate, M., (1988), Waste Disposal Underground - An Opportunity for Solving Environmental Problems, Gluckauf, Translation Vol. 124, No. 4/5, 3rd March, pp. 122-126.
- Porter, I. and Aziz, N.I., (1985), The Relationship Between Rock Competency and Convergence on Longwall Facelines (Private Communication).
- Pouska, G.A. and Link, J.M., (1981), Differential Flow Rheometer, Proc. of the 6th Int. Tech. Conf. on Slurry Transportation, 26th-28th March, Sahara Tahoe, Lake Tahoe, Nevada, pp. 120-126.
- Pramono, E. and Willam, K., (1989), Fracture Energy-Based Plasticity Formulation of Plain Concrete, Engrg. Mech., ASCE, 115(6), pp. 1183-1204.

Recklinghausen, W.K., Marl, D.S. and Walsum, K.I., (1972), Suppressing
Convergence through the Gateroad Side Pack from Anhydrite, Gluckauf, Vol
108 No.21, pp. 980-982.

- Pundit Manual for Use with the Portable Ultrasonic Non-Destructive Digital Indicating Tester, C.N.S. Instruments Ltd., London, 35 Pages.
- Ramachandra, V.S., (1976), Calcium Chloride in Concrete Science and Technology, Applied Science Publishers Ltd., London.
- Ramachandra, V.S., (1984), Concrete Admixtures Handbook, Properties, Science and Technology, Noyes Publications.
- Rao, Y.V.A. and Vutukuri, V.S., (1983), Some Aspects of Recovery of Pillars Adjacent to Uncemented Sandfilled Stopes, Proceedings of the International Symposium on Mining with Backfill, Lulea, 7th-9th June, 1983, pp. 397-403.
- Raring, L.M., (1980), The Hydraulic Disposal of Colliery Waste Material, Proc. of the 5th. Int. Conf. on Slurry and Transportation, 26th-28th March, Sahara Tahoe, Nevada, pp. 120-126.
- Richmond, A.J., (1981), Investigation into Monolithic Pump Packing as a Means of Underground Roof Support, Part A: Laboratory Studies to Determine Pack Properties, P.R. 81-8, ACIRL, August, 34 Pages.
- Richmond, A.J., Skybey, G., Ross, A., Wypych, P. and Lama, R.D., (1985), Evaluation of Cementitious Support for Increased Recovery of Coal Mines, Progress Report, NERDDP Project Contract No. 84/4149.
- Roberts, A., (1977), Geotechnology, An Introduction Text for Students and Engineers, Pergamon Press.

- Rockey, K.C., Evans, H.R., Griffiths, D.W. and Nethercot, D.A., (1983), The Finite Element Method, A Basic Introduction for Engineers, 2nd Edition, Granada.
- Rose, B.W., (1988), Planning and Preparing a Pneumatically Stowed Face in the Northern Take of Haus Aden Colliery, Gluckauf, Translation Vol. 124, No. 8, 21st April, pp.240-245.
- Ruban, V.A. and Shpirt, M.Y., (1987), Utilization of Mining Operations and Coal Preparation Processes Wastes in the USSR and the principles of Their Classification, Second International Symposium on the Reclamation, Treatment and Utilization of Coal Mining Wastes, Edited by Rainbow, A.K.B., Elsevier, 7th-11th September, Nottingham University, pp. 45-54.
- Ruston, R., (1986). Yield Pillar - Overseas Experience and Plans for Experimentation at West Cliff Mine, Supplementary Paper, Ground Movement and Control Related to Coal Mining Symposium, Illawarra Branch - The AusIMM, The University of Wollongong, N.S.W., Australia, 26th-29th August, 6 Pages.
- Ruston, R., Lama, R.D. and Cutifani, M., (1988), Roof Control Technology under Abnormal Conditions, The AusIMM Illawarra Branch, 21st Century Higher Production Coal Mining Systems, Their Implications, Wollongong, N.S.W., Australia, April, pp. 145-157.
- Schaller, S. and Savidis, G., (1983), Investigation into Innovative Means of Secondary Gate Road Support, Paper 11, Proceedings of Longwall Mining Design, Development and Extraction Seminar, Sydney, NSW, Australia.

Senyur, G., (1989), Flow Characteristics Through Hydraulic Filling Materials Produced from Coal Washery Rejects, 4th International Symposium on Mining with Backfill, Innovations in Backfill Technology, Edited by Hassani, F.P., Scoble, M.J. and Yu, T.R., Montreal, Quebec, 2nd-5th October, pp. 307-314.

Scheffé, H., (1958), Experiments with Mixtures, J. of Royal Statistical Society, Series B 20, pp. 344-360.

Schmidt, L.C. and Wu, Y.H., (1989), Numerical Evaluation of Dynamic Pressures Exerted by Broken-ore in Underground Storage Structures, Submitted to Computer Systems in the Aust. Mining Industry, The University of Wollongong, N.S.W., Australia, September, pp. 112-116.

Schmidt, L.C., Wu, Y.H. and Lu, J.P., (1989), Effect of Tectonic Stresses on the Stability of Slope, Second Large Open Pit Mining Conf., Latrobe Valley Branch-The AusIMM, Australia, April, pp. 217-220.

Schroer, D., (1987), Use of Packing Materials from Waste Products, Gluckauf, Translation Vol. 123, No.22, 19th November, pp. 621-625.

Serata, S., (1982), Stress Control Methods: Quantitative Approach to Stabilizing Mine Openings in Weak Ground, First International Conference on Stability in Underground Mining, Vancouver, British Columbia Canada, Editor Brawner, C.O., SME/AIME, Published by SME of the AIMM, and PE, Inc., New York, 16th-18th August, pp. 52-98.

Serata, S. and Galagoda, H.M., (1987), Integration of Finite Element Analysis and Field Instrumentation for Application of the Stress Control Method in Underground Coal Mining, 28th US Symposium on Rock Mechanics, Tucson, USA, 29th June-1st July, pp. 265-272.

Serata, S., Gardner, B.H. and Shrinivasan, K., (1986), Integrated Instrumentation Method of Stress State, Material Property, and Deformation Measurement for

- Stress Control Method of Mining, Proceedings Fifth Conference on Ground Control in Mining, 11th-13th June, pp. 123-133.
- Serata, S., Gardner, B.H. and Preston, M., (1986), Optimization of the Stress Control Method to Improve Productivity and Safety in Underground Coal Mining, Proceedings Fifth Conference on Ground Control in Mining, 11th-13th June, pp. 156-166.
- Shephard, P., (1986), The Use of Yield Pillars at West Cliff Colliery - A Union View, Supplementary Paper, Ground Movement and Control Related to Coal Mining Symposium, Illawarra Branch - The AusIMM, the University of Wollongong, NSW, Australia, 26th-29th August, 5 Pages.
- Singh, R.N., Atkins, A.S. and El-Mherig, A.M., (1985), An Approach to Solve Some of the Problems of Coal Mines Liquid Tailings Disposal in the UK National Symposium on Surface Mining, Hydrology, Sedimentology and Reclamation, Lexington, Kentucky, USA, 10 Pages.
- Sinha, K.M., (1989), Hydraulic Stowing - A Solution for Subsidence Due to Underground Mining in the USA, 30th U.S. Symposium on Rock Mechanics, West Virginia University, Morgantown, West Virginia, U.S.A. 19th-22th June, pp. 827-834.
- Sleeman, W., (1987), The Economics of Minestone Utilization, 3rd International Symposium on the Reclamation, Treatment and Utilization of Coal Mining Wastes, The Kelvin Conference Centre, Wolfson Hall, The University of Glasgow, UK, 3rd-7th September, pp.1-20.

Smart, B.G.D. and Aziz, N.I., (1986), The Influence of Caving in the Hirst and Bulli Seams on Powered Support Rating, The AusIMM Illawarra Branch, Ground Movement and Control Related to Coal Mining Symposium, Edited by Aziz, N.I., Wollongong, N.S.W., Australia, August, pp. 182-193.

- Smart, B.D.G., (1986), Monolithic Partitions for the Wide Drivages - Some Design Considerations, The AusIMM Illawarra Branch, Ground Movement and Control Related to Coal Mining Symposium, Wollongong, Australia, August, 1986, pp. 247-252.
- Smart, B.D.G., Davies, D.O. and Issac, A.K., (1982), Conclusions from Strata Mechanics Investigations Conducted by Cardiff and Strathclyde Universities at Longwall Faces, *Mining Engineer*, Vol. 141, No. 246, March, pp. 539-545.
- Smart, B.D.G., Isaac, A.K. and Roberts, D., (1982), Pack Design Criteria at Betws Colliery, *Mining Engineer*, Vol. 141, No. 230, July, pp. 15-21.
- Smith, I., (1976), Experience with Anhydrite Packing (ANPAC) at Easington Colliery, *Mining Engineer*, Vol. 135, No. 186, October, pp. 47-51.
- Smith, I.A., (1967), The Design of Fly-Ash Concretes, *Proceedings of the Institution of Civil Engineers*, Vol. 36, pp. 769-790.
- Standish, N., (1983), A Study of Size Separation by Screening, MMIJ/AusIMM Joint Symposium, Sendai, pp. 129-144.
- Standish, P., (1989), Report on Performance of Seco-Titan Roof Bits, Uniadvice, the University of Wollongong, Wollongong, Australia, 11/89 (Unpublished Report).
- Statham, C.A., (1980), Roadside-Pack Construction Demonstration, *Colliery Guardian*, Vol. 228, No. 9, September, pp. 553-554.

Taylor, R.K., (1984), Composition and Engineering Properties of British Colliery Discards, British Coal Mining Department, pp. 244.

Thomas, E.G., Lama, R.D. and Wiryanto, K., (1989), Preparation of an Early-Strength Fill Material for Roof Support in Longwall Mining of Coal, 4th International Symposium on Mining with Backfill, Innovations in Backfill Technology, Edited by Hassani, F.P., Scoble, M.J. and Yu, T.R., Montreal, Quebec, 2nd-5th October, pp. 297-306.

- Stockes, H. and Kitching, F., (1980), The Effect of Mechanisation on Strata Control at Face-Ends, Symposium Paper No. 5, Presented at a Symposium on Face-Ends Technology, Harragat, 10th-12th December, pp. 5.1-5.6
- Sydenham, P.H., (1982), Handbook of Measurement Science, Vols. 1 & 2, John Wiley & Sons.
- Szwiski, A.B. and Whittaker, B.N., (1975), Control of Strata Movement around Face-ends, The Mining Engineer, July, pp. 515-524.
- Teale, R., (1965). The Concept of Specific Energy in Rock Drilling, Int. Journal of Rock Mech. Min. Sci., Vol. 2, pp. 57-73.
- Teychenne, D.C., Franklin, R.E. and Erntroy, H.C., (1975), Design of Normal Concrete Mixes, Department of the Environment, Her Majesty's Stationery Office, London, UK, 30 pages.
- Thomas, E.G., (1978), Fill Permeability and its Significance in Mine Fill Practice, Mining with Backfill, 12th Canadian Rock Mechanics Symposium, Sudbury, Ontario, 23th-25th May, pp. 139-145.
- Thomas, E.G., (1986), Report on Laboratory Strength Testing of West Cliff Washplant Reject, School of Mining Engineering, the University of New South Wales, N.S.W., Australia, pp. 1-40.
- Thomas, E.G. and Cowling, R., (1978), Pozzolanic Behaviour of Ground Isa Mine Slag in Cemented Hydraulic Mine Fill at High Slag/Cement Ratios, Mining with Backfill, 12th Canadian Rock Mechanics Symposium, Sudbury, Ontario, 23th-25th May, pp. 129-132.

- Todd, G., (1983), Development and Use of Gate Roads at Appin Colliery, Paper 4, Proceedings of Longwall Mining Design, Development and Extraction Seminar, Sdney, NSW, Australia.
- Tong, G.X. and Wu, Y.H., (1985), Logarithmic Yield Criterion and Its Implementation in Finite Element Analysis, Internal Report, Beijing University of Iron and Steel Technology, pp. 14.
- Tsang, P., Peng, S.S. and Hsiung, S.M., (1989), Yield Pillar Application under Strong Roof and Strong Floor Condition - A Case Study, 30th U.S. Symposium on Rock Mechanics, West Virginia University, Morgantown, West Virginia, U.S.A. 19th-22th June, pp. 411-418.
- Verkerk, C.G., (1986), The Transportation of Flyash and Bottom Ash in Slurry Form, 2nd International Conference on Bulk Materials Storage Handling and Transportation, Wollongong, N.S.W., Australia, 7th-9th July, pp. 34-38.
- Vernard, J.K. and Street, R.L., (1976), Elementary Fluid Mechanics, 5th Edition, John Wiley and Sons, Inc., pp. 521-528.
- Vutukuri, V.S., Lama, R.D. and Saluja, S.S., (1974), Handbook on Mechanical Properties of Rocks, Vol. 1, Series of Rock and Soil Mechanics, Trans Tech Publication, Germany.
- Whittaker, B.N., (1974), An Appraisal of Strata Control Practice, The Mining Engineer, Vol.134, Nos. 166-175, October, pp. 9-58.

- Whittaker, B.N. and Woodrow, G.J.M., (1977), Design Loads for Gateside Packs and Support Systems, *The Mining Engineer*, Vol. 136, No. 189, February, pp. 263-275.
- Wilson, A.H., (1975), Support Load Requirements on Longwall Faces, *Mining Engineer*, Vol. 134, No. 173, June, pp. 479-488.
- Wiryanto, K., (1989), Strength Characteristics of Cemented Coal Reject as Pump Packing Material, M.E. Thesis, the Department of Mining Engineering, School of Mines, The University of New South Wales, Australia, pp. 1-91.
- Wood, J.K., (1986), Expanded Cement: New Solutions for Age-old Problems, *Proceedings Fifth Conference on Ground Control in Mining, USA*, 11th-13th June, pp. 1-5.
- Woodley, J.N.L. and Osborne, B.A., (1980), MRDE Experience with Pump Packing, *Mining Engineer*, Vol. 140, No. 231, December, pp. 437-443.
- Wu, Y.H., Hii, J.K. and Aziz, N.I., (1989), A New Yield Function for CCWR Concretes, *First Conference on Concrete and Structures*, Kuala Lumpur, Malaysia, 3rd-4th October, pp 173-176.
- Wypych, P.W. and Armitage, W.R., (1986), The Operation of a Large Pneumatic Conveying Test Rig in Australia, *2nd International Conference on Bulk Materials Storage Handling and Transportation*, Wollongong, N.S.W., Australia, 7th-9th July, pp. 29-33.
- Zadeh, A.H., Barkhordarian, A., Mills, P.S., Atkins, A.S. and Singh, R.N., (1987), An Investigation into Cheaper Monolithic Packing Materials Utilization

Colliery Tailings, Second International Symposium on the Reclamation, Treatment and Utilization of Coal Mining Wastes, Edited by Rainbow, A.K.B., Elsevier, 7th-11th September, Nottingham University, pp. 369-380.

Zhou, X. and Zhang, S., (1989), Stability Evaluation of Alternative Designs of Drift-and-fill Stopping in Zhaoyuan Gold Mine, P.R. China, 30th U.S. Symposium on Rock Mechanics, West Virginia University, Morgantown, West Virginia, U.S.A. 19th-22nd June, pp. 285-292.

Zienkiewicz, O.C., (1986), The Finite Element Method, 3rd. Edition, McGraw-Hill.

Zienkiewicz, O.C., Vallippan, S. and King, I.P., (1969), Elastic-plastic Solutions of Engineering Problems, 'Initial Stress', Finite Element Approach, Int. J. Numerical Methods in Eng., (1), pp. 75.

Zhang, S. and Hii, J.K., (1990a), An Analytical Approach for the Estimation of Pillar Strength, Ninth Conference, Ground Control in Mining, Edited by Peng, S.S., 4th-6th June, Sheraton Lakeview Resort and Conference Center Morgantown, WV 26505 USA, in Press.

Zhang, S. and Hii, J.K., (1990b), A Computer Model for the Prediction of Fully Mobilized Pillar Strength, 3rd Conference on Ground Control Problems in the Illinois Coal Basin, Edited by Chugh, Y.P., Southern Illinois University at Carbondale, USA, 8th-10th August, in Press.

APPENDIX I

PROGRAM PRINTOUT

Listing of the logarithmic yield function program

```

C   #LOGARITHMIC YIELD FUNCTION#
    DIMENSION X(50),Y(50),YC(50),DY(50)
    COMMON N,A,B,X,Y
    READ(5,*) NPROBL
    DO 1 NP=1,NPROBL
    READ(5,*) N,C0,CE,EPS
    READ(5,*)(X(I1),Y(I1),I1=1,N)
    CALL OBTF(C0,F0)
    CALL OBTF(CE,FE)
    IF (F0*FE.LT.0.0) GOTO 2
    WRITE(6,*) NP,NP,C0,F0,CE,FE
    STOP
2   D=CE-C0
    IF(D.GT.EPS) GOTO 3
    CALL OBTF(CE,FE)
    C=C0+D*F0/(F0-FE)
    CALL OBTF(C,F)
    NN=NN+1
    SUMY=0.0
    DO 4 K=1,N
4   SUMY=SUMY+Y(K)
    YB=SUMY/N
    Q=0.0
    QQ=0.0
    QS=0.0
    DO 5 K=1,N
    YC(K)=A+B*ALOG(X(K)+C)
    D=Y(K)-YC(K)
    DY(K)=D
    Q=Q+ABS(D)
    QQ=QQ+D*D
    QS=QS+(Y(K)-YB)**2
5   CONTINUE
    R=1.0-QQ/QS
    DYB=Q/N
    WRITE(6,6667) NP
6667 FORMAT(1X,////////,6X,'**.PROBLEM.',I2,'**.')
    WRITE(6,10) A,B,C
    WRITE(6,12) DYB,R,F
12  FORMAT(5X,6HDCGM1=,F8.2,2X,'R=',F8.4,2X,'F=',F8.4,/)
    WRITE(6,6665)
6665 FORMAT(5X,'.NO.',6X,'.C3M.',7X,'.C1M.',7X,'.C1C.',7X,'.DC1.',/)
    WRITE(6,11) (I,X(I),Y(I),YC(I),DY(I),I=1,N)
10  FORMAT(1X,/,4X,'CGM1=',F9.2,'+',F8.2,'*ALOG(CGM3+',F7.2,')')
11  FORMAT(5X,I2,1H),4X,F8.2,4X,F8.2,4X,F8.2,4X,F8.2)
    GOTO 1002
3   CT=CE
    CE=0.5*(CE+C0)

```

```

      CALL OBTF(CE,FE)
      IF(F0*FE.LT.0.0) GOTO 2
      C0=CE
      F0=FE
      CE=CT
      GOTO 2
1  CONTINUE
      STOP
      END
C
      SUBROUTINE OBTF(C,F)
      DIMENSION X(50),Y(50)
      COMMON N,A,B,X,Y
      A11=N
      A12=0
      A22=0
      B1=0
      B2=0
      C1=0
      C2=0
      C3=0
      DO 1 K=1,N
      T1=X(K)+C
      T2=ALOG(T1)
      A12=A12+T2
      A22=A22+T2*T2
      B1=B1+Y(K)
      B2=B2+Y(K)*T2
      C1=C1+Y(K)/T1
      C2=C2+1.0/T1
      C3=C3+T2/T1
1  CONTINUE
      T4=1.0/(A11*A22-A12*A12)
      A=(B1*A22-B2*A12)*T4
      B=(B2*A11-B1*A12)*T4
      F=C1-C2*A-C3*B
      RETURN
      END

```

APPENDIX II

EXPERIMENTAL DATA

Table AII.1 Experimental data of sieve analysis one of CWR before processing.

Total weight of CWR sample = 26344.7 gm.

Sieve size (mm)	Weight retained (g)	% of weight retained (%)	% of weight passing (%)
+37.5	5803.1	21.99	78.01
+26.5-37.5	3054.9	11.58	66.43
+19.0-26.5	2766.0	10.58	55.95
+13.2-19.0	3137.5	11.89	43.95
+9.5-13.2	2331.5	8.84	35.12
+6.7-9.5	1975.1	7.48	27.64
+4.75-6.7	1606.4	6.09	21.55
+2.36-4.75	1861.6	7.05	14.50
+1.18-2.36	1324.0	5.02	9.48
+0.60-1.18	863.3	3.27	6.21
+0.30-0.60	647.7	2.45	3.75
+0.212-0.30	240.9	0.91	2.84
+0.150-0.212	214.4	0.81	2.03
+0.075-0.150	272.8	1.03	1.01
under-sized	289.8	1.01	---

 $\Sigma = 26389.0$ $\Sigma = 100.0\%$

$$\% \text{ of error} = \frac{26389.0 - 26344.7}{26344.7} \times 100\%$$

$$= 0.168\%$$

Table AII1.2 Experimental data of sieve analysis two of CWR after processing.

Total weight of CWR sample = 3766.9 gm.

Sieve size (mm)	Weight retained (g)	% of weight retained (%)	% of weight passing (%)
+10.0	0	0	0
+8.0-10.0	740.8	19.70	80.33
+6.7-8.0	535.9	14.23	66.10
+4.75-6.7	747.3	19.84	46.26
+3.35-4.75	413.7	10.98	35.28
+2.5-3.35	332.9	8.84	26.44
+2.0-2.5	243.5	6.46	19.98
+1.7-2.0	138.3	3.67	16.31
+1.18-1.7	196.5	5.22	11.09
+0.850-1.18	119.2	3.16	7.93
+0.600-0.850	89.6	2.38	5.55
+0.425-0.600	67.1	1.78	3.77
+0.300-0.425	44.5	1.18	2.59
+0.212-0.300	32.7	0.87	1.72
+0.150-0.212	30.1	0.80	0.92
+0.105-0.150	9.4	0.25	0.67
+0.075-0.105	12.9	0.34	0.33
+0.063-0.075	4.6	0.12	0.21
+0.053-0.063	6.4	0.17	0.04
under-sized	1.5	0.04	---

 $\Sigma = 3766.9$ $\Sigma = 100.03\%$

$$\% \text{ of error} = \frac{3766.9 - 3766.9}{3766.9} \times 100\%$$

$$= 0\%$$

Table AII1.3(a) Experimental data of sieve analysis three of CWR after processing.

Total weight of CWR sample = 1814.2 gm.

Sieve size (mm)	Weight retained (g)	% of weight retained (%)	% of weight passing (%)
+10.0	0	0	100.00
+8.0-10.0	289.1	15.95	84.05
+6.7-8.0	189.1	10.43	73.62
+4.75-6.7	301.4	16.63	60.00
+3.35-4.75	169.5	9.35	47.65
+2.5-3.35	148.2	8.17	39.47
+2.0-2.5	88.6	4.89	34.59
+1.7-2.0	67.4	3.72	30.87
+1.18-1.7	103.8	5.73	25.14
+0.600-1.18	146.1	8.06	17.09
+0.425-0.600	57.4	3.17	13.92
+0.300-0.425	53.6	2.96	10.96
+0.212-0.300	69.4	3.83	7.14
+0.125-0.212	73.92	4.08	3.06
+0.106-0.125	23.95	1.32	1.74
+0.063-0.106	24.56	1.36	0.38
+0.038-0.063	6.86	0.38	0.004
under-sized	0.07	0.004	---

 $\Sigma = 1812.97$ $\Sigma = 100.03\%$

$$\% \text{ of error} = \frac{1812.97 - 1814.2}{1814.2} \times 100\%$$

$$= -0.068\%$$

Table AII1.3(b) Grain size distribution of sieve analysis three of CWR
after processing.

Total Weight (%)	Weight Percentage (%)	General Remarks
67.75	29.0	Lower medium gravel fraction.
	38.75	Fine gravel fraction.
31.87	14.75	Coarse sand fraction
	12.50	Medium sand fraction
	4.618	Fine sand fraction
0.38	0.38	Coarse silt fraction

Table AII1.4 Experimental data of sieve analysis four of CWR after processing.

Total weight of CWR sample = 2319.5 gm.

Sieve size (mm)	Weight retained (g)	% of weight retained (%)	% of weight passing (%)
+10.0	0	0	0
+8.0-10.0	401.6	17.34	82.66
+6.7-8.0	274.1	11.83	70.83
+4.75-6.7	379.1	16.37	54.46
+3.35-4.75	199.4	8.61	45.85
+2.5-3.35	176.8	7.63	38.22
+2.0-2.5	128.2	5.53	32.69
+1.7-2.0	91.6	3.95	28.73
+1.18-1.7	155.7	6.72	22.01
+0.600-1.18	199.4	8.61	13.40
+0.425-0.600	70.6	3.05	10.35
+0.300-0.425	53.4	2.31	8.05
+0.212-0.300	44.7	1.93	6.12
+0.125-0.212	57.1	2.47	3.65
+0.106-0.125	14.7	0.63	3.02
+0.063-0.106	24.83	1.07	1.95
+0.038-0.063	23.52	1.02	0.93
under-sized	21.59	0.93	---
$\Sigma = 2316.34$		$\Sigma = 99.99\%$	

$$\begin{aligned} \text{\% of error} &= \frac{2316.3 - 2319.5}{2319.5} \times 100\% \\ &= -0.14\% \end{aligned}$$

Table AII1.4(b) Grain size distribution of sieve analysis four of CWR
after processing.

Total Weight (%)	Weight Percentage (%)	General Remarks
71.0	32.0	Lower medium gravel fraction.
	39.0	Fine gravel fraction.
28.0	16.5	Coarse sand fraction
	7.5	Medium sand fraction
	4.0	Fine sand fraction
1.0	1.0	Coarse silt fraction

Table AII1.5 Experimental data of sieve analysis of West Cliff CWR sample 1.
(after Richmond et al, 1985)

Size (μm)	Weight retained (g)	Weight %	Cumulative Weight %
12700	5600	39.0	39.0
6350	2881	20.1	59.1
3350	1691	11.8	70.9
1700	1204	8.4	79.3
850	501	3.5	82.8
425	399	2.8	85.5
212	304	2.1	87.7
106	101	0.7	88.4
53	146	1.0	89.4
38	52	0.4	89.7
-38	1471	10.3	100.0
	14350	100.0	

Table AII1.6 Experimental data of sieve analysis of West Cliff CWR sample 2.
(after Richmond et al, 1985)

Size (μm)	Weight retained (g)	Weight %	Cumulative Weight %
12700	8280	63.2	63.2
6350	1455	11.1	74.3
3350	820	6.3	80.6
1700	507	3.9	84.4
850	319	2.4	86.9
425	170	1.3	88.2
212	178	1.4	89.5
106	232	1.8	91.3
53	118	0.9	92.2
38	146	1.1	93.3
-38	875	6.7	100.0
	13100	100.0	

Table AII1.7 Experimental data of sieve analysis of West Cliff CWR sample 3.
(after Richmond et al, 1985)

Size (μm)	Weight retained (g)	Weight %	Cumulative Weight %
12700	9885	63.4	63.4
6350	1615	10.4	73.7
3350	979	6.3	80.0
1700	405	2.6	82.6
850	288	1.8	84.4
425	278	1.8	86.2
212	345	2.2	88.4
106	286	1.8	90.3
53	263	1.7	91.9
38	89	0.6	92.5
-38	1167	7.5	100.0
	15600	100.0	

Table AII1.8 Experimental data of sieve analysis of West Cliff CWR sample 4.
(after Richmond et al, 1985)

Size (μm)	Weight retained (g)	Weight %	Cumulative Weight %
12700	6278	55.6	55.6
6350	1826	16.2	71.7
3350	1075	9.5	81.2
1700	657	5.8	87.0
850	364	3.2	90.3
425	250	2.2	92.5
212	164	1.5	93.9
106	82	0.7	94.7
53	76	0.7	95.3
38	36	0.3	95.6
-38	492	4.4	100.0
	11300	100.0	

Table AII1.9 Experimental data of sieve analysis of West Cliff CWR sample 5.
(after Richmond et al, 1985)

Size (μm)	Weight retained (g)	Weight %	Cumulative Weight %
12700	7378	62.7	62.7
6350	1667	14.2	76.8
3350	933	7.9	84.8
1700	446	3.8	88.6
850	256	2.2	90.7
425	178	1.5	92.3
212	142	1.2	93.5
106	125	1.1	94.5
53	93	0.8	95.3
38	46	0.4	95.7
-38	506	4.3	100.0
	11770	100.0	

Table AII1.10 Experimental data of sieve analysis of West Cliff CWR sample 6.
(after Richmond et al, 1985)

Size (μm)	Weight retained (g)	Weight %	Cumulative Weight %
12700	5917	66.5	66.5
6350	1219	13.7	80.2
3350	562	6.3	86.5
1700	383	4.3	90.8
850	212	2.4	93.2
425	107	1.2	94.4
212	81	0.9	95.3
106	83	0.9	96.2
53	83	0.9	97.2
38	25	0.3	97.4
-38	228	2.6	100.0
	8900	100.0	

Table AII1.11 Experimental data of sieve analysis of West Cliff CWR sample 7.

(after Richmond et al, 1985)

Size (μm)	Weight retained (g)	Weight %	Cumulative Weight %
12700	6370	46.7	46.7
6350	1620	11.9	58.6
3350	1235	9.1	67.6
1700	735	5.4	73.0
850	451	3.3	76.3
425	200	1.5	77.8
212	148	1.1	78.9
106	188	1.4	80.3
53	524	3.8	84.1
38	75	0.5	84.6
-38	2094	15.4	100.0
	13640	100.0	

Table AII1.12 Experimental data of sieve analysis of West Cliff CWR sample 8.
(after Richmond et al, 1985)

Size (μm)	Weight retained (g)	Weight %	Cumulative Weight %
12700	9825	71.4	71.4
6350	1369	9.9	81.3
3350	770	5.6	86.9
1700	480	3.5	90.4
850	287	2.1	92.5
425	144	1.0	93.5
212	118	0.9	94.4
106	90	0.7	95.0
53	69	0.5	95.5
38	43	0.3	95.9
-38	570	4.1	100.0
	13765	100.0	

Table AII1.13 Experimental data of sieve analysis of West Cliff CWR sample 9.
(after Richmond et al, 1985)

Size (μm)	Weight retained (g)	Weight %	Cumulative Weight %
12700	7208	56.3	56.3
6350	1884	14.7	71.0
3350	1107	8.6	79.7
1700	642	5.0	84.7
850	373	2.9	87.6
425	287	2.2	89.9
212	164	1.3	91.1
106	138	1.1	92.2
53	122	1.0	93.2
38	64	0.5	93.7
-38	811	6.3	100.0
	12800	100.0	

Table AII1.14 Experimental data of sieve analysis of West Cliff CWR sample 10.
(after Richmond et al, 1985)

Size (μm)	Weight retained (g)	Weight %	Cumulative Weight %
12700	11980	63.9	63.9
6350	1740	9.3	73.1
3350	1062	5.7	78.8
1700	829	4.4	83.2
850	401	2.1	85.4
425	278	1.5	86.8
212	168	0.9	87.7
106	189	1.0	88.7
53	183	1.0	89.7
38	79	0.4	90.1
-38	1850	9.9	100.0
	18759	100.0	

Table AII2.2 Sonic velocity measured during curing for 15.0% C-14.72W specimens (m/s).

CURING TIME (DAYS)	SPECIMEN 15.6%C-14.72%W																
	1-2	1-3	7-1	7-2	7-3	14-1	14-2	14-3	28-1	28-2	28-3	60-1	60-2	60-3	90-1	90-2	90-3
1	2061	2029	2184	2141	2303	2168	2191	2138	2193	2185	2181	2239	2187	1919	2141	2092	2189
5			2465	2262	2343	2295	2257	2237	2494	2347	2282	2242	2257	2292	2458	2247	2259
7			2437	2470	2466	2443	2524	2465	2407	2450	2492	2500	2387	2318	2496	2442	2387
14						2553	2537	2462	2580	2483	2460	2582	2462	2389	2568	2454	2474
21									2426	2453	2527	2545	2576	2503	2562	2477	2518
28									2535	2477	2565	2617	2677	2559	2648	2501	2582
51												2671	2602	2591	2719	2564	2589
60												2743	2727	2659	2669	2658	2698
90															2954	2759	2748

Table AII2.3 Sonic velocity measured during curing for 15.0% C-21.0W specimens (m/s).

CURING TIME (DAYS)	SPECIMEN																	
	15.0%C-21.0%W																	
	1-1	1-2	1-3	7-1	7-2	7-3	14-1	14-2	14-3	28-1	28-2	28-3	60-1	60-2	60-3	90-1	90-2	90-3
1	1982	2091	2024	2188	1948	2252	1914	2155	2281	1928	2114	2005	2214	2226	2290	2100	2103	1897
4				2358	2209	2421	2381	2408	2506	2208	2304	2322	2439	2407	2451	2227	2422	2257
7				2469	2379	2557	2469	2519	2564	2421	2409	2422	2518	2541	2569	2358	2518	2433
10							2457	2519	2544	2364	2433	2457	2563	2460	2583	2392	2537	2427
14							2518	2626	2625	2506	2531	2569	2609	2628	2623	2493	2608	2551
21										2544	2531	2643	2616	2601	2686	2525	2628	2551
28										2610	2590	2657	2609	2656	2693	2512	2670	2617
45													2650	2677	2782	2551	2677	2570
60													2767	2781	2829	2652	2712	2673
75																2680	2734	2710
90																2680	2764	2710

Table AII2.4 Sonic velocity measured during curing for 12.5% C-13.0%W specimens (m/s).

CURING TIME (DAYS)	SPECIMEN 12.5%C-13.0%W																	
	1-1	1-2	1-3	7-1	7-2	7-3	14-1	14-2	14-3	28-1	28-2	28-3	60-1	60-2	60-3	90-1	90-2	90-3
1	2387	2061	2029															
3				2560	2450	2462	2544	2559	2367	2330	2632	2456	2488	2354	2367	2482	2447	2390
7				2700	2675	2554	2709	2635	2618	2570	2659	2619	2584	2593	2569	2666	2548	2720
14							2771	2770	2850	2602	2674	2684	2537	2602	2705	2608	2676	2738
23										2906	2901	2719	2847	2802	2865	2841	2785	2716
28										2906	2901	2793	2895	2849	2898	2873	2855	2746
44													2962	2914	2956	2865	2778	2798
60													2971	2931	2948	2931	2954	2886
90																2957	2946	2870

Table AIІ2.5 Sonic velocity measured during curing for 12.5% C-16.5%W specimens (m/s).

CURING TIME (DAYS)	SPECIMEN																	
	12.5%C-16.5%W																	
	1-1	1-2	1-3	7-1	7-2	7-3	14-1	14-2	14-3	28-1	28-2	28-3	60-1	60-2	60-3	90-1	90-2	90-3
1	2018	2077	2158	2086	2067	1933	1994	2102	2100	1980	2037	2074	2111	2096	2135	2083	2154	2116
4				2334	2351	2328	2281	2403	2346	2323	2356	2367	2427	2367	2391	2411	2413	2361
7				2556	2563	2589	2482	2592	2583	2506	2543	2537	2703	2512	2558	2518	2597	2623
10							2563	2673	2685	2628	2648	2588	2747	2594	2591	2594	2665	2671
14							2643	2805	2742	2741	2704	2711	2831	2690	2752	2740	2737	2707
21										2749	2762	2733	2831	2718	2766	2785	2812	2789
28										2825	2800	2839	2887	2808	2828	2800	2828	2812
45													2945	2871	2876	2871	2908	2883
60													2970	2887	2884	2871	2908	2883
75																2911	2933	2900
90																2911	2933	2800

Table AII.2.7 Sonic velocity measured during curing for 10.0% C-12.0W specimens (m/s).

[illegible]

Table AII2.8 Sonic velocity measured during curing for 10.0% C-13.8W specimens (m/s).

CURING TIME (DAYS)		SPECIMEN 10.0%C-13.8%W															
1-1	1-2	1-3	7-1	7-2	7-3	14-1	14-2	14-3	28-1	28-2	28-3	60-1	60-2	60-3	90-1	90-2	90-3
1	2037	2049	1984	2119	2127	2112	2067	2156	2092	1992	2000	2080	2117	2192	2144	2112	2130
3				2192	2187	2208	2169	2302	2168	2208	2208	2183	2205	2317	2248	2203	2263
7				2366	2353	2401	2281	2277	2220	2257	2292	2275	2280	2371	2331	2361	2336
14						2366	2366	2389	2300	2340	2334	2332	2360	2463	2386	2350	2347
28									2370	2394	2476	2408	2428	2531	2455	2423	2414
60												2789	2434	2867	2498	2458	2473
90															2491	2476	2455

Table AI12.9 Sonic velocity measured during curing for 10.0% C-19.12%W specimens (m/s).

CURING TIME (DAYS)	SPECIMEN																	
	10.0%C-19.12%W																	
	1-1	1-2	1-3	7-1	7-2	7-3	14-1	14-2	14-3	28-1	28-2	28-3	60-1	60-2	60-3	90-1	90-2	90-3
1	1851	1884	2013	2003	1994	1876	1876	2005	2054	1961	1784	2015	2029	2032	2003	1992	2082	1998
4				2231	2286	2186	2225	2270	2267	2279	2181	2307	2303	2239	2215	2265	2259	2122
7				2411	2428	2319	2393	2434	2428	2439	2337	2457	2308	2399	2378	2432	2445	2282
10							2393	2434	2428	2445	2343	2457	2452	2416	2423	2432	2469	2262
14							2500	2531	2518	2512	2451	2500	2518	2493	2493	2479	2506	2406
21										2531	2451	2500	2518	2493	2536	2503	2506	2452
28										2603	2475	2602	2568	2544	2536	2553	2609	2518
45													2575	2596	2607	2585	2630	2543
60													2641	2630	2627	2639	2671	2594
75																2639	2686	2594
90																2645	2686	2594

Table AII2.10 Sonic velocity measured during curing for 7.5% C-12.6W specimens (m/s).

CURING TIME (DAYS)	SPECIMEN 7.5%C-12.6%W																	
	1-1	1-2	1-3	7-1	7-2	7-3	14-1	14-2	14-3	28-1	28-2	28-3	60-1	60-2	60-3	90-1	90-2	90-3
1	1963	1996	1953															
2				2091	2115	2164	2116	2104	2073	2161	2080	2114	2131	2004	2176	2056	2146	2123
7				2191	2262	2202												
9							2276	2087	2161	2203	2169	2182	2167	2028	2200	2059	2286	2183
14							2329	2172	2166	2222	2178	2200	2186	2203	2263	2173	2296	2192
28										2287	2266	2254	2225	2189	2263	2246	2296	2246
60													2290	2282	2278	2256	2296	2251
90																2291	2371	2317

Table AI2.11 Sonic velocity measured during curing for 7.5% C-16.5%W specimens (m/s).

CURING TIME (DAYS)	SPECIMEN																	
	7.5%C-16.5%W																	
	1-1	1-2	1-3	7-1	7-2	7-3	14-1	14-2	14-3	28-1	28-2	28-3	60-1	60-2	60-3	90-1	90-2	90-3
1	1851	2295	1956	1823	1984	1858	1659	1610	1796	1603	1790	1892	1752	1843	1906	1795	1616	1839
4				1944	2161	1827	1910	1875	1961	1847	1957	1976	2037	2223	2056	2019	1928	2087
7				2181	2355	2286	2266	2015	2160	2184	2398	2323	2394	2394	2328	2383	2328	2385
10							2276	2085	2197	2222	2403	2366	2394	2428	2366	2388	2388	2402
14							2439	2375	2421	2422	2528	2440	2452	2452	2475	2451	2434	2460
21										2481	2553	2446	2518	2543	2512	2512	2475	2508
28										2506	2592	2500	2518	2543	2575	2531	2500	2514
45													2518	2543	2575	2531	2518	2514
60													2518	2556	2575	2531	2518	2565
75																2531	2543	2565
90																2531	2543	2565

Table AII2.12 Sonic velocity measured during curing for 7.5% C-19.0%W specimens (m/s).

CURING TIME (DAYS)	SPECIMEN																	
	7.5%C-19.0%W																	
	1-1	1-2	1-3	7-1	7-2	7-3	14-1	14-2	14-3	28-1	28-2	28-3	60-1	60-2	60-3	90-1	90-2	90-3
1	1860	1839	1912	1861	1885	1830	1910	1851	1913	1880	1806	1930	1781	1946	1894	1928	1864	1840
4				2198	2193	2080	2236	2120	2147	2209	2172	2293	2042	2172	2121	2161	2080	2199
7				2339	2276	2288	2377	2286	2339	2340	2264	2334	2204	2279	2285	2289	2243	2315
10							2394	2312	2361	2345	2321	2372	2289	2365	2300	2359	2326	2342
14							2422	2355	2394	2367	2343	2378	2316	2370	2337	2359	2326	2348
21										2446	2376	2434	2365	2445	2445	2398	2415	2387
28										2446	2445	2452	2428	2457	2481	2427	2427	2445
45													2458	2487	2506	2439	2500	2481
60													2495	2512	2537	2445	2506	2500
75																2445	2506	2500
90																2445	2506	2500

Table АП2.13 Sonic velocity measured during curing for 5.0% C-12.0W specimens (m/s).

CURING TIME (DAYS)	SPECIMEN 5.0%C-12.0%W														
	1-1	1-2	1-3	7-1	7-2	7-3	14-1	14-2	14-3	28-1	28-2	28-3	60-1	60-2	60-3
1	1800	1741	1700	1877	1804	1783	---	1822	1719	1898	1798	1898	1835	1721	1711
5							1744	---	---	1908	---	1908	---	---	---
7				1973	1890	1877	1844	1933	1722	2036	1811	1919	1981	1891	1861
14							1872	1998	1830	2078	1874	2002	1992	1983	1910
28										2087	1888	2339	2077	2454	2028
60													2134	2097	2020
90													2076	1936	2000

Table АИІ3.2 Specimen weight values measured during curing for 15%С-14.72%W specimens (grams).

CURING TIME (DAYS)	SPECIMEN 15.6%C-14.72%W																	
	1-1	1-2	1-3	7-1	7-2	7-3	14-1	14-2	14-3	28-1	28-2	28-3	60-1	60-2	60-3	90-1	90-2	90-3
1	1553	1558	1535	1638	---	1619	1633	1643	1610	1535	1624	1603	1641	1631	1629	1624	1630	1632
5				1634	1629	1615												
7				1637	1640	1618	1632	1643	1610	1534	1623	1603	1640	1631	1628	1624	1630	1632
8							1631	1642	1607	1530	1621	1601	1638	1629	1627	1621	1628	1630
14										1527	1618	1597	1635	1627	1624	1616	1625	1625
21										1525	1616	1595	---	---	---	---	---	---
28													1632	1625	1621	1613	1623	1622
29													1626	1615	1618	1605	1620	1613
50													1625	1631	1617	1640	1628	1628
60																1629	1626	1614
90																		

Table AII3.3 Specimen weight values measured during curing for 15.0% C-21.0W specimens (grams).

CURING TIME (DAYS)	SPECIMEN																	
	15.0%C-21.0%W																	
	1-1	1-2	1-3	7-1	7-2	7-3	14-1	14-2	14-3	28-1	28-2	28-3	60-1	60-2	60-3	80-1	90-2	90-3
1	1619	1636	1603	1619	1456	1532	1536	1529	1499	1608	1604	1615	1631	1616	1653	1576	1616	1606
4				1620	1456	1533	1537	1530	1500	1607	1605	1614	1631	1616	1653	1578	1617	1610
7				1621	1457	1533	1538	1534	1501	1611	1607	1617	1635	1619	1655	1579	1621	1614
10							1537	1534	1501	1611	1606	1617	1635	1619	1655	1579	1621	1614
14							1636	1534	1500	1613	1608	1621	1636	1622	1657	1580	1623	1617
21										1611	1606	1619	1635	1620	1657	1580	1623	1616
28										1615	1610	1622	1637	1623	1660	1583	1624	1617
45													1634	1618	1657	1581	1621	1612
60													1637	1620	1660	1583	1622	1615
75																1584	1622	1615
90																1581	1622	1614

Table AII3.4 Specimen weight values measured during curing for 12.5%C-13.0%W specimens (grams).

[illegible]

Table АПЗ.6 Specimen weight values measured during curing for 12.5% C-19.13%W specimens (grams).

CURING TIME (DAYS)	SPECIMEN																	
	12.5%C-19.13%W																	
	1-1	1-2	1-3	7-1	7-2	7-3	14-1	14-2	14-3	28-1	28-2	28-3	60-1	60-2	60-3	90-1	90-2	90-3
1	1625	1626	1608	1618	1617	1615	1617	1620	1595	1619	1624	1643	1614	1608	1618	1632	1607	1617
4				1618	1618	1613	1616	1619	1593	1620	1626	1641	1614	1608	1620	1633	1608	1605
7				1620	1622	1615	1624	1622	1595	1624	1631	1647	1618	1612	1622	1636	1613	1611
10					1624	1623	1624	1624	1594	1624	1633	1647	1617	1612	1622	1635	1612	1611
14					1623	1622	1623	1622	1594	1623	1632	1647	1617	1612	1622	1635	1612	1611
21										1626	1631	1645	1622	1615	1627	1639	1617	1613
28										1627	1632	1646	1625	1618	1628	1642	1618	1616
45													1623	1617	1626	1641	1618	1614
60													1621	1615	1625	1640	1617	1611
75																1642	1618	1615
90																1638	1615	1610

Table AII3.7 Specimen weight values measured during curing for 10.0% C-12.0W specimens (grams).

[illegible]

Table AII3.8 Specimen weight values measured during curing for 10.0%C-13.8%W specimens (grams).

CURING TIME (DAYS)	SPECIMEN 10.0%C-13.8%W																	
	1-1	1-2	1-3	7-1	7-2	7-3	14-1	14-2	14-3	28-1	28-2	28-3	60-1	60-2	60-3	90-1	90-2	90-3
1	1548	1562	1566	1640	1656	1652	1656	1636	1659	1651	1657	1672	1653	1635	1641	1639	1647	1632
4				1636	1652	1649	1652	1633	1656	1648	1653	1669	1651	1632	1638	1637	1644	1630
7				1635	1651	1647	1650	1632	1655	1647	1653	1669	1650	1631	1637	1637	1643	1629
14						1647	1647	1628	1652	1640	1649	1667	1647	1627	1635	1636	1640	1625
28										1635	1647	1664	1642	1620	1629	1631	1637	1621
60													1667	1609	1651	1620	1631	1619
90																1601	1619	1600

Table АИІ3.9 Specimen weight values measured during curing for 10.0% C-19.12%W specimens (grams).

CURING TIME (DAYS)	SPECIMEN																	
	10.0%С-19.12%W																	
	1-1	1-2	1-3	7-1	7-2	7-3	14-1	14-2	14-3	28-1	28-2	28-3	60-1	60-2	60-3	90-1	90-2	90-3
1	1620	1634	1646	1639	1626	1631	1606	1624	1630	1604	1587	1607	1640	1598	1634	1626	1603	1639
4				1637	1625	1630	1605	1623	1628	1604	1586	1607	1640	1599	1634	1627	1604	1639
7				1639	1626	1631	1607	1627	1631	1605	1588	1609	1641	1600	1636	1628	1605	1640
10							1607	1627	1631	1605	1587	1608	1640	1600	1636	1628	1605	1640
14										1605	1592	1613	1643	1605	1640	1632	1609	1644
21							1608	1627	1632	1605	1591	1613	1641	1603	1639	1632	1609	1642
28										1605	1592	1614	1642	1605	1641	1634	1609	1642
45													1643	1604	1639	1631	1607	1640
60													1643	1603	1639	1631	1607	1642
75																1631	1607	1642
90																1631	1607	1642

Table AII3.10 Specimen weight values measured during curing for 7.5%C-12.6%W specimens (grams).

CURING TIME (DAYS)	SPECIMEN 7.5%C-12.6%W																	
	1-1	1-2	1-3	7-1	7-2	7-3	14-1	14-2	14-3	28-1	28-2	28-3	60-1	60-2	60-3	90-1	90-2	90-3
1	1665	1669	1652															
2				1656	1668	1670	1667	1648	1663	1666	1656	1667	1647	1656	1670	1653	1668	1667
7				1653	1666	1667												
9							1664	1640	1655	1662	1650	1661	1639	1645	1665	1647	1664	1663
14							1662	1637	1649	1659	1645	1659	1634	1642	1663	1644	1663	1661
28										1656	1641	1655	---	---	---	---	---	---
30													1625	1625	1653	1636	1659	1657
60													1630	1605	1637	1637	1646	1638
90																1607	1628	1590

Table АП3.12 Specimen weight values measured during curing for 7.5% C-19.0%W specimens (grams).

CURING TIME (DAYS)		SPECIMEN 7.5%С-19.0%W																
1-1	1-2	1-3	7-1	7-2	7-3	14-1	14-2	14-3	28-1	28-2	28-3	60-1	60-2	60-3	90-1	90-2	90-3	
1	1658	1642	1662	1652	1645	1629	1640	1643	1650	1655	1638	1659	1609	1623	1628	1629	1615	1622
4			1653	1646	1629	1643	1643	1651	1656	1639	1660	1610	1610	1623	1628	1619	1615	1623
7			1657	1649	1632	1644	1647	1654	1659	1642	1662	1613	1613	1626	1629	1622	1620	1626
10						1645	1647	1655	1659	1642	1663	1613	1613	1626	1630	1623	1621	1626
14						1645	1647	1655	1660	1643	1663	1614	1614	1628	1632	1623	1621	1626
21									1659	1642	1663	1614	1614	1628	1632	1623	1620	1626
28									1658	1641	1662	1613	1613	1628	1631	1623	1620	1625
45												1615	1629	1633	1624	1622	1627	
60												1615	1629	1633	1624	1622	1627	
75															1624	1622	1627	
90															1620	1618	1624	

Table AII3.13 Specimen weight values measured during curing for 5.0%C-12.0%W specimens (grams).

CURING TIME (DAYS)	SPECIMEN 5.0%C-12.0%W																	
	1-1	1-2	1-3	7-1	7-2	7-3	14-1	14-2	14-3	28-1	28-2	28-3	60-1	60-2	60-3	90-1	90-2	90-3
1	1636	1657	1696	1653	1647	1641	1608	1608	1664	1589	1688	1656	1645	1644	1664	1618	1652	1566
5				1650	---	1640	1673	---	---	1645	---	---	---	---	---	1643	---	---
7				1648	1644	1637	1667	1603	1654	1636	1681	1653	1660	1647	1659	1637	1641	1560
14							1661	1600	1645	1631	1675	1650	1656	1639	1655	1632	1635	1556
28										1648	1663	1645	1650	1652	1650	1624	1636	1545
60													1635	1638	1631	1599	1593	1516
90																1566	1557	1490

Table AII4.1 Results of compressive strength testing (15.6%C-14.72%W, mix 1).

SPECIMEN	MAX. LOAD (KN)	MAX. STRESS (MPa)	E (GPa)	ν	LOAD RATE (mm/s)
15.6%-1-1	20.720	2.638	--	--	0.0015
15.6%-1-2	20.000	2.546	0.403	0.358	0.0015
15.6%-1-3	20.000	2.583	0.369	0.250	0.0015
AVERAGE	20.240	2.589	0.386	0.304	0.0015
15.6%-7-1	47.400	5.733	1.750	0.111	0.0015
15.6%-7-2	46.800	5.688	0.947	0.053	0.0015
15.6%-7-3	48.500	5.901	1.685	0.077	0.0015
AVERAGE	47.567	5.774	1.461	0.080	0.0015
15.6%-14-1	53.000	6.417	1.104	0.024	0.0015
15.6%-14-2	55.500	6.750	1.137	0.027	0.0015
15.6%-14-3	55.000	6.691	1.051	0.015	0.0015
AVERAGE	54.500	6.620	1.097	0.022	0.0015
15.6%-28-1	57.500	7.156	0.841	0.025	0.0015
15.6%-28-2	61.900	7.546	1.067	0.021	0.0015
15.6%-28-3	64.800	7.915	1.110	0.017	0.0015
AVERAGE	61.400	7.539	1.006	0.021	0.0015
15.6%-60-1	78.500	9.607	1.916	0.109	0.0015
15.6%-60-2	73.600	9.007	1.622	0.072	0.0015
15.6%-60-3	75.400	9.361	1.282	0.110	0.0015
AVERAGE	75.830	9.325	1.607	0.097	0.0015
15.6%-90-1	81.000	9.971	1.658	0.106	0.0015
15.6%-90-2	69.600*	8.585*	1.162	0.015	0.0015
15.6%-90-3	86.200	10.593	---	---	0.0015
AVERAGE	83.600	10.282	1.658	0.106	0.0015

* Not included in the average.

Table AII4.2 Specimen experimental data (15.6%C-14.72%W, mix 1).

SPECIMEN	ρ_{wet} (t/m ³)	ρ_{dry} (t/m ³)	WATER CONTENT (%)	TEMP. (°C)	DURATION (mins)
15.6%-1-1	1.958	1.653	15.60	----	----
15.6%-1-2	1.964	1.657	15.60	----	----
15.6%-1-3	1.969	1.662	15.60	----	----
15.6%-7-1	1.960	1.669	14.87	----	13.7
15.6%-7-2	1.950	1.658	15.00	----	12.8
15.6%-7-3	1.926	1.638	14.94	----	12.7
15.6%-14-1	1.936	1.655	14.49	----	20.0
15.6%-14-2	1.958	1.672	14.63	----	16.0
15.6%-14-3	1.940	1.651	14.83	----	16.0
15.6%-28-1	1.876	1.621	13.61	19.5	17.0
15.6%-28-2	1.935	1.674	13.50	19.0	16.0
15.6%-28-3	1.908	1.647	13.64	19.5	15.0
15.6%-60-1	1.943	1.721	11.40	18.0	58.0
15.6%-60-2	1.950	1.723	11.63	17.8	62.0
15.6%-60-3	1.968	1.739	11.62	17.8	63.0
15.6%-90-1	1.957	1.667	14.82	20.0	43.3
15.6%-90-2	1.971	1.703	13.59	20.1	50.0
15.6%-90-3	1.935	1.674	13.50	21.8	53.0

Table AII4.3 Results of compressive strength testing (12.5%C-13.0%W, mix 2).

SPECIMEN	MAX. LOAD (KN)	MAX. STRESS (MPa)	E (GPa)	ν	LOAD RATE (mm/s)
12.5%-1.5H	0.642	0.082	---	---	0.0125
12.5%-2.0H	1.188	0.151	---	---	0.0750
12.5%-2.5H	2.100	0.267	0.008	0.193	0.0125
12.5%-4.25H	8.000	1.021	0.088	0.077	0.0125
12.5%-4.5H	9.920	1.251	0.905	0.172	0.0015
12.5%-1-1	41.700	5.054	0.588	0.004	0.0015
12.5%-1-2*	33.000	4.023	0.641	0.023	0.0015
12.5%-1-3	43.000	5.221	0.863	0.060	0.0015
AVERAGE	42.520	5.138	0.726	0.032	
12.5%-7-1	76.800	9.399	1.509	0.059	0.0015
12.5%-7-2	73.900	9.009	2.716	0.049	0.0015
12.5%-7-3	68.840	8.169	1.349	0.023	0.0015
AVERAGE	73.180	8.859	1.858	0.044	
12.5%-14-1	87.500	10.666	2.129	0.231	0.0015
12.5%-14-2	86.000	10.422	2.123	0.085	0.0015
12.5%-14-3	88.000	10.748	1.642	0.047	0.0015
AVERAGE	87.167	10.612	1.905	0.121	
12.5%-28-1	89.600	10.859	4.524	0.173	0.0015
12.5%-28-2	82.150©	9.975	6.460	0.243	0.0015
12.5%-28-3	96.000©	11.680	2.345	0.025	0.0015
AVERAGE	89.250	10.838	4.443	0.147	
12.5%-60-1	124.150	15.046	2.430	0.098	0.0015
12.5%-60-2	121.450	14.805	3.171	0.144	0.0015
12.5%-60-3	125.570	15.367	3.017	0.055	0.0015
AVERAGE	123.723	15.073	2.873	0.099	
12.5%-90-1	146.600	17.940	2.757	0.070	0.0015
12.5%-90-2	139.300	17.048	2.948	0.100	0.0015
12.5%-90-3	121.000	14.808	2.836	0.100	0.0015
AVERAGE	135.633	16.599	2.847	0.090	

* Not included in the average.

© Specimen subjected to re-loading.

Table AII4.4 Specimen experimental data (12.5%C-13.0%W, mix 2).

SPECIMEN	ρ_{wet} (t/m ³)	ρ_{dry} (t/m ³)	WATER CONTENT (%)	TEMP. (°C)	DURATION (mins)
12.5%-1.5H	2.034	---	---	---	16.8
12.5%-2.0H	2.032	---	---	---	9.0
12.5%-2.5H	2.002	---	---	---	8.3
12.5%-4.25H	2.015	1.789	11.22	---	9.0
12.5%-4.5H	1.995	1.772	11.19	---	18.0
12.5%-1-1	2.011	1.800	10.47	---	20.0
12.5%-1-2	1.907	1.705	10.61	---	14.0
12.5%-1-3	1.991	1.780	10.61	---	15.0
12.5%-7-1	2.017	1.817	9.70	15.0	15.3
12.5%-7-2	1.983	1.796	9.77	16.3	14.3
12.5%-7-3	1.994	1.808	9.76	16.3	15.6
12.5%-14-1	2.004	1.820	9.20	18.5	20.0
12.5%-14-2	2.003	1.819	9.20	19.0	16.5
12.5%-14-3	1.997	1.817	9.00	19.0	19.0
12.5%-28-1	1.931	1.761	8.79	18.5	15.0
12.5%-28-2	1.946	1.767	9.20	18.8	15.0
12.5%-28-3	1.981	1.808	8.75	19.3	14.0
12.5%-60-1	1.978	1.841	6.93©	22.0	50.8
12.5%-60-2	1.925	1.794	6.84©	22.5	45.2
12.5%-60-3	1.918	1.775	7.42©	22.5	55.0
12.5%-90-1	1.958	1.837	6.20©	26.0	45.0
12.5%-90-2	1.953	1.823	6.65©	25.5	48.0
12.5%-90-3	1.956	1.822	6.85©	25.5	50.0

© Small portion only of specimen used in the determination of water content. Hence low resultant value.

Table AII4.5 Results of compressive strength testing (10.0%C-13.8%W, mix 3).

SPECIMEN	MAXIMUM LOAD (KN)	MAXIMUM STRESS (MPa)	MAXIMUM STIFFNESS (KN/mm)	E (GPa)	ν	LOAD RATE (mm/s)
10%-1.5H	0.310	0.039	0.110	0.001	0.451	0.0125
10%-2.0H	0.330	0.042	0.102	0.001	0.427	0.0125
10%-1-1	14.400	1.833	19.699	0.252	0.210	0.0015
10%-1-2	14.100	1.795	19.190	0.245	0.025	0.0050
10%-1-3	14.000	1.768	18.510	0.237	0.012	0.0050
AVERAGE	14.167	1.799	19.133	0.245	0.019	
10%-7-1	27.750	3.396	50.664	0.630	0.018	0.0015
10%-7-2	27.400	3.353	30.583	0.381	0.010	0.0015
10%-7-3	29.400	3.598	76.660	0.740	0.017	0.0015
AVERAGE	28.183	3.449	52.636	0.584	0.015	
10%-14-1	30.950	3.788	87.871	1.100	0.014	0.0015
10%-14-2	31.750	3.886	63.469	0.700	0.010	0.0015
10%-14-3	32.450	3.971	116.958	1.250	0.042	0.0015
AVERAGE	31.717	3.882	89.433	1.017	0.022	
10%-28-1	35.400	4.344	89.325	1.053	0.012	0.0015
10%-28-2	35.200	4.326	157.841	1.866	0.070	0.0020
10%-28-3	35.650	4.363	114.858	1.207	0.067	0.0020
AVERAGE	35.417	4.344	120.675	1.379	0.050	
10%-60-1	35.380	4.330	144.646	1.433	0.087	0.0015
10%-60-2	41.450	5.073	137.039	1.542	0.085	0.0015
10%-60-3	38.350	4.693	---	---	---	0.0015
AVERAGE	38.393	4.699	140.843	1.488	0.086	
10%-90-1	47.060	5.752	109.298	1.247	0.037	0.0015
10%-90-2	45.590	5.579	96.203	1.110	0.060	0.0015
10%-90-3	45.440	5.561	73.251	0.896	0.047	0.0015
AVERAGE	46.030	5.631	92.917	1.084	0.048	

Table AII4.6 Specimen experimental data (10.0%C-13.8%W, mix 3).

SPECIMEN	ρ_{wet} (t/m ³)	ρ_{dry} (t/m ³)	WATER CONTENT (%)	TEMP. (°C)	DURATION (mins)
10%-1.5H	1.990	1.707	14.2	---	11.3
10%-2.0H	2.007	1.712	14.7	---	11.0
10%-1-1	1.961	1.690	13.8	19.0	25.0
10%-1-2	1.961	1.694	13.6	19.5	10.0
10%-1-3	1.951	1.686	13.6	19.5	11.0
10%-7-1	1.971	1.729	12.3	18.5	18.0
10%-7-2	1.983	1.727	12.9	20.0	20.5
10%-7-3	1.980	1.721	13.1	20.0	19.5
10%-14-1	1.977	1.737	12.12	20.0	20.0
10%-14-2	1.953	1.707	12.59	20.0	18.0
10%-14-3	1.982	1.734	12.49	20.5	20.0
10%-28-1	1.967	1.723	12.43	17.5	20.0
10%-28-2	1.975	1.726	12.61	17.8	14.2
10%-28-3	1.992	1.734	12.94	17.8	15.0
10%-60-1	1.993	1.728	13.54	22.0	48.0
10%-60-2	1.950	1.728	11.38	22.0	50.0
10%-60-3	2.001	1.723	13.91	25.0	55.0
10%-90-1	1.932	1.757	9.07	22.0	60.0
10%-90-2	1.943	1.749	10.00	22.0	55.0
10%-90-3	1.908	1.726	9.56	21.5	58.0

Table AII4.7 Results of compressive strength testing (7.5%C-12.6%W, mix 4).

SPECIMEN	MAXIMUM LOAD (KN)	MAXIMUM STRESS (MPa)	MAXIMUM STIFFNESS (KN/mm)	E (GPa)	ν	LOAD RATE (mm/s)
7.5%-1.5H	0.300	0.038	0.106	0.001	0.413	0.0125
7.5%-2.0H	0.330	0.042	0.098	0.001	0.576	0.0200
7.5%-4.25H	1.300	0.166	0.263	0.003	0.287	0.0125
7.5%-4.5H	1.460	0.186	0.363	0.004	0.402	0.0125
7.5%-5.0H	1.470	0.187	0.404	0.005	0.281	0.0125
7.5%-1-1	13.180	1.613	13.509	0.168	0.046	0.0015
7.5%-1-2	13.250	1.622	16.824	0.210	0.028	0.0030
7.5%-1-3	13.500	1.652	16.181	0.201	0.045	0.0030
AVERAGE	13.310	1.629	15.505	0.193	0.039	
7.5%-7-1	23.600	2.888	36.209	0.436	0.014	0.0015
7.5%-7-2	22.120	2.681	27.091	0.302	0.010	0.0030
7.5%-7-3	21.000	2.424	41.722	0.410	0.022	0.0030
AVERAGE	22.240	2.664	35.007	0.383	0.015	
7.5%-14-1	24.750	3.029	50.834	0.629	0.020	0.0015
7.5%-14-2	25.130	3.045	35.784	0.392	0.020	0.0030
7.5%-14-3	25.400	3.078	56.775	0.655	0.070	0.0030
AVERAGE	25.093	3.152	47.582	0.559	0.031	
7.5%-28-1	28.600	3.500	92.396	1.124	0.054	0.0020
7.5%-28-2	28.000	3.365	30.156	0.325	0.006	0.0020
7.5%-28-3	27.000	3.272	35.152	0.369	0.014	0.0020
AVERAGE	27.870	3.379	52.568	0.606	0.024	
7.5%-60-1	31.200	3.941	104.241	1.266	0.072	0.0015
7.5%-60-2	34.400	4.210	68.006	0.833	0.053	0.0015
7.5%-60-3	34.370	4.165	50.399	0.541	0.016	0.0015
AVERAGE	33.320	4.105	74.215	0.880	0.047	
7.5%-90-1	38.000	4.605	71.281	0.842	0.056	0.0015
7.5%-90-2	36.500	4.423	80.572	0.973	0.044	0.0015
7.5%-90-3	39.600	4.846	63.452	0.788	0.052	0.0015
AVERAGE	38.033	4.625	71.768	0.877	0.051	

Table AII4.8 Specimen experimental data (7.5%C-12.6%W, mix 4).

SPECIMEN	ρ_{wet} (t/m ³)	ρ_{dry} (t/m ³)	WATER CONTENT (%)	TEMP (°C)	DURATION (mins)
7.5%-1.5H	2.029	1.737	14.4	18.5	11.2
7.5%-2.0H	2.043	1.753	14.2	19.0	6.3
7.5%-4.25H	1.990	1.711	14.0	19.5	11.0
7.5%-4.5H	2.026	1.738	14.2	19.0	11.0
7.5%-5.0H	2.022	1.741	13.9	19.5	11.0
7.5%-1-1	2.000	1.738	13.1	18.5	28.0
7.5%-1-2	2.000	1.735	13.3	18.8	14.3
7.5%-1-3	1.994	1.731	13.2	19.0	15.0
7.5%-7-1	2.003	1.747	12.79	19.5	23.0
7.5%-7-2	1.989	1.732	12.90	19.5	14.0
7.5%-7-3	1.990	1.735	12.80	19.5	15.0
7.5%-14-1	1.994	1.754	12.03	20.0	18.0
7.5%-14-2	1.964	1.733	11.74	20.0	13.0
7.5%-14-3	1.959	1.728	11.81	20.0	13.0
7.5%-28-1	1.987	1.749	12.00	20.0	16.0
7.5%-28-2	1.979	1.749	11.60	20.0	20.0
7.5%-28-3	1.968	1.735	11.80	20.3	21.0
7.5%-60-1	1.975	1.751	11.37	18.8	66.0
7.5%-60-2	1.925	1.748	9.20©	19.5	88.0
7.5%-60-3	1.951	1.762	9.70©	20.1	72.0
7.5%-90-1	1.900	1.737	8.60©	16.0	60.0
7.5%-90-2	1.944	1.800	7.40©	16.0	63.0
7.5%-90-3	1.917	1.777	7.31©	17.3	53.0

© Small portion only of specimen used in the determination of water content. Hence low resultant value.

Table AII4.9 Results of compressive strength testing (5.0%C-12.0%W, mix 5).

SPECIMEN	MAXIMUM LOAD (KN)	MAXIMUM STRESS (MPa)	MAXIMUM STIFFNESS (KN/mm)	E (GPa)	ν	LOAD RATE (mm/s)
5.0%-3.0H	1.070	0.136	0.642	0.007	0.370	0.0125
5.0%-4.0H	2.000	0.255	1.553	0.010	0.407	0.0125
5.0%-4.5H	1.970	0.251	1.539	0.005	0.310	0.0125
5.0%-1-1	9.500	1.149	19.976	0.199	0.134	0.0030
5.0%-1-2	10.000	1.214	15.941	0.166	0.106	0.0030
5.0%-1-3	10.400	1.260	10.594	0.114	0.198	0.0030
AVERAGE	9.967	1.208	15.504	0.160	0.146	
5.0%-7-1	16.060	1.965	15.267	0.190	0.174	0.0015
5.0%-7-2	15.500	1.882	23.412	0.240	0.127	0.0030
5.0%-7-3	14.550	1.781	23.623	0.260	0.101	0.0030
AVERAGE	15.370	1.876	20.767	0.230	0.134	
5.0%-14-1	17.300	2.117	32.129	0.401	0.203	0.0015
5.0%-14-2	15.650	1.904	28.649	0.354	0.100	0.0030
5.0%-14-3	17.350	2.103	22.957	0.282	0.052	0.0030
AVERAGE	16.770	2.041	27.912	0.346	0.118	
5.0%-28-1	19.100	2.338	18.414	0.220	0.057	0.0030
5.0%-28-2	20.500	2.509	23.837	0.273	0.151	0.0030
5.0%-28-3©	15.300	1.872	16.286	0.187	0.175	0.0030
AVERAGE	19.800	2.432	19.512	0.247	0.104	
5.0%-60-1	21.150	2.588	25.238	0.315	0.059	0.0015
5.0%-60-2	19.500	2.363	25.777	0.319	0.037	0.0015
5.0%-60-3	20.650	2.527	28.122	0.328	0.210	0.0015
AVERAGE	20.433	2.493	26.379	0.321	0.102	
5.0%-90-1	27.410	3.350	47.588	0.448	0.189	0.0015
5.0%-90-2	28.000	3.426	40.734	0.480	0.201	0.0015
5.0%-90-3	22.500	2.754	39.634	0.468	0.080	0.0015
AVERAGE	27.705	3.388	42.652	0.465	0.157	

© Not included in the average because values abnormally low.

Table АП4.10 Specimen experimental data (5.0%C-12.0%W, mix 5).

SPECIMEN	ρ_{wet} (t/m ³)	ρ_{dry} (t/m ³)	WATER CONTENT (%)	TEMP (°C)	DURATION (mins)
5.0%-3.0H	2.040	1.785	12.51	21.0	10.2
5.0%-4.0H	2.042	1.787	12.51	20.5	9.0
5.0%-4.5H	2.048	1.790	12.59	20.5	9.4
5.0%-1-1	1.946	1.723	11.44	19.5	17.0
5.0%-1-2	1.972	1.746	11.47	19.3	16.0
5.0%-1-3	2.007	1.775	11.56	19.5	17.0
5.0%-7-1	1.996	1.778	10.92	18.5	23.0
5.0%-7-2	1.992	1.763	11.51	18.8	15.0
5.0%-7-3	1.964	1.748	11.02	19.0	15.0
5.0%-14-1	1.993	1.788	10.29	18.8	29.0
5.0%-14-2	1.917	1.710	10.80	19.5	15.1
5.0%-14-3	1.966	1.768	10.07	19.0	16.5
5.0%-28-1	1.993	1.781	10.60	19.0	28.0
5.0%-28-2	1.985	1.792	9.71	18.5	30.0
5.0%-28-3	1.987	1.758	11.54	19.0	31.0
5.0%-60-1	1.962	1.788	8.88©	18.5	68.0
5.0%-60-2	1.945	1.739	10.56	19.5	58.0
5.0%-60-3	1.957	1.982	8.97©	20.8	66.0
5.0%-90-1	1.907	1.793	6.00©	21.0	88.0
5.0%-90-2	1.868	1.780	4.70©	22.3	83.0
5.0%-90-3	1.805	1.702	5.75©	22.8	76.0

© Small portion only of specimen used in the determination of water content. Hence low resultant value.

Table AII5.1 Post failure modulus and residual strength results of
CCWR specimens (15.6%C-14.72%W, mix 1).

Specimen	% of U.C.S.	E_f (GPa)	Residual Strength
15.6% - 7 - 1	84%*	0.244	
2	90%*	0.200	
3	93%*	0.221	
15.6% - 14 - 1	85%*	0.206	
2	90%*	0.232	
3	84%*	0.186	
15.6% - 28 - 1	90%*	0.195	
2	85%*	0.305	
3	73%*	0.419	
15.6% - 60 - 1	61%	0.338	
	35%	0.186	2.142
	22%	0.104	
2	65%	0.346	1.836
	20%	0.046	
3	60%	0.417	1.24
	13%	0.045	
15.6% - 90 - 1	50%	0.305	
	22%	0.365	1.165
	14%	0.077	
2 ⁺	26%	0.128	1.703
3	26%	0.303	1.571

* Rate of loading was increased after ultimate compressive strength has been obtained.

+ Value anomalously low

Table AII5.2 Post failure modulus and residual strength results of
CCWR specimens (12.5%C-13.0%W, mix 2).

Specimen	% of U.C.S.	E_f (MPa)	Residual Strength (MPa)
12.5% - 1 - 1 2 3	84% 90%	205* 208.4*	
12.5% - 7 - 1 2 3	88% 85% 80%	450* 492* 464*	
12.5% - 14 - 1 2 3	60% 58% 71%	1554.0* 1934.2* 687.4*	
12.5% - 28 - 1 2 3	56% 55% 40%	1782* 6839* 1254*	
12.5% - 60 - 1 2 3	10% 10% 16%	137.5 87.4 135.0	1.212 1.341 1.224
12.5% - 90 - 1 2 3	8% 18% 13%	66.53 272.15 486.94	1.591 1.657 1.657

* Rate of loading was increased after ultimate compressive strength has been obtained.

Table AII5.3 Post failure modulus and residual strength results of
CCWR specimens (10.0%C-13.8%W, mix 3).

Specimen	% of U.C.S.	E_f (MPa)	Residual Strength (MPa)
10% - 7 - 1	89%	79.05*	
2	89%	77.94*	
3	86%	95.51*	
10% - 14 - 1	88%	115.97*	
2	81%	116.21	
3	84%	115.97*	
10% - 28 - 1	70%	220.73*	
2	77%	239.71	
3	72%	229.49*	
10% - 60 - 1	35%	114.57	0.612
2	39%	149.37	0.979
3	36%	130.02	0.612
10% - 90 - 1	42%	182.49	0.428
2	33%	169.91	0.428
3	33%	186.14	0.490

* Rate of loading was increased after
ultimate compressive strength has
been obtained.

Table AII5.4 Post failure modulus and residual strength results of
CCWR specimens (7.5%C-12.6%W, mix 4).

Specimen	% of U.C.S.	E_f (MPa)	Residual Strength (MPa)
7.5%-1-1	91% [®]	13.55	--
2	93% [®]	14.04	--
3	89% [®]	15.05	--
7.5%-7-1	93% [®]	54.81	--
7.5%-14-1	73% [®]	84.02	--
2	81% [®]	74.51	--
3	73% [®]	12.88	--
7.5%-28-1	73% [®]	78.02	--
2	76% [®]	91.81	--
3	76% [®]	90.05	--
7.5%-60-1	43%	80.90	--
2	13%	27.78	0.17
3	15%	27.00	0.19
7.5%-90-1	28%	84.99	0.42
2	40%	99.58	0.30
3	15%	130.75	0.31

® Rate of loading was increased after ultimate compressive
strength has been obtained.

Table AII5.5 Post failure modulus and residual strength results of
CCWR specimens (5.0%C-12.0%W, mix 5).

Specimen	% of U.C.S.	E_f (MPa)	Residual Strength (MPa)
5%-14-1	69% [®]	57.21	--
2	72% [®]	45.74	--
3	71% [®]	56.32	--
5%-28-1	75% [®]	50.90	--
2	77% [®]	51.91	--
3	76% [®]	37.90	--
5%-60-1	26%	24.97	--
2	39%	40.50	0.22
3	28%	42.59	0.15
5%-90-1	26%	54.28	0.43
2	29%	71.91	0.25
3	89%	58.86	--

® Rate of loading was increased after ultimate compressive strength has been obtained.

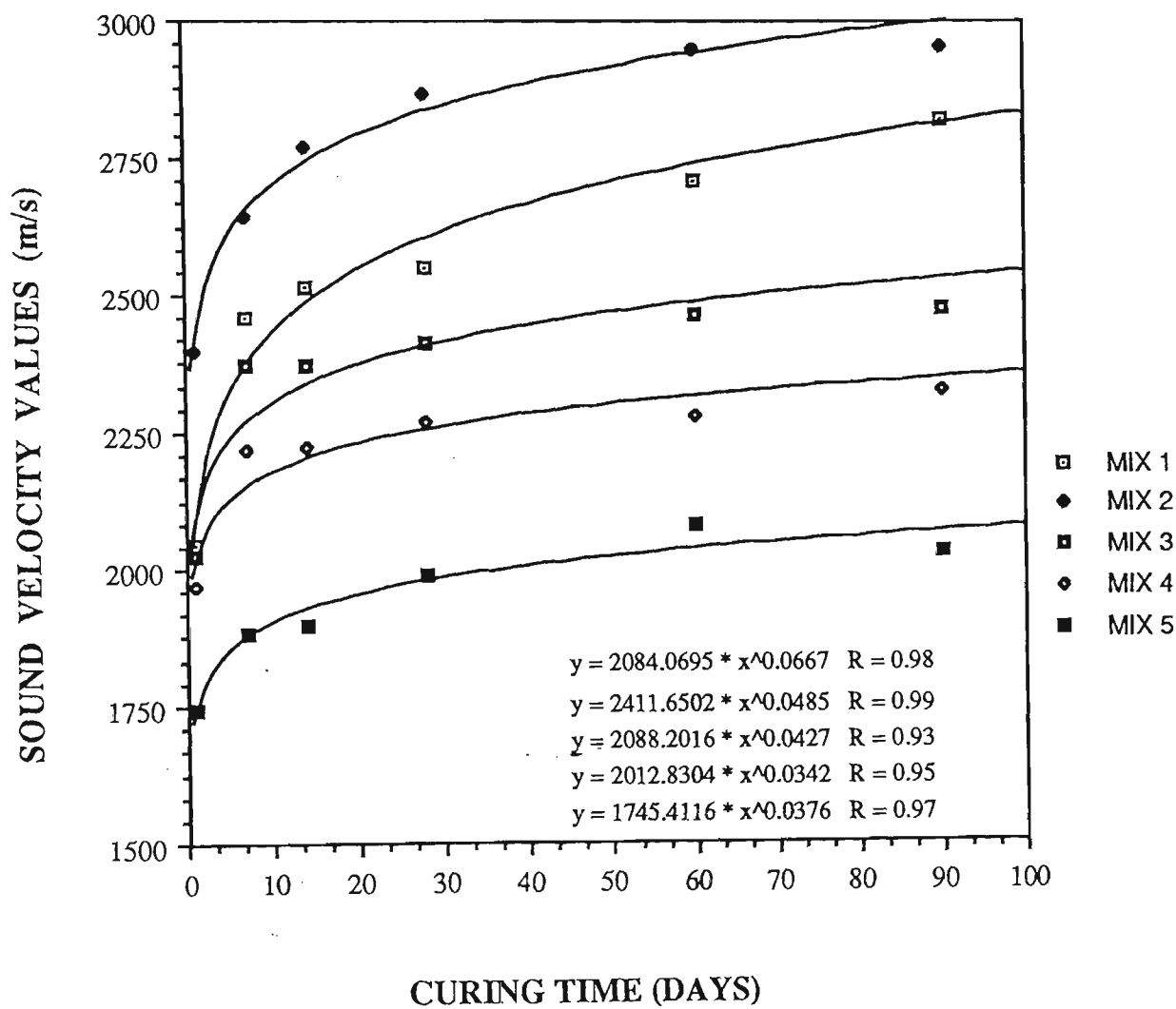


Figure AII6.1 Sonic velocity-curing time graph of CCWR specimens for mixes 1 through 5.

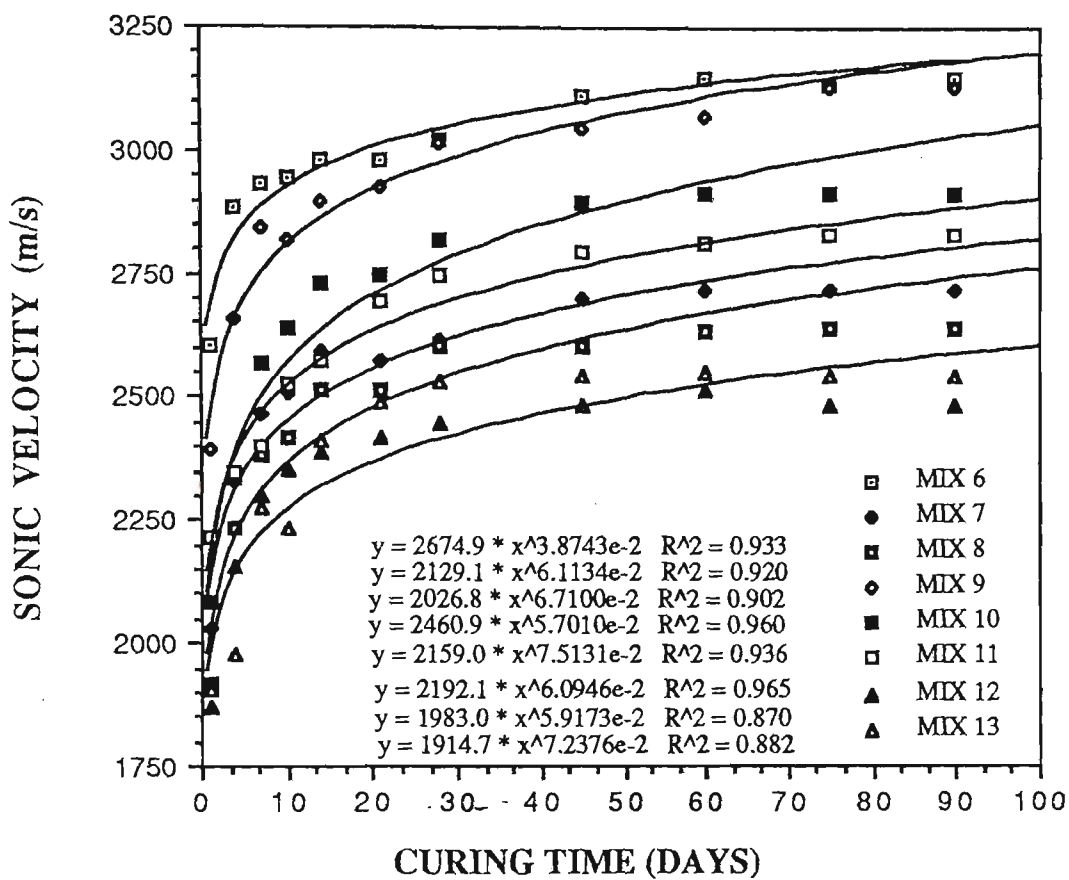


Figure AII6.2 Sonic velocity-curing time graph of CCWR specimens for mixes 6 through 13.

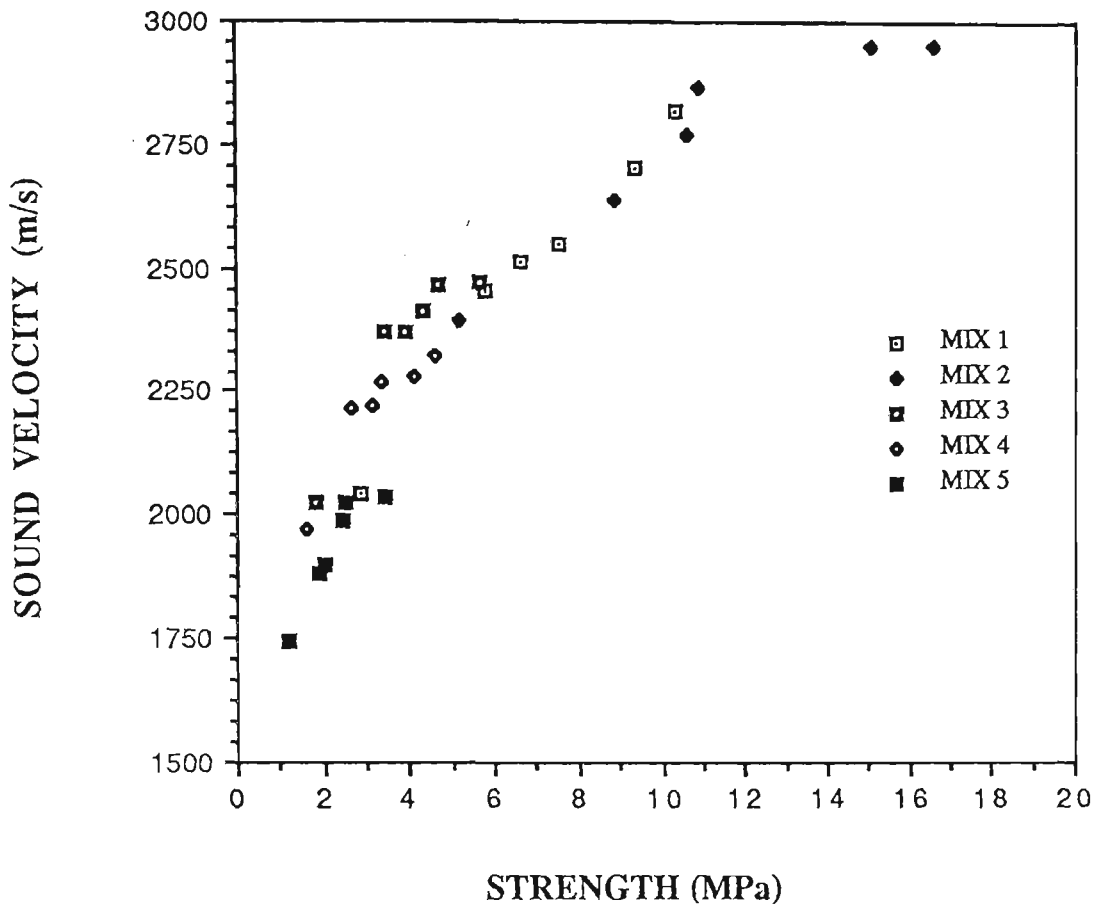


Figure AII6.3 Sonic velocity-strength graph of CCWR specimens for mixes 1 through 5.

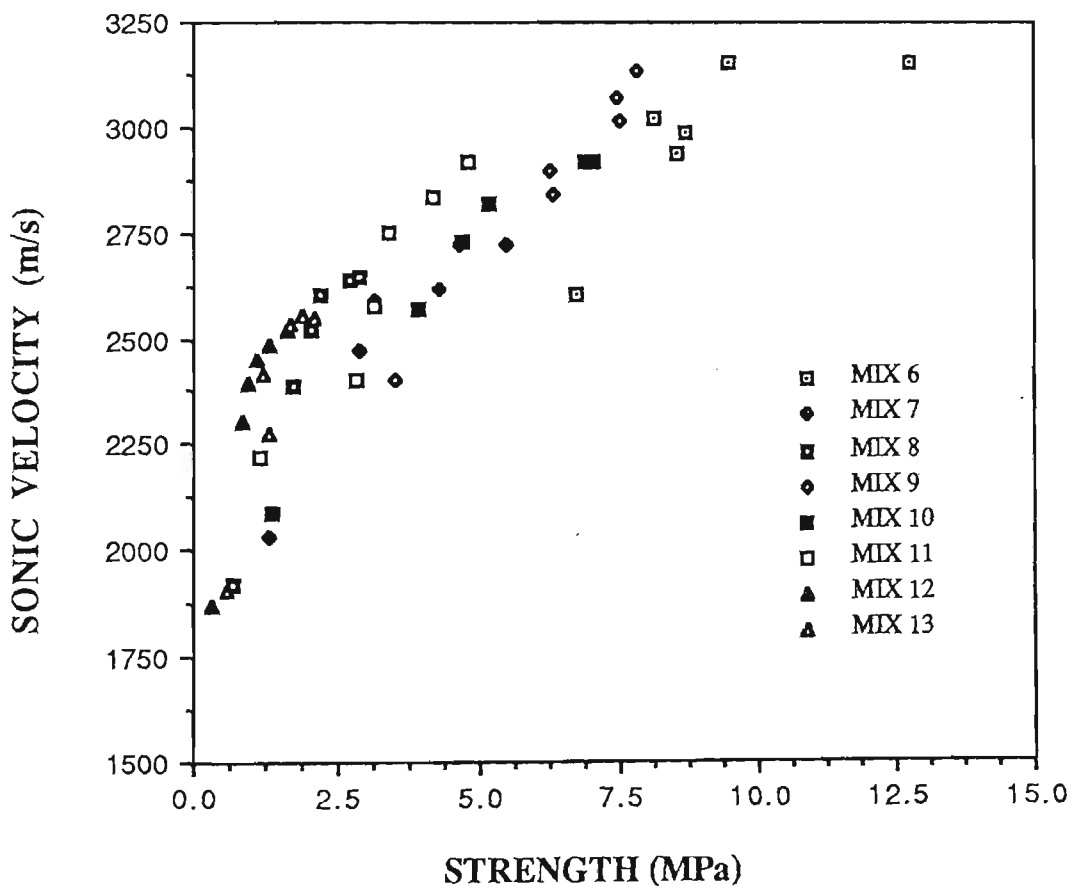


Figure AII6.4 Sonic velocity-strength graph of CCWR specimens for mixes 6 through 13.

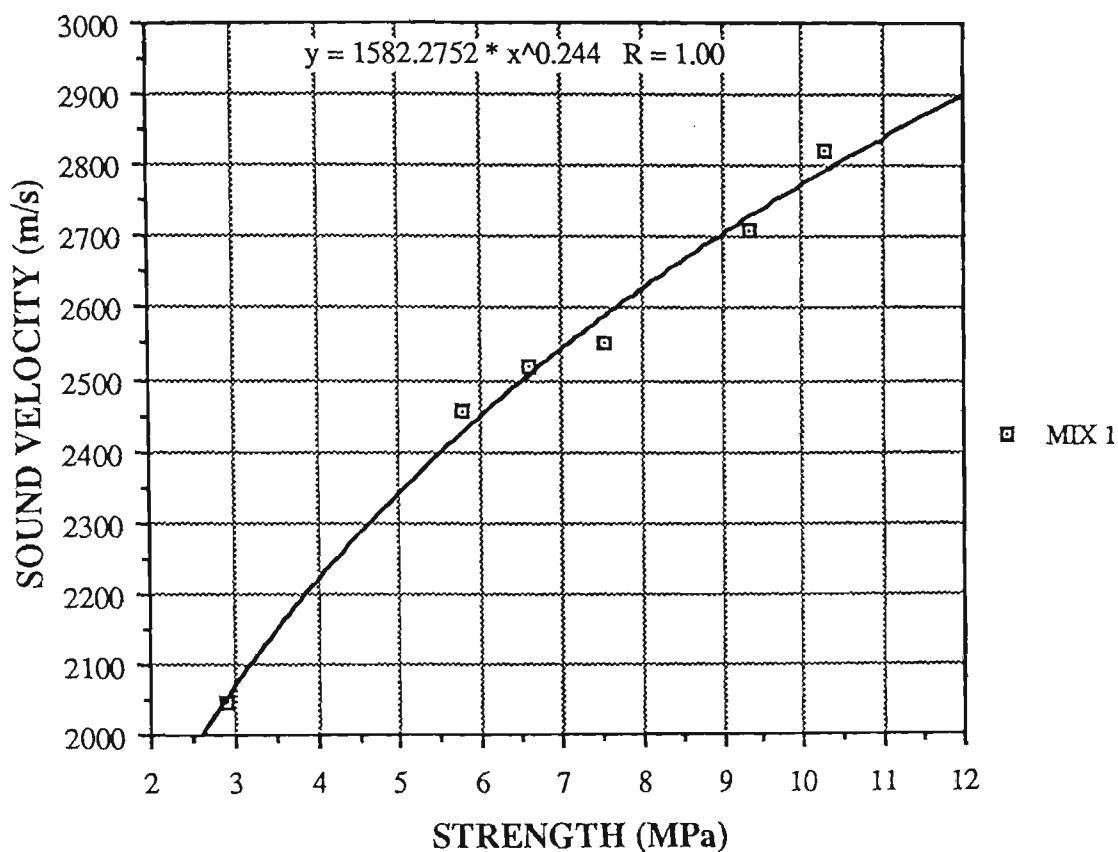


Figure AII6.5 Sonic velocity-strength graph of CCWR specimens (mix 1).

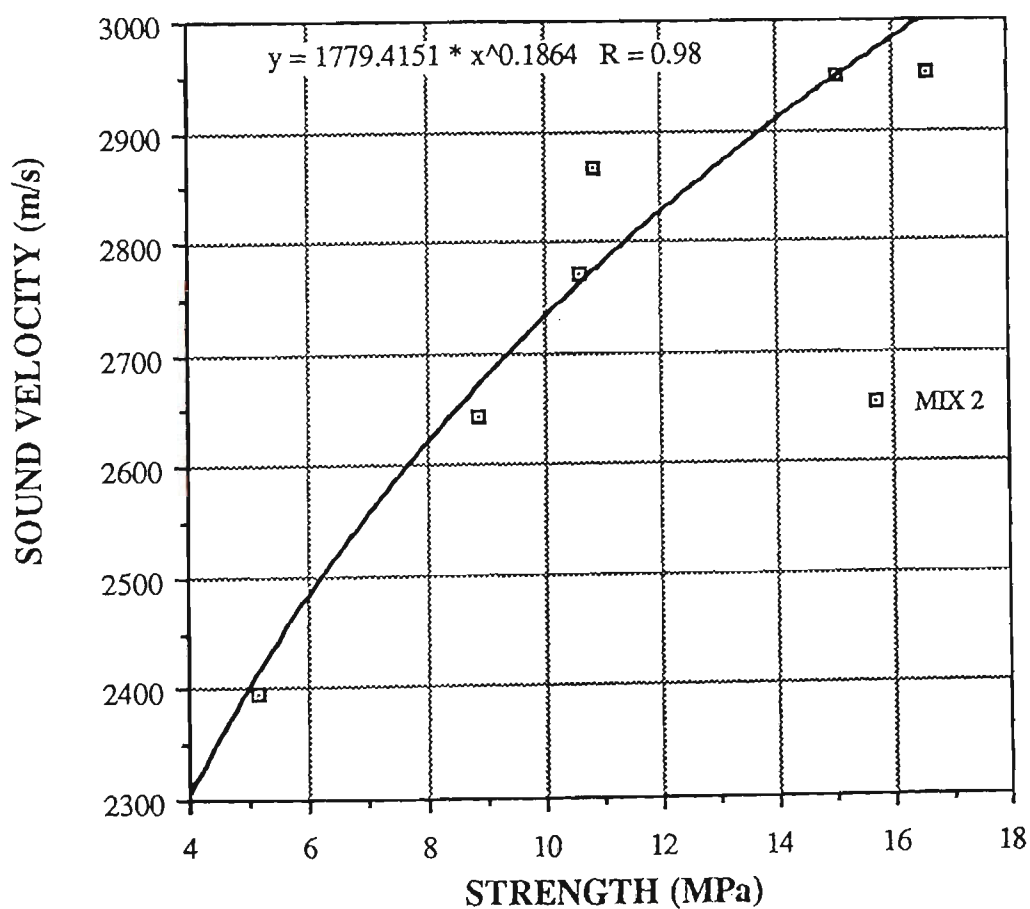


Figure AII6.6 Sonic velocity-strength graph of CCWR specimens (mix 2).

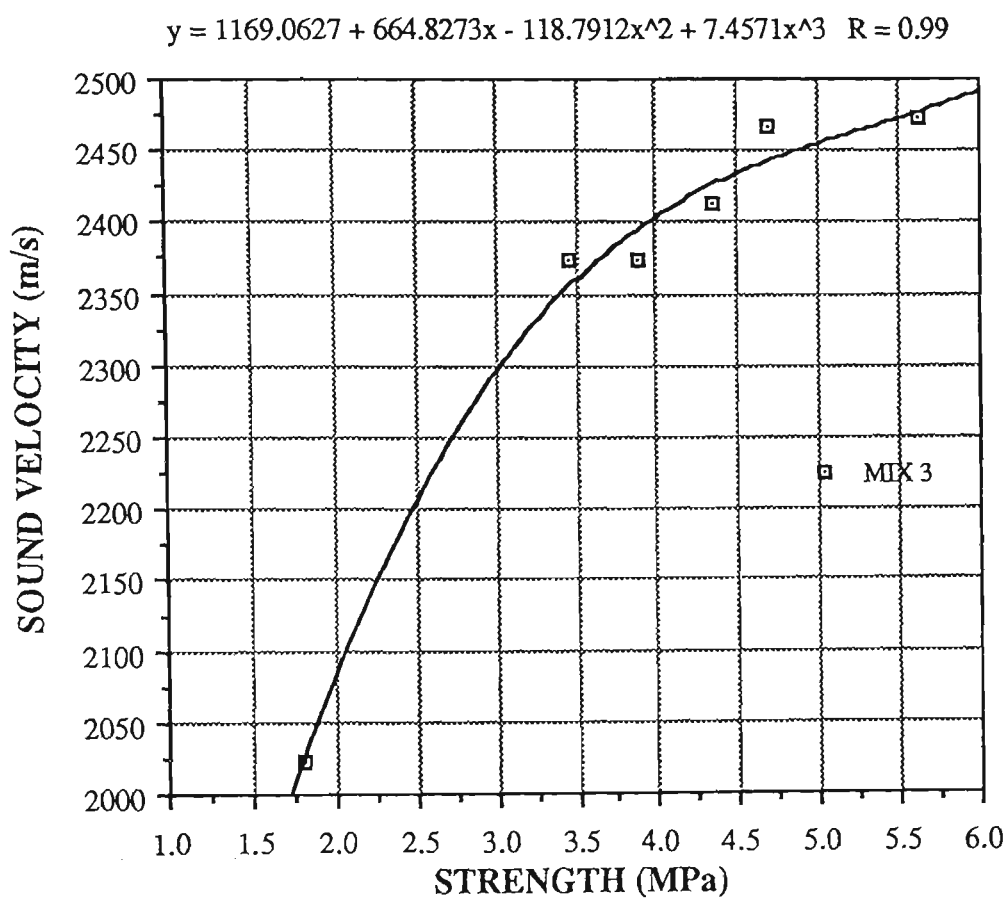


Figure AII6.7 Sonic velocity-strength graph of CCWR specimens (mix 3).

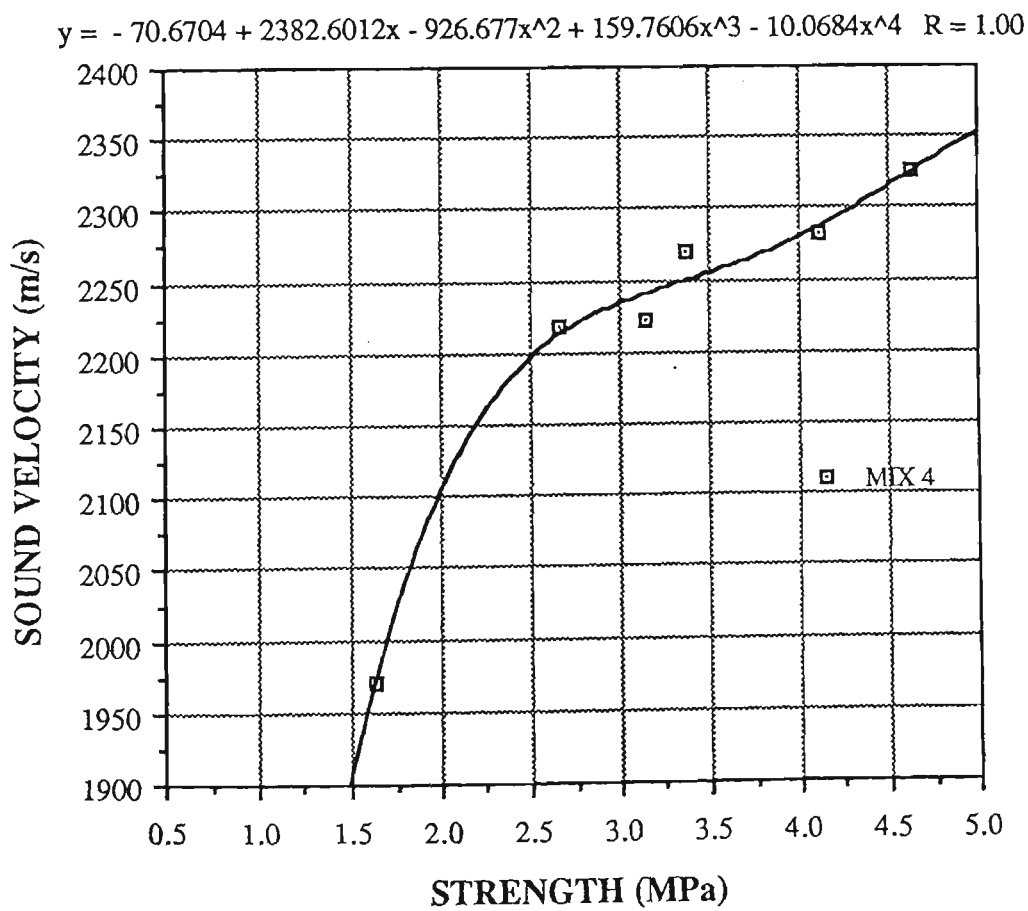


Figure AII6.8 Sonic velocity-strength graph of CCWR specimens (mix 4).

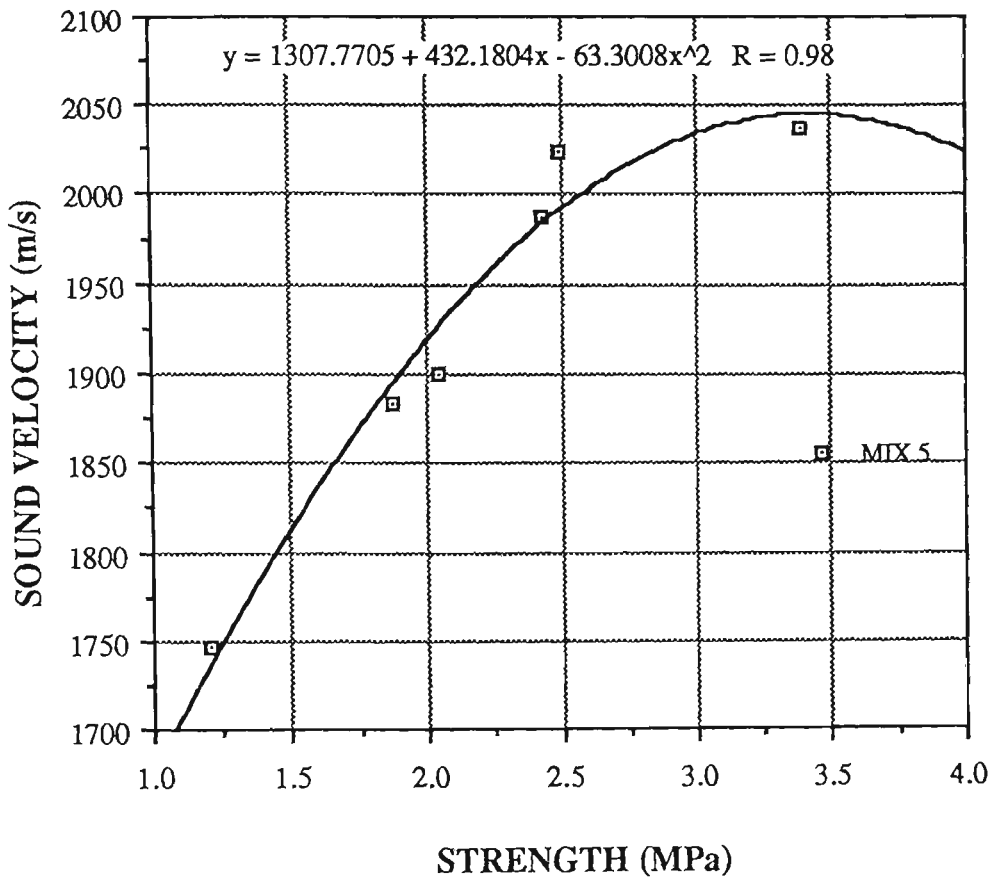


Figure AII6.9 Sonic velocity-strength graph of CCWR specimens (mix 5).

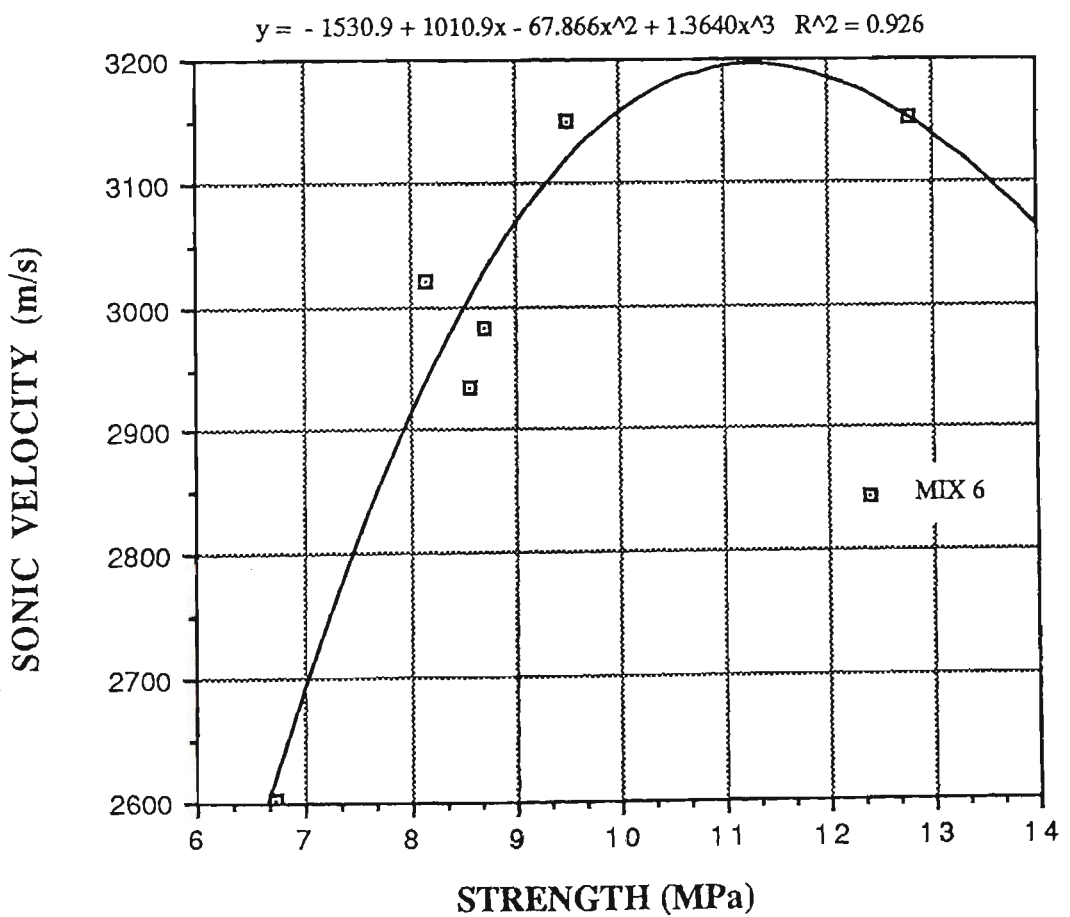


Figure AII6.10 Sonic velocity-strength graph of CCWR specimens (mix 6).

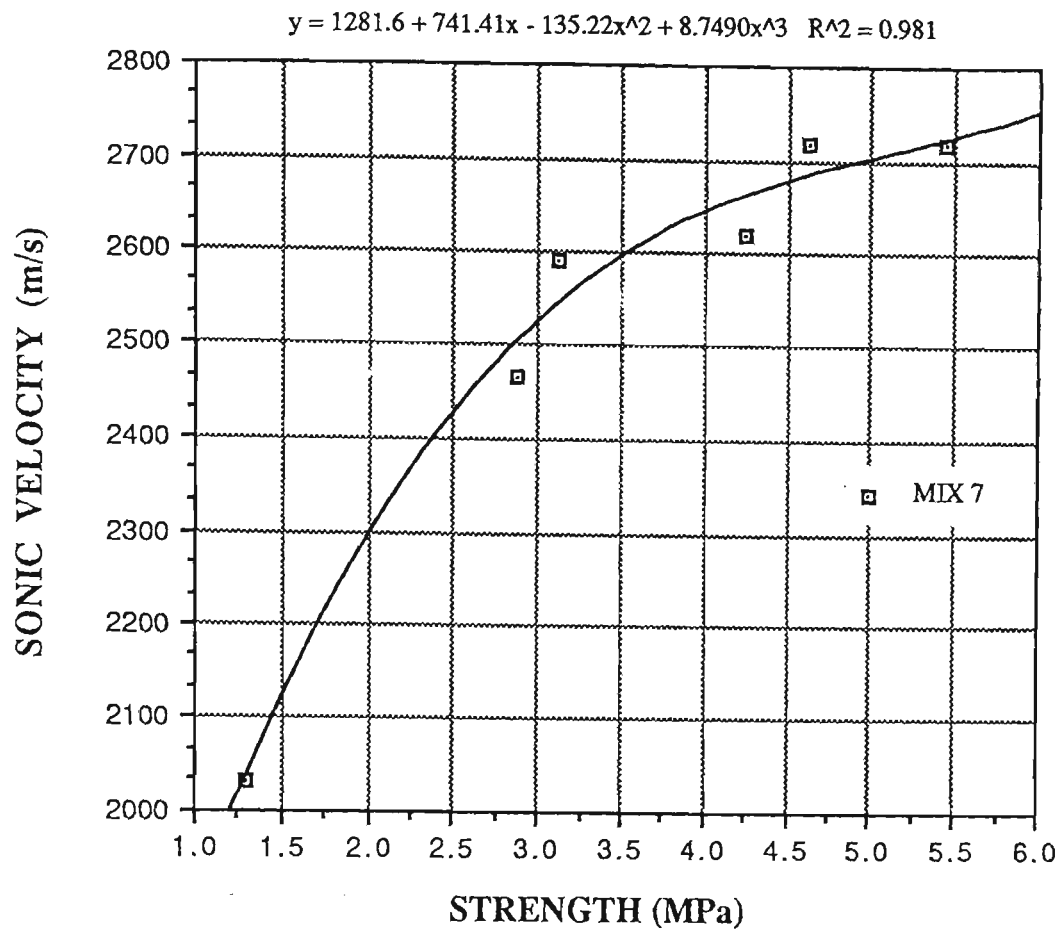


Figure AII6.11 Sonic velocity-strength graph of CCWR specimens (mix 7).

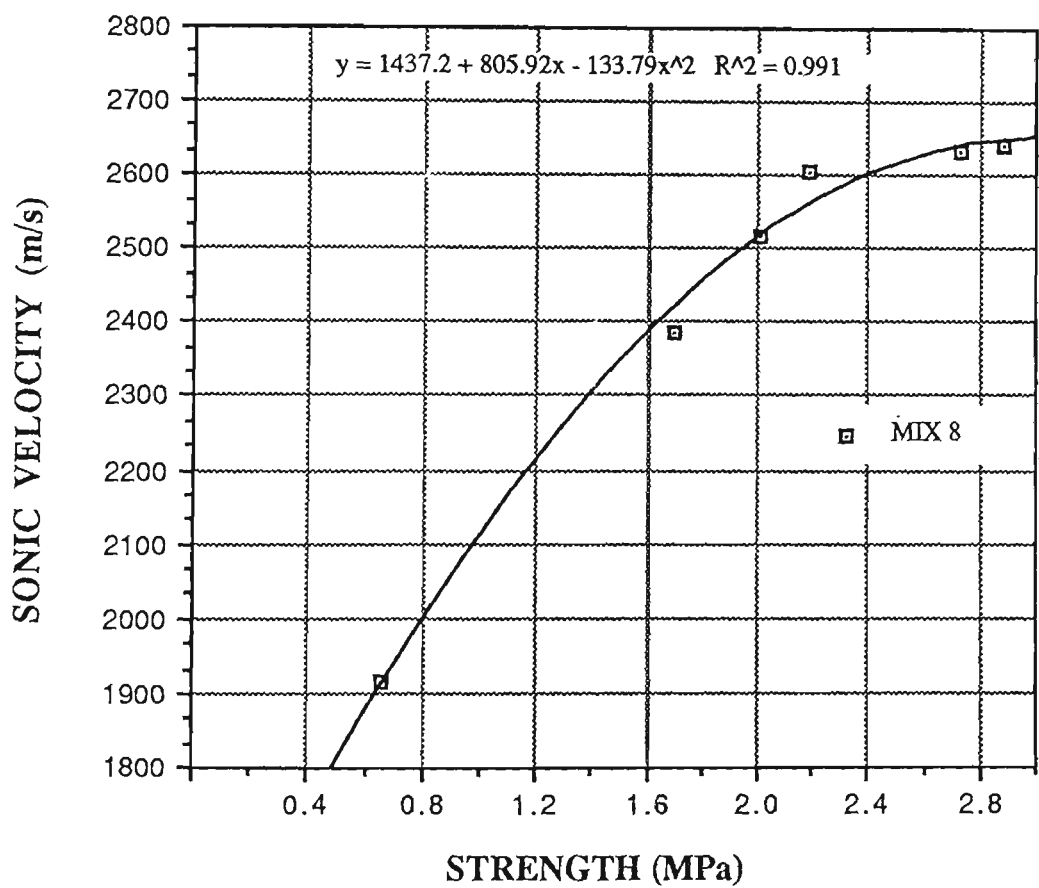


Figure AII6.12 Sonic velocity-strength graph of CCWR specimens (mix 8).

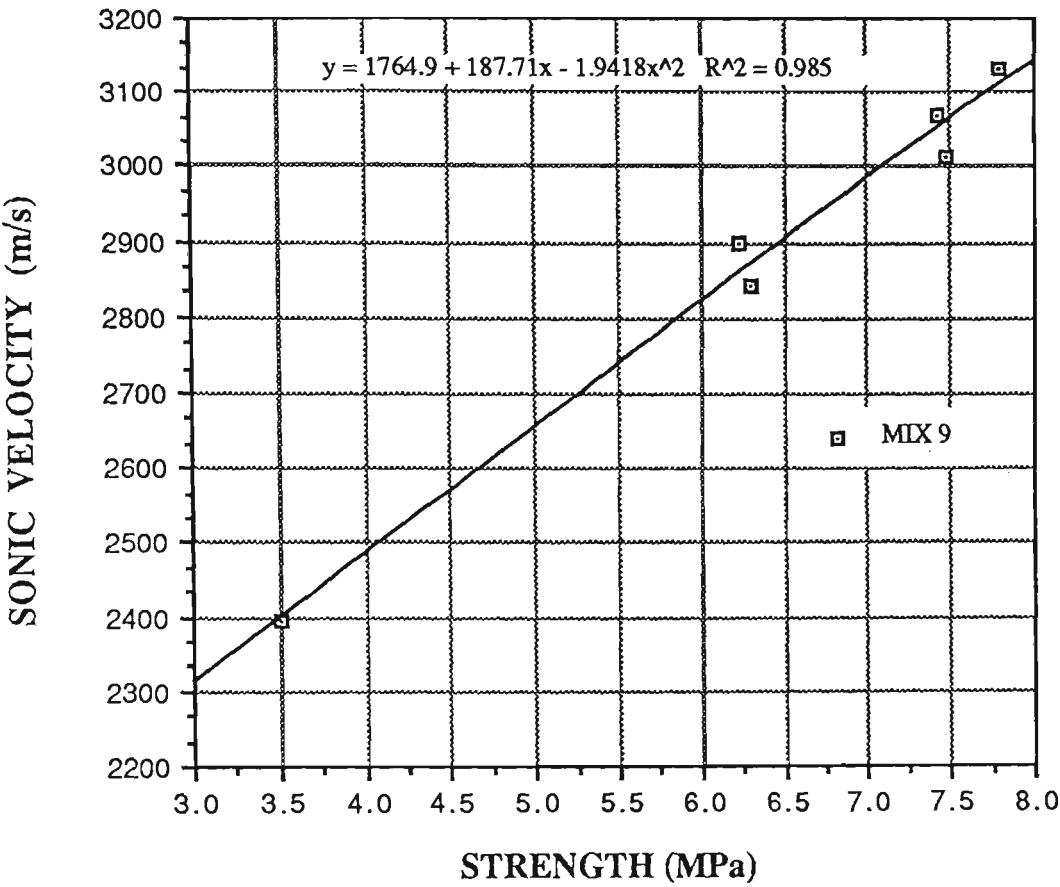


Figure AII6.13 Sonic velocity-strength graph of CCWR specimens (mix 9).

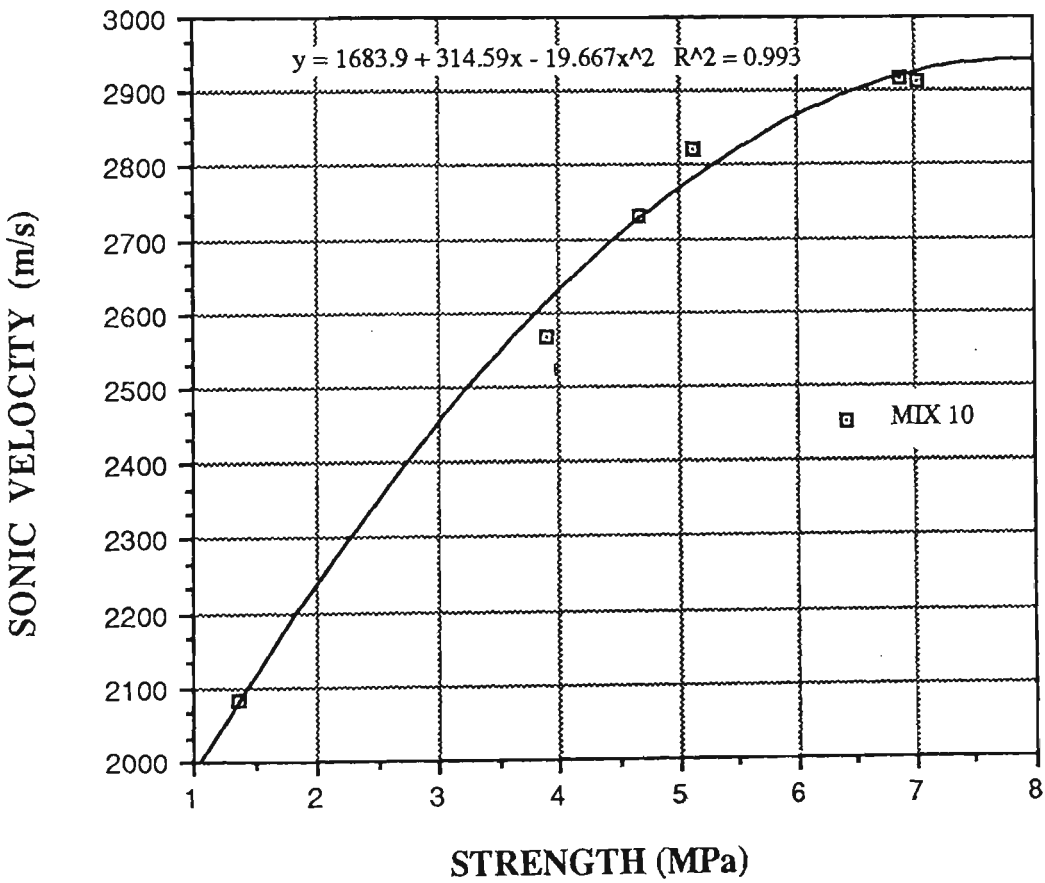


Figure AII6.14 Sonic velocity-strength graph of CCWR specimens (mix 10).

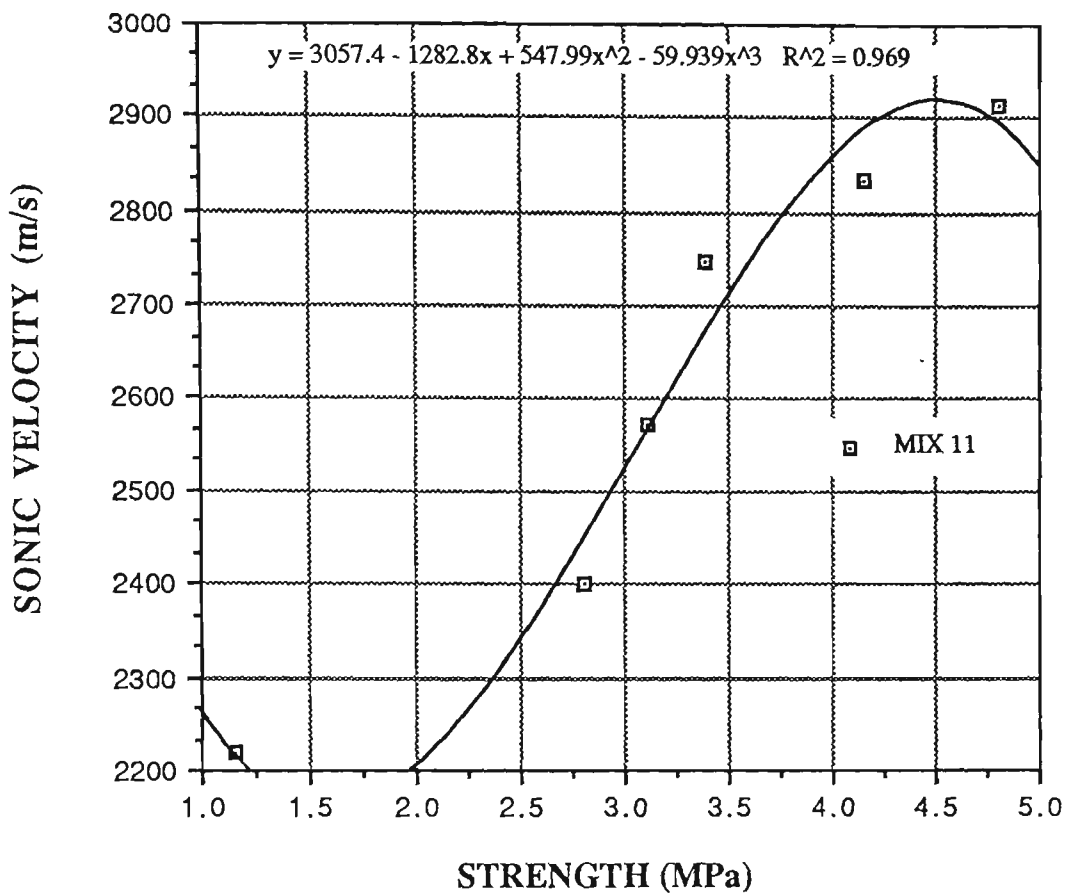


Figure AII6.15 Sonic velocity-strength graph of CCWR specimens (mix 11).

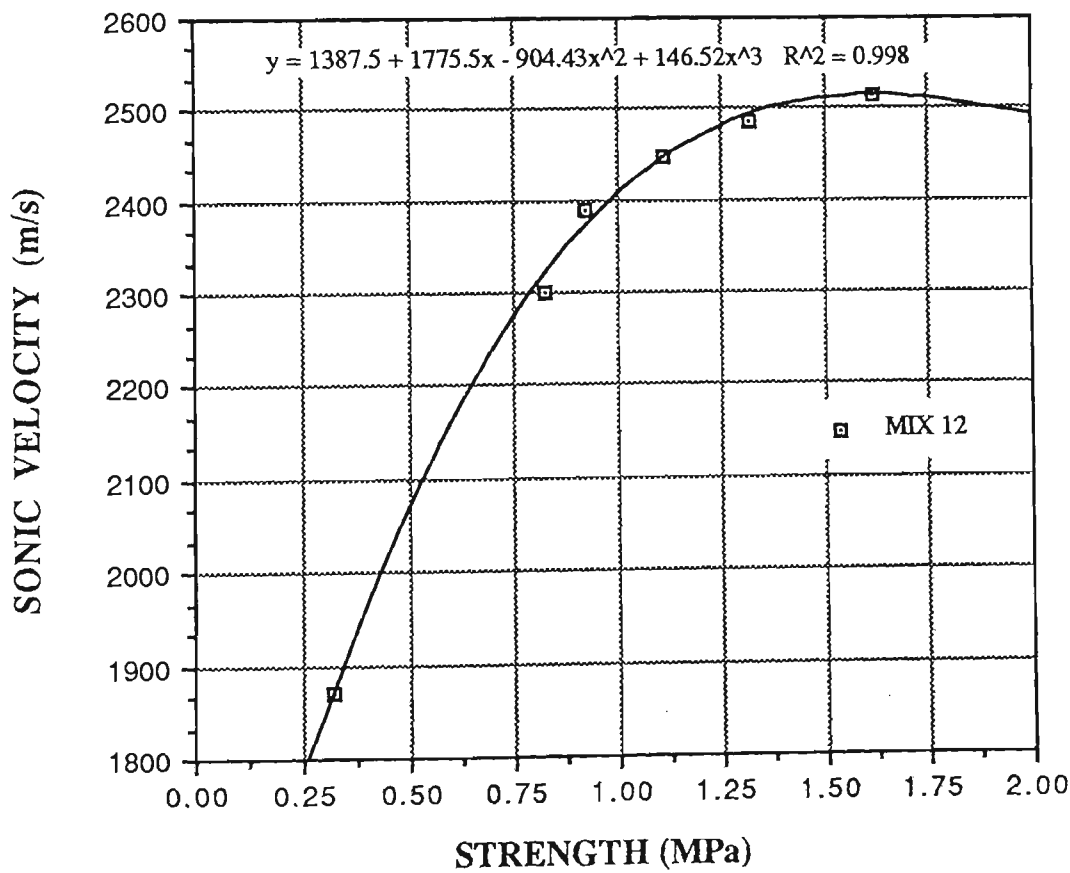


Figure AII6.16 Sonic velocity-strength graph of CCWR specimens (mix 12).

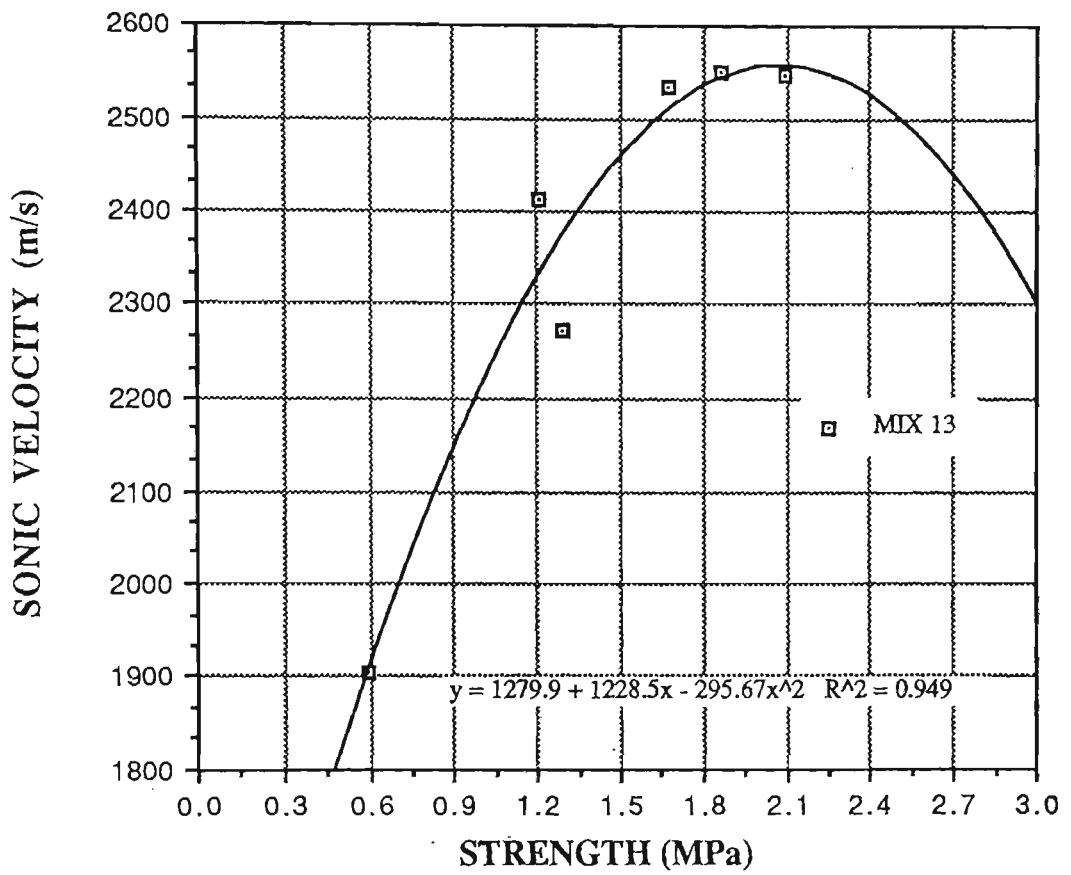


Figure AII6.17 Sonic velocity-strength graph of CCWR specimens (mix 13).

Table AII7.1 Flow test results of CWR.

Water Content (%)	Run NO.	Flow Factor ξ	Slope of Flow-tube ($^{\circ}$)	Temp. of Atmosphere ($^{\circ}\text{C}$)	Remarks
2	1	2.04	38.5 $^{\circ}$	23 $^{\circ}$	A. very dry mix and hence very rapid flow. The flow-ability is amongst the highest
	2	2.72			
	3	2.42			
	4	2.31			
	5	2.17			
	\bar{x}	2.33	$\sigma_n=0.23$	$\sigma_{n-1}=0.26$	
Flowability = 42.88					
5	1	---	38.5 $^{\circ}$	25 $^{\circ}$	A. very stiff mix as well as a very cohesive mix was observed.
	2	---			
	3	---			
	No Flow				
10	1	2.54	38.5 $^{\circ}$	18 $^{\circ}$	Relatively rapid flow was observed
	2	2.61			
	3	2.44			
	4	2.15			
	5	2.48			
		\bar{x}	2.44	$\sigma_n=0.16$	$\sigma_{n-1}=0.18$
Flowability = 40.92					
15	1	9.46	38.5 $^{\circ}$	18.5 $^{\circ}$	The mix is on the limit of saturation. @ Flow like a solid plug Typical of the so-called Bingham fluid.
	2	8.13			
	3	10.31 [®]			
	4	11.22			
	5	8.75			
		\bar{x}	9.57	$\sigma_n=1.10$	$\sigma_{n-1}=1.23$
Flowability = 10.44					

Table AII7.2 Flow test results of CWR.

Water Content (%)	Run No.	Flow Factor ξ	Slope of Flow-tube ($^{\circ}$)	Temp. of Atmosphere ($^{\circ}$ C)	Remarks
20	1	13.38	38.5	23.5	The mix appeared to be saturated with water. A little free water existed in the mix. Reasonably quick flow was observed.
	2	10.74			
	3	10.46			
	4	9.40			
	5	11.20			
	\bar{x}	10.45	$\sigma_n=0.66$	$\sigma_{n-1}=0.76$	
	Flowability = 9.60				
20	1	4.95	40.0	18.0	Again with a little free water. Laterally collapsed slump was observed.
	2	4.77			
	3	4.49			
	4	4.69			
	5	3.60			
	\bar{x}	4.50	$\sigma_n=0.47$	$\sigma_{n-1}=0.53$	
	Flowability = 22.22				
25	1	2.70	38.5	24.5	A rather saturated mix with a considerable amount of free water. A high flowability mix.
	2	3.26			
	3	3.30			
	4	2.86			
	\bar{x}	3.03	$\sigma_n=0.26$	$\sigma_{n-1}=0.30$	
	Flowability = 33.00				
25	1	1.55	40.0	18.5	Again a rather saturated mix with considerable amount of free water
	2	1.75			
	3	1.59			
	4	1.98			
	5	1.69			
	\bar{x}	1.71	$\sigma_n=0.15$	$\sigma_{n-1}=0.17$	
	Flowability = 58.41				

Table AII7.3 Flow test results of CWR.

Water Content (%)	Run No.	Flow Factor ξ	Slope of Flow-tube ($^{\circ}$)	Temp. of Atmosphere ($^{\circ}\text{C}$)	Remarks
30	1	1.98	38.5	23.0	An extremely saturated mix with plenty of free water. As expected, it flows very rapidly. There was a considerable amount of separation between the tailings and the water.
	2	1.59			
	3	1.81			
	4	1.79			
	5	1.70			
	\bar{x}	1.77	$\sigma_n=0.13$	$\sigma_{n-1}=0.14$	
Flowability = 56.50					
30	1	1.79	40.0	20.0	Again plenty of free water was observed. It is the mix with the highest mass per cent of water content and consequently it is also the mix with the highest flowability.
	2	1.39			
	3	1.47			
	4	1.72			
	5	1.58			
	\bar{x}	1.59	$\sigma_n=0.15$	$\sigma_{n-1}=0.177$	
Flowability = 62.89					

Table AII7.4 Flow test results of CWR.

Water Content (%)	Run No.	Flow Factor \bar{x}	Slope of Flow-tube (°)	Temp. of Atmosphere (°C)	Remarks
2	1	1.04	45	18.0	This is by far the best slope for the flow tests. A considerably quicker flow was experienced at this slope, c.f. 38.5°.
	2	1.14			
	3	1.15			
	4	1.27			
	5	1.27			
	\bar{x}	1.17	$\sigma_n=0.09$	$\sigma_{n-1}=0.10$	
Flowability = 85.47					
5	1	1.68	45	18.0	A very stiff material. It flowed quite rapidly at this slope.
	2	1.47			
	3	1.36			
	4	1.36			
	5	1.37			
	\bar{x}	1.45	$\sigma_n=0.12$	$\sigma_{n-1}=0.14$	
Flowability = 69.06					
10	1	1.62	45	18.0	A rapid flowing material. It has a low slump value of 15 mm.
	2	1.52			
	3	1.49			
	4	1.50			
	5	1.36			
	\bar{x}	1.50	$\sigma_n=0.08$	$\sigma_{n-1}=0.09$	
Flowability = 66.76					

Table AII7.5 Flow test results of CWR.

Water Content (%)	Run No.	Flow Factor δ	Slope of Flow-tube ($^{\circ}$)	Temp. of Atmosphere ($^{\circ}\text{C}$)	Remarks
15	1	2.96	45	18.5	This material has the lowest flowability. However, it is a fairly consistent mix.
	2	3.54			
	3	2.35			
	4	2.70			
	5	2.30			
	\bar{x}	2.77	$\sigma_n=0.45$	$\sigma_{n-1}=0.51$	
Flowability = 36.10					
20	1	1.90	45	18.0	Almost has the same flowability value as the 15% water content mix.
	2	1.95			
	3	2.10			
	4	2.19			
	5	2.12			
	\bar{x}	2.05	$\sigma_n=0.11$	$\sigma_{n-1}=0.53$	
Flowability = 48.73					
25	1	1.36	45	18.5	The mix had considerable amount of free water. A rapid flowing mix.
	2	1.31			
	3	1.34			
	4	1.34			
	5	1.50			
	\bar{x}	1.37	$\sigma_n=0.07$	$\sigma_{n-1}=0.08$	
Flowability = 72.99					
30	1	1.18	45	18.5	The mix had a high lateral collapse slump value of 200mm. Very little cohesive property of the material was observed.
	2	1.22			
	3	1.33			
	4	1.30			
	5	1.39			
	\bar{x}	1.28	$\sigma_n=0.08$	$\sigma_{n-1}=0.08$	
Flowability = 77.88					

Table AII7.6 Flow test results of CWR.

Water Content (%)	Run No.	Flow Factor \bar{x}	Slope of Flow-tube ($^{\circ}$)	Temp. of Atmosphere ($^{\circ}\text{C}$)	Remarks
2	1	1.20	50	18.0	Very little cohesive property was observed of the material.
	2	1.49			
	3	1.12			
	4	1.10			
	5	1.12			
	\bar{x}	1.21 $\sigma_n=0.15$ $\sigma_{n-1}=0.16$			
	Flowability = 82.95				
5	1	1.62	50	18.0	A very stiff material with zero slump value. This material did not flow at 38.5 deg. slope.
	2	1.06			
	3	1.15			
	4	1.06			
	5	1.03			
	\bar{x}	1.18 $\sigma_n=0.22$ $\sigma_{n-1}=0.25$			
	Flowability = 84.46				
10	1	0.99	50	18.0	The flowability value of this mix is similar to that of the previous mix at this angle.
	2	1.16			
	3	1.18			
	4	1.12			
	5	1.10			
	\bar{x}	1.11 $\sigma_n=0.07$ $\sigma_{n-1}=0.07$			
	Flowability = 90.09				
15	1	1.96	50	18.5	This mix has a typically low flowability value, indicating a particularly high internal shear strength of the material at this water content.
	2	1.65			
	3	1.97			
	4	1.60			
	5	1.71			
	\bar{x}	1.78 $\sigma_n=0.16$ $\sigma_{n-1}=0.18$			
	Flowability = 56.24				

Table AII7.7 Flow test results of CWR.

Water Content (%)	Run No.	Flow Factor δ	Slope of Flow-tube (°)	Temp. of Atmosphere (°C)	Remarks
20	1	1.81	50	18.0	A collapsed slump was observed. Flowability value is similar to the previous mix.
	2	1.68			
	3	1.80			
	4	1.76			
	5	1.66			
	\bar{x}	1.74	$\sigma_n = 0.06$	$\sigma_{n-1} = 0.07$	
	Flowability = 57.41				
25	1	1.21	50	18.5	A considerable amount of free water was observed. A high flowability is evident.
	2	1.42			
	3	1.17			
	4	1.20			
	5	1.24			
	\bar{x}	1.25	$\sigma_n = 0.09$	$\sigma_{n-1} = 0.10$	
	Flowability = 80.13				
30	1	0.99	50	18.0	Again a lot of free water was observed. The material flowed rather quickly.
	2	0.95			
	3	1.02			
	4	0.84			
	5	0.82			
	\bar{x}	0.92	$\sigma_n = 0.08$	$\sigma_{n-1} = 0.09$	
	Flowability = 108.23				

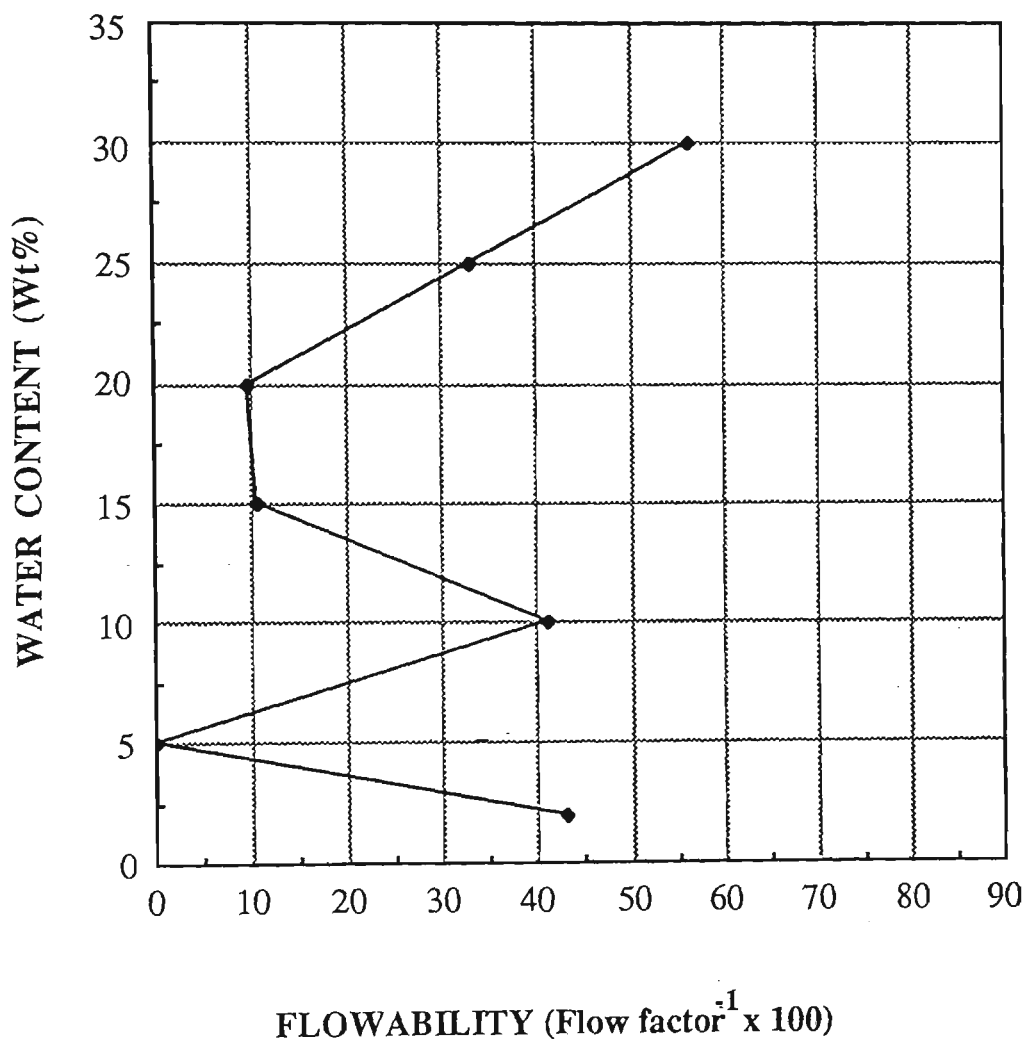


Figure AII7.1 Water content-flowability graph of CWR at 38.5° Slope.

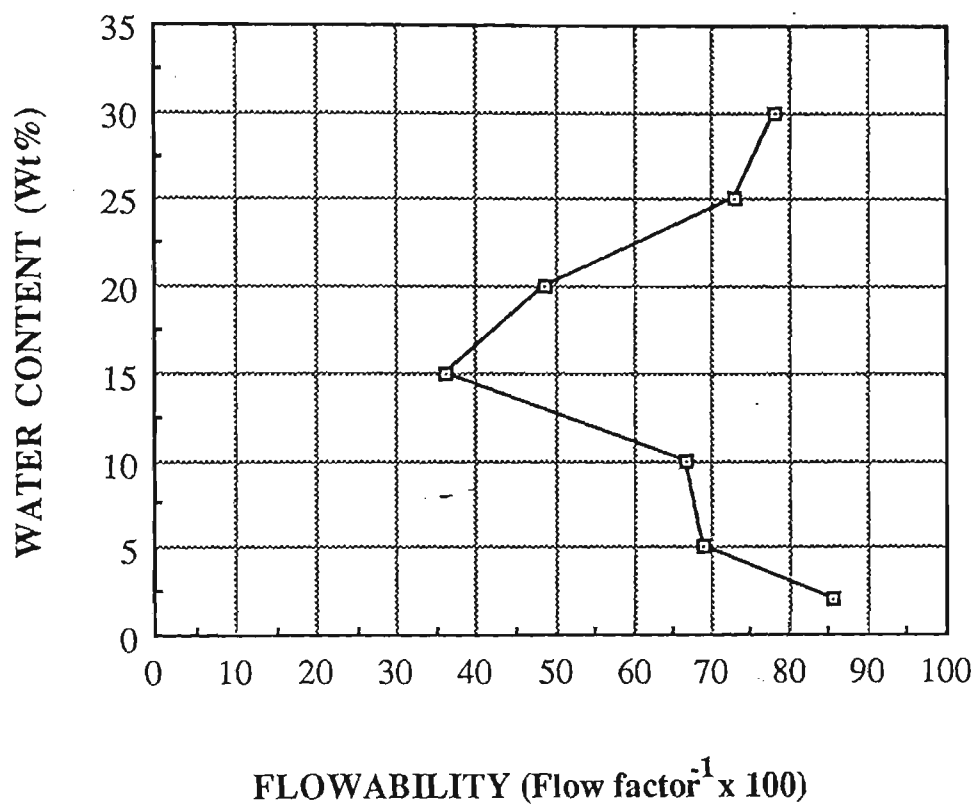


Figure AII7.2 Water content-flowability graph of CWR at 45.0° Slope.

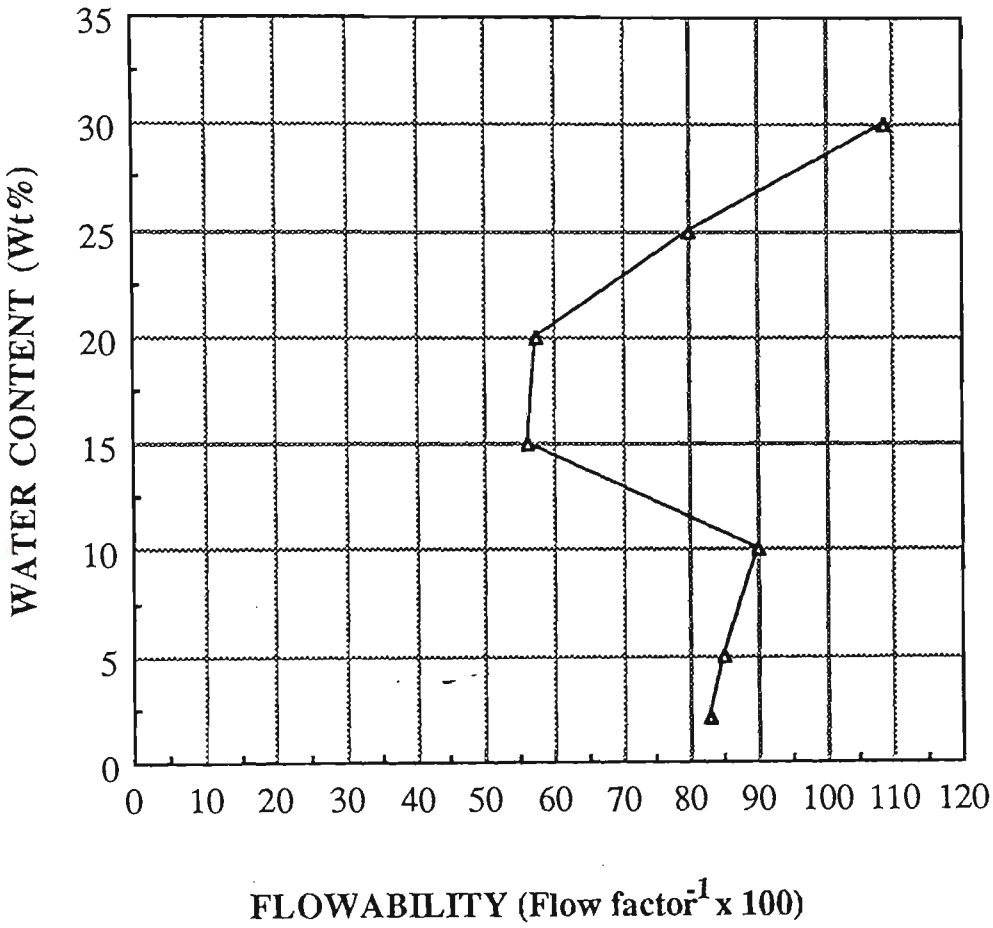
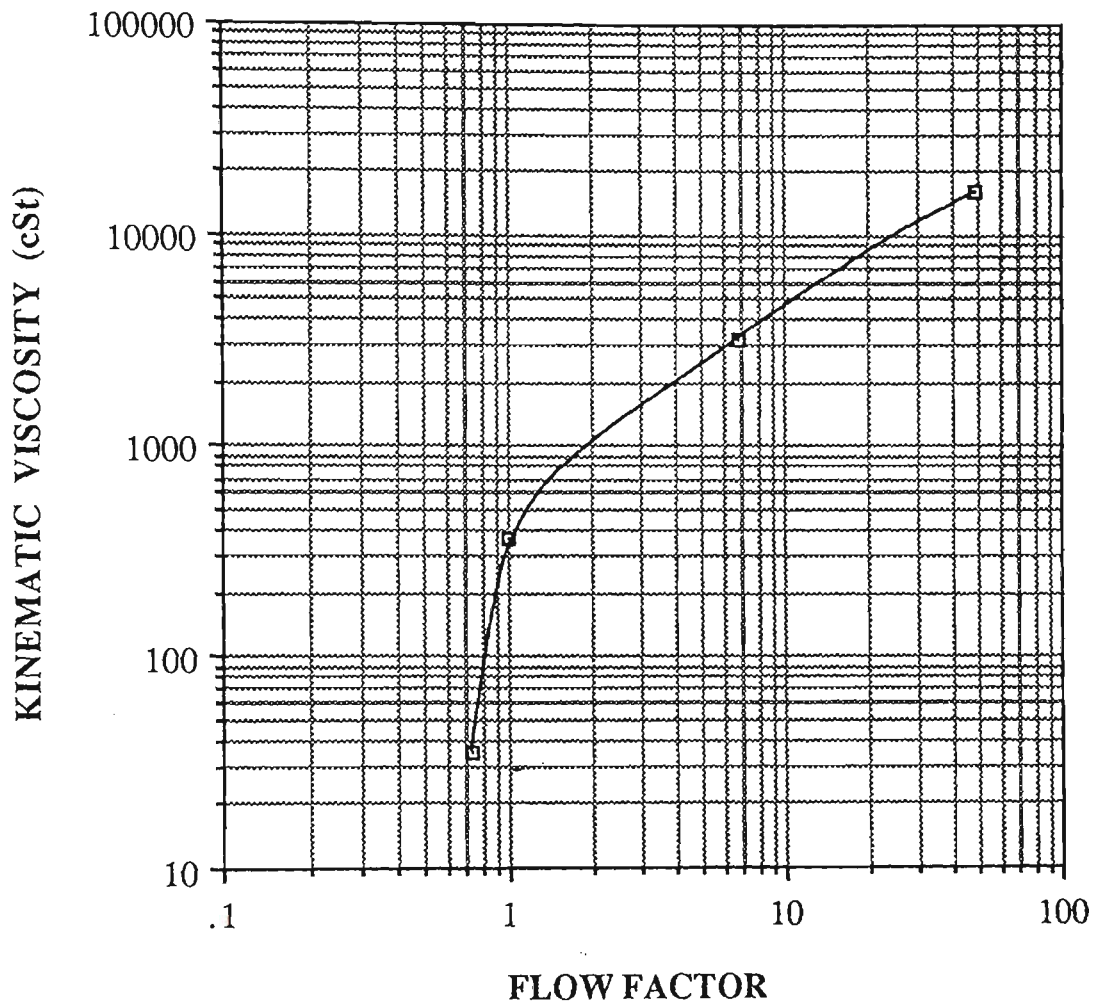
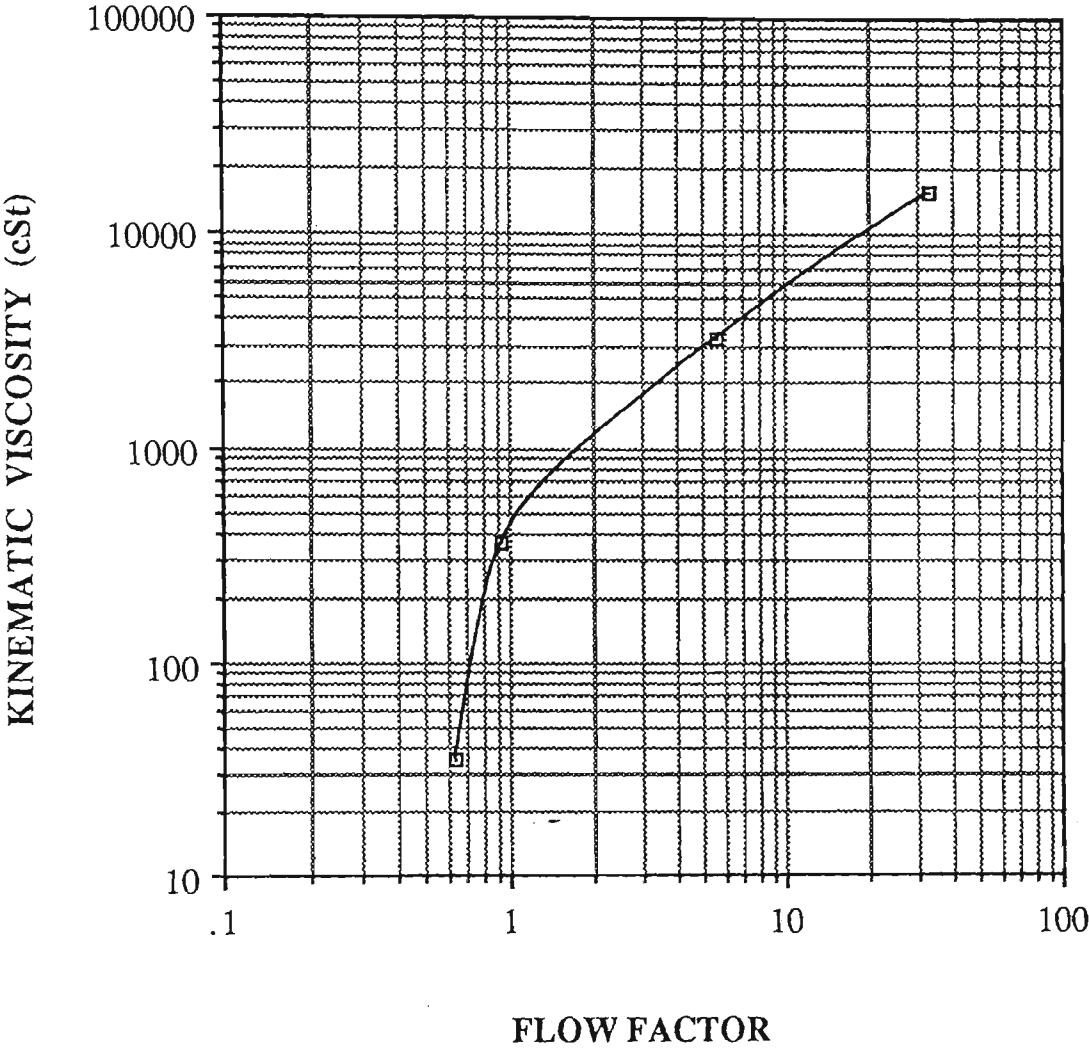


Figure AII7.3 Water content-flowability graph of CWR at 50.0° Slope.



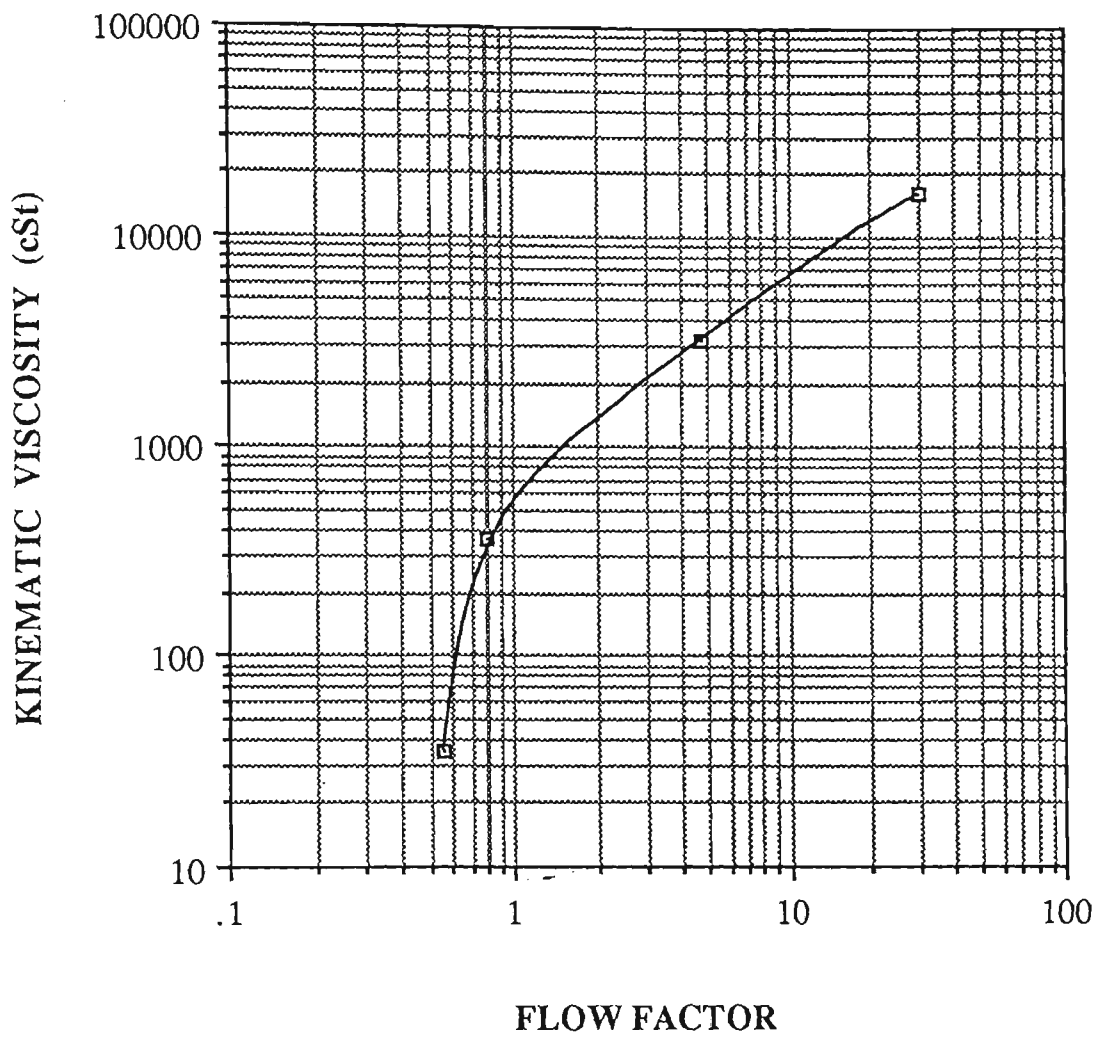
Average values of each of the five runs for each oil at 38.5° slope were used to plot this graph.

Figure AII7.4 Graph of kinematic viscosity-flow factor of different calibration oils at 38.5° Slope.



Average values of each of the five runs for each oil at 45° slope were used to plot this graph.

Figure AII7.5 Graph of kinematic viscosity-flow factor of different calibration oils at 45.0° Slope.



Average values of each of the five runs for each oil at 50° slope were used to plot this graph.

Figure AII7.6 Graph of kinematic viscosity-flow factor of different calibration oils at 50.0° Slope.